

**SK Potassium and TRPM7 Ion
Channel Role in CNS Cell Survival
and Breast Cancer Cell Death
Decisions**



A thesis submitted to Cardiff University in accordance with
the requirements for the degree of Philosophiae Doctor

by

Zana Azeez Abdulkareem

September 2015

School of Pharmacy and Pharmaceutical Sciences
Cardiff University

United Kingdom

Summary

Cell survival is modulated by a cocktail of ion channels engaging cell life and death decisions through controlling key cellular messages such as apoptosis and proliferation. Unnatural regulation of these processes results in various disorders, for example neurodegenerative diseases, as well as the cancers. Nowadays, these pathologies are affecting millions of people per year in the world. Potassium (K^+) ion channels appear to play a potent role in such illnesses since they can control many cellular gates in cell physiology such as ionic homeostasis and signalling cascades. Amongst the K^+ channels, small (SK1-3) and intermediate (SK4) conductance Ca^{2+} -activated potassium ion channels have recently been shown to save cells, thereby protecting mitochondrial function which serves as a cell survival platform. In the case of other ion channels, for instance transient receptor potential melastatin 7 (TRPM7), it is also repeatedly stated that such membrane channels shows an impressive and differential role in excitable and non-excitable cell survival. This channel also modulates ionic homeostasis of crucial ions in cellular physiology such as Ca^{2+} . This study reveals that central nervous system (CNS) and breast cancer cells differentially express SK1-4 ion channel subtypes, and their functional presence is pharmacologically confirmed, however, in most cases these results were further clarified through small interference RNA (siRNA) method. Similarly, functional TRPM7 channel expression in CNS cells is also confirmed. In the CNS, SK1-4 channel activation rescues neurons from oxidative stress, whereas, TRPM7 channel inhibition protects CNS cells from this hydrogen peroxide (H_2O_2) harmful effect, as well as hypoxia and apoptosis, so improving cell survival. Excitingly, SK1-4 channels differentially exist between wild-type and Huntington's affected mouse striatal cells, where diseased cells lack SK1-3 channels, key players in action potential activity. Interestingly, SK2 or SK3 channel subtypes are also functionally expressed in breast cancer cells with various phenotypes. This study established that these ion channels are powerful agents in a survival role, in fact controlling growth through cross-talk with an apoptotic avenue "intrinsic pathway". SK2 or SK3 channel activation enhances cell viability, while its inhibition dampens cell growth. It is very noteworthy that SK2 and SK3 channels are not expressed in non-tumorigenic breast cells.

In brief, SK1-4 and TRPM7 molecules are clearly implicated in the survival of diverse cell types through an apoptotic route, indicating that these ionic regulators are promising targets in channelopathies related to cellular degeneration and growth.

Publications relevant to this thesis

This manuscript is currently under peer-review for publication by British Journal of Pharmacology:

Abdulkareem Z. A., Cox C. D., Gee M.W. J., and Wann K. T. (2015) Small conductance Ca^{2+} -activated potassium channel knockdown is potently cytotoxic in breast cancer cell lines. Br J Pharmacol.

Acknowledgements

I would like to thank my principal supervisor Prof Kenneth Wann. His kind offer to study my PhD in his lab was a tremendous opportunity. I am deeply indebted to him for his support, guidance and all scientific advice over last four years. I will be forever grateful for his help and kindness.

I would like to also thank Prof Gary Baxter, Prof Anthony Campbell and Dr Emma Kidd who have supported me and guided me throughout my PhD study, the greatest academic group in the school of Pharmacy and Pharmaceutical Sciences.

Many thanks to my lab colleagues: Dr Charles Cox, Dr Zhang Jin, Dr Rhian Thomas, Dr Dwaine Burley, Dr Justin Bice and Mr Benyamin Ertefai who shared intelligent scientific comments and views, and also shared their lab experience with me. In addition, Pharmacy project students and Erasmus students proved very enjoyable to work with.

An enormous thanks also to my main sponsor the Kurdistan Regional Government of Iraq. Here, it is important to thank also Cardiff University that supported me to complete a PhD degree.

Finally, thank you very much to my family that they were always very kind and supportive.

Abbreviations

AHP	Afterhyperpolarisation
ATP	Adenosine-5-triphosphate
BCA	Bicinchoninic acid assay
Bcl-2	B-cell lymphoma 2
bp	Base pairs
CaM	Calmodulin
cDNA	Complementary DNA
CK2	Casein kinase 2
CNS	Central nervous system
CoCl₂	Cobalt (II) chloride
CREB	Cyclic AMP response element binding protein
DAG	Diacylglycerol
dNTP	Deoxynucleotide triphosphate
DTT	Dithiothreitol
EBIO	Ethyl-2-benzimidazolinone
EC₅₀	Half maximal effective concentration
ECL	Enhanced chemiluminescence
ER	Endoplasmic reticulum
ER⁺	Estrogen receptor +ve
fAHP	Fast afterhyperpolarisation
FasL	Fas ligand
GAP-43	Growth Associated Protein 43
GAPDH	Glyceraldehyde 3-phosphate dehydrogenase
GPCRs	G-protein coupled receptors
GTP	Guanosine triphosphate
H₂O₂	Hydrogen peroxide
HER2	Human epidermal growth factor receptor 2
HIF-1	Hypoxia-inducible transcription factor 1
IC₅₀	Half maximal inhibitory concentration
IP3	Inositol triphosphate
K_d	Dissociation constant
mAHP	Medium afterhyperpolarisation
mRNA	Messenger ribonucleic acid
NMDA	N-Methyl-D-Aspartate
NO	Nitric oxide
PIP2	Phosphatidylinositol 4,5-bisphosphate

PLC	Phospholipase C
PP2A	Protein phosphatase 2A
PR	Progesterone receptor
ROS	Reactive oxygen species
RT-PCR	Reverse transcription-polymerase chain reaction
RyRs	Ryanodine receptors
sAHP	Slow afterhyperpolarisation
SK1-3	Small-conductance Ca ²⁺ -activated K ⁺ channels
SK4	Intermediate-conductance Ca ²⁺ -activated K ⁺ channels
SOCE	Store-operated Ca ²⁺ entry
SR/ER	Sarco/Endoplasmic reticulum
TAE	Tris-acetate-EDTA
tBID	Truncated BID
TNFα	Tumour necrosis factor-alpha
TraIL	TNF-related apoptosis-inducing ligand
TRPC	Transient receptor potential canonical
TRPC1	Transient receptor potential canonical 1
TRPC5	Transient receptor potential canonical 5
TRPM2	Transient receptor potential melastatin 2
TRPM3	Transient receptor potential melastatin 3
TRPM4	Transient receptor potential melastatin 4
TRPM7	Transient receptor potential melastatin 7
TRPV	Transient receptor potential vanilloid
TRPV2	Transient receptor potential vanilloid 2
V_m	Membrane potential
VOCs	Voltage-operated channels

List of figures

Figure 1.1 The structure of SK ion channels.....	5
Figure 1.2 Chemical structures of the SK channel activators.	11
Figure 1.3 Chemical structures of SK channel inhibitors.	12
Figure 1.4 Phylogenetic tree of TRP channels according their homology	16
Figure 1.5 Transmembrane and the quaternary structure of TRP channels.....	19
Figure 1.6 Possible mechanisms for TRP channel activation	21
Figure 1.7 Chemical structure of 2-aminoethyl diphenylborinate	23
Figure 1.8 Mechanisms of cell death	25
Figure 1.9 Extrinsic and intrinsic modes of apoptosis, mode one	27
Figure 1.10 Extrinsic and intrinsic modes of apoptosis, mode two	28
Figure 1.11 Simplified picture of calcium signalling in cells	32
Figure 3.1 SK channel mRNA investigation in undifferentiated SH-SY5Y cells...	73
Figure 3.2 SK channel mRNA investigation in differentiated SH-SY5Y cells.....	73
Figure 3.3 Representative immunoblot of SK1 channel subtype in SH-SY5Y cells.	74
Figure 3.4 Representative immunoblot of SK3 channel subtype in SH-SY5Y cells.	74
Figure 3.5 Representative immunoblot of growth associated protein-43 (GAP-43) in SH-SY5Y cells.	75
Figure 3.6 The effect of the SK1 channel activator, GW542573X, on undifferentiated SH-SY5Y cell viability.	77
Figure 3.7 The effect of the SK1 channel activator, GW542573X, on differentiated SH-SY5Y cell viability.....	77

Figure 3.8 The effect of the SK2-3 channel activator, CyPPA, on undifferentiated SH-SY5Y cell viability.	78
Figure 3.9 The effect of the SK2-3 channel activator, CyPPA, on differentiated SH-SY5Y cell viability.	78
Figure 3.10 The effect of SK1-3 channel blocker, UCL1684, on undifferentiated SH-SY5Y cell viability.	80
Figure 3.11 The effect of SK1-3 channel blocker, UCL1684, on differentiated SH-SY5Y cell viability.	80
Figure 3.12 The effect of SK1-3 channel blocker, NS8593, on undifferentiated SH-SY5Y cell viability.	81
Figure 3.13 The effect of SK1-3 channel blocker, NS8593, on differentiated SH-SY5Y cell viability.	81
Figure 3.14 The effect of H ₂ O ₂ on undifferentiated SH-SY5Y cell viability.	83
Figure 3.15 The effect of H ₂ O ₂ on differentiated SH-SY5Y cell viability.	83
Figure 3.16 The effect of GW542573X, SK1 channel activation, on the survival of undifferentiated SH-SY5Y cells exposed to H ₂ O ₂ -induced oxidative stress.	85
Figure 3.17 The effect of GW542573X, an SK1 channel activator, in the presence of SK1-3 blocker, UCL1684, on the survival of undifferentiated SH-SY5Y cells exposed to H ₂ O ₂ -induced oxidative stress.	85
Figure 3.18 The effect of GW542573X, an SK1 channel activator, on the survival of differentiated SH-SY5Y cells exposed to H ₂ O ₂ -induced oxidative stress.	86
Figure 3.19 The effect of GW542573X, an SK1 channel activator, in the presence of SK1-3 channel blocker, UCL1684, on the survival of differentiated SH-SY5Y cells exposed to H ₂ O ₂ -induced oxidative stress.	86

Figure 3.20 The effect of CyPPA, SK3 channel activation, on the survival of undifferentiated SH-SY5Y cells exposed to H ₂ O ₂ -induced oxidative stress.	88
Figure 3.21 The effect of CyPPA, an SK2-3 channel activator, in the presence of the SK1-3 channel blocker, UCL1684, on the survival of undifferentiated SH-SY5Y cells exposed to H ₂ O ₂ -induced oxidative stress.	88
Figure 3.22 The effect of CyPPA, an SK2-3 channel activator, in the presence of SK1-3 channel blocker, NS8593, on the survival of undifferentiated SH-SY5Y cells exposed to H ₂ O ₂ -induced oxidative stress.	89
Figure 3.23 The effect of CyPPA, SK3 channel activation, on the survival of differentiated SH-SY5Y cells exposed to H ₂ O ₂ -induced oxidative stress.	90
Figure 3.24 The effect of CyPPA, an SK2-3 channel activator, in the presence of SK1-3 blocker, UCL1684, on the survival of differentiated SH-SY5Y cells exposed to H ₂ O ₂ -induced oxidative stress.	90
Figure 3.25 The effect of CyPPA, an SK2-3 channel activator, in the presence of SK1-3 channel blocker, NS8593, on the survival of differentiated SH-SY5Y cells exposed to H ₂ O ₂ -induced oxidative stress.	91
Figure 3.26 SK channel mRNA investigation in wild-type <i>Hdh^{+/+}</i> cells.	94
Figure 3.27 SK channel mRNA investigation in heterozygous mutant <i>Hdh^{Q111}/Hdh⁺</i> cells.	94
Figure 3.28 SK channel mRNA investigation in homozygous mutant <i>Hdh^{Q111}/Hdh^{Q111}</i> cells.	94
Figure 3.29 Representative immunoblot of SK2 channel subtype in heterozygous mutant <i>Hdh^{Q111}/Hdh⁺</i> cells.	95
Figure 3.30 Representative immunoblot of SK3 channel subtype in wild-type <i>Hdh^{+/+}</i> cells.	95

Figure 3.31 The effect of SK2-3 channel activator, CyPPA, on wild-type <i>Hdh^{+/Hdh⁺}</i> cell viability.	97
Figure 3.32 The effect of SK4 channel activator, NS309, on wild-type <i>Hdh^{+/Hdh⁺}</i> cell viability.	97
Figure 3.33 The effect of SK2-3 channel activator, CyPPA, on heterozygous mutant <i>Hdh^{Q111/Hdh⁺}</i> cell viability.	98
Figure 3.34 The effect of SK4 channel activator, NS309, on homozygous mutant <i>Hdh^{Q111/Hdh^{Q111}}</i> cell viability.	98
Figure 3.35 The effect of SK1-3 channel blocker, NS8593, on wild-type <i>Hdh^{+/Hdh⁺}</i> cell viability.	100
Figure 3.36 The effect of SK4 channel blocker, TRAM-34, on wild-type <i>Hdh^{+/Hdh⁺}</i> cell viability.	100
Figure 3.37 The effect of SK4 channel blocker, NS6180, on wild-type <i>Hdh^{+/Hdh⁺}</i> cell viability.	101
Figure 3.38 The effect of SK1-3 channel blocker, UCL1684, on heterozygous mutant <i>Hdh^{Q111/Hdh⁺}</i> cell viability.....	101
Figure 3.39 The effect of SK4 channel blocker, TRAM-34, on homozygous mutant <i>Hdh^{Q111/Hdh^{Q111}}</i> cell viability.	102
Figure 3.40 The effect of SK4 channel blocker, NS6180, on homozygous mutant <i>Hdh^{Q111/Hdh^{Q111}}</i> cell viability.	102
Figure 3.41 The effect of H ₂ O ₂ on wild-type <i>Hdh^{+/Hdh⁺}</i> cell viability.	104
Figure 3.42 The effect of H ₂ O ₂ on heterozygous mutant <i>Hdh^{Q111/Hdh⁺}</i> cell viability.	104
Figure 3.43 The effect of H ₂ O ₂ on homozygous mutant <i>Hdh^{Q111/Hdh^{Q111}}</i> cell viability.	105

Figure 3.44 The effect of CyPPA, SK2 channel activation, on the survival of heterozygous mutant <i>Hdh^{Q111}/Hdh⁺</i> cells exposed to H ₂ O ₂ -induced oxidative stress.....	107
Figure 3.45 The effect of CyPPA, an SK2-3 channel activator, in the presence of SK1-3 blocker, UCL1684, on the survival of heterozygous mutant <i>Hdh^{Q111}/Hdh⁺</i> cells exposed to H ₂ O ₂ -induced oxidative stress.	107
Figure 3.46 The effect of CyPPA, an SK2-3 channel activator, on the survival of wild-type <i>Hdh⁺/Hdh⁺</i> cells exposed to H ₂ O ₂ -induced oxidative stress.....	109
Figure 3.47 The effect of CyPPA, an SK2-3 channel activator, in the presence of SK1-3 blocker, NS8593, on the survival of wild-type <i>Hdh⁺/Hdh⁺</i> cells exposed to H ₂ O ₂ -induced oxidative stress.....	109
Figure 3.48 The effect of NS309, an SK4 channel activator, on the survival of wild-type <i>Hdh⁺/Hdh⁺</i> cells exposed to H ₂ O ₂ -induced oxidative stress.	111
Figure 3.49 The effect of NS309, an SK4 channel activator, in the presence of the SK4 channel blocker, TRAM-34, on the survival of wild-type <i>Hdh⁺/Hdh⁺</i> cells exposed to H ₂ O ₂ -induced oxidative stress.	111
Figure 3.50 The effect of NS309, an SK4 channel activator, in the presence of the SK4 channel blocker, NS6180, on the survival of wild-type <i>Hdh⁺/Hdh⁺</i> cells exposed to H ₂ O ₂ -induced oxidative stress.	112
Figure 3.51 The effect of NS309, SK4 channel activation, on the survival of homozygous mutant <i>Hdh^{Q111}/Hdh^{Q111}</i> cells exposed to H ₂ O ₂ -induced oxidative stress.....	113
Figure 3.52 The effect of NS309, an SK4 channel activator, in the presence of the SK4 channel blocker, TRAM-34, on the survival of homozygous mutant <i>Hdh^{Q111}/Hdh^{Q111}</i> cells exposed to H ₂ O ₂ -induced oxidative stress.	113

Figure 3.53 The effect of NS309, an SK4 channel activator, in the presence of the SK4 channel blocker, NS6180, on the survival of homozygous mutant <i>Hdh^{Q111}/Hdh^{Q111}</i> cells exposed to H ₂ O ₂ -induced oxidative stress.	114
Figure 3.54 The effect H ₂ O ₂ and/or SK3 or SK4 channel activation on Bcl-2 expression in mouse wild-type striatal cells, and human neuroblastoma and astrocytoma cells.....	117
Figure 4.1 SK and TRPM7 channel mRNA in homozygous mutant <i>Hdh^{Q111}/Hdh^{Q111}</i> cells.	141
Figure 4.2 Representative immunoblot of TRPM7 channel subtype in homozygous mutant <i>Hdh^{Q111}/Hdh^{Q111}</i> cells.	141
Figure 4.3 The effect of NS8593, TRPM7 channel inhibition, on homozygous mutant <i>Hdh^{Q111}/Hdh^{Q111}</i> cell viability.	143
Figure 4.4 The effect of UCL1684, TRPM7 channel inhibition, on homozygous mutant <i>Hdh^{Q111}/Hdh^{Q111}</i> cell viability.	143
Figure 4.5 The effect of CoCl ₂ on homozygous mutant <i>Hdh^{Q111}/Hdh^{Q111}</i> cell viability.	145
Figure 4.6 The effect of staurosporine on homozygous mutant <i>Hdh^{Q111}/Hdh^{Q111}</i> cell viability.	145
Figure 4.7 The effect of NS8593, TRPM7 channel inhibition, on the survival of homozygous mutant <i>Hdh^{Q111}/Hdh^{Q111}</i> cells exposed to H ₂ O ₂ -induced oxidative stress.....	147
Figure 4.8 The effect of UCL1684, TRPM7 channel inhibition, on the survival of homozygous mutant <i>Hdh^{Q111}/Hdh^{Q111}</i> cells exposed to H ₂ O ₂ -induced oxidative stress.....	147

Figure 4.9 The effect of NS8593, TRPM7 channel inhibition, on the survival of homozygous mutant <i>Hdh^{Q111}/Hdh^{Q111}</i> cells exposed to CoCl ₂ -induced hypoxia.	148
Figure 4.10 The effect of UCL1684, TRPM7 channel inhibition, on the survival of homozygous mutant <i>Hdh^{Q111}/Hdh^{Q111}</i> cells exposed to CoCl ₂ -induced hypoxia.	148
Figure 4.11 The effect of NS8593, TRPM7 channel inhibition, on the survival of homozygous mutant <i>Hdh^{Q111}/Hdh^{Q111}</i> cells exposed to staurosporine-induced apoptosis.....	149
Figure 4.12 The effect of UCL1684, TRPM7 channel inhibition, on the survival of homozygous mutant <i>Hdh^{Q111}/Hdh^{Q111}</i> cells exposed to staurosporine-induced apoptosis.....	149
Figure 4.13 Representative immunoblot of TRPM7 channel in homozygous mutant <i>Hdh^{Q111}/Hdh^{Q111}</i> cells transfected with specific TRPM7-siRNA.....	151
Figure 4.14 Densitometric measurement of TRPM7 channel in homozygous mutant <i>Hdh^{Q111}/Hdh^{Q111}</i> cells transfected with specific TRPM7-siRNA.....	151
Figure 4.15 The effect of siRNA-mediated knockdown of TRPM7 channel on the survival of homozygous mutant <i>Hdh^{Q111}/Hdh^{Q111}</i> cells exposed to H ₂ O ₂ -induced oxidative stress.....	152
Figure 4.16 The effect of siRNA-mediated knockdown of TRPM7 channel on the survival of homozygous mutant <i>Hdh^{Q111}/Hdh^{Q111}</i> cells exposed to CoCl ₂ -induced hypoxia.....	152
Figure 4.17 The effect of siRNA-mediated knockdown of TRPM7 channel on the survival of homozygous mutant <i>Hdh^{Q111}/Hdh^{Q111}</i> cells exposed to staurosporine-induced apoptosis.	153
Figure 4.18 SK channel mRNA investigation in MOG-G-UVW cells.....	155
Figure 4.19 TRPM7 channel mRNA investigation in MOG-G-UVW cells.	155

Figure 4.20 Representative immunoblot of TRPM7 channel subtype in MOG-G-UVW cells.	155
Figure 4.21 The effect of NS8593, TRPM7 channel inhibition, on MOG-G-UVW cell viability.	157
Figure 4.22 The effect of UCL1684, TRPM7 channel inhibition, on MOG-G-UVW cell viability.	157
Figure 4.23 The effect of H ₂ O ₂ on MOG-G-UVW cell viability.	159
Figure 4.24 The effect of CoCl ₂ on MOG-G-UVW cell viability.	159
Figure 4.25 The effect of staurosporine on MOG-G-UVW cell viability.	160
Figure 4.26 The effect of NS8593, TRPM7 channel inhibition, on the survival of MOG-G-UVW cells exposed to H ₂ O ₂ -induced oxidative stress.	162
Figure 4.27 The effect of UCL1684, TRPM7 channel inhibition, on the survival of MOG-G-UVW cells exposed to H ₂ O ₂ -induced oxidative stress.	162
Figure 4.28 The effect of NS8593, TRPM7 channel inhibition, on the survival of MOG-G-UVW cells exposed to CoCl ₂ -induced hypoxia.	163
Figure 4.29 The effect of UCL1684, TRPM7 channel inhibition, on the survival of MOG-G-UVW cells exposed to CoCl ₂ -induced hypoxia.	163
Figure 4.30 The effect of NS8593, TRPM7 channel inhibition, on the survival of MOG-G-UVW cells exposed to staurosporine-induced apoptosis.	164
Figure 4.31 The effect of UCL1684, TRPM7 channel inhibition, on the survival of MOG-G-UVW cells exposed to staurosporine-induced apoptosis.	164
Figure 4.32 Representative immunoblot of TRPM7 channel in MOG-G-UVW cells transfected with specific TRPM7-siRNA.	166
Figure 4.33 Densitometric measurement of TRPM7 channel in MOG-G-UVW cells transfected with specific TRPM7-siRNA.	166

Figure 4.34 The effect of siRNA-mediated knockdown of TRPM7 channel on the survival of MOG-G-UVW cells exposed to H ₂ O ₂ -induced oxidative stress.....	167
Figure 4.35 The effect of siRNA-mediated knockdown of TRPM7 channel on the survival of MOG-G-UVW cells exposed to CoCl ₂ -induced hypoxia.....	167
Figure 4.36 The effect of siRNA-mediated knockdown of TRPM7 channel on the survival of MOG-G-UVW cells exposed to staurosporine-induced apoptosis.	168
Figure 4.37 TRPM7 channel blocking by the SK channel modulators.	172
Figure 5.1 SK channel mRNA investigation in wild-type MCF-7 cells.....	187
Figure 5.2 SK channel mRNA investigation in endocrine resistant TamR cells.	187
Figure 5.3 SK channel mRNA investigation in endocrine resistant FasR cells. .	187
Figure 5.4 Microarray analysis of SK channel transcripts in the MCF-7 cell lineage.....	188
Figure 5.5 Immunoblot of SK2 channel subtype in the MCF-7 cell lineage.	189
Figure 5.6 Representative immunoblot of SK2 channel in wild-type MCF-7 cells transfected with specific SK2-siRNA.	191
Figure 5.7 Densitometric measurement of SK2-long isoform (SK2-L) channel in wild-type MCF-7 cells transfected with specific SK2-siRNA.	191
Figure 5.8 The effect of siRNA-mediated knockdown of the SK2 channel on MCF-7 cell viability.	192
Figure 5.9 Representative immunoblot of anti-apoptotic Bcl-2 protein in wild-type MCF-7 cells transfected with specific SK2-siRNA.	194
Figure 5.10 Densitometric measurement of anti-apoptotic Bcl-2 protein in wild-type MCF-7 cells transfected with specific SK2-siRNA.	194
Figure 5.11 Representative immunoblot of pro-apoptotic caspase-7 protein in wild-type MCF-7 cells transfected with specific SK2-siRNA.	195

Figure 5.12 Densitometric measurement of full length (FL) pro-apoptotic caspase-7 protein in wild-type MCF-7 cells transfected with specific SK2-siRNA.	195
Figure 5.13 The effect of SK1-3 channel blocker, UCL1684, and SK4 channel blocker, NS6180, on MCF7 cell viability.	197
Figure 5.14 The effect of SK2-3 activator, CyPPA, on MCF-7 cell viability.....	197
Figure 5.15 The effect of SK1-3 channel blocker, UCL1684, on TamR cell viability.	198
Figure 5.16 The effect of SK1-3 channel blocker, UCL1684, on FasR cell viability.	198
Figure 5.17 SK channel mRNA investigation in wild-type BT-474 cells.	199
Figure 5.18 Representative immunoblot of SK2 channel in wild-type BT-474 cells transfected with specific SK2-siRNA.	201
Figure 5.19 Densitometric measurement of SK2-long (SK2-L) isoform channel in wild-type BT-474 cells transfected with specific SK2-siRNA.	201
Figure 5.20 The effect of siRNA-mediated knockdown of SK2 channel on BT-474 cell viability.	202
Figure 5.21 Representative immunoblot of anti-apoptotic Bcl-2 protein in wild-type BT-474 cells transfected with specific SK2-siRNA.	204
Figure 5.22 Densitometric measurement of anti-apoptotic Bcl-2 protein in wild-type BT-474 cells transfected with specific SK2-siRNA.....	204
Figure 5.23 Representative immunoblot of pro-apoptotic caspase-7 protein in wild-type BT-474 cells transfected with specific SK2-siRNA.....	205
Figure 5.24 Densitometric measurement of full length (FL) pro-apoptotic caspase-7 protein in wild-type BT-474 cells transfected with specific SK2-siRNA.....	205

Figure 5.25 The effect of SK1-3 channel blocker, UCL1684, on BT-474 cell viability.	207
Figure 5.26 The effect of SK2-3 activator, CyPPA, on BT-474 cell viability.	207
Figure 5.27 SK channel mRNA investigation in wild-type MDA-MB-231 cells. ...	208
Figure 5.28 Representative immunoblot of SK3 channel in wild-type MDA-MB-231 cells transfected with specific SK3-siRNA.	210
Figure 5.29 Densitometric measurement of SK3 channel in wild-type MDA-MB-231 cells transfected with specific SK3-siRNA.	210
Figure 5.30 The effect of siRNA-mediated knockdown of SK3 channel on MDA-MB-231 cell viability.....	211
Figure 5.31 Representative immunoblot of anti-apoptotic Bcl-2 protein in wild-type MDA-MB-231 cells transfected with specific SK3-siRNA.	213
Figure 5.32 Densitometric measurement of anti-apoptotic Bcl-2 protein in wild-type MDA-MB-231 cells transfected with specific SK3-siRNA.....	213
Figure 5.33 Representative immunoblot of pro-apoptotic caspase-7 protein in wild-type MDA-MB-231 cells transfected with specific SK3-siRNA.....	214
Figure 5.34 Densitometric measurement of full length (FL) pro-apoptotic caspase-7 protein in wild-type MDA-MB-231 cells transfected with specific SK3-siRNA..	214
Figure 5.35 The effect of SK1-3 channel blocker, UCL1684, on MDA-MB-231 cell viability.	216
Figure 5.36 The effect of SK1-3 channel blocker, NS8593, on MDA-MB-231 cell viability.	216
Figure 5.37 The effect of the SK2-3 activator, CyPPA, on MDA-MB-231 cell viability.	217

List of tables

Table 1.1	Pharmacology of SK ion channel modulators	10
Table 2.1	The passage numbers of the cells used in this study	45
Table 3.1	Primer sequences for human SK channel transcripts and positive control in the human cell types.	69
Table 3.2	Primer sequences for mouse SK channel transcripts and positive control in the mouse cell types.	69
Table 4.1	Primer sequences for human SK channel transcripts and positive control in the human cell type.	135
Table 4.2	Primer sequences for mouse SK channel transcripts and positive control in the mouse cell type.	136
Table 4.3	Primer sequences for human and mouse TRPM7 channel transcript and positive control in the human and mouse cell types.	136
Table 5.1	Biological features of breast cancer cell lines.	181
Table 5.2	Primer sequences for both human SK channel transcripts and the positive control in the human cell lines.	182

Table of Contents

1	Chapter One: General Introduction.....	1
1.1	Neurodegeneration and cancer.....	1
1.2	Ion channels.....	1
1.3	Potassium (K ⁺) ion channels.....	2
1.3.1	Overview.....	2
1.3.2	Introduction.....	2
1.3.3	Classification of K ⁺ ion channels.....	3
1.3.4	SK potassium ion channels.....	3
1.3.4.1	Cloning, structure, and diversity.....	4
1.3.4.2	Gating of SK channels.....	6
1.3.4.3	Calcium (Ca ²⁺) sources for SK channel activation.....	7
1.3.4.4	SK channel pharmacology.....	8
1.3.4.5	SK channel and intrinsic excitability.....	13
1.4	TRP ion channels.....	15
1.4.1	Overview.....	15
1.4.2	Classification of TRP ion channels.....	15
1.4.3	Cloning, structure and diversity.....	17
1.4.4	Gating of TRP channels.....	20
1.4.5	TRPM7 biological features.....	21
1.4.6	TRPM7 channel pharmacology.....	23
1.5	Cell death mechanisms.....	24
1.6	Cellular Ca ²⁺ in pathophysiology.....	29

1.7	Cell models	34
1.7.1	CNS cell lines	34
1.7.1.1	SH-SY5Y cell model.....	34
1.7.1.2	STH <i>dh</i> cell model.....	35
1.7.1.3	BV-2 cell model	36
1.7.1.4	MOG-G-UVW cell model.....	36
1.7.2	Breast cancer and non-tumorigenic cell lines	37
1.7.2.1	Wild-type breast cancer cell models.....	37
1.7.2.2	Endocrine resistance cell models.....	38
1.7.2.3	Non-tumorigenic epithelial cell model.....	38
1.8	General hypothesis and aims.....	40
2	Chapter Two: General Methods and Materials	41
2.1	Cell lines.....	41
2.2	Culture conditions	42
2.3	Preparation of primary culture and subculturing	43
2.4	Gene expression assessment	46
2.4.1	Qualitative gene expression assessment	46
2.4.1.1	Primer design	46
2.4.1.2	RNA extraction	46
2.4.1.3	RNA precipitation	46
2.4.1.4	DNase treatment.....	47
2.4.1.5	RNA quantification	47
2.4.1.6	Reverse transcription	47

2.4.1.7	Polymerase chain reaction	48
2.4.1.8	Electrophoresis	48
2.4.2	Quantitative gene expression assessment	49
2.5	Protein blotting	51
2.5.1	Protein extraction	51
2.5.2	Protein quantification	51
2.5.3	Polyacrylamide Gel Electrophoresis (PAGE)	52
2.5.4	Western blotting	53
2.6	MTS preparation	55
2.7	Pharmacological modulation	55
2.7.1	Plate preparation	55
2.7.2	MTS cell proliferation assays	56
2.8	Gene silencing	57
2.8.1	Design, source and storage	57
2.8.2	Plate preparation	57
2.8.3	Transfection	58
2.9	Cell storage	59
2.10	Preparation of chemicals	59
2.11	Densitometric analysis	60
2.12	Data analysis	61
3	Chapter Three: SK Ion Channel in Survival of Neurons and brain astrocytes	62
3.1	Introduction	62
3.2	Hypothesis and aims	65

3.3	Materials and methods	67
3.3.1	Cell origins and features	67
3.3.2	Polymerase chain reaction	68
3.3.3	Western blotting.....	70
3.3.4	SK channel pharmacology	71
3.4	Results	72
3.4.1	SK ion channel expression and modulation in human neuroblastoma SH-SY5Y cells	72
3.4.1.1	SK channel mRNA and protein investigation in human neuroblastoma SH-SY5Y cells	72
3.4.1.2	Neuroblastoma SH-SY5Y cell differentiation.....	75
3.4.1.3	The effect of SK channel modulators alone on human neuroblastoma SH-SY5Y cell viability	76
3.4.1.4	The effect of SK channel blockers alone on SH-SY5Y cell viability 79	
3.4.1.5	The dose-response curve for hydrogen peroxide in human neuroblastoma SH-SY5Y cells	82
3.4.1.6	Pharmacological modulation of SK1 and SK3 channels in human neuroblastoma SH-SY5Y cells	84
3.4.2	SK ion channel expression and modulation in mouse model of Huntington's (<i>STHdh</i>) striatal cells.....	92
3.4.2.1	SK channel mRNA and protein investigation in mouse <i>STHdh</i> striatal cells.....	92

3.4.2.2	The effect of SK channel modulators alone on mouse <i>STHdh</i> striatal cells.....	96
3.4.2.3	The dose-response curve for hydrogen peroxide in mouse <i>STHdh</i> striatal cells.....	103
3.4.2.4	Pharmacological modulation of SK channels in mouse <i>STHdh</i> striatal cells.....	106
3.4.3	SK ion channel expression and modulation in human brain astrocytoma cells	115
3.4.4	The effect of H ₂ O ₂ and/or SK3-4 channel activation on Bcl-2 expression in wild-type mouse striatal, human neuroblastoma, and astrocytoma cells	116
3.5	Discussion.....	118
3.6	Conclusions.....	128
3.7	Recommendations and future work.....	129
4	Chapter Four: TRPM7 Ion Channel in Survival of Astrocytes and Neurons.	130
4.1	Introduction	130
4.2	Hypothesis and aims	133
4.3	Materials and methods.....	134
4.3.1	Cell origins and features	134
4.3.2	Polymerase chain reaction	134
4.3.3	Small interference RNA	137
4.3.4	Western blotting.....	138
4.3.5	TRPM7 channel pharmacology.....	139
4.4	Results	140

4.4.1	TRPM7 ion channel expression in mouse model of Huntington's homozygous <i>STHdh^{Q111}/Hdh^{Q111}</i> cells	140
4.4.1.1	TRPM7 channel mRNA and protein investigation in <i>STHdh^{Q111}/Hdh^{Q111}</i> cells	140
4.4.1.2	The effect of pharmacological TRPM7 channel inhibition on <i>STHdh^{Q111}/Hdh^{Q111}</i> cell viability	142
4.4.1.3	The dose-response curve for cellular insults in <i>STHdh^{Q111}/Hdh^{Q111}</i> cells	144
4.4.1.4	Pharmacological inhibition of TRPM7 channel against striatal cell insults in <i>STHdh^{Q111}/Hdh^{Q111}</i> cells	146
4.4.1.5	Small interference RNA-mediated modulation of TRPM7 channel against cellular insults in <i>STHdh^{Q111}/Hdh^{Q111}</i> cells.....	150
4.4.2	TRPM7 ion channel expression in human astrocytoma MOG-G-UVW cells	154
4.4.2.1	TRPM7 channel mRNA and protein investigation in MOG-G-UVW cells	154
4.4.2.2	The effect of pharmacological TRPM7 channel inhibition on MOG-G-UVW cell viability	156
4.4.2.3	The dose-response curve for cellular insults in MOG-G-UVW cells	158
4.4.2.4	Pharmacological inhibition of TRPM7 channel against cellular insults in MOG-G-UVW cells	161
4.4.2.5	Small interference RNA-mediated modulation of TRPM7 channel against cellular insults in MOG-G-UVW cells.....	165

4.5	Discussion.....	169
4.6	Conclusions.....	175
4.7	Recommendations and future work.....	176
5	Chapter Five: SK Ion Channel in Death of Breast Cancer Cells	177
5.1	Introduction	177
5.2	Hypothesis and aims	180
5.3	Materials and methods	181
5.3.1	Cell origins and features	181
5.3.2	Polymerase chain reaction	181
5.3.3	Small interference RNA	183
5.3.4	Western blotting.....	184
5.3.5	SK channel pharmacology.....	185
5.4	Results	186
5.4.1	SK channel expression and modulation in wild-type and endocrine resistant MCF-7 cells	186
5.4.1.1	SK channel mRNA investigation and analysis.....	186
5.4.1.2	SK2 channel protein expression in wild-type MCF-7 cells.....	189
5.4.1.3	siRNA-mediated modulation of SK2 channel in MCF-7 cells....	190
5.4.1.4	The effect of siRNA-mediated knockdown of SK2 channel on apoptosis in MCF-7 cells	193
5.4.1.5	Pharmacological modulation of SK2 channel in the MCF-7 lineage	196
5.4.2	SK channel expression and modulation in BT-474 cells	199

5.4.2.1	SK channel mRNA investigation	199
5.4.2.2	SK2 channel protein expression and siRNA-mediated modulation of SK2 channel in BT-474 cells.....	200
5.4.2.3	The effect of siRNA-mediated knockdown of SK2 channel on apoptosis in BT-474 cells	203
5.4.2.4	Pharmacological modulation of SK2 channel in BT-474 cells ..	206
5.4.3	SK channel expression and modulation in MDA-MB-231 cells	208
5.4.3.1	SK channel mRNA investigation	208
5.4.3.2	SK3 channel protein expression and siRNA-mediated modulation of SK3 channel in MDA-MB-231 cells.....	209
5.4.3.3	The effect of siRNA-mediated knockdown of SK3 channel on apoptosis in MDA-MB-231 cells.....	212
5.4.3.4	Pharmacological modulation of SK3 channel in MDA-MB-231 cells	215
5.5	Discussion.....	218
5.6	Conclusions.....	225
5.7	Recommendations and future work.....	226
6	Chapter Six General Discussion	227
6.1	The major findings of this study:.....	227
6.2	SK channel role in cell survival.....	229
6.3	TRPM7 channel role in CNS cell survival.....	233
7	Appendix.....	239
8	References	251

1 Chapter One: General Introduction

1.1 Neurodegeneration and cancer

Neuronal degeneration or abnormal cell growth are related cell life or death-related cases which under an umbrella range of circumstances can affect cell survival and cell growth. In neuronal loss, several factors are touted as drivers in the progression of neurodegenerative diseases, for example β -amyloid (Glennner and Wong 1984) which impacts in Alzheimer's pathology, while α -synuclein (Polymeropoulos *et al.* 1997) accumulation results in Parkinson's disease (Bredesen *et al.* 2006; Guo *et al.* 2013). In abnormal cell gain "cancer", this ocean of diseases is characterised by uncontrolled cell acquisition where loss of apoptosis is an accepted feature (Brown and Attardi 2005). These pathological states are more prevalent in recent decades. It has been reported, for example, that about 44 million people in the world experience dementia to date (Alzheimer's disease international statistics, 2015). Also, the American Cancer Society has reported that nearly 1.6 million recent cases were diagnosed in 2013 (Litan and Langhans 2015). Indeed this condition is the chief cause of death nowadays worldwide. However, meaningful any progress has been made accepting underlying mechanisms of these pathological actions, there is yet no favourable outcome in the clinic.

1.2 Ion channels

Ion channels in membranes have attracted considerable attention: they have been intensively studied over many years with the production of some beautiful data and the resulting field has generated several Nobel prizes (Hodgkin and Huxley 1952; MacKinnon 2004). They have a well-defined role in excitable cells. However they also exist in many varieties of non-excitable cells where they clearly hold a non-

classical role, for example in guiding proliferation, differentiation or survival of cells (Pardo and Stuhmer 2014). More recently attention has turned to this non-classical role in excitable cells also (Dolga *et al.* 2013). The big questions are: which classes of ion channels, if any, are most relevant in this respect? Also how precisely do they achieve these tasks to modulate cellular function? Is it for example solely through their capacity to translocate ions? Just how this new role is achieved is however unclear.

1.3 Potassium (K⁺) ion channels

1.3.1 Overview

There is now a substantial body of data to support the view that particularly in the case of potassium (K⁺) channels, a very diverse family of proteins, with varying amino acid sequences and topologies, they can modify diverse cellular functions (Dolga and Culmsee 2012). Over the past few decades, numerous studies have established that plasma membrane ion translocation is involved in cellular electrogenesis and electrical excitability. In addition, a number of researchers have shown the contribution of ion channels to basic cellular processes including tissue homeostasis (Lang *et al.* 2005; Razik and Cidlowski 2002; Schonherr 2005). Further studies suggest that not only cellular but also subcellular membranes play a pivotal role, for instance, in the initiation and progression of cell death gates, such as through Kca (SK) channels (Dolga *et al.* 2014).

1.3.2 Introduction

Potassium channels are K⁺ carrying proteins and form the largest family amongst ion channels, which are widely expressed in cells including both excitable and non-excitable cells and may trigger various physiological functions. Upon activation, K⁺

channels lower membrane excitability due to hyperpolarisation (Yuan and Chen 2006). In neurons, it is known that K^+ channels are differentially expressed at different cellular and subcellular sites and serve multiple tasks (Lujan 2010). Their role in non-excitable cells is perhaps less clear, but may be concerned here with growth.

1.3.3 Classification of K^+ ion channels

Currently, five major ion classes of this type have been identified in cells: voltage-gated (K_v) class, Ca^{2+} -activated K^+ (K_{ca} or SK) channels, ATP-sensitive (K_{ATP}) channels, inwardly rectifying K^+ (K_{IR}) channels, and two-pore domain K^+ (K_{2P}) channels (Yuan and Chen 2006).

1.3.4 SK potassium ion channels

SK channels are intermediate, termed SK4 or IK channels, and small conductance (SK1-3) Ca^{2+} -activated potassium channels, which are largely found throughout the central nervous system (CNS), as well as in glial cells. SK channels were described originally in red blood cells, more than 50 years ago, suggesting that these channels are involved in hyperpolarisation (Gardos 1958). In neurons, the SK currents were first identified in the mollusc (Meech 1972), followed by cat spinal motor neurons (Krnjevic and Lisiewicz 1972). In the 1980s, it was shown in the mammalian hippocampus that SK currents lead to afterhyperpolarisations (AHP)(Alger and Nicoll 1980). Further studies have shown that Ca^{2+} activated K^+ channels directly contribute to various respects of electrolyte transport, for instance osmolarity regulation (Marty 1989).

In SK channel classification, electrophysiological experiments have confirmed three forms of Ca^{2+} -activated potassium channels, based on biophysical, molecular and

pharmacological properties, which differentially respond to elevations in cytosolic Ca^{2+} . Firstly, the big-conductance K^+ channels (BK) have a single-channel conductance of 100-200 pS and are voltage-dependent, whereas small-conductance Ca^{2+} -activated K^+ channels (SK1-3) with conductances of 10-20 pS, are less voltage but more Ca^{2+} dependent. Last, the intermediate-conductance Ca^{2+} -activated K^+ channels (SK4) have a single-channel conductance of about 46 pS: these are similar to SK channels in aspects of structure, and function, being part of the same gene family, and are strictly Ca^{2+} dependent (Adelman *et al.* 2012; Blatz and Magleby 1986; Dutta *et al.* 2009; Syme *et al.* 2000). It is becoming increasingly difficult to overlook the role of SK channels in ionic signalling pathways, and based on current knowledge SK channels may be proposed as therapeutic targets.

1.3.4.1 Cloning, structure, and diversity

Nowadays, the International Union of Pharmacology has placed SK and IK channels in one gene family, the KCNN gene, which includes $\text{Kca}_{2.1}$, $\text{Kca}_{2.2}$, $\text{Kca}_{2.3}$ (SK1, SK2, and SK3 respectively) and $\text{Kca}_{3.1}$ (SK4) channels (Wei *et al.* 2005). SK channels are structurally homomeric tetramers (Figure 1.1) and are highly homologous, consisting of four subunits (Kohler *et al.* 1996). The SK1, SK2, SK3 mRNAs are expressed in central neurons (Stocker and Pedarzani 2000), whereas the SK4 subtype is absent (Adelman *et al.* 2012). In 1996, the Adelman laboratory first cloned SK1, SK2, SK3 channels from mammalian brain, and the SK4 subtype was then cloned from Chinese hamster ovary cells (Joiner *et al.* 1997).

In the context of the coding region, the $\text{Kca}_{2.1}$ gene has nine exons, while $\text{Kca}_{2.2}$ and $\text{Kca}_{2.3}$ have eight exons (Stocker 2004). These channels are composed of six serpentine transmembrane (S1-S6) domains, and cytosolic N- and C- termini, sharing this with voltage-gated K^+ channels. In the Kv channels, the fourth segment

is decorated with seven positively charged amino acids, which are thought to be located on the face of the α -helix and act as a voltage sensor (Bezanilla 2000; Catterall 2010), whereas there are only three positively charged residues in the SK channels (Li and Aldrich 2011). The transmembrane pore in SK channels (like other K^+ channels) contains the K^+ selective signature sequence, and is located between S5 and S6. Despite numerous attempts have been made by researchers, the splicing mechanism is not fully understood (Adelman et al. 2012).

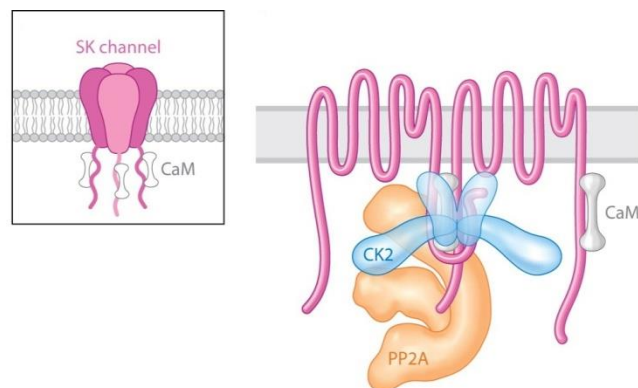


Figure 1.1 The structure of SK ion channels (Adelman et al. 2012).

1.3.4.2 Gating of SK channels

The SK1-4 channels show much less voltage-dependence than BK channels: alternatively Ca^{2+} gates the SK1-4 channels and is indeed essential in the gating mechanism (Keen *et al.* 1999). Such molecules are multiprotein complex channels and are constitutively associated with calmodulin (CaM), casein kinase 2 (CK2), and protein phosphatase 2A (PP2A) (Adelman *et al.* 2012). Calmodulin, as a Ca^{2+} sensor, is abundantly present in eukaryotic cells. Upon stimulation, CaM may initiate numerous cellular signalling pathways, most importantly, calmodulin can act through conformational changes, thus binding with other proteins, ultimately influencing diverse cellular functions, including ion channel modulation, synaptic transmission, plasticity, enzymatic activity, as well as gene expression (Zhang *et al.* 2012). Notably, calmodulin is composed of two globular domains, the C- and N-lobe, which are separated by a flexible central linker. Each CaM lobe presents two EF hand sites that may be involved in Ca^{2+} binding. The C-lobe and the central linker of CaM serve mainly as the linkage part between the SK channels and CaM. In this complex, the N-lobe can bind Ca^{2+} , thereby gating SK channels (Li *et al.* 2009). Furthermore, the CK2 and PP2A, which allosterically modulate SK channels, are known to be largely expressed in the brain, particularly in neuronal soma and dendrites (Allen *et al.* 2007).

The pore-forming subunits alone do not generate a fully functional channel, due to the lack of the Ca^{2+} -binding domain, which must therefore be associated constitutively with calmodulin. This can be regulated by protein kinase and phosphatase interactions. In fact, SK channels are modulated by two particular types of gating apparatus i.e. two constitutive components. In this paradigm, SK channels can be directly modulated by intracellular Ca^{2+} ions via CaM (Maylie *et al.*

2004), and are also gated by a Ca^{2+} -independent mechanism this being dependent on protein kinase and phosphatase interactions. More recently, it has been reported that CaM itself “belongs” to SK channel intrinsically (Adelman 2015).

Generally, calmodulin can directly initiate Ca^{2+} gating, thereby activating SK channels. On the other hand, the phosphorylation of CK2 on SK-associated CAM is associated with a decrease in the SK channel activity (Allen et al. 2007). On detailed inspection, the CaM binds to a highly conserved CaM-binding domain, and each channel subunit is thought to bind one CaM. During channel opening, the Ca^{2+} ions can bind to the N-lobe EF hands of CaM, and the bound CaM is then induced to bind with a neighbouring CaM, to generate dimerization, which may lead to conformational changes through a rotary force to the pore (Bruening-Wright *et al.* 2002). Importantly, CaM can be phosphorylated by casein kinase 2 and that may lead to a decrease in Ca^{2+} sensitivity of SK channels: in contrast protein phosphatase 2A acting on open SK channels counterbalances CK2 effects and results in an increase in Ca^{2+} sensitivity of the SK channels (Allen et al. 2007).

Although little is known about the precise gating mechanism for SK channels, the mechanism above is part of the story although a key fundamental question in this process is under what physiological condition the Ca^{2+} sensitivity of SK channels can be modified by CK2 and PP2A.

1.3.4.3 Calcium (Ca^{2+}) sources for SK channel activation

The SK channel is modulated through intracellular Ca^{2+} changes being elicited by Ca^{2+} from different sources (Xia *et al.* 1998). Obviously, SK channels are more reactive to activation by Ca^{2+} ions near the channel, so the location and sources of Ca^{2+} are influential (Adelman et al. 2012; Hirschberg *et al.* 1998). Within neurons, Ca^{2+} can be provided by either Ca^{2+} influx through voltage-gated Ca^{2+} channels,

Ca²⁺ entry via Ca²⁺-permeable ligand-gated ion channels, for instance NMDA receptors (Oliver *et al.* 2000), and released Ca²⁺ from intracellular origins i.e. cellular organelles based on inositol trisphosphate generation via G protein-coupled receptors and Ca²⁺-induced Ca²⁺ release, or both (Nahorski 1988).

1.3.4.4 SK channel pharmacology

In functional studies, it was shown that rat or mouse SK2 and SK3, and human SK1 expression are functional and homologous plasma membrane channels (Hosseini *et al.* 2001; Monaghan *et al.* 2004). Conversely, expression of rat or mouse SK1 failed to form functional channels, which may interact with the SK2 channel subtype (Benton *et al.* 2003). Although SK channels are highly similar in respect of structure, function and Ca²⁺-gating mechanism (Catacuzzeno *et al.* 2012), they have different biophysical and pharmacological properties.

Early studies showed that SK1, SK2 and SK3 channel subtypes can be differentially inhibited by apamin, which is a potent neurotoxin isolated from bee venom (Habermann 1984). The rat SK2 exhibits most sensitivity, the rat SK3 shows an intermediate sensitivity, whereas the hSK1 is less sensitive to the toxin, with IC₅₀ values of 27 pM, 4 nM, and 196 nM respectively (Grunnet *et al.* 2001). In apamin binding assays, three different binding sites have been suggested. A first study revealed that two amino acids on sides of deep pore can confer apamin sensitivity (Ishii *et al.* 1997). Further study has indicated that one amino acid, which is located between S3 and S4 transmembrane domains, is responsible for this sensitivity (Nolting *et al.* 2007). Interestingly, recent work suggests that the effect of apamin depends on an allosteric mechanism rather than classically occluding the pore (Lamy *et al.* 2010). Contrary to the small conductance SK subtypes, the IK subtype

possesses most sensitivity to maurotoxin isolated from scorpion venom, with an IC_{50} of 1 nM (Castle *et al.* 2003), the toxin binding to the channel pore vestibule via tyrosine-32 (Visan *et al.* 2004).

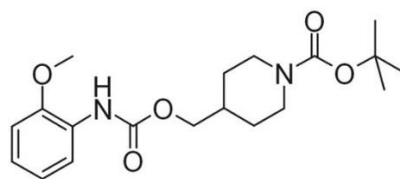
In addition to peptide toxins, organic compounds have been found to block SK channels. For example, d-Tubocurarine, UCL1684, UCL1848, TRAM-34, and NS8593 differentially inhibit SK members (Pedarzani and Stocker 2008), and most recently another SK4 channel blocker (UCL6180) has been generated (Strobaek *et al.* 2013), which is more potent than TRAM-34 on SK4: these interact with threonine250 and valine275 at S5-P-S6 regions (Strobaek *et al.* 2013; Wulff *et al.* 2001). Currently, several positive modifiers are available to probe SK channel molecules. Among these activators, EBIO was first identified in colonic epithelial cells, thereby activating basolateral IK (SK4) channels to enhance secretion. Many efforts then have been made by researchers to increase its potency and selectivity, subsequently introducing DC-EBIO (Singh *et al.* 2001) and later the NS309 compound (Strobaek *et al.* 2004), which is four times more potent on the SK4 channel subtype. Two recent SK1-3 channel activators are now available. The first SK-subtype selective activator (GW542573X) was more selective on the SK1 channel than SK2 and SK3, this compound possibly interacting with serine293 on the deep pore gating region of SK channel protein (Hougaard *et al.* 2009). The second SK-subtype selective opener (CyPPA) exhibits more selectivity for SK2 and SK3 channel subtypes in the order SK3 > SK2 >> SK1, but its pharmacological profile at SK1 is not well documented.

SK channels can currently be modulated by a wide variety of modifiers based on their biophysical and pharmacological characteristics, and applying highly specific

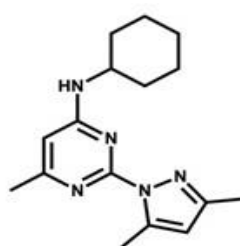
subtype blockers or activators is vital to distinguish and assess the functional role for each SK subtype.

Modulators	Selectivity	EC₅₀	IC₅₀
Activators			
GW542573X	SK1	8.2 μ M	
CyPPA	SK2 and SK3	5.6 and 14 μ M	
NS309	SK4	~30 nM	
Blockers			
UCL1684	SK1, 2 and 3		0.76, 0.36 and 9.5 nM
NS8593	SK1, 2 and 3		0.42, 0.60 and 0.73 μ M
TRAM-34	SK4		55 nM
NS6180	SK4		9 nM

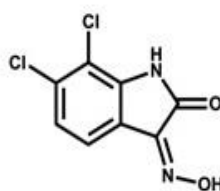
Table 1.1 Pharmacology of SK ion channel modulators. EC₅₀ and IC₅₀ values are shown for each SK channel subtype (Fanger *et al.* 2001; Fioretti *et al.* 2006; Hougaard *et al.* 2007; Hougaard *et al.* 2009; Strobaek *et al.* 2013; Strobaek *et al.* 2006; Strobaek *et al.* 2004).

**GW542573X**

4-[[[(2-Methoxyphenyl)amino]carbonyl]oxy]methyl]-piperidinecarboxylic acid-1,1-dimethylethyl ester

a**CyPPA**

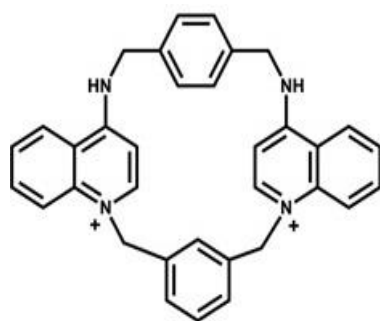
N-Cyclohexyl-*N*-[2-(3,5-dimethyl-pyrazol-1-yl)-6-methyl-4-pyrimidinamine

b**NS309**

6,7-Dichloro-1*H*-indole-2,3-dione 3-oxime

c

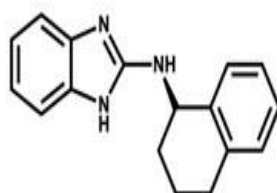
Figure 1.2 Chemical structures of the SK channel activators. a) SK1 channel activator b) SK2-3 channel activator c) SK4 channel activator (Hougaard et al. 2009; Wulff and Kohler 2013).



a

UCL 1684

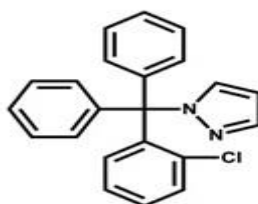
6,12,19,20,25,26-Hexahydro-5,27:13,18:21,24-trietheno-11,7-metheno-7*H*-dibenzo [*b,n*] [1,5,12,16]tetraazacyclotricosine-5,13-dium dibromide



b

NS8593

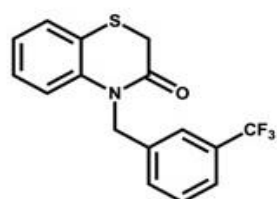
N-[(1*R*)-1,2,3,4-Tetrahydro-1-naphthalenyl]-1*H*-benzimidazol-2-amine hydrochloride



c

TRAM-34

1-[(2-Chlorophenyl)diphenylmethyl]-1*H*-pyrazole



d

NS6180

4-[[3-(Trifluoromethyl)phenyl]methyl]-2*H*-1,4-benzothiazin-3(4*H*)-one

Figure 1.3 Chemical structures of SK channel inhibitors. a) SK1-3 channel blocker b) SK1-3 channel blocker c) SK4 channel blocker d) SK4 channel blocker (Wulff and Kohler 2013).

1.3.4.5 SK channel and intrinsic excitability

SK channels couple intracellular Ca^{2+} transients and cellular membrane potential. Rises in cytosolic Ca^{2+} leads to activation of SK channels and enhances K^+ ion exit, causing hyperpolarisation, thus reducing Ca^{2+} entry through other Ca^{2+} -dependent channels, which eventually limits the firing frequency of action potentials, to form spike frequency adaptation (Barrett and Barret 1976; Madison and Nicoll 1982). This intrinsic property of neurons is vital to achieve a central homeostatic mechanism influenced by numerous internal and external stimuli that may alter neuronal phenotypes, and subsequently alter neuronal networks.

Three forms of afterhyperpolarisations have been identified that have overlapping kinetic properties. The fast afterhyperpolarisation (fAHP) can participate in the falling phase of action potential and overlaps spike repolarisation, lasting 10-20 ms: BK channels are thought to be involved in this form of AHP (Storm 1987). The mAHP begins rapidly, and lasts hundreds of milliseconds. This AHP component produces modest changes in the shape of action potentials and is frequently mediated by SK channels (Zhang and Krnjevic 1987). Finally, the sAHP lasts over several seconds, the underlying current having an initial rising phase which decays in hundreds of milliseconds: its activation has recently been determined and is due to the SK4 channel (King *et al.* 2015).

Apamin (bee venom peptide) has been widely used to distinguish components of AHP and this in fact blocks the mAHP in the many cells tested, including spinal motor neurons (Zhang and Krnjevic 1987), supraoptic neurons (Bourque and Brown 1987), vagal motoneurons (Sah and McLachlan 1992), pyramidal neurons in the sensory cortex (Schwindt *et al.* 1988), basolateral amygdala (Power and Sah 2008), nucleus reticularis thalamic neurons (Avanzini *et al.* 1989), cholinergic nucleus

basalis neurons (Williams *et al.* 1997), CA1 hippocampal interneurons (Zhang and McBain 1995), stratum radiatum (Savic *et al.* 2001), midbrain dopamine neurons (Shepard and Stump 1999), rat subthalamic neurons (Hallworth *et al.* 2003), cerebellar Purkinje neurons (Edgerton and Reinhart 2003), suprachiasmatic nucleus neurons (Teshima *et al.* 2003), striatal cholinergic neurons (Goldberg and Wilson 2005), mitral cells in olfactory bulb (Maher and Westbrook 2005), and finally paraventricular neurons (Chen and Toney 2009).

It can be assumed that SK channels therefore underlie the mAHP but not the sAHP. In response to exogenous Ca^{2+} , small conductance SK channels can be opened rapidly: in contrast the sAHP activates slowly. Further, it was shown that buffering cytosolic Ca^{2+} does not afford a rapid reduction in the sAHP current (Sah and Clements 1999). Lastly, in CA1 pyramidal neurons, the underlying current of the sAHP has been recorded using transgenic mice lacking small conductance SK channels (Bond *et al.* 2004).

1.4 TRP ion channels

1.4.1 Overview

Transient receptor potential (TRP) channels control plasma membrane ion movements, and are a super-family comprising nearly 50 genes which represents ~20% of ion channels to date in the animal kingdom species. The TRP channel message has been found in many different cell types, embracing both excitable and non-excitable varieties. Emerging evidence indicates that certain TRP members can act as calcium release ion channels. Most TRP proteins generate active role in manifold biological functions such as membrane depolarisation (Eijkelkamp *et al.* 2013; Gees *et al.* 2010). Interestingly, this class of ion channels has a unique intrinsic domain, namely a kinase domain, and are widely implicated in both biological and diseased conditions, for example TRPM7 channels contribute to cytosolic Ca²⁺ homeostasis (Mederos y Schnitzler *et al.* 2008), oxidative stress modulation (Simon *et al.* 2013), and anoxic cell loss (Aarts *et al.* 2003). Therefore, these molecules seem an interesting target when dealing with cancer and neurodegeneration as these proteins can serve as a powerful channel in the regulation of ions recognised as dangerous elements once deregulated in pathological conditions.

1.4.2 Classification of TRP ion channels

In the ion channel tree, TRP members form the most diverse division amongst ion channels (Venkatachalam and Montell 2007). The International Union of Pharmacology currently lists 28 TRP channel genes i.e. isoforms, and six protein families, which include the canonical (TRPC), vanilloid (TRPV), melastatin (TRPM), ankyrin (TRPA), mucolipin (TRPML) and polycystin (TRPP) channels (Clapham *et*

al. 2005). The TRPM family has eight channel members, and TRPM7 has been repeatedly targeted in neuroscience, cancer and other areas. Genes in this family are termed TRPM as the first gene was identified in a melanoma (Duncan *et al.* 1998). The work described here only focused on the TRPM7 channel, addressing its role in neurodegeneration.

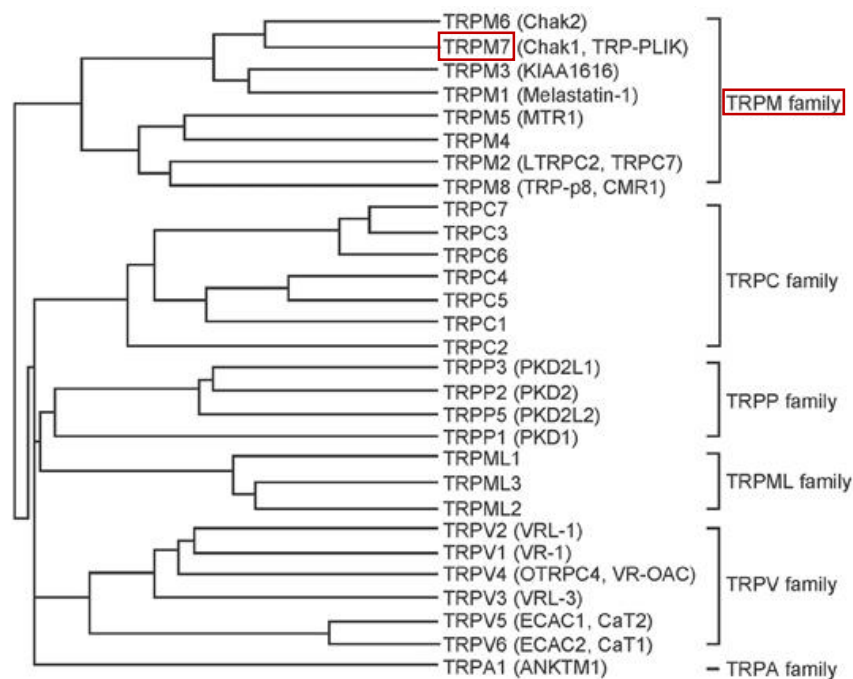


Figure 1.4 Phylogenetic tree of TRP channels according to their homology (Takahashi *et al.* 2012).

1.4.3 Cloning, structure and diversity

In 1969, the first TRP gene was electrophysiologically discovered in *Drosophila melanogaster*, a mutant fly which suffered impaired vision due to disruption of inositol triphosphate (IP₃)-dependent Ca²⁺ influx after phototransduction (Cosens and Manning 1969), and the gene was named as TRP gene. After 20 years, the gene was cloned (Montell and Rubin 1989; Wong *et al.* 1989), and in 1991, this gene was found to generate a functional ion channel protein (Hardie 2011). In mammals, Wes and his colleagues first cloned TRPC1 (Wes *et al.* 1995). Structural studies found that the TRP channel platform has six transmembrane (S1-S6) segments, and intracellular linked N- and C- termini, which usually assemble as tetramers (Fleig and Penner 2004). In the N- region, TRPMs have a longer N-terminus by nearly 400 amino acids compared with other classes, namely TRPC and TRPV families (Perraud *et al.* 2003). TRPM channels have variable C-terminus size of up to 2000 amino acids (Montell 2005), moreover, the N- domain has a known region of TRPM homology (Perraud *et al.* 2004). TRPM channels also differentially share protein identities, for example, the TRPM6 protein sequence demonstrates ~49% similarity to TRPM7 (Ullrich *et al.* 2005). A mutation search indicated, in HEK293 cells, that these TRPM members can produce multimeric channels (Chubanov *et al.* 2004). The transmembrane pore which contains “cation selective” signature complexes is formed between S5 and S6. It is believed that the channel pore presents three negatively charged amino acids (Yee *et al.* 2014), essential for its function, thereby modulating ionic conductance. TRPM7 gene is resident in chromosome 15, and has 39 exons. However, studies have revealed that this gene has nine splice variants, with four transcripts providing a protein message.

In the case of TRPM7, it is assumed that it can act as an ion channel and kinase (Runnels *et al.* 2001), and it has further been reported that the TRPM7 channel kinase can serve as a sensor of the cell and as its transducer (Clapham 2003; Takahashi *et al.* 2012). The kinase uses an amino acid segment, which starts from 1553 to 1562, as a fundamental part of its action (Crawley and Cote 2009). Here, the nucleotide binding site occupies the end of this track, and this is where the kinase lobes may combine (Yamaguchi *et al.* 2001). In the relationship between TRPM7 and its kinase, it is not clear whether there is direct cross-talk or not (Park *et al.* 2014).

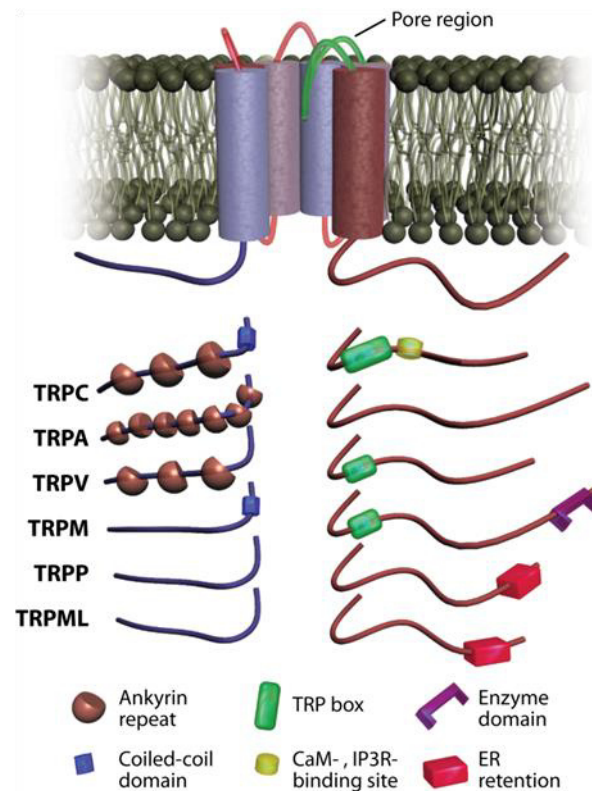
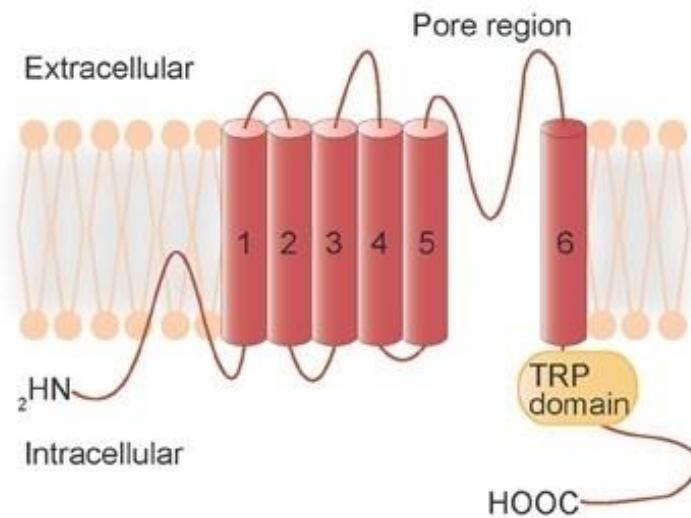


Figure 1.5 Transmembrane and the quaternary structure of TRP channels. The ankyrins may increase plasticity through the channels. The TRP box may contribute to channel gating. The ER retention domains may be relevant for channel localisation within the cell. The calmodulin IP₃ receptor binding domain seems to facilitate channel gating (Eijkelkamp et al. 2013; Takahashi et al. 2012).

1.4.4 Gating of TRP channels

TRP gating is caused by direct activation and also through signalling pathways. Temperature and pH changes, mechanical forces (Figure 1.6), and second messengers have been proposed as potential gating mechanisms, which are directly sensed or mediated through receptor operated pathways. In Chinese hamster ovary cells transfected with TRPV2 (CHO knock-in TRPV2), membrane tension on an elastic membrane caused TRPV2 activation and significantly increased $[Ca^{2+}]_i$ (Muraki *et al.* 2003). In patch-clamp recording, TRPM7 channel activity was significantly increased in HEK293 knock-in TRPM7 cells by osmotic swelling and membrane expansion (Numata *et al.* 2007). Activation of HEK293 knock-in TRPV channels produced by increasing hypertonic solution temperature to 36°C, resulted in a marked rise in $[Ca^{2+}]_i$ (Nishihara *et al.* 2011). Also, it has been accepted that TRPM7 channels are vulnerable to pH modulation since reducing the pH below the physiological 7.4 level lowers TRPM7 channel affinity for ions, namely Ca^{2+} and Mg^{2+} (Jiang *et al.* 2005). Subsequently, it was found that cytosolic acidification to a pH of 6.3 represents an IC_{50} block of TRPM7 channels in HEK293 cells (Chokshi *et al.* 2012b). It has been proposed that G proteins play a role in the activation of TRP channels via second messengers. In this context, G-protein coupled receptors (GPCRs) may activate phospholipase C (PLC), which hydrolyses PIP2 to generate diacylglycerol (DAG) and IP_3 . DAG acts as candidate for TRP channel activation (Eijkelkamp *et al.* 2013). In *Drosophila* microvilli photoreceptors, it has been highlighted recently that PLC hydrolysis of PIP2, and resultant DAG in the membrane may cause physical changes and membrane expansion through light sensing, with ultimate activation of TRP channels (Hardie and Franze 2012). However these ideas are still limited and remain open to debate.

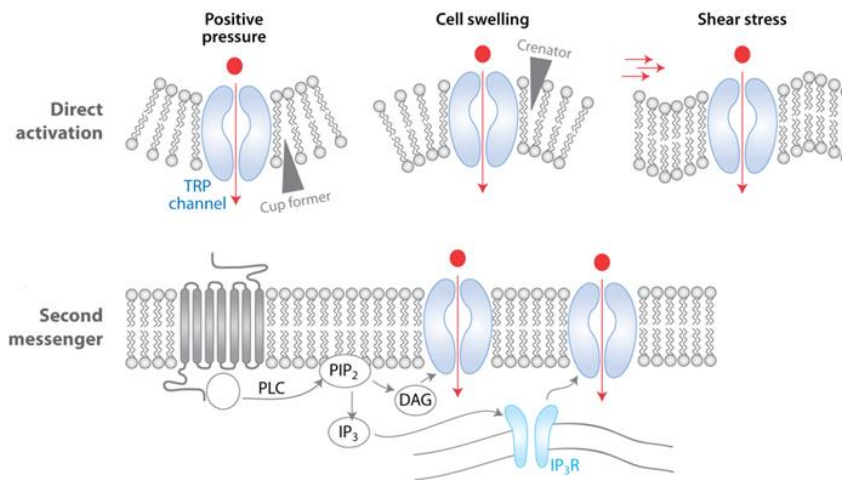


Figure 1.6 Possible mechanisms for TRP channel activation (Eijkelkamp et al. 2013).

1.4.5 TRPM7 biological features

TRP channels are involved in three main physiological processes, which include sensory tasks, ion homeostasis, and motile functions such as muscle contraction (Eijkelkamp et al. 2013; Gees et al. 2010). Their prominent role in the regulation of Ca^{2+} homeostasis, but not in all subtypes, is fascinating indeed. However, although TRP channel biophysical characterisation is well progressed, in contrast, function is not well-known. Since, for example TRPM7 channels serve as the conduit for physiologically crucial ions in terms of membrane potential, i.e. Ca^{2+} , of course this gate influences membrane voltage. The channel is constitutively active (Monteilh-Zoller *et al.* 2003), conducting Ca^{2+} and Mg^{2+} inward currents at -40 mV to -80 mV and 105 pS has been reported for TRPM7 single channel conductance (Bae and Sun 2011; Runnels et al. 2001). In resting cells, physiological Mg^{2+} concentration

can restrain TRPM7 activity (Nadler *et al.* 2001). In contrast, for example lowering either $[Mg^{2+}]_i$ or Mg.ATP (Nadler *et al.* 2001), cytosolic alkalinisation \sim pH= 8.4 (Kozak *et al.* 2005) and cAMP (Langeslag *et al.* 2007) can all activate the TRPM7 channel. TRPM members have a different signature to recognise and permit Ca^{2+} ions to flow through the channels, ranging from high permeability (TRPM3) to impermeability (TRPM4) channels (Gees *et al.* 2010). In human atrial fibroblasts, Ca^{2+} influx was markedly reduced (maximum achieved was 62%) when TRPM7 expression was down-regulated by siRNA (Du *et al.* 2010). These findings clearly indicate that tight modulation of the TRPM7 channel is required in cell physiology (Bae and Sun 2013), otherwise any dysregulation results in global ionic concentration changes in the cell, thereby triggering ionic cell signalling that indeed produces diseased cells, such as those in cancer and neurodegeneration. Generally, in cancer cells, TRPM7 plays a necessary role for cell growth, whereas in other cells, such as neurons, TRPM7 inhibition improves cell survival (Yee *et al.* 2014) in the face of various insults such as ischaemia (Sun *et al.* 2009). Intriguingly, a recent study has shown that TRPM7 channel knockout caused a hind leg paralysis, affecting neural crest advances in mouse dorsal root ganglion (Jin *et al.* 2012). In addition, it has been well documented that TRPM7 as a Mg^{2+} channel can be involved in both cellular and whole body Mg^{2+} regulation (Ryazanova *et al.* 2010). In brief, the TRPM7 member of TRPM family regulates various important ions in the tissue, so that this ion channel is a big player in both physiological and pathological decisions.

1.4.6 TRPM7 channel pharmacology

To date, neither TRPM7 channel activators nor selective TRPM7 blockers are available. However, several chemicals have been shown to block TRPM7, for example 2-aminoethyl diphenylborinate (2-APB) (Chokshi *et al.* 2012a), but these are not specific. In this paradigm, researchers have found that 2-APB can also block other TRP members, at least TRPM2 (Togashi *et al.* 2008), and TRPC5 (Xu *et al.* 2005). Fluorescence recording reported that 2-APB at 100 μM acidifies the cellular pH in single cell imaging, thus inactivating TRPM7 (Chokshi *et al.* 2012a). Most recently, Chubanov and his colleagues have documented that SK channel modulators can also block TRPM7 channels (Chubanov *et al.* 2012), for example, SK1-3 blocker (NS8593, 30 μM) can fully block the channel current, but this blocks SK1-3 channels at nanomolar ranges. This finding was surprising, but valuable, since the work here was designed to focus only on SK channels, using those modulators that have been researched by Chubanov's group. This finding is mentioned and discussed further in chapter four (See chapter four, discussion).

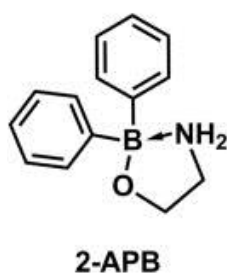


Figure 1.7 Chemical structure of 2-aminoethyl diphenylborinate (Hofer *et al.* 2013).

1.5 Cell death mechanisms

The first type of cell loss amongst cell death mechanisms, was discovered when considering the morphology of cells (Kerr *et al.* 1972), and was named apoptosis or programmed cell death. Apoptosis is not the only type of cell death, but is certainly the most prevalent. Cell death is regulated by different processes, including apoptosis, necrosis, autophagy, necroptosis, oncosis, and pyroptosis (Figure 1.8) (Bortner and Cidlowski 2014). Basically, there are two major mechanisms that may induce apoptosis. Firstly, receptor-mediated apoptosis that may activate death-inducing signalling such as caspases. Secondly, apoptotic-signalling pathways can also be triggered by chemicals: for example hydrogen peroxide (H₂O₂) leads to the destruction of the mitochondrion and thus releases cytochrome c into the cytosol (Fiers *et al.* 1999; Yang *et al.* 1997). The term apoptosis refers to pathological and also physiological death, an example of programmed cell death, which involves the activation of cascades, thus orchestrating the damaging of the cell (Friedlander 2003). This cell death is identified by cell shrinking, involving mitochondria (Kerr *et al.* 1972). Unlike apoptosis, which is caspase-dependent, necrosis is a pathologic process, which is caused by external stimuli, for instance ischemia (Majno and Joris 1995). In addition to apoptosis and necrosis, the term autophagy is a relatively new kind of cell death, which is an intracellular catabolic process (Martin 2010), surrounding and destructing subcellular organelles (Kang *et al.* 2011). Apoptosis is different from necrosis in its histological and biochemical signature (Friedlander 2003). Also, necrosis and apoptosis are different, morphologically and mechanistically, from autophagy (Martin 2010). Recently, necrotic cell death has been linked to passive cell death, termed necroptosis, which is activated by TNF α , FasL, and Trail ligands (Christofferson and Yuan 2010). Most recently, two other

types were added to the catalogue of the cell demise pathways. In oncosis, this death mechanism is thought to cause ionic imbalance which is characterised by cytosolic vacuole creation, and an increase in size of various organelles, namely the nucleus and mitochondria, as well as an enlarging of the cytoplasm, thus producing cell loss (Weerasinghe and Buja 2012). This can occur through cell ischaemia, for instance, via radiation injury. Finally, another form of programmed cell death has been shown to occur during inflammation in response to microbes, involving caspase-1 awakening (Franchi *et al.* 2012).

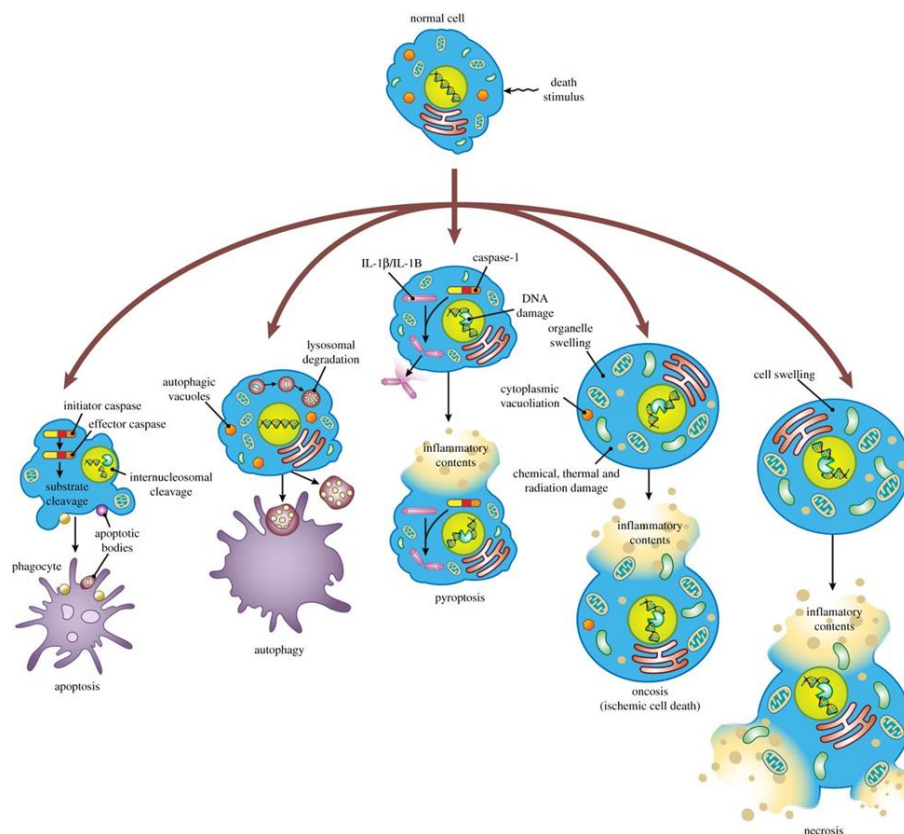


Figure 1.8 Mechanisms of cell death (Bortner and Cidlowski 2014).

In apoptotic signalling two platforms are shown. Caspase members have been categorised, based on their mechanisms, initiators involving both caspase-8 and caspase-9, while caspase-3, -6, and -7 are touted as executioner caspases (McIlwain *et al.* 2013). Extrinsic avenues occur through external triggers where these stimuli, in the form of ligands, at the plasma membrane first bind to a death receptor (DR), delivering a message to death effector domain (DED) of caspase-8, which is a central driver in this form of apoptosis (Figure 1.9). This engages death domains, the adapter proteins either FAS-associated or TNFR-associated death domains (Varfolomeev *et al.* 1998; Yeh *et al.* 1998), abbreviated as FADD or TRADD respectively, thus awakening caspase-8 activity. This produces new caspase activities propagating caspase-3 and caspase-7. Alternatively, active caspase-8 can trigger an intrinsic route first via BID, where its cleavage form (tBID) enhances apoptosis through mitochondria (Schug *et al.* 2011), releasing cytochrome c into the cytosol. On the other hand, an intrinsic type generated by stressors from internal sources, is linked to mitochondria - so called "mitochondrial apoptosis". Different factors induce this picture of apoptosis, such as hypoxia and accumulation of unfolded proteins. Mitochondrial apoptosis uses caspase-9 as initiator, when its interacting domain, termed a caspase recruitment domain (CARD), binds to its counterpart the adapter protein apoptotic protease-activating factor-1 (APAF1) (Shiozaki *et al.* 2002). This and caspase-9 are present in the cytosol, but they require cytochrome c action, therefore the pathway can commence in response to stresses. Cytochrome c interacting with APAF1 results in a conformational change. This is followed by further conformational change (Acehan *et al.* 2002), which ultimately activates caspase-9 in a complex known as an apoptosome (Cain *et al.* 2002).

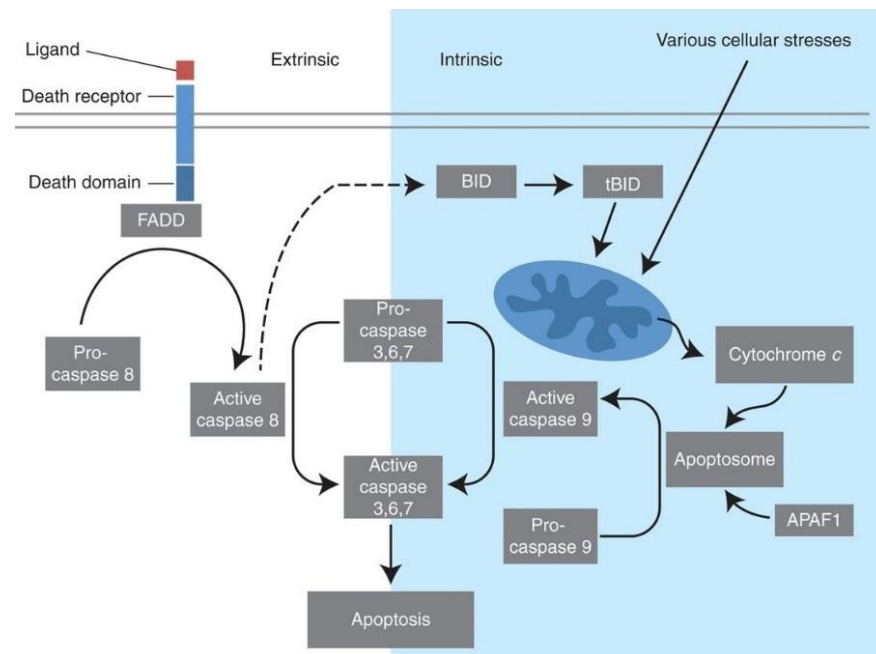


Figure 1.9 Extrinsic and intrinsic modes of apoptosis, mode one (McIlwain et al. 2013).

In mitochondrial apoptosis, BH3-only members, are also connected, which act as apoptotic initiators after cytotoxic stimulation, thereby blocking pro-survival effectors, namely Bcl-2 proteins (Figure 1.10). Subsequently, BAX and BAK effectors generate the oligomers, thus triggering the mitochondrial outer membrane permeability. This action causes cytochrome c formation, which can activate caspase-9 through APAF1, or in contrast, produces a second mitochondria-derived activator of caspases (SMAC), which prevents the caspase inhibitor XIAP, a short hand for X-linked inhibitor of apoptosis protein (Czabotar *et al.* 2014).

The role of Bcl-2 protein family, such as Bcl-2 effector, is emerging in the curing of disease, since such a player illustrates a principal role in cell life and death decisions, including neurons (Anilkumar and Prehn 2014) and cancer cells (Correia *et al.* 2015). In this respect, there has been more interest in Bcl-2 in the neuronal

survival in Huntington's degenerative cell loss. It was discovered that in cells affected with the Huntington's phenotype that elevating Bcl-2 expression is in fact protective in the face of mutant Huntingtin protein (Ju *et al.* 2011). So, the Bcl-2 is currently considered a novel target in such models of diseases, as well as in the cancers (Sassone *et al.* 2013).

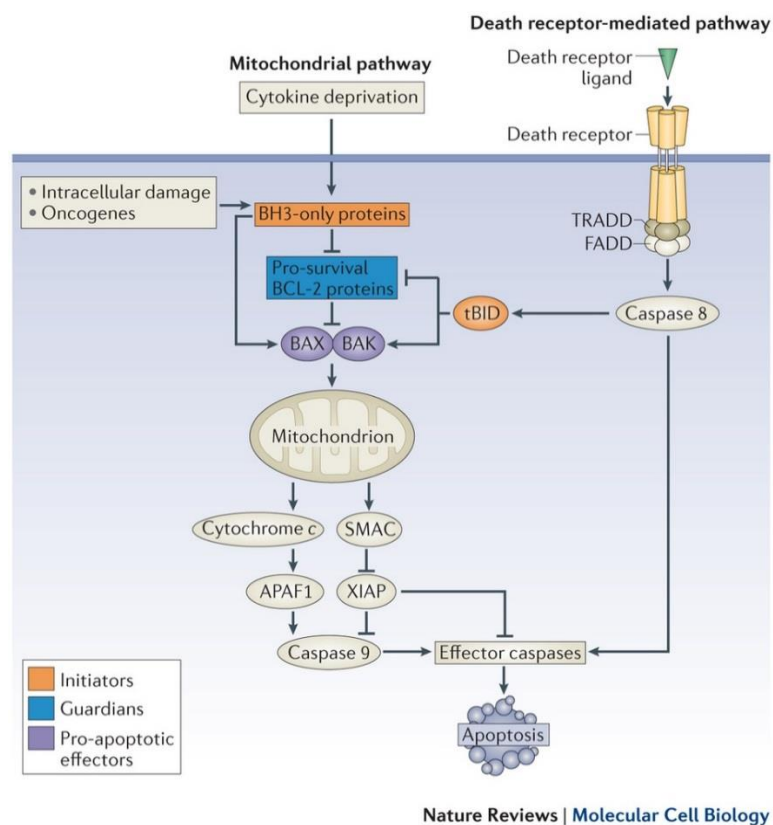


Figure 1.10 Extrinsic and intrinsic modes of apoptosis, mode two (Czabotar *et al.* 2014).

In pathological conditions, for example neuronal “survival” and cancer “growth”, apoptotic determinants are widely implicated. Interestingly, ion channel roles are well-linked to the heart of apoptosis (Bortner and Cidlowski 2014; Burg *et al.* 2006). It is indeed very exciting that ion channels are unique targets for cancer search

(Kunzelmann 2005; Li and Xiong 2011; Pardo and Stuhmer 2014), since these molecules are very powerful not only in arresting cell growth, but also in dampening cancer invasion. In neurons, programmed cell death, particularly apoptotic power, is a major element in degeneration, as well as aging cell loss such as occurs in Alzheimer's disease (Ghavami *et al.* 2014).

1.6 Cellular Ca²⁺ in pathophysiology

Calcium signalling is pivotal in normal cellular function with changes in intracellular Ca²⁺ being a key message or signal for cell growth, secretion, excitability, contraction or gene expression. However changes in intracellular Ca²⁺ are also very much at the heart of pathophysiological processes, playing a key role in cellular dysfunction and even death (Campbell 2014) .

In the early 1880s, Sydney Ringer published four papers in which he described the key role of calcium in physiological processes. The most obvious finding to emerge from this study was the quantitative amount of calcium, potassium and sodium ions necessary to maintain the heart contraction (Miller 2004). In subsequent studies, this view was supported by number of researchers (Campbell 1983), and the competing processes of calcium efflux and influx were highlighted and linked. It has been shown that store filling occurs by receptor activation (Casteels and Droogmans 1981). From the mid to late twentieth century, there has been a progressive increase in the number of biomedical scientific publications on calcium (Putney 2011). In recent years, there has been increasing curiosity in Ca²⁺ homeostasis, and interestingly, the past decade has seen continued rapid growth in the field of calcium research.

In the CNS, Ca^{2+} plays a central role in long-term depression and potentiation, which are forms of synaptic plasticity, dendritic development, synaptogenesis, membrane excitability, and information processing (Berridge 1998). Indeed, Ca^{2+} influx into a cell leading to an increase in local Ca^{2+} concentration results in a number of synaptic alterations. Larger elevations in $[\text{Ca}^{2+}]_i$ are cytotoxic (Mattson 2007) by either changing cell signalling or by damaging of cellular components through enzymes and free radicals. On the other hand, disruption of the proliferation-apoptosis balance results in abnormal cell growth and further cancer cell metastasis (Farfariello *et al.* 2015). Therefore, the role of cytosolic Ca^{2+} in both cancer progress and neurodegeneration is extremely interesting.

Cell signalling pathways are initiated by either elevating or reducing intracellular Ca^{2+} levels, therefore each physiological and pathological phenotype is characterized by a specific “calcium signature”, comprising kinetics, localization, and amplitude (Lehen'kyi *et al.* 2011). Evidence shows that the resting concentration of cytosolic free Ca^{2+} lies in the range of 100 nM to 200 nM (Decuyper *et al.* 2011; Marambaud *et al.* 2009). Upon stimulation, it can increase to low micromole levels through calcium influx from the outside milieu, and also calcium efflux from internal stores (Marambaud *et al.* 2009).

Ca^{2+} diffusion is limited by several mechanisms, termed homeostatic mechanisms, including Ca^{2+} buffering proteins, for instance parvalbumin, membrane pumps, and carriers, which influence the Ca^{2+} concentration gradient, triggering cellular signalling (Augustine *et al.* 2003). Clearly, diffused calcium ions can bind to Ca^{2+} -binding effectors proteins and cell Ca^{2+} -sensors, such as neurocalcin, thus activating physiological processes (Ames *et al.* 1996; Augustine *et al.* 2003).

A correct calcium homeostasis is essential to maintain cell function. For this central regulation, there are various factors and mechanisms such as voltage-operated, receptor-operated, and store-operated calcium channels, which are located at different cellular sites (Ghosh and Greenberg 1995). The influx of Ca^{2+} from the extracellular space can be modulated by either receptor-operated channels, such as NMDA receptors or voltage-operated channels (VOCs) which in turn trigger the release of neurotransmitters following action potentials.

In the mammalian nervous system, glutamate is the most common neurotransmitter, which is particularly important in respect of memory. In the neuronal membrane, glutamate can bind to both metabotropic and ionotropic receptors. Interestingly, metabotropic receptors were shown to be involved in calcium homeostasis by driving Ca^{2+} from internal stores through GTP-binding protein-dependent pathways (Marambaud et al. 2009). Moreover, glutamate is transported by different plasma membrane transporters, which are reversible and inward under physiological conditions, in contrast glutamate can also be transported in the outward direction, termed reversed transport, for instance when intracellular $[\text{Na}^+]$ / extracellular $[\text{K}^+]$ increase (Szatkowski et al. 1990). It is well known that overstimulation of glutamate receptors is associated with neuronal toxicity. Glutamate receptors respond to various agonists such as hormones and growth factors. Importantly, they activate phospholipase-C hydrolysing phosphatidyl inositol 4,5-biphosphate (PIP₂) to generate inositol 1,4,5 triphosphate (IP₃), which acts as a second messenger (Figure 1.11). IP₃ then acts on IP₃ receptors, ultimately releasing Ca^{2+} from the ER (Zhang et al. 2011b). In addition, the IP₃R can be influenced by various modulators such as Ca^{2+} , ATP, CaM, and protein kinases (Foskett et al. 2007; Mikoshiba 2007).

It is clear that endoplasmic reticulum (ER) Ca^{2+} homeostasis plays a prominent role in controlling diverse neuronal functions. The ER intraluminal Ca^{2+} level is approximately 4 to 5 orders of magnitude higher than the surrounding milieu. Therefore, this concentration gradient leads to Ca^{2+} leaving the ER upon activation of receptors or channels such as IP_3Rs and RyRs , which differ in conductance, expression profile, and regulation. On the other hand, the sarcoplasmic-endoplasmic reticulum Ca^{2+} ATPase pump can accumulate Ca^{2+} in the SR/ER lumen through ATP hydrolysis (Stutzmann and Mattson 2011). In addition, the store-operated calcium entry system is involved in the refilling of intracellular Ca^{2+} stores by a complex process, termed store-operated Ca^{2+} entry, which is activated by reducing intracellular stores in the ER (Putney 2011).

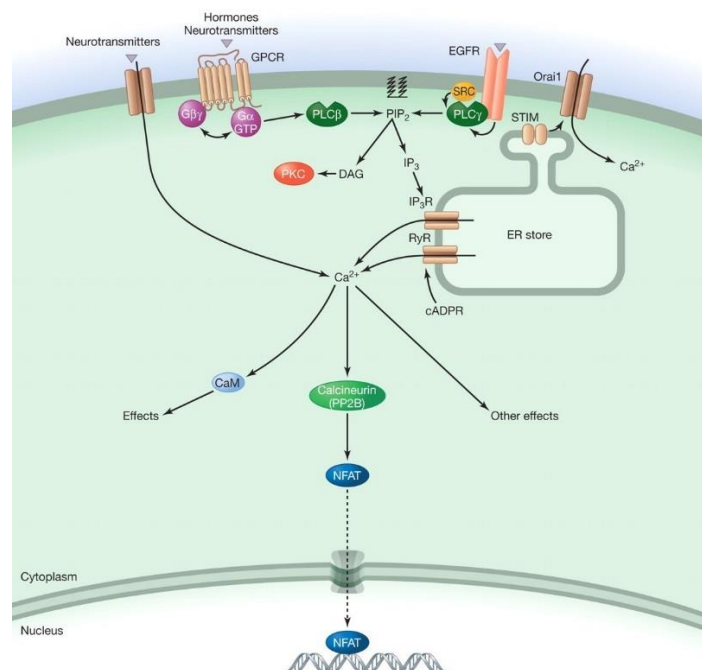


Figure 1.11 Simplified picture of calcium signalling in cells (Bootman 2012).

The mitochondrion in cells is a multi-functional organelle. In addition to producing ATP, it plays an essential role in numerous cellular functions such as Ca^{2+} homeostasis and cell death pathways. It is generally accepted that mitochondrial perturbations are involved in the neurological diseases such as an interruption in oxygen to the brain (Zorov *et al.* 2007). Under normal physiological conditions, neurons are exposed to a baseline degree of oxidative stress from different sources. Elevated oxidative stress is a pathological condition leading to increased production of reactive oxygen species (ROS) and free radicals, thereby reacting with DNA, lipids and proteins, and causes cellular damage and dysfunction (Choi *et al.* 2009; Suh *et al.* 2008). Importantly, it has been determined that cross-link between redox signals and Ca^{2+} plays critical role in neuronal function. Furthermore, ROS can alter Ca^{2+} signalling proteins, amplitudes, and kinetics. Also, oxidation of (NO) can be induced by ROS and reacts with free thiol in the RyR, to generate S-nitrosothiol, which mediates Ca^{2+} release from the ER. Likewise, it has also been reported that ROS can activate IP_3Rs . On the other hand, ROS is thought to be implicated in the inhibition of both the sarcoplasmic-endoplasmic reticulum Ca^{2+} ATPase and the plasma membrane Ca^{2+} ATPase (Foskett *et al.* 2007; Sutko and Airey 1996).

In addition, the Cyclic AMP response element binding protein (CREB), is a nuclear transcription factor, which regulates genes important for neuronal survival (Tsokas *et al.* 2007). Interestingly, phosphorylation and activation of CREB is switched on by rises in intracellular Ca^{2+} accompanying neuronal activity. Conversely, CREB levels are decreased in transgenic models of Alzheimer's disease following beta-amyloid treatment of neurons (Pugazhenthii *et al.* 2011). Further, CREB function has also been recently linked to expression of some subclasses of K^+ channel in brain slice cultures (Tong *et al.* 2010).

In cell growth mechanism(s) mapping, it is clear that Ca^{2+} play a powerful role beyond cancer considerations, such as through canonical and non-canonical role of K^+ channels (Huang and Jan 2014) in modulating membrane potential and $[\text{Ca}^{2+}]_i$ signalling, thus changing cell cycle progression (Ouadid-Ahidouch and Ahidouch 2013; Yang and Brackenbury 2013). These concepts are well reviewed in chapter five. Unfortunately, research efforts have not made further progress, and it is still not clear how Ca^{2+} upmodulation in cells sustains “switch on” cell growth mechanisms. More, “How Ca^{2+} oscillations, apoptosis and cell growth are linked is still a big question”. Thus, understanding calcium signalling rules in cancerous cells is currently very poor.

Accordingly, the study of cellular mechanisms, which participate in the perturbation of cellular Ca^{2+} signalling, though not clear, are fundamental in investigating pathogenesis and disease mechanisms, and in recognising therapeutic targets.

1.7 Cell models

1.7.1 CNS cell lines

1.7.1.1 SH-SY5Y cell model

The human neuroblastoma line, SH-SY5Y, was established from bone marrow tissue in cell culture. First, it was shown that its parental line, SK-N-SH, shows dopamine beta-hydroxylase activity, thus expressing a neuronal phenotype (Biedler *et al.* 1978). Subsequently, it is frequently used in disease models, most commonly in neuroblastoma, Parkinson’s and Alzheimer’s models as disease-specific phenotypes. Evidence demonstrates that undifferentiated SH-SY5Y cells exhibits immature catecholaminergic neuronal phenotype at a biochemical level, lacking mature neuronal markers (Biedler *et al.* 1978; Gilany *et al.* 2008). Therefore, this

cell type might not be an appropriate model for neurodegenerative models, such as Parkinson's disease, since mature and differentiated dopaminergic neurons are affected in the brain through PD. Interestingly, multiple lines of research evidence on the SH-SY5Y cells highlight that differentiation of this model, through certain treatments e.g. retinoic acid, produces a more SH-SY5Y neuronal phenotype, with cholinergic, noradrenergic and dopaminergic properties, and alters the SH-SY5Y cell morphology to one similar to mature neurons (Xie *et al.* 2010). More recently, genomic mapping of SH-SY5Y cells, through sequencing the whole genome, has found that specific genes existing in Parkinson's pathways, were also expressed in the SH-SY5Y genome (Krishna *et al.* 2014).

1.7.1.2 *STHdh* cell model

A cell model of Huntington's disease was also used in this study. In this model, wild-type mouse striatal cells (*STHdh*^{+/+}/*Hdh*⁺), heterozygous (*STHdh*^{Q111}/*Hdh*⁺), as well as homozygous cells (*STHdh*^{Q111}/*Hdh*^{Q111}) were established from wild-type and Huntington disease (*Hdh*^{Q111}) knock-in embryos (Trettel *et al.* 2000; Wheeler *et al.* 2000). This study found that a full-lengthening glutamine track in Huntington protein produces dominant phenotypes in mouse striatal cells. The Huntington's disease collaborative research group (1993) reported that the human Huntington's disease mutation shows an expanded CAG repeat that extends a poly glutamine portion to 37 or more residues. This reveals that the trinucleotide repeat in Huntington gene is unstable and mutations produces different CAG repeat length. This phenomenon can affect HD case severity (Trettel *et al.* 2000) and its onset, as longer CAG repeat accelerates HD onset (Pouladi *et al.* 2013). Two HD mice models, R6/1 and R6/2, found that these show different CAG repeats in exon 1, 116 and 144 CAG repeats respectively, using the human Huntington promoter (Mangiarini *et al.* 1996). In HD

pathogenesis, studies report that full-length mutant protein actually promotes mutant amino-terminal fragment into amyloid (Scherzinger *et al.* 1997; Scherzinger *et al.* 1999). Furthermore, it is believed to date that all models that generate truncated N-terminal fragment shows similar symptoms, for example cognitive and behavioural abnormalities (Pouladi *et al.* 2013).

1.7.1.3 BV-2 cell model

Other CNS cells were also used in this study, thus addressing the role of channels of interest not only in neurons but also in glial cells in the brain. A murine cell line, BV-2, was used in the study, since it represents a valid cell model for primary microglia (Henn *et al.* 2009). BV-2 cells were originally derived from a mouse primary microglial cell culture (Blasi *et al.* 1990). The study of BV-2 properties, as an immune cells in CNS, has shown that these cells have phagocytic ability, including secretory properties for instance lysozyme, tumour necrosis factor, as well as interleukin 1 (Blasi *et al.* 1990). Such cells indeed present antimicrobial activities, more importantly against microorganisms that involve in CNS pathologies (Bocchini *et al.* 1992). Further study compared lipopolysaccharide-activated primary microglia and the BV-2 response pattern, and has indicated that their functional responses were highly similar, through modulating interferon gamma and NO regulation (Henn *et al.* 2009), that play an important role in neuroinflammation.

1.7.1.4 MOG-G-UVW cell model

Finally, the human brain astrocytoma cell line, MOG-G-UVW, was a line of interest because previous studies did not address the role of channels of interest in the seminal element “astrocytes” in the brain in the context of neuronal insults. MOG-G-UVW cells were established from anaplastic astrocytoma of adult human brain in

tissue culture (Frame *et al.* 1984). It is surprising that growing evidences points out emerging roles of this CNS resident cell in neurological disorders. In this paradigm, it has been mentioned that these cells, for example, are involved in neuroplasticity (Clarke and Barres 2013).

1.7.2 Breast cancer and non-tumorigenic cell lines

1.7.2.1 Wild-type breast cancer cell models

The cancer work in this study was carried out in three wild-type breast cancer cell lines, which include MCF-7, BT-474 and MDA-MB-231 cell lines. The reason was to explore whether breast cancer cells which express different phenotypes show either similar or different expression pattern in the context of channels of interest as well as their role in breast cancer cell growth, if any. MCF-7 line is the most commonly used cell line so far, these cells being derived from a primary culture of 734B cell culture from human pleural effusion which was originally isolated from a metastatic mammary carcinoma (Soule *et al.* 1973). These cells have (ER⁺, PR⁺ and HER2⁻) status (See section 5.3.1), which represent approximately 70% of breast cancer cases to date (Lumachi *et al.* 2013). Another line, BT-474, has a triple positive (ER⁺, PR⁺ and HER2⁺) expression pattern, and is less common (~15%) among breast cancer patients compare to MCF-7 line phenotype (Alba *et al.* 2014; Neve *et al.* 2006). These cells were also derived from human pleural effusions from an invasive ductal carcinoma (Lasfargues *et al.* 1978). Furthermore, another breast cancer phenotype was also utilised in the study, namely MDA-MB-231 cells, which demonstrate (ER⁻, PR⁻ and HER2⁻) phenotype i.e. triple negative status (Neve *et al.* 2006). This phenotype is also less common and constitutes about 15% compare to (ER⁺, PR⁺, HER2⁻) status of MCF-7 cell line, and was derived from pleural

effusions (Cailleau *et al.* 1974). This indicates that these different cells have different growth signature through various mechanisms i.e. pathological features. Breast cancer cell lines are also classified, based on molecular characterisation, into five models: luminal A (MCF-7), luminal B (BT-474), HER2 (MDA-MB-453), Basal (MDA-MB-468) and claudin-low (MDA-MB-231) (Perou *et al.* 1999; Perou *et al.* 2000). In breast cancer study, there is little doubt that these cell lines improved the understanding of breast cancer pathogenesis at the molecular level as *in vitro* models of breast cancer.

1.7.2.2 Endocrine resistance cell models

The work in this study also utilised endocrine resistance cell models, it is assumed that resistance mechanism understanding is highly complex and challenging in its clinical outcome. In this regard, it has been reported that about 45% of estrogen receptor casualties which were treated with endocrine therapy, such as tamoxifen and fulvestrant, will eventually relapse (Jafaar *et al.* 2014). This was the reason that endocrine MCF-7 resistance cell models, namely TamR (Knowlden *et al.* 2003) and FasR (Nicholson *et al.* 2005), were investigated to test whether the channels of interest play any role in the context of their expression and their functional activities (See sections 2.1 and 5.3.1).

1.7.2.3 Non-tumorigenic epithelial cell model

This cancer research was followed by asking whether these ion channel targets occur in a human breast epithelial cell line, namely MCF 10A. This line was generated from human fibrocystic mammary tissue (Soule *et al.* 1990). Such cells exhibit normal characteristic of breast epithelial cells, when several parameters are considered. For instance, MCF 10A cells lack of tumorigenicity phenotype, their

growth in culture can be modulated by using growth factors, and these cells can form a dome pattern in confluent culture (Soule et al. 1990).

1.8 General hypothesis and aims

It has become clear that intracellular Ca^{2+} perturbations trigger cell survival and so are involved in several pathologies, more importantly in neurodegeneration and cancer. In neurons, Ca^{2+} overload is cytotoxic, whereas an increase in intracellular Ca^{2+} is required for abnormal cell growth, namely in cancer. Thus, SK and TRPM7 ion channel modulation will modify “on-off” switching cell survival capabilities.

In this *in vitro* study, the main aims are:

1. To establish a role, if any, for SK and TRPM7 ion channels in CNS cell survival against neuronal insults.
2. To establish a role, if any, for the SK ion channel in breast cancer cell growth.
3. To explore whether SK and TRPM7 ion modulation is involved in any underlying “molecular” mechanisms such as apoptosis, causing either neurodegeneration or modified cell growth.

2 Chapter Two: General Methods and Materials

2.1 Cell lines

SH-SY5Y cells, a human neuroblastoma line were subcloned and isolated from a four year-old female. MOG-G-UVW cells, is a human brain astrocytoma line, and both lines were purchased from the European Collection of Cell Cultures, United Kingdom (UK). Mouse striatal cells, a mouse striatal cell model of Huntington's disease, which include a wild type $STHdh^+/Hdh^+$, a heterozygous mutant $STHdh^{Q111}/Hdh^+$ and a homozygous mutant $STHdh^{Q111}/Hdh^{Q111}$, were a gift from Professor Lesley Jones, Institute of Psychological Medicine and Clinical Neurosciences, School of Medicine, Cardiff University, UK. BV-2 cells, a primary mouse brain microglia line, were provided courtesy of Professor Rosario Donato, Department of Experimental Medicine and Biochemical Sciences, University of Perugia, Italy.

Also used were MCF-7 cells (Luminal A: ER⁺, HER2⁻), and a human breast adenocarcinoma isolated from a 69-year old Caucasian female, a widely studied endocrine resistant model, being Tamoxifen-resistant (TamR) and Fulvestrant-resistant (FasR) lines, and originally derived from primary MCF-7 cells. Other breast cancer cell lines of varying phenotype, namely BT-474 (Luminal B: ER⁺, HER2⁺), and MDA-MB-231 cells (Basal B: ER⁻, HER2⁻) were kindly provided by Tenovus Centre for Breast Cancer Research, School of Pharmacy and Pharmaceutical Sciences, Cardiff University, UK. A non-tumorigenic cell line, namely MCF 10A was a gift from Prof Arwyn Jones, School of Pharmacy and Pharmaceutical Sciences, Cardiff University, UK.

2.2 Culture conditions

SH-SY5Y cells were grown in Eagles Minimum Essential Medium in a ratio 1:1 with F12 nutrient mixture (Sigma-Aldrich, UK), 15% (v/v) foetal bovine serum (Gibco® Life Technologies, United Kingdom), and 1% (v/v) non-essential amino acids (Sigma-Aldrich, UK). For SH-SY5Y differentiation, regular medium was supplemented with 10 µM retinoic acid for seven days, a commonly used protocol to differentiate neuroblastoma cells into a neuronal phenotype. MOG-G-UVW cells were cultured in Dulbecco's Modified Eagle Medium (Gibco® Life Technologies, UK) in a ratio 1:1 with F10 nutrient mixture (Sigma-Aldrich, UK), and 10% (v/v) foetal bovine serum. Mouse striatal cells, namely the wild type *STHdh⁺/Hdh⁺*, the heterozygous mutant *STHdh^{Q111}/Hdh⁺* and the homozygous mutant *STHdh^{Q111}/Hdh^{Q111}* cells were cultured in Dulbecco's Modified Eagle Medium, and 10% (v/v) foetal bovine serum. Mouse microglial BV-2 cells were cultured in Roswell Park Memorial Institute-1640 medium containing phenol red (Gibco® Life Technologies, UK) and 10% (v/v) foetal bovine serum. MCF-7 cells were grown in Roswell Park Memorial Institute-1640 medium containing phenol red, supplemented with 5% (v/v) foetal bovine serum. Tamoxifen resistant and Fulvestrant resistant cells were exposed to 100 nM 4-hydroxytamoxifen (Sigma-Aldrich, UK) and Fulvestrant (Sigma-Aldrich, UK) for eighteen and twenty seven months respectively, thereby generating a short term endocrine resistant model, and their replication maintained in Roswell Park Memorial Institute-1640 medium, supplemented with 5% (v/v) charcoal-stripped foetal bovine serum (Appendix 1). BT-474 cells were grown in in Dulbecco's Modified Eagle Medium, and 10% (v/v) foetal bovine serum. MDA-MB-231 cells were grown in Dulbecco's Modified Eagle Medium in a ratio 1:1

with F12 nutrient mixture, and 10% (v/v) foetal bovine serum. MCF 10A cells were cultured in Dulbecco's Modified Eagle Medium in a ratio 1:1 with F12 nutrient mixture, and 5% (v/v) horse serum, supplemented by 100 µl of insulin (10 mg/ml), 5 µl of epidermal growth factor (400 µg/ml), and 50 µl of hydrocortisone 1 mg/ml, which were purchased from Sigma-Aldrich, UK.

All cultures were maintained at 37°C, except BV-2 cells which were maintained at 33°C, in a standard humid atmosphere of 5% CO₂, supplemented with 2 mM (v/v) L-glutamine (Sigma-Aldrich, UK), and 100 IU/ml penicillin-100 µg/ml streptomycin (Gibco® Life Technologies, UK).

2.3 Preparation of primary culture and subculturing

Working with a cell culture environment requires an aseptic (closed) system. Therefore the laminar flow cabinet was "preconditioned" being switched on and left at its normal setting for 15 minutes, the work area being sprayed with ethanol 70% (v/v) using clean tissues before starting the culture procedure and setting up. Moreover, reagents necessary for the cell culture such as Dulbecco's phosphate buffered saline and trypsin, were pre-warmed (37°C) in a clean water bath for 15 minutes, which were aseptically opened in the cabinet. Cells were frozen and stored either in the cryo-freezer (-80°C) for short-term storage or in liquid nitrogen (-196°C) for long-term storage. Primary cultures were generated by transferring the frozen vials to the water bath and allowing them to thaw for about 5 minutes before gently pipetting into Eppendorf tubes: the suspension containing cells was immediately centrifuged at 1000 rpm for 3 minutes. The old medium was then discarded and cells were recovered with fresh growth medium (1 ml) by disintegrating the pellet and pipetting down in order to have a homogenous suspension. Cells were then

distributed into the culture flask (Thermo Fisher Scientific, UK), and as a result cells can grow leaving the quiescence state which can differ for each line of cells. Cells were examined on a daily basis under the microscope. Although each cell line has specific culture demands, the technology and procedures are similar in terms of subculturing for all. Cell passaging regime at regular intervals limits the cell biomass in the form of monolayer culture, thereby maintaining cultures by continuous transferring a determined volume of each respective cell number in the confluent flasks. The “dilution” of cells in the new culture is typically in the range of a ratio 1:2-1:10 as necessary, based on the goals of subculturing with optimum growing efficiency and the requirements of further experimental work. Moreover, the number of flasks required for further use, were considered in advance being based on the experimental design, for example the number of technical and biological replicates and the planned time course. For subculturing (Cell splitting), the regular medium in 25 cm² tissue culture flasks was aspirated and cells rinsed with Dulbecco’s phosphate buffered saline (1 ml), which was then sucked away using an aspiration pump. Adhered cells were detached in trypsin (0.5 ml) after incubation at 37°C for 3-6 minutes. Flasks were retained and examined under the microscope to ensure complete cell detachment, gently tapping if necessary. Trypsin activity is immediately ceased by adding the normal medium (1 ml) and swirling. The solution was then transferred to an Eppendorf tube, which was then centrifuged at 1000 rpm for 3 minutes resulting in a suspended pellet: again the supernatant was discarded, the pellet recovered in normal medium (1 ml) and pipetted up and down to reach an homogenous distribution of cells. In the pre-seeding step, variations in the cell suspension densities were assessed using a haemocytometer in order to achieve

the desired culture density. An unknown cell population (in 1 ml) was added to normal medium (4 ml) in a universal tube and pipetted. The counting chambers and coverslip were sprayed with 70% ethanol (v/v) and cleaned using lens tissue. The suspension was mixed well and then 10 μ l injected to the V-shaped area under the coverslip on both sides with a pipette. Cells in all squares were counted under the microscope thus providing values for the volumes that the cell suspension and the medium need to be mixed in for further experimental work such as culture maintenance, using the equation (Total cells counted in 10 in squares/ 10) X 10⁴).

Cell models	Passage number
CNS	
Undifferentiated SH-SY5Y	17-20
Differentiated SH-SY5Y	17-20
MOG-G-UVW	18-22
BV-2	19-21
STHdh ^{+/+} Hdh ⁺	7-10
STHdh ^{Q111/} Hdh ⁺	7-10
STHdh ^{Q111/} Hdh ^{Q111}	7-10
Breast cancer	
MCF-7	8-12
TamR	40-44
FasR	100-104
BT-474	8-11
MDA-MB-231	6-10
Non-tumorigenic	
MCF 10A	9-12

Table 2.1 The passage numbers of the cells used in this study.

2.4 Gene expression assessment

2.4.1 Qualitative gene expression assessment

2.4.1.1 Primer design

Forward and reverse primers in original DNA sequences were designed using the National Centre for Biotechnology Information online database. The Basic Local Alignment Search (Blast) tool compares sequences producing significant similarity. Primer 3 tool (Version 0.4.0) accesses predesigned primers. Sequences were retrieved in an Ensemble database to verify where the primers bind in the exons in question.

2.4.1.2 RNA extraction

Total RNA from cultured cells was extracted using 2.5 ml of Trizol (Ambion® Life Technologies, UK) spread over the entire surface of 75 cm² culture flask (Thermo Fisher Scientific, UK). The cell lysate was pipetted several times to form a homogenous cell suspension, which was transferred into two Eppendorf tubes, and 250 µl of chloroform (Sigma-Aldrich, UK) was added to each tube. After brief incubation, the mix was centrifuged at 12,000 rpm for 10 minutes at room temperature. The supernatant, which contains RNA, was isolated into a fresh Eppendorf tube. In this, and all subsequent steps, a controlled workstation within a PCR hood was used.

2.4.1.3 RNA precipitation

After generation of the aqueous (RNA containing) phase, this was re-suspended in 625 µl of isopropyl alcohol (Thermo Fisher Scientific, UK), thus recovering RNA. Following incubation at room temperature for 10 minutes, the mix was then

centrifuged at 12,000 rpm for 5 minutes. The resultant precipitant was eluted in 75% ethanol (500 µl) after which RNA samples were vortexed, and centrifuged at 12,000 rpm for 5 minutes at room temperature. The supernatant was aspirated, and the pellet was incubated at room temperature for a few minutes. To rehydrate the RNA, 25 µl of RNase free water was added, and the samples were stored overnight at -80°C.

2.4.1.4 DNase treatment

DNase treatment was performed to ensure the purity of the RNA samples, thereby eliminating contaminating genomic DNA. Samples were combined in a 500 µl tube, followed by RNA purification using Precision™ DNase kit (PrimerDesign, United Kingdom), which was treated with Precision 10x DNase reaction buffer (5 µl) and precision DNase enzyme (1µl) for 10 minutes at 30°C in a DNA thermal cycler (Perkin-Elmer). DNase enzyme was heat inactivated after incubation of the mix for 5 minutes at 55°C, thus terminating reactions. RNA samples were immediately cooled on ice, before proceeding to the RNA quantification step.

2.4.1.5 RNA quantification

The Du 730 spectrophotometer (Beckman coulter®) was calibrated, followed by a 50 times dilution of the samples in a cuvette using nuclease free water, and the amount of RNA per microliter was quantified at 540 nm. As per manual, the ratio index (260 nm/ 280 nm) yields the RNA amount for further assays.

2.4.1.6 Reverse transcription

The resultant mRNA was reverse transcribed using precision nanoScript™ Reverse Transcription kit (PrimerDesign, United Kingdom) to produce complementary DNA

(cDNA). The annealing step reaction involved 1 µg of RNA template, RT primers 1 µl of each Oligo-dT (20 µM) and Random nonamer (40 µM), and RNase/DNase free water up to 10 µl. The mixture was incubated at 65°C for 5 minutes in a DNA thermal cycler, which was immediately cooled in an ice bath for optimal performance. The extension RT reaction was conducted using the following constituents: nanoScript 10x buffer (2 µl), dNTP (10 mM) mix (1 µl), 2 µl of DTT (100 mM), RNase/DNase free water (4 µl), and 1 µl nanoScript enzyme (17.5 u/µl), which were added to the sample on an ice bath. After a pulse spin, tubes were incubated at 25°C for 5 minutes and then at 55°C for 20 minutes. This reaction was then terminated by incubation at 75°C for 15 minutes.

2.4.1.7 Polymerase chain reaction

Polymerase chain reaction (PCR) was undertaken to investigate the presence of messages in all target cells, this technique using specific primers to replicate a DNA target. Promega PCR assay uses nuclease free water (7.43 µl), 5x Green GoTaq Flexi buffer (2.5 µl), 0.75 µl MgCl₂ (25mM), 0.25 µl dNTP (10 mM), 0.0625 µl GoTaq polymerase (5 u/µl), and 0.5 µl of each primer (10 µM). The mixture was placed in a UNO-Thermoblock machine (Biometra) using an appropriate PCR protocol, so producing multiple DNA amplified segments from the isolated cDNA.

2.4.1.8 Electrophoresis

Following the development of DNA copies, gel electrophoresis, using an agarose matrix (1%) was performed to facilitate the separation of DNA populations, according to biomolecule sizes. Gels were cast using 700 mg agarose gel (Invitrogen™ Life Technologies, UK), and 70 ml Tris-acetate-EDTA (Thermo Fisher Scientific, UK), the mixture briefly microwaved, and stained using 0.5 µg/ml ethidium

bromide (BIO-RAD, UK) in a Mini-Gel tray (BIO-RAD, UK). Following 30 minutes incubation at room temperature, the gel was placed in an electrophoresis chamber, the comb removed and the wells then covered with TAE buffer (1x). The wells were loaded with 10 μ l of DNA of interest and β -actin samples, which is ubiquitously expressed in eukaryotic cells. Product sizes were referenced using an 10 μ l HyperLadder™50bp (BioLine, UK), which yields blue and yellow dyes, and to monitor migrating molecules through a gel, the device was set at 100 mV, 200 mA for up to 60 minutes. When the front dye approached the end of gel, the migration progress was ceased, and the resulting gel was photographed by a UV gel documentation system.

2.4.2 Quantitative gene expression assessment

A quantitative expression profiling supplementary to qualitative approach (PCR) was performed using the Affymetrix GeneChip® 1.0 ST array system, which provides data on the concordant expression of transcripts encoding genes of interest. Assays used RNA compiled from experimental and reference samples at three passage numbers, the RNA quantity was scored, and the quality was verified through PCR. The technique involves transcribing of RNA to cDNA, which was differentially labeled with fluorescence. The hybridisation involves the labeled DNA molecules pairing with the complementary sequence of the DNA probe to form double stranded DNA on the chip, on which thousands of spots were printed. The arrays were then scanned, the data processed, analysed, and normalised using GENESIFTER software, which results in a log transformed expression pattern, as well as a heatmap that provides a snapshot of changes in gene expression. In this profile, spot colours reflect simultaneous gene expression, red colour meaning the

target gene is up-regulated, in contrast down-regulation appears as green, and black signifies no change in expression. Experiments were conducted by the Tenovus Centre for Breast Cancer Research, School of Pharmacy and Pharmaceutical Sciences, Cardiff University, UK.

Additional details can be found at:

http://media.affymetrix.com/support/technical/datasheets/gene_1_0_st_datasheet.pdf

2.5 Protein blotting

2.5.1 Protein extraction

Total protein was lysed from cells cultured in six well plates: either regular or experimental medium was aspirated, the culture was rinsed with appropriate amount of ice cooled phosphate buffered saline (Sigma-Aldrich, UK), and 200 μ l was retained in each well. After 15 minutes incubation on ice whilst maintaining constant rocking, adherent cells were mechanically dislodged using a plastic cell scraper (Thermo Fisher Scientific, UK), and the suspension was transferred into pre-cooled Eppendorf tubes. The lysate was fractioned by centrifuging for 5 minutes at 4°C, pellets recovered and cells disintegrated in a mixture of Pierce lysis IP buffer (Thermo Fisher Scientific, UK) and Halt™ protease inhibitor cocktail (Thermo Fisher Scientific, UK) in a ratio (100:1). The cocktail protects the proteins from uncontrolled losses through degradation. For this preliminary treatment, samples were incubated on ice for 30 minutes. Centrifugation for 15 minutes at 12,000 rpm resulted in a solution at the top, which carries proteins, which can then be determined.

2.5.2 Protein quantification

Unknown concentrations were determined using an accurate colorimetric assay (Thermo Fisher Scientific, UK). The bicinchoninic acid assay (BCA) uses the biuret reaction in which peptide bonds reduce cupric (Cu^{2+}) to cuprous (Cu^+) that chelates with bicinchoninic acid molecules whereby the products stain a purple colour with light adsorbing at 560 nm, and the absorbance correlates with the protein amount that can be displayed in a linear relationship. A series of different and known protein concentrations were required for normalisation using standard albumin (10 mg/ml). BCA component A and B were mixed in a ratio (7 ml: 140 μ l) and then added to the

wells containing protein samples. The reactions were developed by incubation at 37°C for 30 minutes, and the absorbance was read using a LT-5000MS ELISA reader (Labtech). Proteins were washed in the most common sample buffer (1:1), Laemmli (Sigma-Aldrich, UK), which masks an inherent charge, so that proteins are negatively charged. Finally, proteins were aliquoted and stored at -20°C.

2.5.3 Polyacrylamide Gel Electrophoresis (PAGE)

The PAGE is an electrophoretic separation technique in which proteins migrate based on their sizes and can be detected as bands through the matrix. In principle, the matrix is mounted between the anode (-) and cathode (+) running buffers in the upper and lower chambers, respectively. The gel is porous through which negatively charged proteins can be forced toward the cathode (+) in the unit. As the migration pattern depends on molecule charge and size, large molecules are retarded in their mobility compared to smaller molecules. In this format, a typical matrix comprises two sections which vary in concentration, a running (Appendix 2) and stacking (Appendix 2) gel solution. Prior to casts set, the module needed for gel solidification was assembled using Mini-PROTEAN Tetra Cell system (BIO-RAD, UK). Separating gel solutions were poured into glass plates on the casting stand, topped with isopropyl alcohol (Thermo Fisher Scientific, UK) to achieve a glossy surface, and allowed to stand for 40 minutes at room temperature. When the separating gel set, the gel was overlaid by stacking gel, and a comb was inserted to form the wells. When layers were set, the module was placed in the buffer tank, and the running (1x) Tris-Glycine-SDS buffer (Sigma-Aldrich, UK) was poured into the chambers. After removing a comb, wells were uncovered and rinsed with the buffer using a Pasteur pipette. The lanes were loaded with the same amount of protein as

recommended, in order to achieve the same expression level between lanes. In all cases, the control well was loaded with the same amount of total protein (20 µg) as treated cells. Samples were run at a constant voltage and current of 120 V and 400 mA until the coloured band reference line was reached. For all runs, the first well was reserved for a molecular weight marker, namely Precision Plus Protein™ Kaleidoscope Standards (BIO-RAD, UK): molecules in the samples are in parallel wells and migrate a distance according to size, which can then be determined. Once protein bands reached the reference line, the current was stopped in the run.

2.5.4 Western blotting

This technique expands the workflow that starts with the contemporary method, referred to as electrotransfer that permits immobilising of separated proteins on a membrane, in which proteins are captured at their relative positions, mirroring the pattern achieved by electrophoresis in the gel. This setting used a wet transfer system, where in response to an electrical current, proteins could then be transferred. The transfer sandwich uses the cassette, in which the layers start with a sponge followed by a filter paper, the membrane in contact with the gel, a second filter paper and second sponge. It is vital to ensure expulsion of air bubbles and to avoid creases in the construct, which compromises uniform transfer. Prior to the sandwich preparation, all constituents were immersed in transfer buffer. Further, the buffer contains methanol that activates the membrane, the degree to which leads to efficient binding. The sandwich was then submerged in refrigerated (1x) Tris-Glycine buffer in the transfer tank. As buffers would generate heat and require an ice block, this is therefore considered in the design. In the transfer apparatus, the stack was run at a constant current of 100 V and 400 mA fixed, ensuring that the membrane

was orientated towards the cathode (+). Once the membrane was lined with proteins that were originally established on the gel, which itself would complete in about 1 hour, the current was disconnected in the stack.

As nonspecific binding is detrimental, it is recommended to incubate the fresh membranes with 5% (w/v) dried skimmed milk and Tris buffered Saline with Tween®-20 regularly for three hours, a strategy which blocks the spaces that are not occupied by target molecules.

For detection of target proteins, the membrane is incubated overnight with the primary antibodies diluted in 5% (w/v) dried skimmed milk and Tris buffered Saline with Tween®-20, a more sensitive treatment which allows the probes to bind only the protein in question in the whole sample isolate. Known target proteins are thus labelled at 4°C overnight. An additional manipulation is required, as a high background alters the signal to noise ratio. After three washings (15 minutes/wash), again using 5% (w/v) dried skimmed milk and Tris buffered Saline with Tween®-20, the appropriate secondary antibody (1:10000), Anti-rabbit IgG HRP-linked (#7074), which is affinity purified goat anti-rabbit IgG format, is directed against a first reporter, the primary antibody for 60 minutes, because the primary antibody itself does not generate a signal. After a series of washes as above, the membrane which carries an immune complex and has provided the horseradish peroxidase activity developed in Supersignal™ West Dura Chemiluminescent substrate layered by Amersham Hyperfilm™ ECL, enables the determination of specific protein present using a film cassette, which can be visualised and then quantified after 3 minutes in a darkroom. In most applications, reprobing the resolved membrane is required for identifying other targets, which can be achieved by stripping the prewashed

membrane with Restore™ Plus Western Blot Stripping Buffer for 8 minutes at room temperature.

2.6 MTS preparation

The cell proliferation experiments used the MTS method to assess cell viability in the culture in a colorimetric fashion, thereby staining viable cells present per population, and in principle monitoring the cytotoxicity of pharmacological probes. In essence, living cells have a dehydrogenase (NADPH) activity which is normally abundant in the mitochondria that can reduce the tetrazolium dye (MTS) to a formazan product, which can be quantified through an absorbance function that yields a picture of cell proliferation, being a surrogate for the number of healthy cells. Based on the Promega procedure, MTS powder reagent (42 mg) was weighed and added into phosphate buffered saline (21 ml) using a Corning® 50 ml tube: the mixture allowed to dissolve at 37°C for 15 minutes, followed by adjusting the pH (6.0-6.5). Then this filtered using a syringe filter, as cell culture requires an aseptic approach, the stock was stored at -20°C. This procedure also required an electron coupling reagent phenazine methosulfate (PMS) combined with MTS in a ratio 1:20 to form an MTS-PMS mix. Again the PMS stock demands the same storage conditions as the MTS solution.

2.7 Pharmacological modulation

2.7.1 Plate preparation

For this work, confluent flasks (80-90%) were used to harvest fresh cells, and the density assessed using a haemocytometer as described above. The resultant solution with known cell population was further diluted in the relevant medium in

order to achieve sufficient volume of the suspension based on the experimental strategies. In all cases, experiments used formatted 96-well plates, where only inner wells had cells so ensuring less chance to lose aseptic conditions and medium evaporation, particularly in long-term assays. Cells in a final volume (100 μ l) were distributed among wells, using a multi-channel pipette for convenience and uniform delivery with desired densities, thereby optimising cell seeding for different scenarios. In CNS experiments, SH-SY5Y cells were seeded at a density of 15×10^3 , and all other cell lines were seeded at a density of 10×10^3 cells per well. Breast cancer cells were also pharmacologically managed, all lines being seeded at a density of 8×10^3 cells per well. It is essential to use the same medium for control “blank” wells (without cells) for each respective group, so removing the any background considerations in the statistical treatment. Transferred fresh cells were allowed to adhere and recover for 24 hours in the incubator.

2.7.2 MTS cell proliferation assays

The next day after cells had been maintained for 24 hours in normal conditions, test cells were kept either unchallenged, as respective controls, or treated with insults and/or ion channel modulators for the desired period. The medium was aspirated from the wells using a Pasteur pipette and then replaced, controls being only refreshed with normal medium (100 μ l each), whereas other cell groups were challenged using normal medium (100 μ l each) containing test treatments. Treating CNS derived cells with test compounds used a 24 hour challenge in parallel with both insult and ion channel modulators, as well as each probe alone. On the other hand, in experiments with cancer cells, these were challenged for 72 hours, refreshing the medium and treatment every 24 hours, and cells were observed

under the microscope. Three hours before each examination point to determine any changes, the plates were retrieved and the pre-warmed MTS-PMS (20 μ l) was added in a ratio of 1:5 to each well using the repeating pipette, protected from light and further incubated for 3 hours in the incubator. Results were obtained using a LT-5000MS ELISA reader machine in the form of an absorbance function (490 nm) and the responses were then profiled.

2.8 Gene silencing

2.8.1 Design, source and storage

The siRNAs wherein the double stranded RNAs, namely sense and antisense templates were designed to direct against genes of interest, and to bind to silence the target mRNA, thus identifying a unique sequence particularly in the case of the intended targets. However, it is important to candidate an additional cDNA template, thus limiting off-target results. The Eurofins Genomics database was consulted using the IDs of genes in the NCBI database that had been utilised previously for PCR. The target and control siRNAs needed for this study were commercially synthesized by Eurofins Genomics, diluted in appropriate buffer (50 μ M each) based on the manufacture's instruction, and stored at 4°C.

2.8.2 Plate preparation

For transfection assay with breast cancer and CNS derived cell lines, fresh cells were prepared from confluent flasks, as described above. Then six well plates were cultured, at a density of 200 X 10³ cells per well in normal medium (2 ml), and allowed to stand for 24 hours to attain 50-60% confluence.

2.8.3 Transfection

On transfection day after 24 hours, cells in cultured plates were first retrieved and observed under the microscope to ensure the quality of the culture. Normal medium was replaced twice by adding the same amount of Opti-MEM® medium, thereby washing cells which were then incubated for 15 minutes. The siRNA procedure was carried out according to the manufacturer's instructions, accompanied by previously normalised and published protocol (Al Soraj *et al.* 2012). To deliver 50 nM siRNA into cells of interest per well, the following reagents with indicated concentrations were sequentially applied. First, the siRNA transfection medium Opti-MEM® (179 µl) was transferred to Eppendorf tubes of the target and control siRNA, and then oligonucleotides (1 µl) were diluted in each tube. Also, Oligofectamine™, the transfection reagent, (8 µl) was diluted in Opti-MEM® medium (32 µl). Next the diluted oligofectamine (20 µl) was combined with the diluted siRNA solutions, an homogenous mix ensured, and incubated for 30 minutes. Before adding the siRNA-oligofectamine complex, the medium in wells was replaced by Opti-MEM® medium (800 µl) without serum and antibiotics, and the complex (200 µl) was added onto specific wells of the target and control siRNA. At four hours post-transfection, wells were supplemented with Opti-MEM® medium containing 12% (v/v) serum, and further incubated for 72 hours.

In siRNA knockdown and apoptosis experiments, medium was replaced with Dulbecco's phosphate buffered saline (300 µl) per well and incubated on ice using a shaker for 10 minutes. Cells were then harvested into Dulbecco's phosphate buffered saline by scraping, with cell suspensions from three wells subjected to the same condition being combined in order to obtain appropriate protein concentrations

per sample, which were then pelleted by centrifuging at 1000 rpm for 5 minutes at 4°C. The supernatant was discarded and the pellet was resuspended in Pierce lysis IP buffer-Halt™ protease inhibitor cocktail mix (150 µl), before proceeding to protein quantification and immunoblotting, as described above.

In cell proliferation assays, cells were washed with Dulbecco's phosphate buffered saline (1 ml), harvested in trypsin (300 µl) after incubation for 5 minutes, and normal medium (600 µl) was immediately added. Also, suspensions from three wells were combined to achieve sufficient cell numbers in the sample. Cells were counted, and seeded in 96-well plates using the growth medium.

2.9 Cell storage

Prolonged examining of cells with continuous subculturing runs the risk that cells become contaminated and lose their characteristics. In this study, cells were frozen in cryovials using Recovery™ Cell Culture Freezing Medium (300 X 10³ cells per ml), yielding higher cell maintenance. The procedure covered all steps of cell preserving, Cryovials were first placed into a Nalgene freezing container (-1°C /Minute) then into a cryofreezer (-80°C), followed by their transfer to a liquid nitrogen container (-196°C).

2.10 Preparation of chemicals

The pharmacological SK modulators, GW542573X (Cat. No. 4311), CyPPA (Cat. No. 2953), NS309 (Cat. No. 3895), UCL1684 (Cat. No. 1310), TRAM-34 (Cat. No. 2946), and NS6180 (Cat. No. 4864), were purchased from Tocris Bioscience, UK, NS8593 (Cat. No. N2538) being obtained from Sigma-Aldrich, UK. Using the online Tocris dilution calculator and instructions, the modulators were all dissolved in

dimethyl sulfoxide (Sigma-Aldrich, UK). The stock solutions of GW542573X (50 mM), CyPPA (50 mM), NS309 (50 mM), UCL1684 (4 mM), TRAM-34 (50 mM), NS6180 (4 mM) and NS8593 (8 mM), were stored at (-20) in aliquots, and used within one month.

In the case of the pharmacological CNS insults, hydrogen peroxide (H₂O₂) (Cat. No. H1009), cobalt (II) chloride (CoCl₂) (Cat. No. 232696), Escherichia Coli lipopolysaccharides (Cat. No. L6529), were purchased from Sigma-Aldrich, UK and staurosporine (Cat. No. 1285) was purchased from Tocris Bioscience, UK. Here, the stock solutions were made using sterile water for H₂O₂ (0.5 M), CoCl₂ (10 mM), and lipopolysaccharides (1mg/ml), and were kept at 4°C. The stock solution of staurosporine (500 µM) was prepared using dimethyl sulfoxide and stored at -20°C. Other test agents, namely 4-Hydroxytamoxifen (Cat. No. L6529), Fulvestrant (Cat. No. 14409), and retinoic acid (Cat. No. R2625) were purchased from Sigma-Aldrich, UK. Former drugs were dissolved in ethanol (Thermo Fisher Scientific, UK) to reach a concentration of (1 mM each) and kept at 20°C. Retinoic acid (10 mM) was made up using dimethyl sulfoxide.

In all cases, specific demands such as light sensitivity were covered.

2.11 Densitometric analysis

The autoradiography films were first scanned by an office scanner in order to semi-quantify and translate the resultant images into values, acquiring an 8-bit scale and a resolution of 600 dots per inch (dpi), this step being referred to as image acquisition. This is followed by a second step which uses computer aided ImageJ software as previously pointed out (Gassmann *et al.* 2009). The software allows the rectangular selection around the relevant bands. The software further enables

estimation of the peak heights of specific signals, based on their size, that can be expressed as a relative percentage of the area (Protein band), which were compared with their corresponding loading controls, again derived from their densities, namely peak heights, of the housekeeping protein bands (GAPDH). Subsequently, the values provided can yield the adjusted optical density for bands of interest by dividing the density of each sample by the loading control. The ImageJ software can correct background due to default settings. This function may often interfere with the densitometric result, though no correction was undertaken in this study.

2.12 Data analysis

In the protein measurement step, experiments used BCA assays to determine unknown protein concentrations in samples (See section 2.5.2). Obtained raw data (absorbance) were retrieved in Excel, means were averaged and the background was removed. The line of best fit was drawn through the absorbance-concentration data (the standard curve). This generates the trendline equation which can be used to assess unknown protein concentrations in fresh samples.

This study used one-way ANOVA as a statistical method. All measures for MTS assays and densitometric analysis were used in GraphPad Prism (Version 6.05, 2015). This software evaluated means, as well as detecting significant outliers, if any, from the rest. Here, the data are presented as means \pm SEM. *p*-values: *, **, ***, **** denotes $P \leq 0.05$, $P \leq 0.01$, $P \leq 0.001$, and $P \leq 0.0001$ respectively i.e. $P \leq 0.05$ was considered “significant”. Amongst post hoc tests, Dunnett’s test was used in all cases, with the exception of the statistical case in quantitative gene expression analysis, where Tukey’s test was performed.

3 Chapter Three: SK Ion Channel in Survival of Neurons and brain astrocytes

3.1 Introduction

SK channels are a Ca^{2+} responsive family of potassium channels, with four channel subtypes (Wei et al. 2005), namely SK1-4, which are expressed at both plasma membrane (Adelman et al. 2012), and more recently, channels such as SK2 channels are also found at the mitochondrial molecular level (Dolga et al. 2013). SK1-3 channel subtypes mediate a small K^+ ion conductance, whereas SK4 (IK) generates an intermediate K^+ ion conductance (Adelman et al. 2012). Pathology of many diseases showed, in both neuronal degeneration (Mattson 2007), and abnormal cell growth aspects (Farfariello et al. 2015), that Ca^{2+} signalling plays a significant role. This system is well characterised in excitable cells, such as neurons (Higley and Sabatini 2012). Here, a calcium role is extremely critical, Ca^{2+} acting either as a survival or criminal element (Berridge 2012). Perturbed Ca^{2+} signalling in neurons is largely implicated in neurodegeneration processes (Kawamoto *et al.* 2012), deregulated Ca^{2+} homeostasis being linked to life or death outcomes, thereby triggering neuronal survival, as well as cancer progression. In neurons, SK1-3 channels are responsible for a medium after-hyperpolarisation (mAHP) function (Zhang and Krnjevic 1987), whereas SK4 channels underlie the slow form of the AHP (King et al. 2015): thus SK channel activation reduces Ca^{2+} influx and potential Ca^{2+} overload (Stocker *et al.* 2004). Their role in non-excitabile cells is perhaps less clear, and may be concerned with cell growth through Ca^{2+} regulation. These proteins are largely expressed in central nervous system (CNS) resident cells, particularly in neurons. In rat CNS, three SK subtypes, namely SK1, SK2, and SK3

channel subtypes exist. For example, the SK1 and SK2 channels are present in the hippocampus region, while SK3 channels are expressed in the supraoptic nucleus (Stocker and Pedarzani 2000). In mouse brain, immunocytochemistry also determined the presence of SK1 and SK2 channels in the hippocampus, but the SK3 channel subtype is resident in other regions, such as the basal ganglia and thalamus (Sailer *et al.* 2004). Mouse dopaminergic neurons express both SK2 and SK3 channel subtypes (Deignan *et al.* 2012). It is surprising that the SK1 channel cDNA, at least in rat and mouse species, does not generate functional channels at the plasma membrane. This channel perhaps interacts with the SK2 channel subtype (Benton *et al.* 2003), although this remains unclear (D'Hoedt *et al.* 2004). It is important to highlight that SK channel expression, if any, was still not studied in astrocytes as CNS resident cells. It was shown that these cells are less sensitive to oxidative stress upmodulation than neurons, for instance H₂O₂-induced oxidative stress (Almeida *et al.* 2001; Dringen 2000; Wilson 1997). Most importantly, *in vitro* mixed cultures of both neurons and astrocytes improved neuronal protection against oxidative stress (Vargas and Johnson 2009; Wilson 1997). This indicates that neighbouring astrocytes in CNS strengthens neuronal defence mechanism to combat this stress. SK channel expression in diseased cells in aging has not been investigated, for example in the Huntington's cell model. For instance, do these cells express SK channels, if any, and also are they differentially expressed compare to the wild-type. This study considers such a big question. It has been well mapped that exacerbated oxidative stress is extensively up-modulated in neuropathology. Interestingly, a recent study using both *in vitro* and *vivo* models has shown that SK2 channel opening can markedly rescue cells from the glutamate toxicity in cerebral ischemia, this protection being linked to Ca²⁺ remodelling, through SK channel

action (Dolga *et al.* 2011). Most recently, molecular level expression of these channels in human dopaminergic neurons has been revealed, and that indeed mitochondria also express SK channels. This seminal study showed that SK2 channel activation significantly challenged mitochondrial dysfunction by rotenone, a complex I inhibitor, thus improving cell survival through modifying mitochondrial membrane potential (Dolga *et al.* 2014), and therefore reveals that this organelle perhaps plays a critical and central role in age-related diseases (Federico *et al.* 2012), for instance Alzheimer's disease. Indeed, understanding has recently been advanced, with the demonstration that increases in calcium influx through the plasma membrane triggers mitochondria, thereby upregulating reactive oxygen species production in vagal neurons (Goldberg *et al.* 2012).

In summary, SK channels not only control membrane potential at the plasma membrane level, but also at the subcellular level. This clearly means that these channels modulate calcium ion oscillations in the world of neuronal cells.

3.2 Hypothesis and aims

Activation of SK channels will have neuroprotective effects against H₂O₂-induced oxidative stress neuronal damage *in vitro*, since abnormal oxidative stress acts as a major contributor in the degeneration processes in neurons.

The principal objectives are:

1. To explore the profile of expression of SK1-4 potassium channels in a human neuroblastoma SH-SY5Y cell line: cell differentiation will also be undertaken.
2. To explore the profile of expression of SK1-4 potassium channels in mouse striatal wild-type *STHdh⁺/Hdh⁺* cells.
3. To explore the profile of expression of SK1-4 potassium channels in mouse striatal Huntington's cell models, namely heterozygous *STHdh^{Q111}/Hdh⁺*, in addition to homozygous *STHdh^{Q111}/Hdh^{Q111}* cells.
4. To explore the profile of expression of SK1-4 potassium channels in human astrocytoma MOG-G-UVW cells.
5. To explore the effect of the SK channel modulation, if any, on the viability of these cells.
6. To measure the LD₅₀ effect of the insult, H₂O₂, on these cells.
7. To establish a role, if any, for SK1-4 potassium channels against H₂O₂-induced oxidative stress:
 - a. To probe any protective effects of SK channel opening on H₂O₂-induced oxidative stress.
 - b. If SK activation is protective, to specify the channel target, and reverse the action by simultaneously blocking the channel target, using the relevant channel blocker.

8. To explore whether any changes in apoptotic mechanisms, through SK1-4 channel modulation and H₂O₂, are involved in any of the effects observed.

3.3 Materials and methods

3.3.1 Cell origins and features

The *in vitro* work of this study used two neuronal cell types, namely human neuroblastoma and mouse striatal cells. The former cell line was subcloned from SH-SY5, this being derived from an SH-SY clone of the SK-N-SH cells, which were isolated from human bone marrow neuroblastoma metastasis (Biedler et al. 1978). Importantly, SH-SY5Y cells were also differentiated to a neuronal phenotype. Thus, both undifferentiated and differentiated SH-SY5Y cells were tested. Experiments also used wild-type mouse striatal (ST) cells, as well as mutated Huntington gene knock-in counterparts. Huntington disease knock-in cells express an abnormal glutamine tract in their *Hdh*⁺ allele, whereas the normal tract has seven glutamines (Q7), as in wild-type cells, which is named *STHdh*^{+/Hdh}⁺. Here, both forms of the mutant cells were considered. In heterozygous cells, only one allele was targeted, thereby inserting CAG repeat generation up to 111 glutamines, hence the formatting *STHdh*^{Q111/Hdh}⁺. Moreover, homozygous cells have two mutant proteins, namely two *Hdh*^{Q111} allele knock-in in striatal neurons of the mice, this is the reason for the abbreviation *STHdh*^{Q111/Hdh}^{Q111} cells (Trettel et al. 2000; Wheeler et al. 2000). This work also used MOG-G-UVW cells, a human brain astrocyte, which were derived from anaplastic astrocytoma, isolated from adult brain tissue (Frame et al. 1984).

3.3.2 Polymerase chain reaction

SK channel transcripts (SK1-4) were interrogated for their messages, if present, at the mRNA level in these cells using RT-PCR. Experiments collected total RNA from the lysed cells, followed by RNA quantification for each sample, and then their integrity were assessed. These were reverse transcribed, thereby producing their cDNA. In these reactions, reverse transcriptase enzyme was used in all the samples, except the negative control sample, which was abbreviated as “No RT”. The resultant cDNA was amplified in the PCR reaction, using specific primers for the SK channel genes in question, and β -actin, which serves as the reference. Indeed, reaction conditions were optimised for each SK channel gene, as well as the reference, here both cycle number and the temperature being varied. Experiments explored the following optimum conditions, in the case of the human primers that were used for human cell lines in this work: denaturation at 95°C for 5 minutes, followed by 30 cycles of incubation consisting of 95°C for 30 seconds, 55°C for 30 seconds, followed by an extension step at 72°C for 1 minute, as well as 72°C for 5 minutes of final extension step. For mouse primers the same profile was used, with the exception that the mouse primers were annealed at 60°C instead of 55°C. RT-PCR product sizes were then assessed on an 1% agarose gel in electrophoresis, after being visualised by UV light.

Gene	Gene ID	Human primer sequences	Sizes (bp)
β-actin	NM_001101	F. 5'-CCCAGCCATGTACGTTGCTA-3'	126
		R. 5'-AGGGCATACCCCTCGTAGATG-3'	
KCNN1 (SK1)	NM_002248.4	F. 5'-TGGACACTCAGCTCACCAAG-3'	208
		R. 5'-TTAGCCTGGTCGTTTCAGCTT-3'	
KCNN2 (SK2)	AF397175.1	F. 5'-CAAGCAAACACTTTGGTGGA-3'	249
		R. 5'-CCGCTCAGCATTGTAAGTGA-3'	
KCNN3 (SK3)	NM_002249.5	F. 5'-AAGCGGAGAAGCACGTTTCATA-3'	180
		R. 5'-CTGGTGGATAGCTTGGAGGAA-3'	
KCNN4 (SK4)	AB128983.1	F. 5'-GAGAGGCAGGCTGTTATTGC-3'	215
		R. 5'-ACGTGCTTCTCTGCCTTGTT-3'	

Table 3.1 Primer sequences for human SK channel transcripts and positive control for the human cell types, and predicted identities. F. denotes forward primer and R. denotes reverse primer.

Gene	Gene ID	Mouse primer sequences	Sizes (bp)
β-actin	NM_007393.3	F. 5'-TGTTACCAACTGGGACGACA-3'	165
		R. 5'-GGGGTGTGAAGGTCTCAA-3'	
KCNN1 (SK1)	NM_032397.2	F. 5'-GAAGCTTGGGTGAACTGAGC-3'	232
		R. 5'-CCATTAAGGAATCCCCAGGT-3'	
KCNN2 (SK2)	AY123778.1	F. 5'-TCTGATTGCCAGAGTCATGC-3'	250
		R. 5'-CCACATTGCTCCAAGGAAGT-3'	
KCNN3 (SK3)	AF357241.1	F. 5'-ACTTCAACACCCGATTCGTC-3'	191
		R. 5'-GGAAAGGAACGTGATGGAGA-3'	
KCNN4 (SK4)	BC010274.1	F. 5'-AAGCACACTCGAAGGAAGGA-3'	215
		R. 5'-CCGTGATTCTCTTCTCCAG-3'	

Table 3.2 Primer sequences for mouse SK channel transcripts and positive control for the mouse cell types, and predicted identities. F. denotes forward primer and R. denotes reverse primer.

3.3.3 Western blotting

Protein blotting experiments used cold Dulbecco's phosphate buffered saline in which cells were lifted using a cell scraper. Harvested cells were then pelleted, and the supernatant was discarded. The full lysate was then recovered in a mixture of Pierce lysis IP buffer and Halt™ protease inhibitor cocktail (100:1), through disintegrating cell proteins, and samples were incubated on ice for 30 minutes. Proteins were then partitioned in the supernatant, after samples being centrifuged. Isolated proteins were directly transferred into fresh tubes, samples subjected to the BCA assay, and protein concentrations were determined.

PAGE electrophoresis was used to separate protein molecules, which were then Western blotted onto membranes. This was followed by incubation of these membranes in a blocking solution, 5% (w/v) dried skimmed milk and Tris buffered Saline with Tween®-20. Blocked membranes were probed with antibodies against protein targets, and a loading control (See section 2.5.4). Antibodies in this work, and their noted dilution ratios are rabbit monoclonal anti-GAP43 (Abcam ab134075, 1:1000), rabbit polyclonal anti-SK1 (Abcam ab66624, 1:5000), rabbit polyclonal anti-SK2 long and short isoforms (Abcam ab85401, 1:1000), rabbit polyclonal anti-SK3 (Abcam ab28631, 1:1000), rabbit monoclonal anti-Bcl-2 (Abcam ab32124, 1:1000), and mouse anti-GAPDH antibody (Sigma-Aldrich G9295, 1:50,000). These were all diluted and incubated with the membranes overnight, for 16 hours, using the blocking solution, with the exception of anti-GAPDH antibody. The next day, this antibody was incubated against the membrane for 45 minutes, after the membrane was washed with Tris buffered Saline with Tween®-20. The developing signals were documented at the following exposure times: 3 minutes, 2 minutes, 2 minutes, 3 minutes, 2 minutes, and 30 seconds, respectively.

3.3.4 SK channel pharmacology

In MTS cell viability experiments, the effect of the insult alone, SK1-4 potassium channel modulators alone, and these modulators in conjunction with the insult were assessed *in vitro* after 24 hours. In the case of survival effects, if any, target specification was ensured by testing the effect of the relevant SK channel blocker along with the SK channel activator-H₂O₂ combination. Briefly, SK channel effects on proliferation were screened in target cells, where there was no action, the next step proceeded to challenge cells with H₂O₂ alone to gain LD₅₀ values, and then these treatments were all combined. In these steps, overall relative viability was measured in MTS assays (See section 2.7.2) after the time indicated above.

3.4 Results

3.4.1 SK ion channel expression and modulation in human neuroblastoma SH-SY5Y cells

3.4.1.1 SK channel mRNA and protein investigation in human neuroblastoma SH-SY5Y cells

In this neurosurvival work and all subsequent sections of this study, experiments began by interrogating the presence of channels of interest, if any, in all cell targets. Here, reverse transcription-polymerase chain reaction (RT-PCR) was used to investigate the presence of the message for SK channel members (SK1-4) in neuroblastoma SH-SY5Y cells. This qualitative investigation indicated the presence of only $K_{ca2.1}$ (SK1), $K_{ca2.3}$ (SK3), and $K_{ca3.1}$ (SK4) channel transcripts (Subtypes) in both undifferentiated (Figure 3.1) and differentiated (Figure 3.2) SH-SY5Y cells.

This work also asked whether these channels are expressed at the protein level. In these two cell types, however, SK4 channel protein expression was not technically managed to be addressed. Unfortunately, specific antibodies used here, which were commercially obtained, did not work. Therefore, Western blotting targeting of this protein did not reveal any SK4 channel expression. Blotting of other proteins, namely SK1 (Figure 3.3) and SK3 (Figure 3.4), showed their protein expression in both forms of SH-SY5Y cells. However, SK1 channel is similarly expressed at the protein level (Figure 3.3). Variable results were found regarding the SK3 channel expression, where SK3 channel is distinctly downregulated in differentiated SH-SY5Y cells (Figure 3.4). This indicates that retinoic acid-induced SH-SY5Y cell differentiation apparently downregulated SK3 channel expression at the protein level.

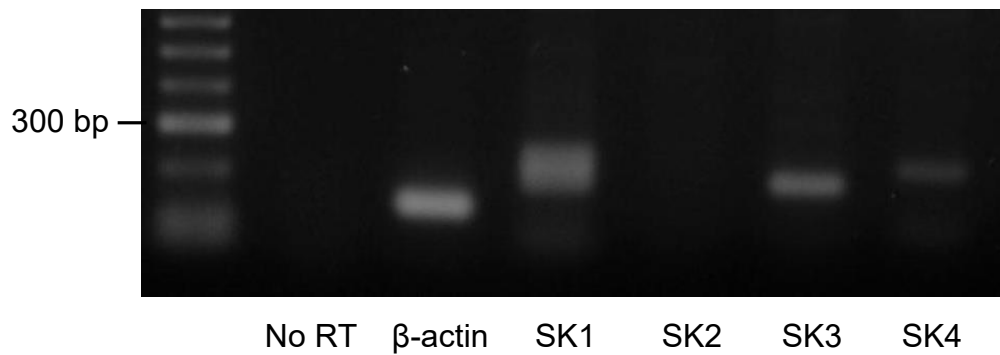


Figure 3.1 SK channel mRNA investigation in undifferentiated SH-SY5Y cells. Only the amplicons for SK1, SK3, and SK4 channels are present and the PCR products are of the predicted size. β -actin serves as the normalising control.

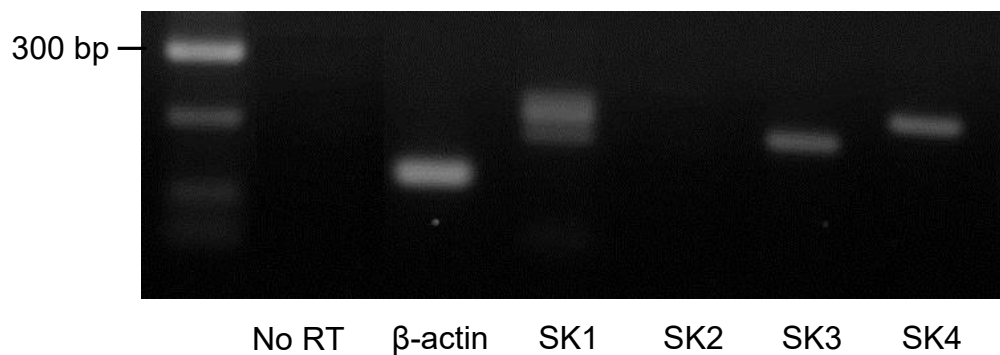


Figure 3.2 SK channel mRNA investigation in differentiated SH-SY5Y cells. Only the amplicons for SK1, SK3, and SK4 channels are present and the PCR products are of the predicted size. β -actin serves as the normalising control.

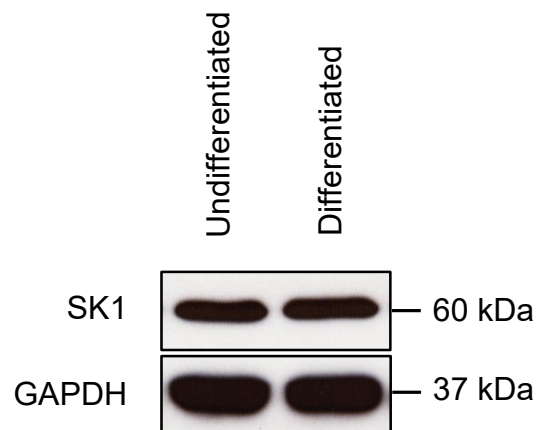


Figure 3.3 Representative immunoblot of SK1 channel subtype in SH-SY5Y cells. SK1 channel protein is expressed similarly in both undifferentiated and differentiated SH-SY5Y cells. GAPDH serves as the normalising control.

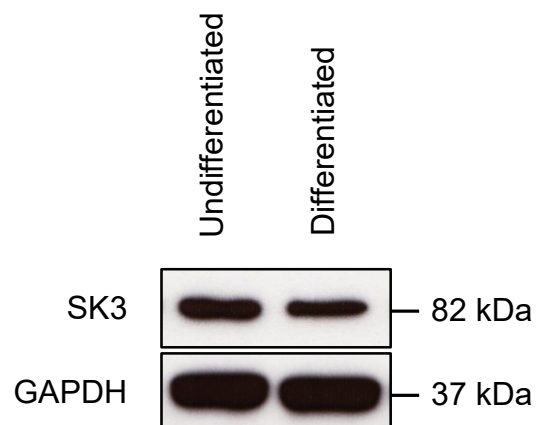


Figure 3.4 Representative immunoblot of SK3 channel subtype in SH-SY5Y cells. SK3 channel protein expression is visibly downregulated in differentiated cells compared to undifferentiated SH-SY5Y cells. GAPDH serves as the normalising control.

3.4.1.2 Neuroblastoma SH-SY5Y cell differentiation

These cells are neuroblastoma, and in this work an attempt was made to differentiate SH-SY5Y cells to a neuronal phenotype. In this protocol, experiments used retinoic acid (10 μ M) in the culture for seven days to achieve the phenotype. The action of this acid on these cells was assessed through monitoring the expression of growth associated protein-43 (GAP-43), a neuronal marker, upon differentiation at three different time courses. Protein blotting of GAP-43 showed that treatment with retinoic acid for 5 days *in vitro* produced a pronounced upregulation of GAP-43 (Figure 3.5). This also established that a seven day exposure to retinoic acid is perhaps sufficient to achieve a neuronal phenotype based on GAP-43 expression observation (Figure 3.5).

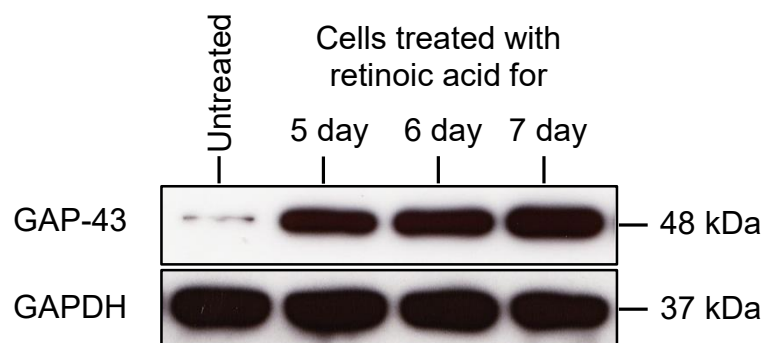


Figure 3.5 Representative immunoblot of growth associated protein-43 (GAP-43) in SH-SY5Y cells. GAP-43 protein expression is distinctly upregulated after treatment with retinoic acid in SH-SY5Y cells after 5 days. GAPDH serves as the normalising control.

3.4.1.3 The effect of SK channel modulators alone on human neuroblastoma SH-SY5Y cell viability

3.4.1.3.1 The effect of SK channel activators alone on SH-SY5Y cell viability

In vitro work then addressed the action of SK channel modulators, namely activators and blockers, alone on the viability of the cells of interest in the culture. The reason was to check whether these modulators alone exert any noticeable action on the viability, i.e. cell numbers, which can relatively be measured by MTS survival assay. This was necessary since these channel modulators were then screened in the presence of the insult of CNS cells, to test whether SK channel modulation, indeed activation based on the hypothesis, can rescue these cells from the degenerative neuronal insult. Here, it is important to note that the MTS viability assay is traditionally referred to as the MTS cell proliferation assay.

In this approach, experiments first considered the effect of SK channel activators, since it was predicted that SK channel activation might afford protection in the face of cellular degeneration using hydrogen peroxide (H₂O₂). In SH-SY5Y cells, SK channel activators were chosen according to the expression pattern in cells, and cells were challenged for 24 hours. It was found that SH-SY5Y cells were not affected by SK1 (Figures 3.6 and 3.7) and SK3 (Figures 3.8 and 3.9) channel openers in either undifferentiated or differentiated cells after 24 hours. Bracketing previously obtained EC₅₀ values, GW542573X (10-50 µM), and CyPPA (10-50 µM) did not significantly change SH-SY5Y cell growth. This was an encouraging result to advance with and to proceed this to the next step.

It is important to mention also that the working concentrations of the vehicle dimethyl sulfoxide (DMSO) had no effect on cell growth (Appendix 3, Figures 7.1, 7.2 and 7.3), and that any confounding effect was constantly considered in this study.

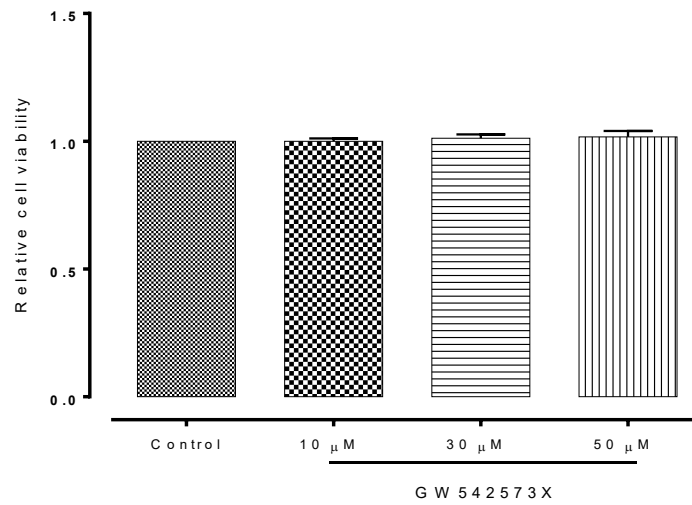


Figure 3.6 The effect of the SK1 channel activator, GW542573X, on undifferentiated SH-SY5Y cell viability. Data are shown as means \pm SEM. One-way ANOVA followed by Dunnett's post hoc test, n=6.

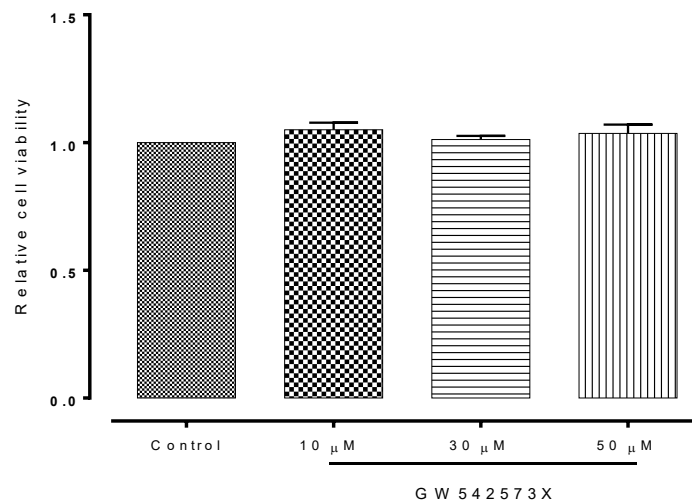


Figure 3.7 The effect of the SK1 channel activator, GW542573X, on differentiated SH-SY5Y cell viability. Data are shown as means \pm SEM. One-way ANOVA followed by Dunnett's post hoc test, n=6.

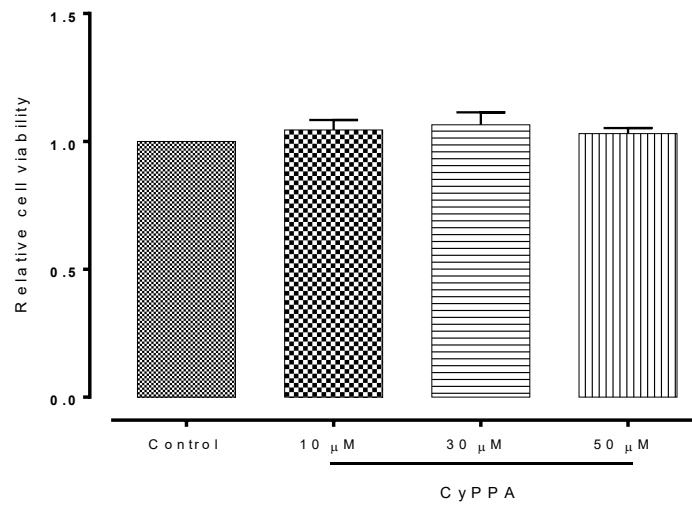


Figure 3.8 The effect of the SK2-3 channel activator, CyPPA, on undifferentiated SH-SY5Y cell viability. Data are shown as means \pm SEM. One-way ANOVA followed by Dunnett's post hoc test, $n=6$.

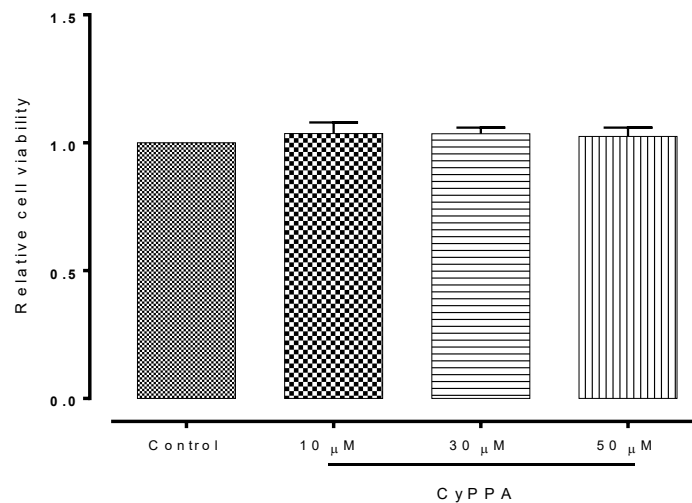


Figure 3.9 The effect of the SK2-3 channel activator, CyPPA, on differentiated SH-SY5Y cell viability. Data are shown as means \pm SEM. One-way ANOVA followed by Dunnett's post hoc test, $n=6$.

3.4.1.4 The effect of SK channel blockers alone on SH-SY5Y cell viability

SK channel blockers, again based on SK channel expression fashion in SH-SY5Y cells, were tested to show whether SK1 or SK3 channel inhibition modulated cell growth of these cells.

MTS viability assay showed that neither SK1 channel inhibition (Figures 3.10 and 3.11) through UCL1684 (3-10 nM), nor SK3 channel inhibition (Figures 3.12 and 3.13) by NS8593 (300 nM -1 μ M) significantly altered the SH-SY5Y growth after 24 hours. This is further demonstrating that not only SK1 and SK3 channel activation, but also SK1 and SK3 channel inhibition has no effect on SH-SY5Y cell viability after the time indicated.

Thus interestingly, SH-SY5Y cells do not favour SK molecules for their normal growth, and SK1 and SK3 channel modulators role can now be assessed in the face of degenerative oxidative stress using H₂O₂ and the MTS assay.

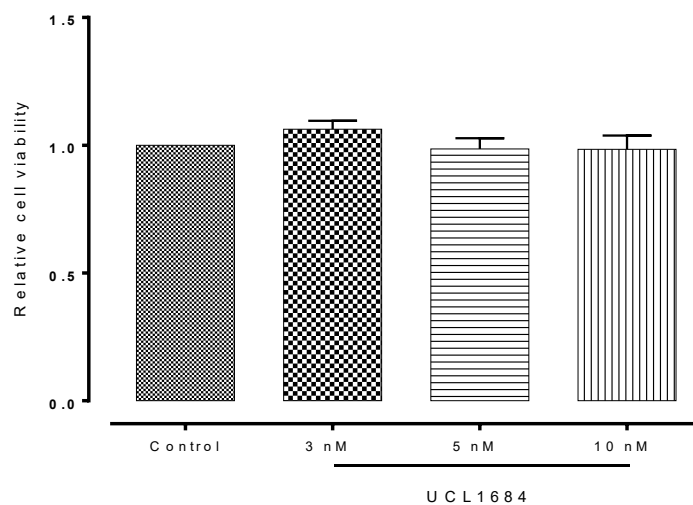


Figure 3.10 The effect of SK1-3 channel blocker, UCL1684, on undifferentiated SH-SY5Y cell viability. Data are shown as means \pm SEM. One-way ANOVA followed by Dunnett's post hoc test, $n=6$.

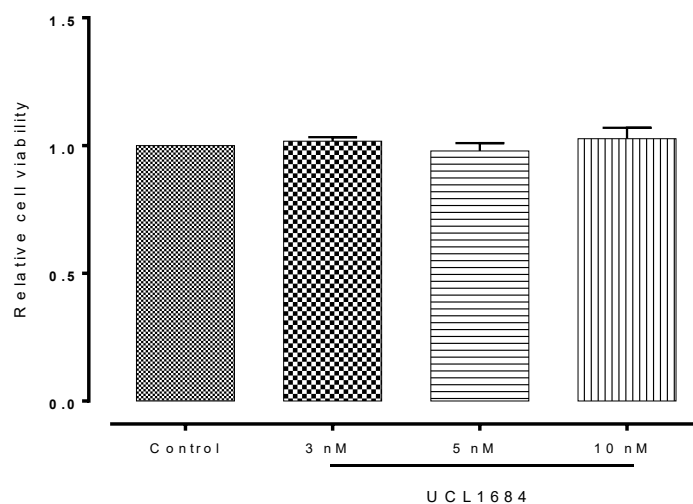


Figure 3.11 The effect of SK1-3 channel blocker, UCL1684, on differentiated SH-SY5Y cell viability. Data are shown as means \pm SEM. One-way ANOVA followed by Dunnett's post hoc test, $n=6$.

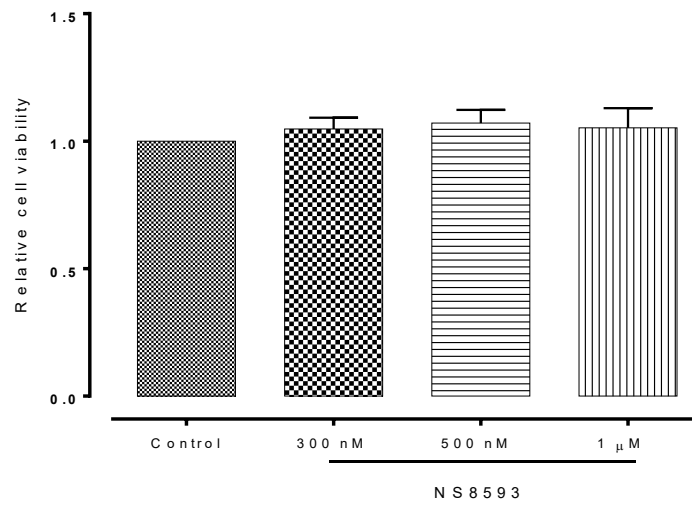


Figure 3.12 The effect of SK1-3 channel blocker, NS8593, on undifferentiated SH-SY5Y cell viability. Data are shown as means \pm SEM. One-way ANOVA followed by Dunnett's post hoc test, $n=6$.

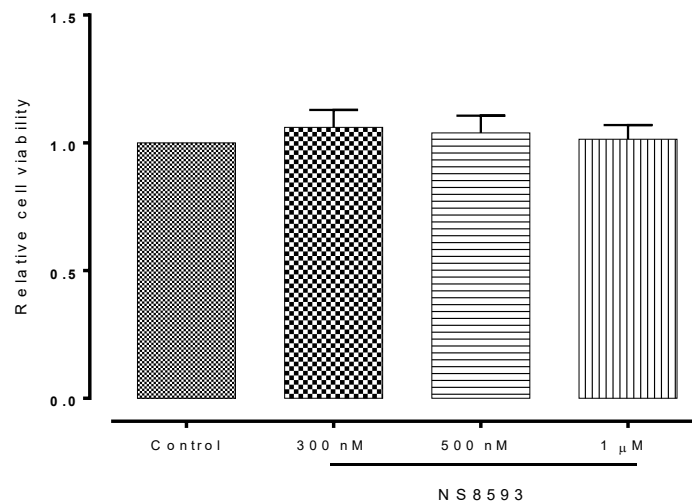


Figure 3.13 The effect of SK1-3 channel blocker, NS8593, on differentiated SH-SY5Y cell viability. Data are shown as means \pm SEM. One-way ANOVA followed by Dunnett's post hoc test, $n=6$.

3.4.1.5 The dose-response curve for hydrogen peroxide in human neuroblastoma SH-SY5Y cells

The effect of the insult, namely H₂O₂, alone was first determined on cells of interest to estimate the median lethal dose (LD₅₀). For these experiments here both undifferentiated and differentiated SH-SY5Y cells were challenged in the presence of H₂O₂ for 24 hours. The MTS assay showed that H₂O₂ itself significantly decreased SH-SY5Y cell numbers in a dose-dependent manner in undifferentiated (Figure 3.14) and differentiated (Figure 3.15) cells, and the LD₅₀ was similar for H₂O₂ in both cell types i.e. 450 µM.

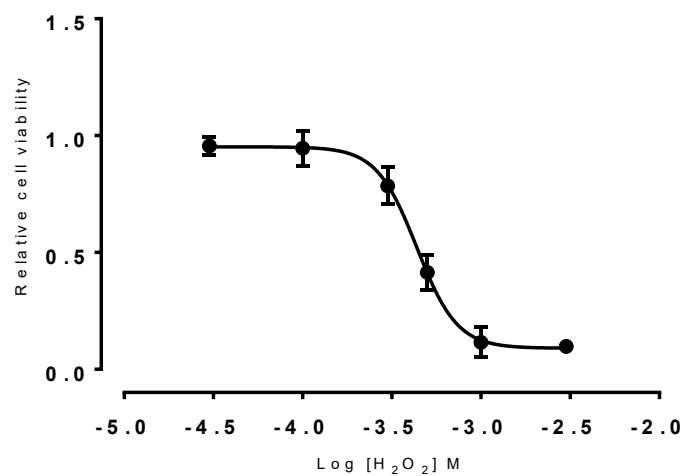


Figure 3.14 The effect of H₂O₂ on undifferentiated SH-SY5Y cell viability. From the line of best fit of the dose-response data, the LD₅₀ was 450 μ M, n= 9.

In this figure and all subsequent plots the data are shown as means \pm SEM.

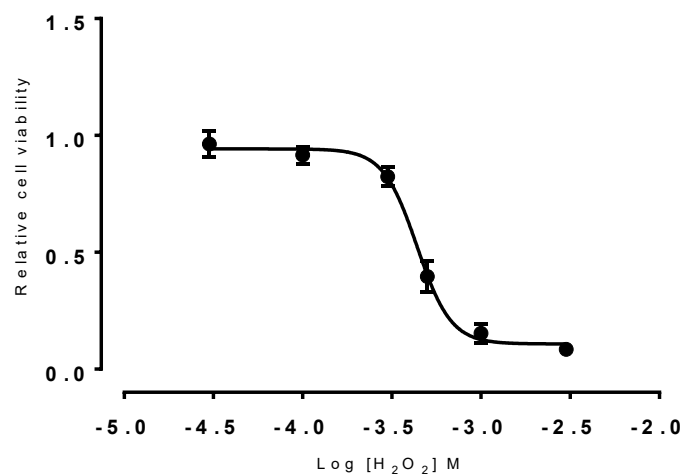


Figure 3.15 The effect of H₂O₂ on differentiated SH-SY5Y cell viability. From the line of best fit of the dose-response data, the LD₅₀ was 450 μ M, n= 9.

3.4.1.6 Pharmacological modulation of SK1 and SK3 channels in human neuroblastoma SH-SY5Y cells

3.4.1.6.1 Hydrogen peroxide-SK1 channel interaction

The next question asked was whether the SK channel subtypes represent a novel target for modulating oxidative stress in neurons? Because SK channels are well characterised molecules in pharmacology, the question can be selectively addressed, first investigating an SK1 channel role followed by an SK3 channel contribution. For the pharmacological approach here and in all subsequent sections, previously reported (EC_{50} s and IC_{50} s) of SK channel modulators were adopted. Commencing with the SK1 channel argument, MTS viability assay revealed that GW542573X (10 μ M - 40 μ M) afforded significant protection (p -value <0.0001 versus insult) against H_2O_2 -induced oxidative stress, which itself markedly reduced SH-SY5Y cell numbers by near 50%, in both undifferentiated and differentiated cells (Figures 3.16 and 3.18, respectively).

Intriguingly, the SK1-3 channel blocker UCL1684 (3 nM), through SK1 channel inhibition, in the presence of GW542573X (10 μ M - 40 μ M) fully abolished the protection achieved against H_2O_2 (Figures 3.17 and 3.19, respectively) in both cell types, this reversal ensured the specificity of channel target. These effects of SK1 channel modulators clearly indicate that these cells have oversight of oxidative stress through SK1 channel modulation.

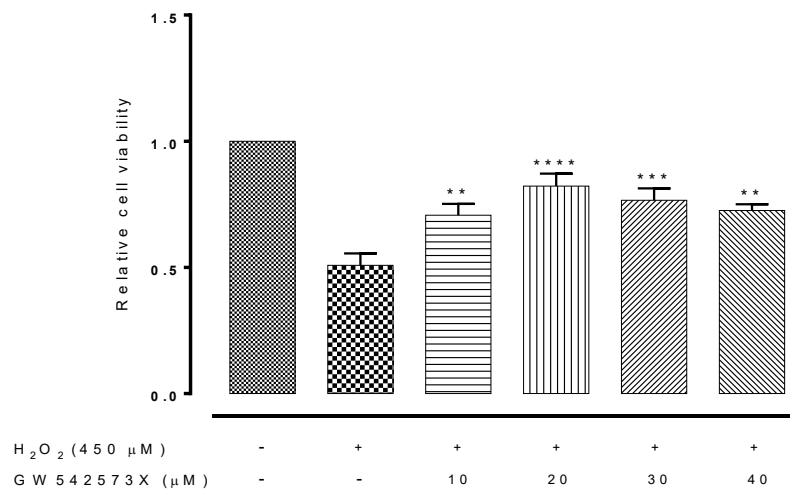


Figure 3.16 The effect of GW542573X, SK1 channel activation, on the survival of undifferentiated SH-SY5Y cells exposed to H₂O₂-induced oxidative stress. Data are shown as means \pm SEM. *****p*-value < 0.0001 versus insult, one-way ANOVA followed by Dunnett's post hoc test, n =9.

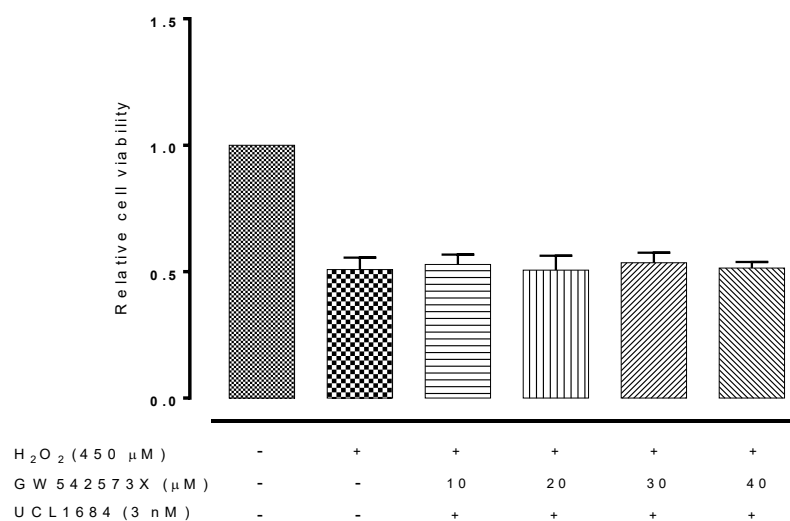


Figure 3.17 The effect of GW542573X, an SK1 channel activator, in the presence of SK1-3 blocker, UCL1684, on the survival of undifferentiated SH-SY5Y cells exposed to H₂O₂-induced oxidative stress. Data are shown as means \pm SEM. One-way ANOVA followed by Dunnett's post hoc test, n=9.

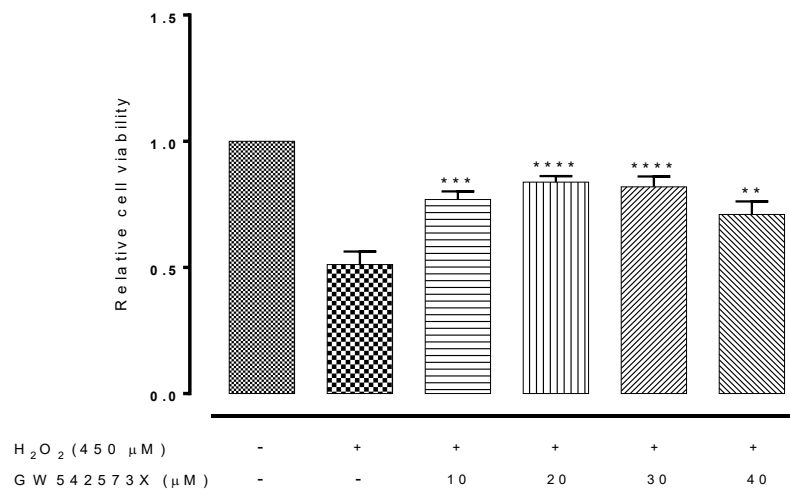


Figure 3.18 The effect of GW542573X, an SK1 channel activator, on the survival of differentiated SH-SY5Y cells exposed to H₂O₂-induced oxidative stress. Data are shown as means \pm SEM. *****p*-value < 0.0001 versus insult, one-way ANOVA followed by Dunnett's post hoc test, n =9.

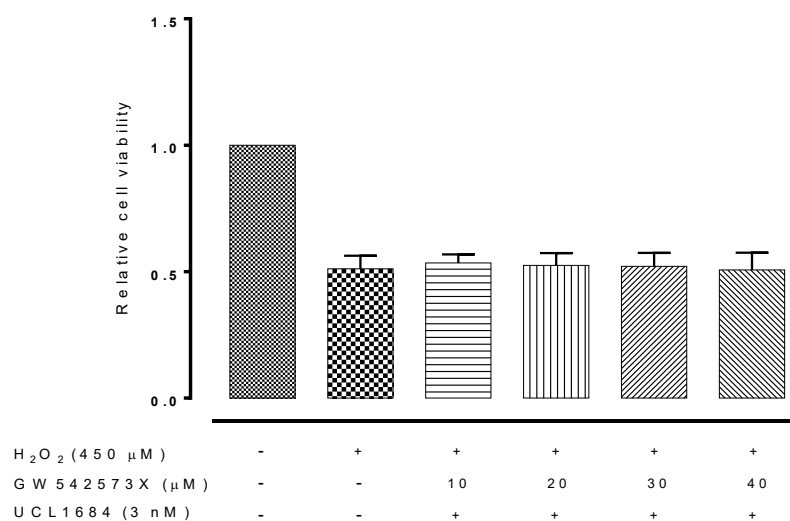


Figure 3.19 The effect of GW542573X, an SK1 channel activator, in the presence of SK1-3 channel blocker, UCL1684, on the survival of differentiated SH-SY5Y cells exposed to H₂O₂-induced oxidative stress. Data are shown as means \pm SEM. One-way ANOVA followed by Dunnett's post hoc test, n=9.

3.4.1.6.2 Hydrogen peroxide-SK3 channel interaction

As shown above SK1 channel opening can rescue SH-SY5Y cells from H₂O₂-induced oxidative stress. The resident SK3 channel was the next candidate to investigate in both undifferentiated and differentiated cells, to test also in the face of oxidative stress with H₂O₂. In MTS viability assay, the insult alone produced a dramatic reduction in cell numbers by near 50%, whereas SK3 channel activation, CyPPA (10 μM- 40 μM), significantly reversed the decrease in undifferentiated (Figure 3.20) and differentiated (Figure 3.23) SH-SY5Y cell numbers produced by H₂O₂. To identify the channel target, an SK1-3 blocker, UCL1684, was first used in the mix to test whether it can abolish the protection afforded by SK3 channel activation. UCL1684 (3 nM) did not abolish the protection mediated by the relevant SK3 activators (Appendix 3, Figure 7.4). It was then decided to raise the concentration of the compound to 10 nM, where it was found that UCL1684 (10 nM) partially reversed the action of the SK3 channel activator in undifferentiated (Figure 3.21) and differentiated (Figure 3.24) SH-SY5Y cells. The reason that UCL1684 had a little action on the SK3 channel induced protection will be addressed in the discussion. Pharmacological experiments then probed another generic SK1-3 channel blocker, NS8593, at the relevant concentration. NS8593 (750 nM) reversed the survival effect afforded by CyPPA, the relevant SK3 activator, in undifferentiated (Figure 3.22) and differentiated (Figure 3.25) SH-SY5Y cells. In the light of these data, further work largely focused on the NS8593 compound, an SK1-3 channel blocker, to target SK3 channel in all subsequent sections.

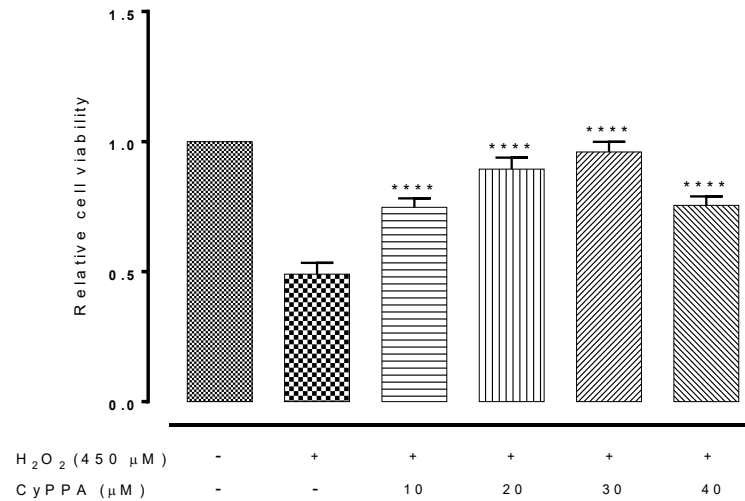


Figure 3.20 The effect of CyPPA, SK3 channel activation, on the survival of undifferentiated SH-SY5Y cells exposed to H₂O₂-induced oxidative stress. Data are shown as means \pm SEM. **** p -value < 0.0001 versus insult, one-way ANOVA followed by Dunnett's post hoc test, $n = 9$.

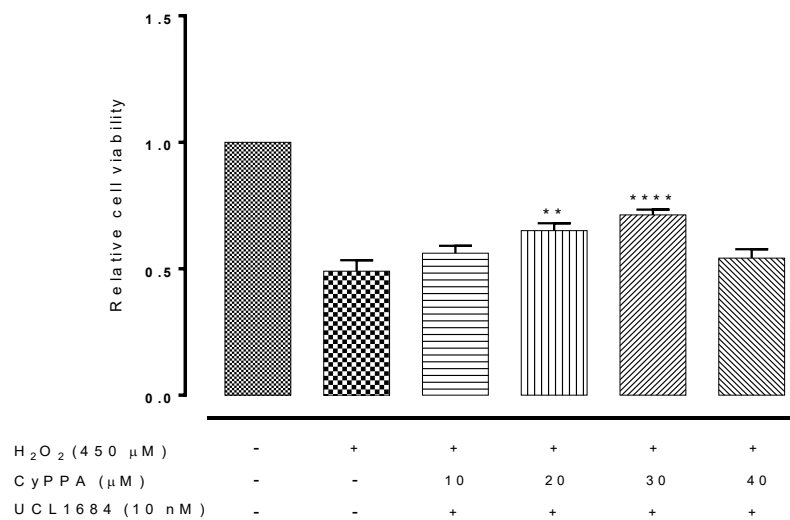


Figure 3.21 The effect of CyPPA, an SK2-3 channel activator, in the presence of the SK1-3 channel blocker, UCL1684, on the survival of undifferentiated SH-SY5Y cells exposed to H₂O₂-induced oxidative stress. Data are shown as means \pm SEM. **** p -value < 0.0001 versus insult, one-way ANOVA followed by Dunnett's post hoc test, $n = 9$.

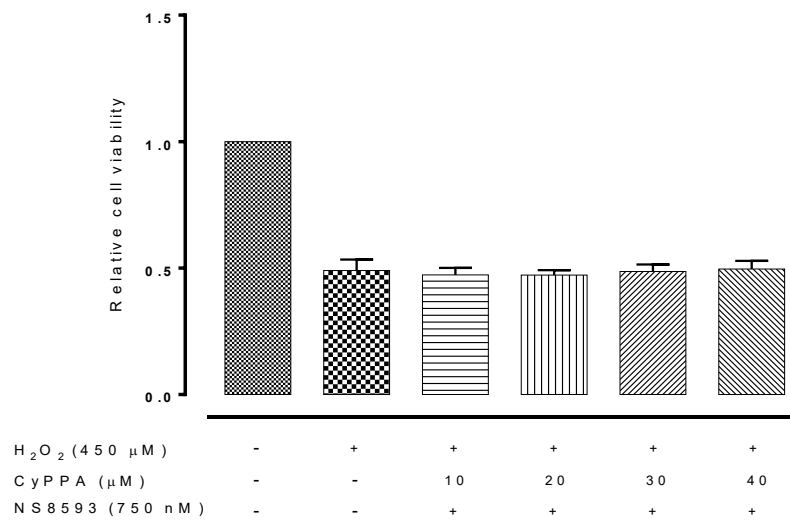


Figure 3.22 The effect of CyPPA, an SK2-3 channel activator, in the presence of SK1-3 channel blocker, NS8593, on the survival of undifferentiated SH-SY5Y cells exposed to H₂O₂-induced oxidative stress. Data are shown as means ± SEM. One-way ANOVA followed by Dunnett's post hoc test, n=9.

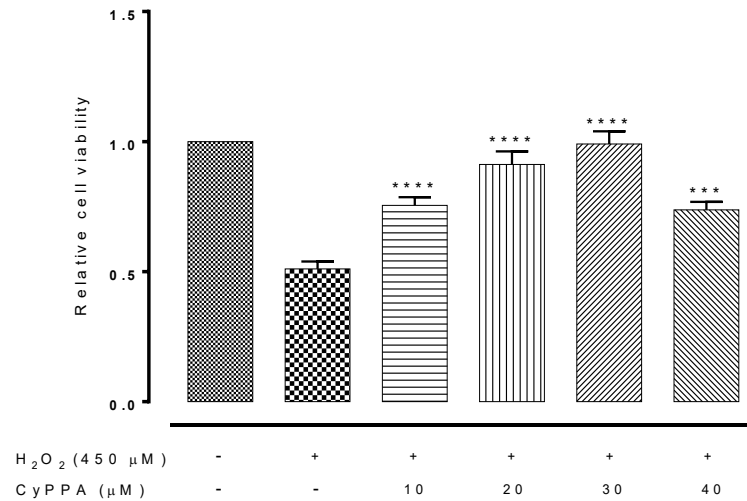


Figure 3.23 The effect of CyPPA, SK3 channel activation, on the survival of differentiated SH-SY5Y cells exposed to H₂O₂-induced oxidative stress. Data are shown as means \pm SEM. *****p*-value < 0.0001 versus insult, one-way ANOVA followed by Dunnett's post hoc test, n =9.

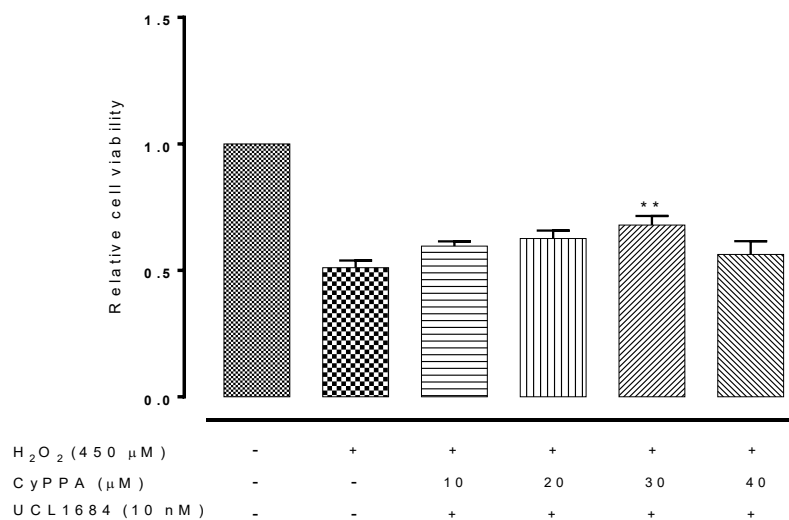


Figure 3.24 The effect of CyPPA, an SK2-3 channel activator, in the presence of SK1-3 blocker, UCL1684, on the survival of differentiated SH-SY5Y cells exposed to H₂O₂-induced oxidative stress. Data are shown as means \pm SEM. ****p*-value < 0.01 versus insult, one-way ANOVA followed by Dunnett's post hoc test, n =9.

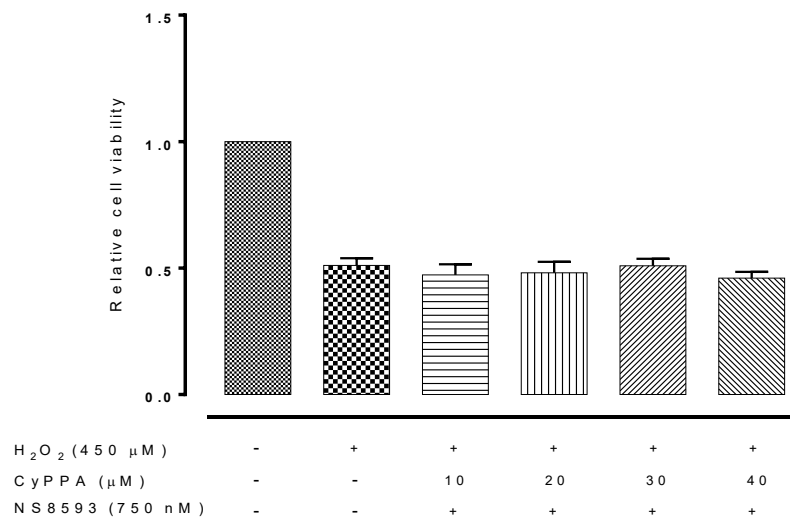


Figure 3.25 The effect of CyPPA, an SK2-3 channel activator, in the presence of SK1-3 channel blocker, NS8593, on the survival of differentiated SH-SY5Y cells exposed to H_2O_2 -induced oxidative stress. Data are shown as means \pm SEM. One-way ANOVA followed by Dunnett's post hoc test, $n=9$.

3.4.2 SK ion channel expression and modulation in mouse model of Huntington's (*STHdh*) striatal cells

To further test the hypothesis, mouse striatal neurons were also used in this work, being attractive candidates for several reasons. Firstly, these cells were directly derived from primary neurons. Secondly, it has been known that striatal cells among CNS neurons are very sensitive to oxidative stress (Trettel et al. 2000). It was thought interesting to test the hypothesis not only on human cells, but also on these mouse cells.

3.4.2.1 SK channel mRNA and protein investigation in mouse *STHdh* striatal cells

Initially, RT-PCR was employed to test for the existence of SK1-4 channels, if any, in the target cells. This proved a fascinating adventure in the context of SK1-4 channel expression in wild-type (*STHdh⁺/Hdh⁺*) and the mutant *Hdh^{Q111}* knock-in mouse striatal cells, namely heterozygous (*STHdh^{Q111}/Hdh⁺*) and homozygous (*STHdh^{Q111}/Hdh^{Q111}*), a cell model of Huntington's disease. Wild-type *STHdh⁺/Hdh⁺* cells exhibit *K_{ca}2.1* (SK1), *K_{ca}2.3* (SK3), and *K_{ca}3.1* (SK4) channel transcripts (Figure 3.26). Mutant heterozygous (*STHdh^{Q111}/Hdh⁺*) cells, however, express only *K_{ca}2.1* (SK1) and *K_{ca}2.2* (SK2) channel messages (Figure 3.27). Intriguingly, mutant homozygous (*STHdh^{Q111}/Hdh^{Q111}*) cells lacked SK2 and SK3 channels (Figure 3.28). It is important to highlight here that it has been shown that SK1 channel cDNA is not functional in mouse and this will be considered in the discussion.

At the protein level, Western blotting confirmed SK2 channel expression in mutant heterozygous *STHdh^{Q111}/Hdh⁺* cells. Here, the anti-SK2 antibody detected both long (SK2-L) and short (SK2-S) isoforms of the channel (Figure 3.29). Western blotting

also showed that the wild-type *STHdh⁺/Hdh⁺* cells express SK3 channels (Figure 3.30) at the protein level. These results mirrored the RT-PCR results in both cell types.

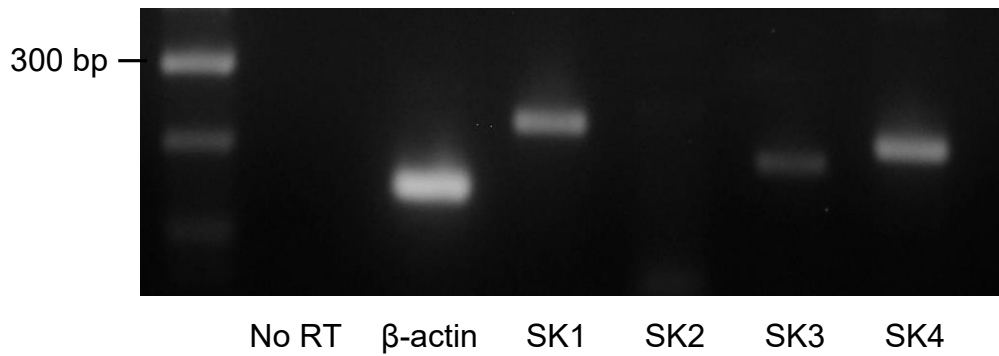


Figure 3.26 SK channel mRNA investigation in wild-type *Hdh^{+/Hdh}* cells. Only the amplicons for SK1, SK3 and SK4 channels are present and the PCR products are of the predicted size. β -actin serves as the normalising control.

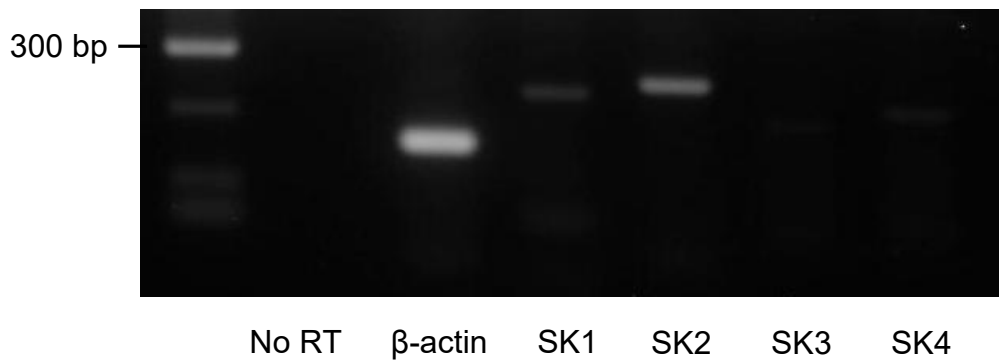


Figure 3.27 SK channel mRNA investigation in heterozygous mutant *Hdh^{Q111/Hdh}* cells. Only the amplicons for SK1 and SK2 channels are present and the PCR products are of the predicted size. β -actin serves as the normalising control.

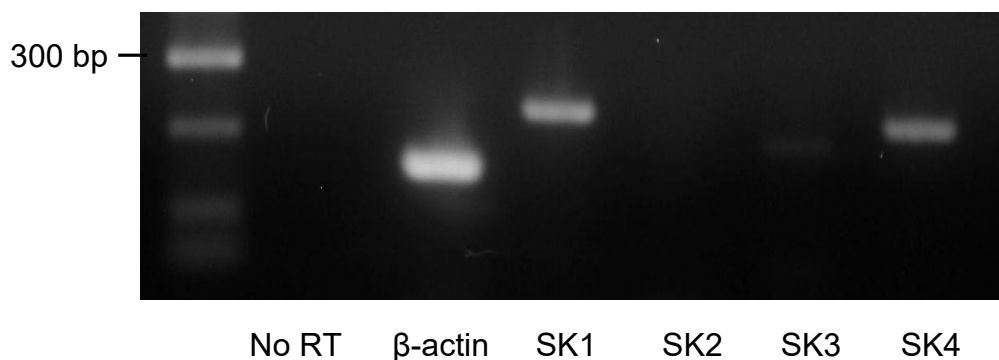


Figure 3.28 SK channel mRNA investigation in homozygous mutant *Hdh^{Q111/Hdh^{Q111}}* cells. Only the amplicons for SK1 and SK4 channels are present and the PCR products are of the predicted size. β -actin serves as the normalising control.

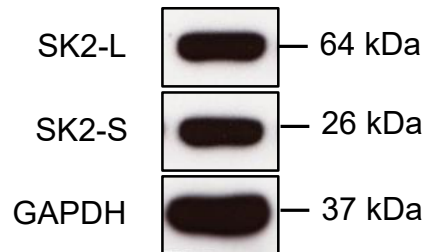


Figure 3.29 Representative immunoblot of SK2 channel subtype in heterozygous mutant *Hdh^{Q111}/Hdh⁺* cells. GAPDH serves as the normalising control. SK2 channel isoforms, SK2 long and SK2 short, are expressed in the cells.

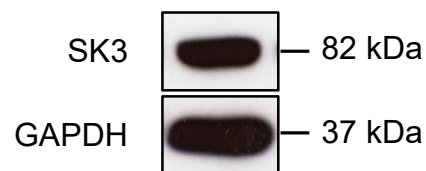


Figure 3.30 Representative immunoblot of SK3 channel subtype in wild-type *Hdh⁺/Hdh⁺* cells. GAPDH serves as the normalising control.

3.4.2.2 The effect of SK channel modulators alone on mouse *STHdh* striatal cells

3.4.2.2.1 The effect of SK channel activators alone on *STHdh* cell viability

As above, the effect of the SK modulators were systematically approached. The viability of mouse striatal cells in culture was challenged in the presence of SK1-4 channel openers alone for 24 hours, to check whether these modulators alone modify cell growth in these cells. The relevant SK channel activators, based on the expression pattern of SK1-4 channels in these cell types, were tested against cell growth. As seen in the case of SH-SY5Y cells, SK channel activation produced no significant change in mouse striatal cells growth rate. Pharmacological modification of the SK3 or SK4 channel using an SK2-3 activator, CyPPA (10-50 μ M), and SK4 channel opener NS309 (30-100 nM) produced no significant effect on wild-type *Hdh^{+/Hdh⁺}* cell viability of mouse striatal cells (Figures 3.31 and 3.32, respectively). Similarly, screening of CyPPA (10-50 μ M) against heterozygous mutant *Hdh^{Q111/Hdh⁺}* viability did not modify cell growth (Figure 3.33). It was not surprising that SK channel modulation was also ineffective on homozygous mutant *Hdh^{Q111/Hdh^{Q111}}* cell viability (Figure 3.34) using NS309 (30-100 nM), an SK4 channel activator. The next step was to test the effect of the SK channel blockers on these cells.

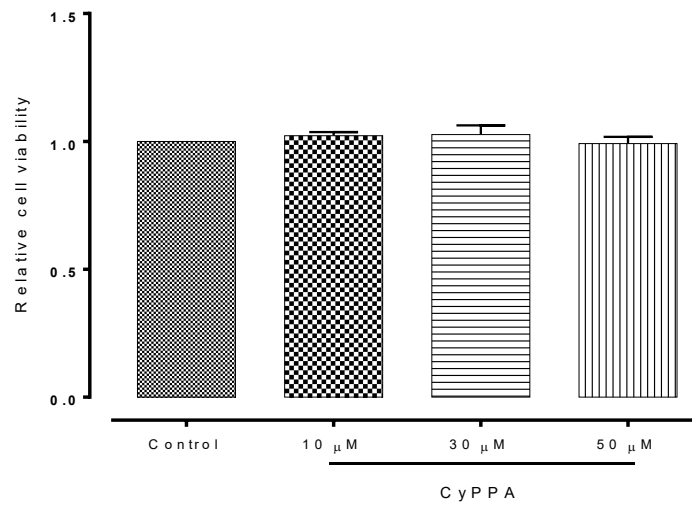


Figure 3.31 The effect of SK2-3 channel activator, CyPPA, on wild-type *Hdh*^{+/Hdh} cell viability. Data are shown as means ± SEM. One-way ANOVA followed by Dunnett's post hoc test, n=6.

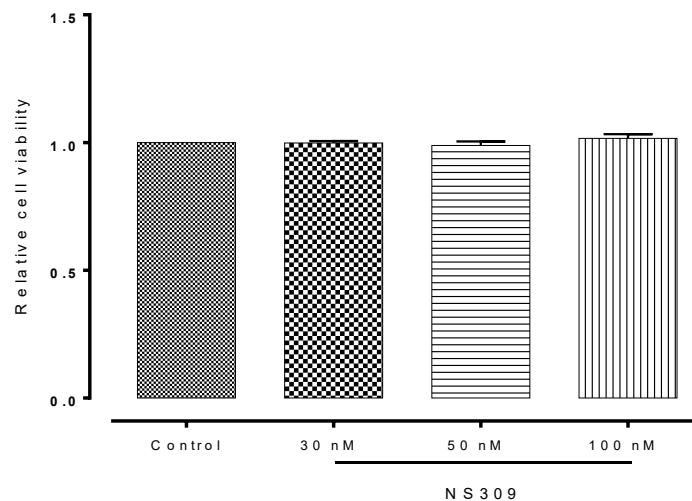


Figure 3.32 The effect of SK4 channel activator, NS309, on wild-type *Hdh*^{+/Hdh} cell viability. Data are shown as means ± SEM. One-way ANOVA followed by Dunnett's post hoc test, n=6.

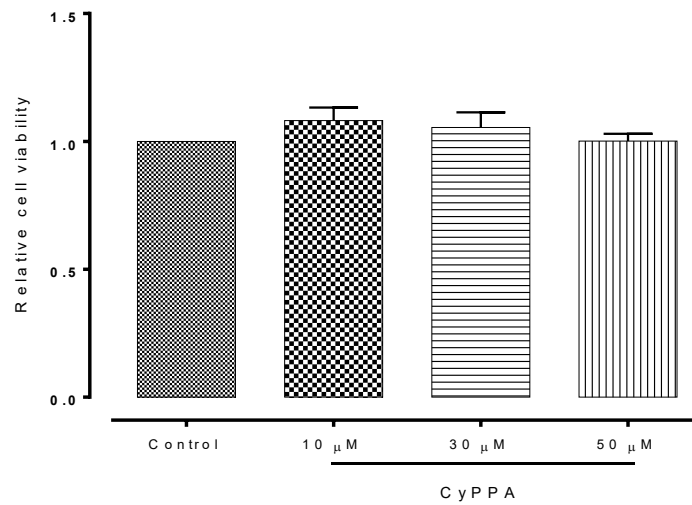


Figure 3.33 The effect of SK2-3 channel activator, CyPPA, on heterozygous mutant *Hdh^{Q111}/Hdh⁺* cell viability. Data are shown as means ± SEM. One-way ANOVA followed by Dunnett's post hoc test, n=6.

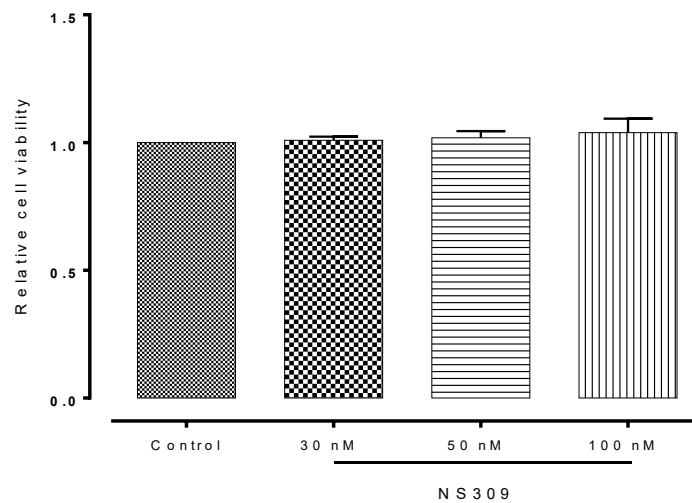


Figure 3.34 The effect of SK4 channel activator, NS309, on homozygous mutant *Hdh^{Q111}/Hdh^{Q111}* cell viability. Data are shown as means ± SEM. One-way ANOVA followed by Dunnett's post hoc test, n=6.

3.4.2.2.2 The effect of SK channel blockers alone on *STHdh* cell viability

To determine whether SK channel blocking impacts on mouse striatal cell growth, the relevant SK1-4 channel blockers were also pharmacologically screened against *STHdh* cell growth. SK1-4 channel inhibition also did not affect cell growth after 24 hours, in an MTS assay. In wild-type cells, neither SK3 channel blockade by NS8593 (300 nM-1 μ M), nor SK4 channel inhibition by the SK4 channel blockers, TRAM-34 (50-300 nM) or NS6180 (10-50 nM), significantly affected *Hdh*^{+/+}*Hdh*⁺ cell numbers (Figures 3.35, 3.36 and 3.37, respectively). Heterozygous mutant *Hdh*^{Q111}/*Hdh*⁺ cells showed a similar lack of response to UCL1684 (3-10 nM), an SK1-3 channel blocker (Figure 3.38). Moreover, homozygous mutant *Hdh*^{Q111}/*Hdh*^{Q111} cells were unresponsive to the SK4 channel blocking action (Figures 3.39 and 40) of TRAM-34 (50-300 nM), and NS6180 (10-50 nM) respectively.

These results meant that the next steps can be performed to finalise the work on neurons beginning with measuring the LD₅₀ of the insult (H₂O₂) on these cell types.

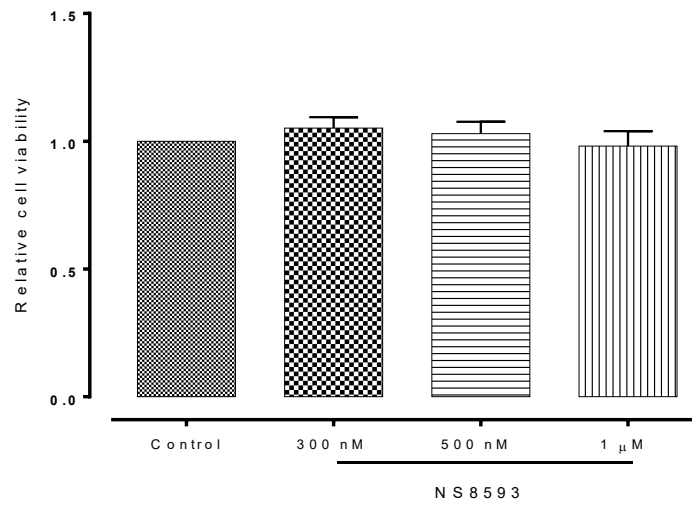


Figure 3.35 The effect of SK1-3 channel blocker, NS8593, on wild-type *Hdh*^{+/+}*Hdh*⁺ cell viability. Data are shown as means ± SEM. One-way ANOVA followed by Dunnett's post hoc test, n=6.

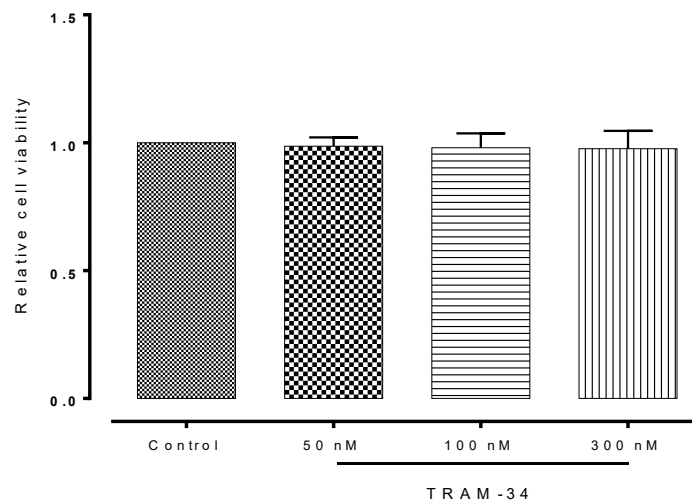


Figure 3.36 The effect of SK4 channel blocker, TRAM-34, on wild-type *Hdh*^{+/+}*Hdh*⁺ cell viability. Data are shown as means ± SEM. One-way ANOVA followed by Dunnett's post hoc test, n=6.

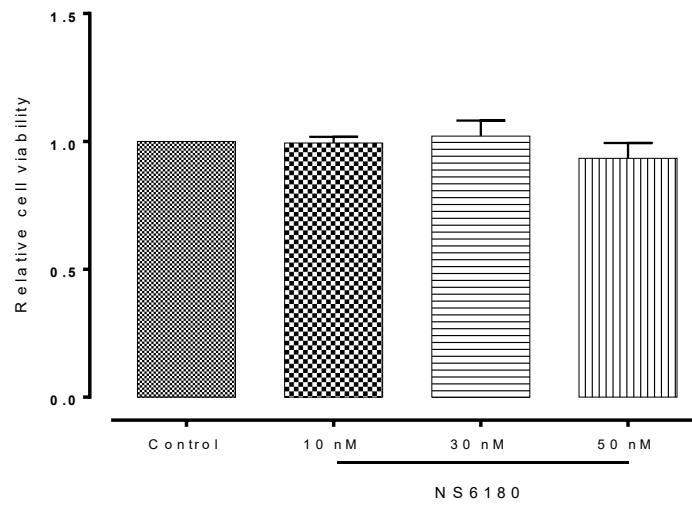


Figure 3.37 The effect of SK4 channel blocker, NS6180, on wild-type *Hdh*^{+/Hdh} cell viability. Data are shown as means ± SEM. One-way ANOVA followed by Dunnett's post hoc test, n=6.

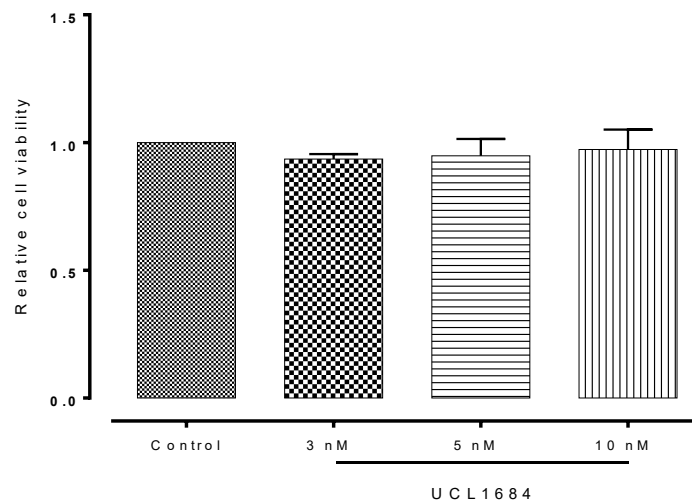


Figure 3.38 The effect of SK1-3 channel blocker, UCL1684, on heterozygous mutant *Hdh*^{Q111/Hdh} cell viability. Data are shown as means ± SEM. One-way ANOVA followed by Dunnett's post hoc test, n=6.

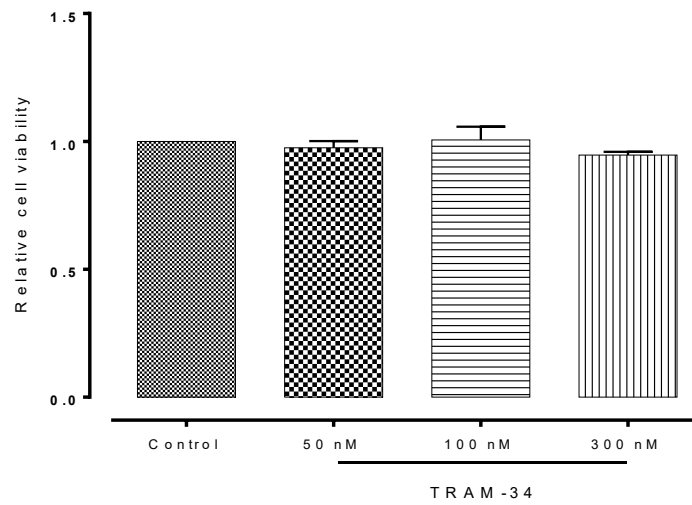


Figure 3.39 The effect of SK4 channel blocker, TRAM-34, on homozygous mutant *Hdh^{Q111}/Hdh^{Q111}* cell viability. Data are shown as means ± SEM. One-way ANOVA followed by Dunnett's post hoc test, n=6.

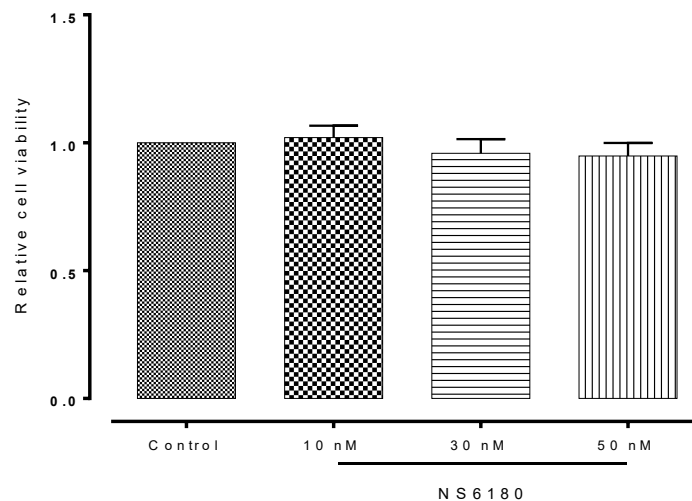


Figure 3.40 The effect of SK4 channel blocker, NS6180, on homozygous mutant *Hdh^{Q111}/Hdh^{Q111}* cell viability. Data are shown as means ± SEM. One-way ANOVA followed by Dunnett's post hoc test, n=6.

3.4.2.3 The dose-response curve for hydrogen peroxide in mouse *STHdh* striatal cells

MTS assay measured the effect of H₂O₂ at 24 hours, and determined from the dose-response curve the LD₅₀. It was clear that wild-type *Hdh*^{+/+}*Hdh*⁺ and mutant *Hdh*^{Q111} striatal cells, namely heterozygous *Hdh*^{Q111}/*Hdh*⁺ and homozygous *Hdh*^{Q111}/*Hdh*^{Q111}, respond similarly to H₂O₂-induced oxidative stress with an approximate LD₅₀ of ~ 1 mM (Figures 3.41, 42 and 3.43, respectively). These data show that the dominating Huntington's gene in mouse striatal cells had no role in terms of responsiveness to oxidative stress compared to its wild-type counterpart.

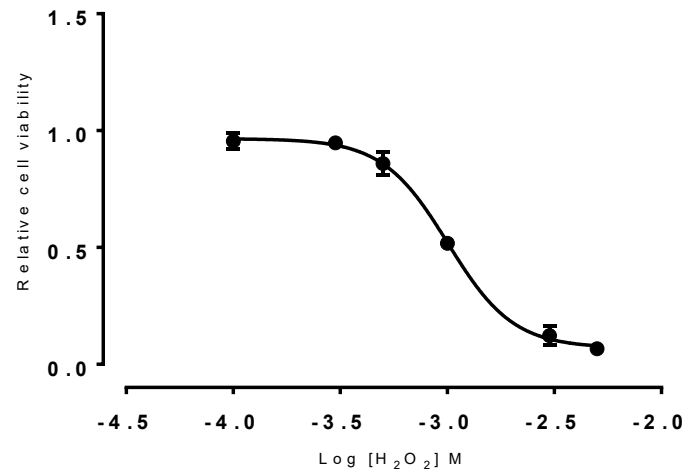


Figure 3.41 The effect of H₂O₂ on wild-type *Hdh*^{+/+} cell viability. From the line of best fit of the dose-response data, the LD₅₀ was 1 mM, n= 9.

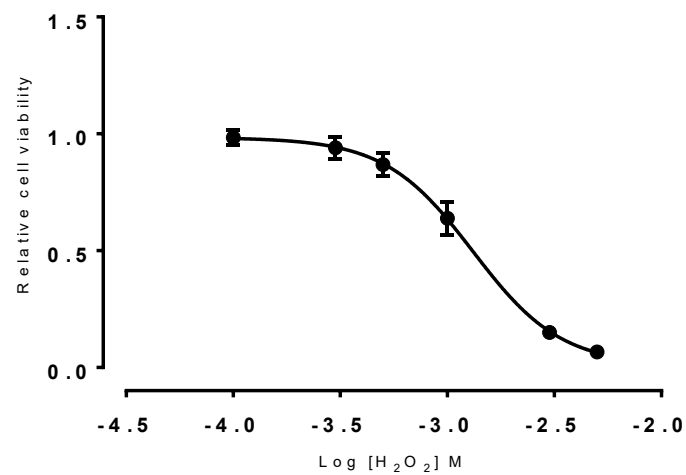


Figure 3.42 The effect of H₂O₂ on heterozygous mutant *Hdh*^{Q111/+} cell viability. From the line of best fit of the dose-response data, the LD₅₀ was 1 mM, n= 9.

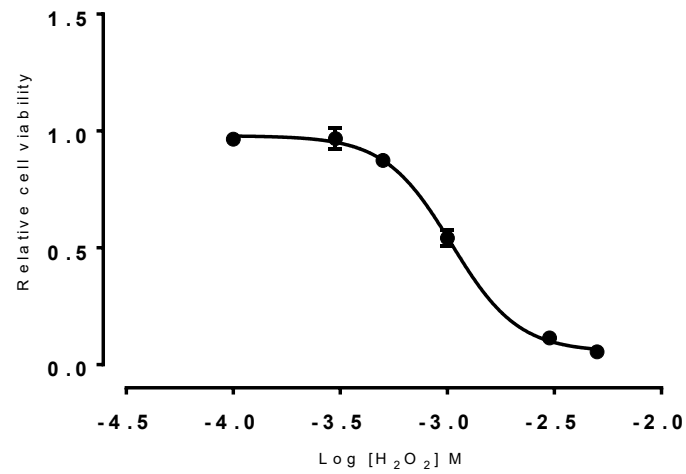


Figure 3.43 The effect of H₂O₂ on homozygous mutant *Hdh*^{Q111}/*Hdh*^{Q111} cell viability. From the line of best fit of the dose-response data, the LD₅₀ was 1 mM, n= 9.

3.4.2.4 Pharmacological modulation of SK channels in mouse STHdh striatal cells

3.4.2.4.1 Hydrogen peroxide-SK2 channel interaction

Experiments then challenged SK channels in the presence of the oxidative stress insult in striatal neurons. Because it was reported that the SK1 gene does not form functional SK1 channel proteins, its role was not addressed in this work. As shown in the SK1-4 channel expression section, SK2 channel was uniquely expressed in heterozygous mutant *Hdh^{Q111}/Hdh⁺* cells. Screening of this mutant cell type with an SK2 channel activator, CyPPA (20 μ M - 40 μ M), in the presence of H₂O₂ significantly (p -value<0.0001 versus insult) rescued mutant *Hdh^{Q111}/Hdh⁺* cells (Figure 3.44). UCL1684 (3 nM) completely reversed (Figure 3.45) the activity of the relevant SK2 channel activator, CyPPA, on the channel.

Since, the SK3 channel is expressed in wild-type cells, a role for this channel is now explored.

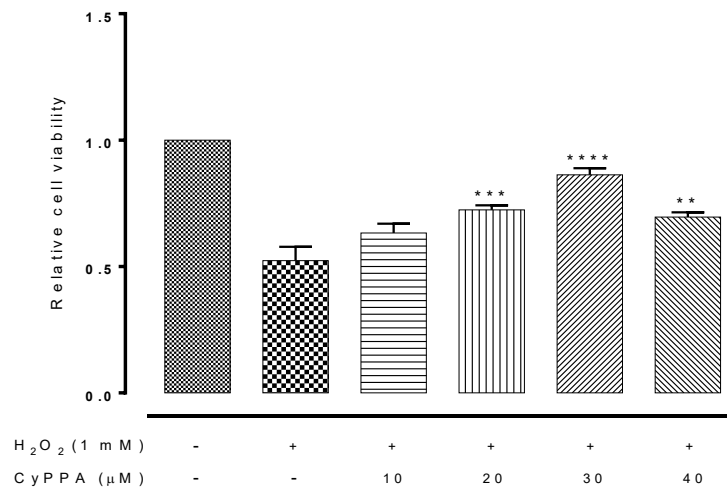


Figure 3.44 The effect of CyPPA, SK2 channel activation, on the survival of heterozygous mutant *Hdh^{Q111}/Hdh⁺* cells exposed to H₂O₂-induced oxidative stress. Data are shown as means ± SEM. *****p*-value < 0.0001 versus insult, one-way ANOVA followed by Dunnett's post hoc test, n=9.

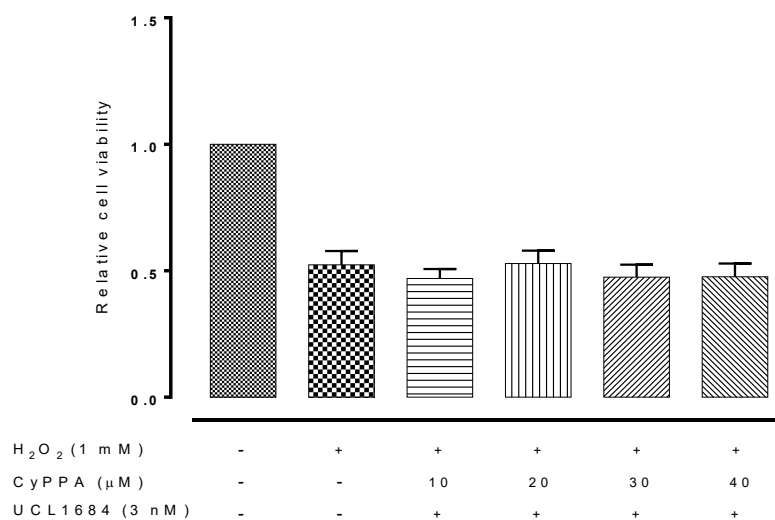


Figure 3.45 The effect of CyPPA, an SK2-3 channel activator, in the presence of SK1-3 blocker, UCL1684, on the survival of heterozygous mutant *Hdh^{Q111}/Hdh⁺* cells exposed to H₂O₂-induced oxidative stress. Data are shown as means ± SEM. One-way ANOVA followed by Dunnett's post hoc test, n=9.

3.4.2.4.2 Hydrogen peroxide-SK3 channel interaction

Whether another SK channel member behaves similarly against oxidative stress was now addressed. In wild-type *Hdh^{+/Hdh⁺}* cells, CyPPA activation of the SK3 channel, under conditions of H₂O₂-induced oxidative stress, again markedly challenged H₂O₂ (*p*-value<0.0001 versus insult) after 24 hours (Figure 3.46). Here, the protective effect of CyPPA was combined with SK3 channel inhibition using NS8593 (750 nM). As expected, this resulted in the abolishing of CyPPA activity (Figure 3.47).

These data would indicate that SK channels are promising targets against the deleterious effects of oxidative stress which is often said to underlie cell demise in neurodegenerative diseases.

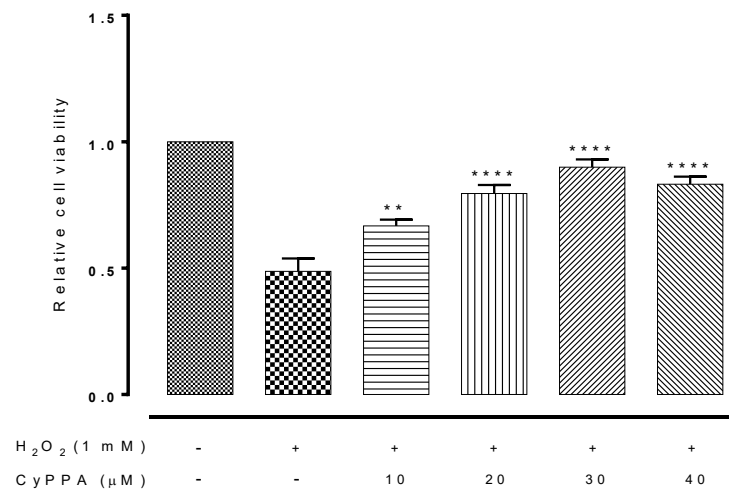


Figure 3.46 The effect of CyPPA, an SK2-3 channel activator, on the survival of wild-type *Hdh*^{+/Hdh} cells exposed to H₂O₂-induced oxidative stress. Data are shown as means ± SEM. *****p*-value < 0.0001 versus insult, one-way ANOVA followed by Dunnett's post hoc test, n =9.

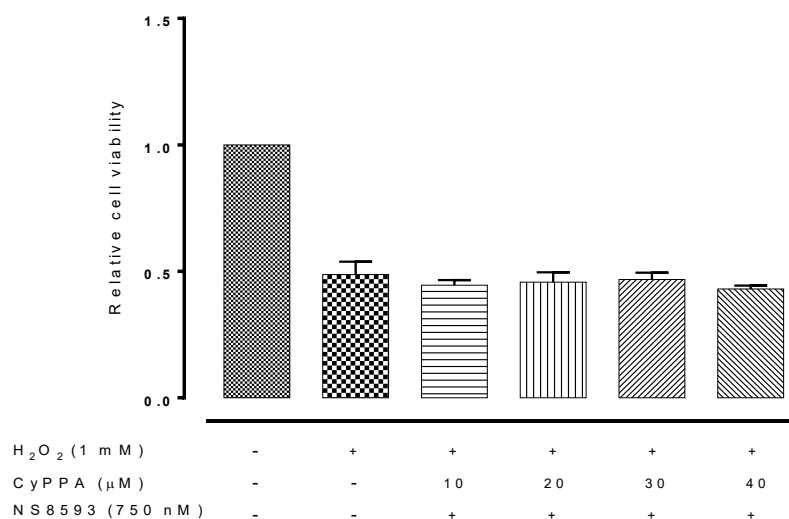


Figure 3.47 The effect of CyPPA, an SK2-3 channel activator, in the presence of SK1-3 blocker, NS8593, on the survival of wild-type *Hdh*^{+/Hdh} cells exposed to H₂O₂-induced oxidative stress. Data are shown as means ± SEM. One-way ANOVA followed by Dunnett's post hoc test, n=9.

3.4.2.4.3 Hydrogen peroxide-SK4 channel interaction

This section concludes by asking whether the SK4 channel subtype is still a target for blocking oxidative stress? The IK (SK4) channel is distinctive, having its own biophysical and pharmacological features. The SK4 resident channel was further targeted in wild-type *Hdh⁺/Hdh⁺* and homozygous mutant *Hdh^{Q111}/Hdh^{Q111}* cells. Results confirmed that SK4 also favoured this category of neurosurvival. Activation of this ion channel by NS309 (20-40 nM) also rescued (p -value<0.0001 versus insult) these cells from oxidative stress (Figures 3.48 and 3.51) in wild-type *Hdh⁺/Hdh⁺* and homozygous mutant *Hdh^{Q111}/Hdh^{Q111}* cells respectively. Experiments then used the SK4 blockers, TRAM-34 (100 nM) and NS6180 (30 nM), to test whether these blockers can eliminate the protection afforded by SK4 channel activation. Parallel blocking of SK4 channel fully blunted the channel protective role of activators in wild-type *Hdh⁺/Hdh⁺* (Figures 3.49 and 3.50, respectively), and mutant homozygous *Hdh^{Q111}/Hdh^{Q111}* (Figures 3.52, and 3.53, respectively) cells. In summary, the data in this chapter identify the novel target (SK channels) that effectively modulate mechanisms of neurodegeneration, at least that caused by oxidative stress.

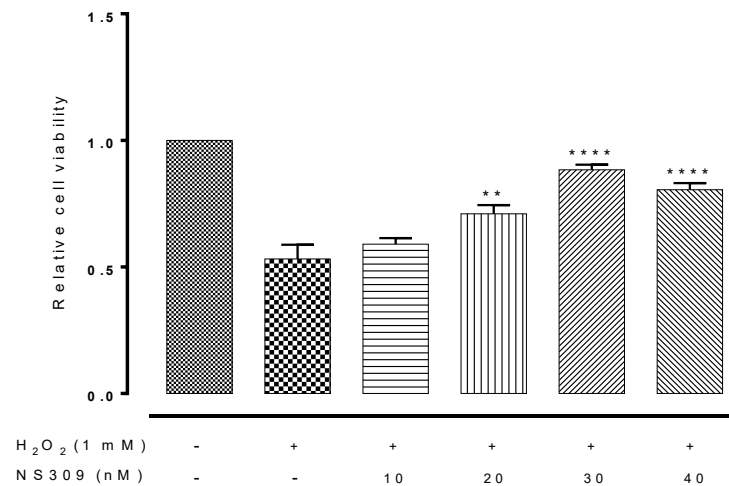


Figure 3.48 The effect of NS309, an SK4 channel activator, on the survival of wild-type *Hdh*^{+/Hdh} cells exposed to H₂O₂-induced oxidative stress. Data are shown as means ± SEM. *****p*-value < 0.0001 versus insult, one-way ANOVA followed by Dunnett's post hoc test, n= 9.

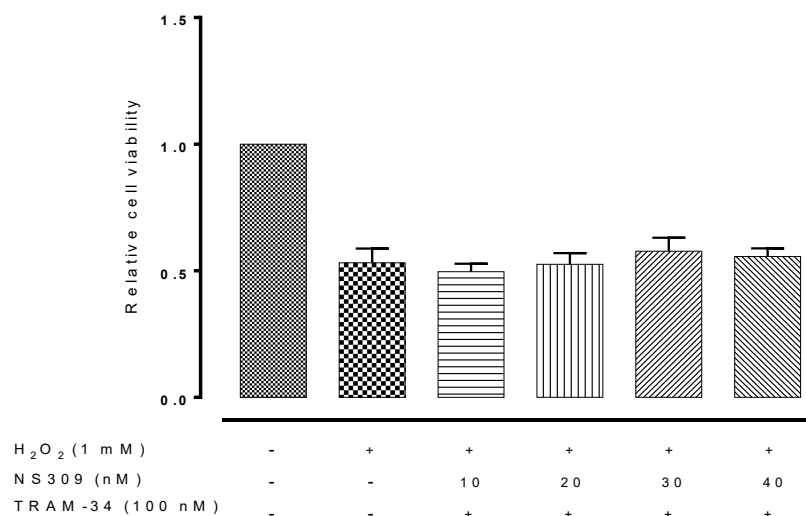


Figure 3.49 The effect of NS309, an SK4 channel activator, in the presence of the SK4 channel blocker, TRAM-34, on the survival of wild-type *Hdh*^{+/Hdh} cells exposed to H₂O₂-induced oxidative stress. Data are shown as means ± SEM. One-way ANOVA followed by Dunnett's post hoc test, n=9.

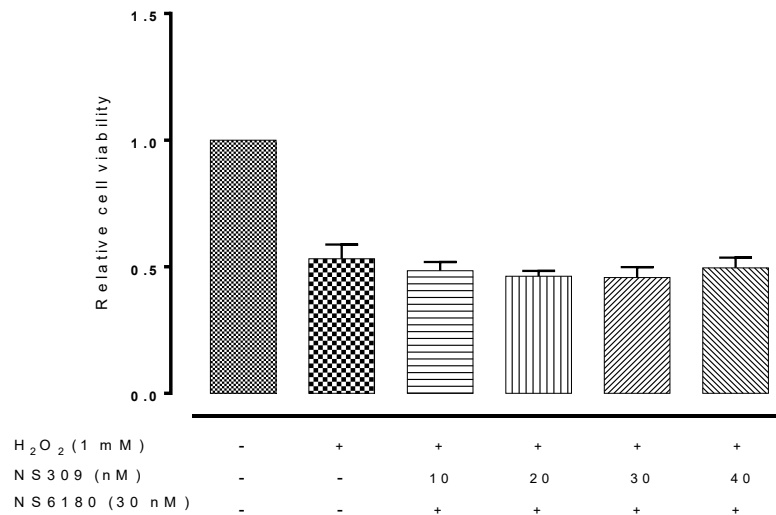


Figure 3.50 The effect of NS309, an SK4 channel activator, in the presence of the SK4 channel blocker, NS6180, on the survival of wild-type *Hdh*^{+/+} cells exposed to H₂O₂-induced oxidative stress. Data are shown as means ± SEM. One-way ANOVA followed by Dunnett's post hoc test, n=9.

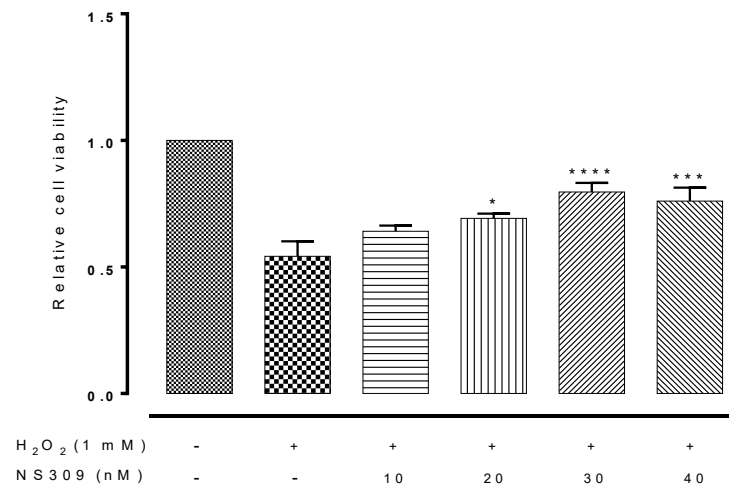


Figure 3.51 The effect of NS309, SK4 channel activation, on the survival of homozygous mutant *Hdh*^{Q111}/*Hdh*^{Q111} cells exposed to H₂O₂-induced oxidative stress. Data are shown as means \pm SEM. *****p*-value < 0.0001 versus insult, one-way ANOVA followed by Dunnett's post hoc test, *n* = 9.

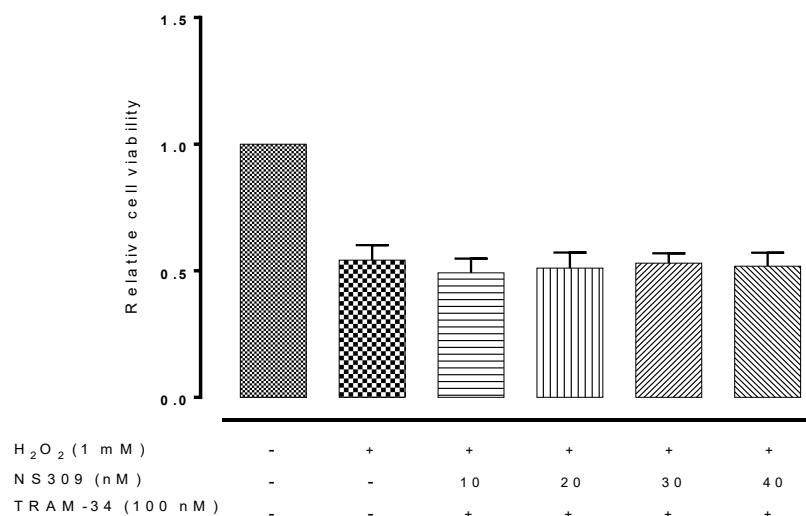


Figure 3.52 The effect of NS309, an SK4 channel activator, in the presence of the SK4 channel blocker, TRAM-34, on the survival of homozygous mutant *Hdh*^{Q111}/*Hdh*^{Q111} cells exposed to H₂O₂-induced oxidative stress. Data are shown as means \pm SEM. One-way ANOVA followed by Dunnett's post hoc test, *n* = 9.

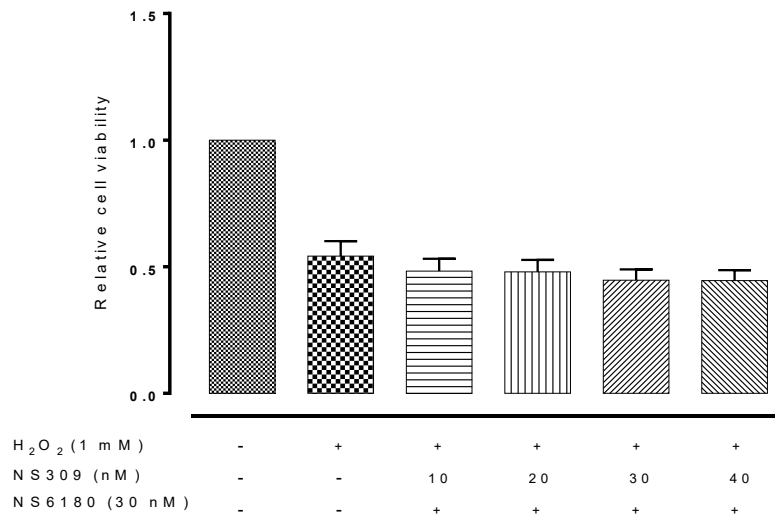


Figure 3.53 The effect of NS309, an SK4 channel activator, in the presence of the SK4 channel blocker, NS6180, on the survival of homozygous mutant *Hdh^{Q111}/Hdh^{Q111}* cells exposed to H₂O₂-induced oxidative stress. Data are shown as means ± SEM. One-way ANOVA followed by Dunnett's post hoc test, n= 9.

3.4.3 SK ion channel expression and modulation in human brain

astrocytoma cells

This work also tested the hypothesis on another CNS resident cell, a human astrocytoma, namely the MOG-G-UVW cell. RT-PCR indicated only the presence of SK4 channel in MOG-G-UVW cells at the mRNA level. Activation of this channel by NS309 (20-40 nM) caused a marked increase (p -value<0.0001) in cell numbers versus LD₅₀ of H₂O₂ (1 mM). Target channel specificity was also verified using SK4 channel blockers, TRAM-34 (100 nM) and NS6180 (30 nM). Again, these blockers abrogated the protection afforded by SK4 channel opening. It is important to mention that these SK channel modulators alone did not significantly change cell viability (Appendix 3, Figures 7.5, 7.6, 7.7 and 7.8).

These data show that SK1-4 channel activation, not only in neurons, but also in brain astrocytes, is protective against oxidative stress. This work is the first to identify an SK channel role in a second CNS resident cell in oxidative stress.

This indicates that SK1-4 molecules are functionally expressed in two types of CNS cells, and they represent in fact a novel and impressive channel against oxidative stress in both brain cells.

3.4.4 The effect of H₂O₂ and/or SK3-4 channel activation on Bcl-2 expression in wild-type mouse striatal, human neuroblastoma, and astrocytoma cells

To investigate which molecular mechanism SK channel modulation adopt to promote survival of neurons from a toxic H₂O₂ effect, an apoptotic avenue was explored. Currently, it is known that Bcl-2 plays a powerful role in neuronal survival, thereby rigidly regulating the path of neuronal apoptosis (Anilkumar and Prehn 2014). Western blotting experiments addressed this using only wild-type cell types. Results showed that the insult markedly diminished the pro-survival target, namely Bcl-2, at the protein level (Figure 3.54). These target cells express the SK3 channel subtype, in *Hdh^{+/-}Hdh⁺* and SH-SY5Y cells, and the SK4 channel subtype in MOG-G-UVW cells. Pharmacological experiments screened CyPPA, an SK2-3 activator, and NS309, an SK4 activator, to test whether they could reverse H₂O₂ action, through the Bcl-2 effector. SK3 and SK4 channel opening significantly (p -value<0.01 versus insult, densitometry relative to GAPDH expression) re-established Bcl-2 expression after 24 hours in these cells (Figure 3.54).

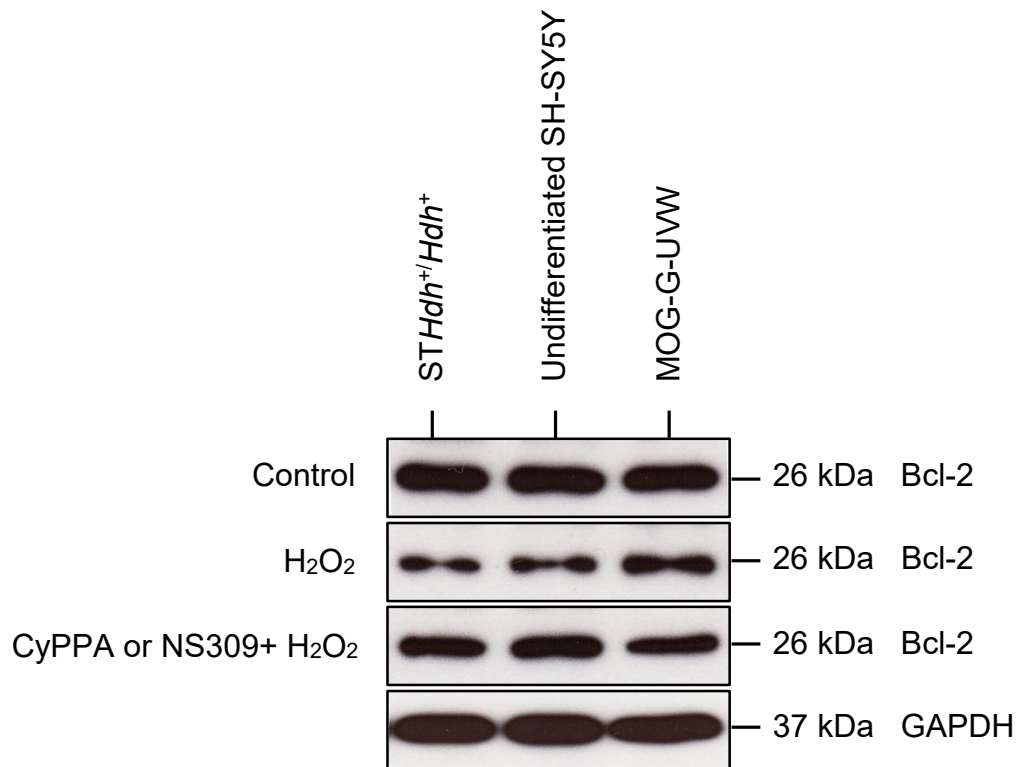


Figure 3.54 The effect H₂O₂ and/or SK3 or SK4 channel activation on Bcl-2 expression in mouse wild-type striatal cells, and human neuroblastoma and astrocytoma cells. LD₅₀ of H₂O₂ produced a significant reduction in Bcl-2 protein expression after 24 hours. CyPPA (30 μM) through SK3 channel activation expression in mouse wild-type *Hdh*^{+/Hdh} striatal cells and human neuroblastoma SH-SY5Y cells, also SK4 channel activation via NS309 (30 nM) in human astrocytoma MOG-G-UVW cells, significantly restored Bcl-2 expression. ***p*-value < 0.01 versus insult. GAPDH serves as the normalising control.

3.5 Discussion

The main findings of this work are:

1. **In human neuroblastoma cells**, $K_{Ca2.1}$ (SK1), $K_{Ca2.3}$ (SK3) and $K_{Ca3.1}$ (SK4) channels are expressed in both undifferentiated and differentiated SH-SY5Y cells at the mRNA (SK1, SK3 and SK4) and protein level (SK1 and SK3).
2. The SK4 channel subtype is noticeably upregulated in differentiated SH-SY5Y cells at the mRNA level.
3. The SK3 channel subtype is noticeably downregulated in differentiated SH-SY5Y cells at the protein level.
4. A neuronal marker, GAP-43, is markedly upregulated after retinoic acid exposure for 5 days.
5. Pharmacological opening of SK1 and SK3 channels did not significantly modify cell growth after 24 hours in either undifferentiated or differentiated SH-SY5Y cells.
6. Pharmacological blocking of SK1 and SK3 channels also did not significantly affect cell growth after 24 hours in both undifferentiated and differentiated SH-SY5Y cells.
7. Both undifferentiated and differentiated SH-SY5Y cells were similarly sensitive to H_2O_2 , the LD_{50} being 450 μM .
8. SK1 or SK3 channel activation significantly rescued undifferentiated and differentiated SH-SY5Y cells from H_2O_2 -induced oxidative stress.
9. Coincident SK1 or SK3 channel inhibition abolished the protection afforded by the relevant SK channel activator against H_2O_2 -induced oxidative stress in undifferentiated and differentiated SH-SY5Y cells.

10. **In mouse striatal cells**, SK channels are differentially expressed between the wild-type and mutant cells. Wild-type *Hdh^{+/+}* cells express K_{Ca2.1} (SK1), K_{Ca2.3} (SK3) and K_{Ca3.1} (SK4) channels at the mRNA level, and SK3 channel protein expression was also confirmed.
11. Heterozygous mutant *Hdh^{Q111/+}* cells only favour K_{Ca2.1} (SK1), K_{Ca2.2} (SK2) channel expression, and here SK2 channel protein expression was also confirmed.
12. Intriguingly, homozygous mutant *Hdh^{Q111/Q111}* cells only showed the presence of K_{Ca2.1} (SK1), K_{Ca3.1} (SK4) channels.
13. Pharmacological opening of SK3 and SK4 channels in wild-type *Hdh^{+/+}* cells, SK2 channels in heterozygous mutant *Hdh^{Q111/+}* cells, and SK4 channels in homozygous mutant *Hdh^{Q111/Q111}* cells, did not significantly change cell growth after 24 hours.
14. Pharmacological blocking of SK3 and SK4 channels in wild-type *Hdh^{+/+}* cells, SK2 channels in heterozygous mutant *Hdh^{Q111/+}* cells, and SK4 channels in homozygous mutant *Hdh^{Q111/Q111}* cells, also did not produce a significant effect on cell growth after 24 hours.
15. These cells respond to H₂O₂ cytotoxic action similarly, the LD₅₀ being nearly 1 mM.
16. Against H₂O₂-induced oxidative stress, activation of SK3 and SK4 channels in wild-type *Hdh^{+/+}* cells, SK2 channels in heterozygous *Hdh^{Q111/+}* cells, and SK4 channels in homozygous *Hdh^{Q111/Q111}* cells, afforded significant protection.
17. Coincident inhibition of SK3 and SK4 channels in wild-type *Hdh^{+/+}* cells, SK2 channels in heterozygous *Hdh^{Q111/+}* cells, and SK4 channels in

homozygous *Hdh^{Q111}/Hdh^{Q111}* cells, also totally reversed the protection demonstrated by the relevant SK channel activator against H₂O₂-induced oxidative stress.

18. **In human brain astrocytes**, RT-PCR showed only the presence of the SK4 channel subtype. SK4 channel opening in MOG-G-UVW cells significantly opposed H₂O₂ toxic action and markedly increased cell numbers.
19. **In questioning molecular mechanisms**, work here also found that H₂O₂-induced oxidative stress downmodulated Bcl-2 protein expression, whereas either SK3 or SK4 channel opening significantly challenged Bcl-2 loss in wild-type mouse *Hdh^{+/+}/Hdh^{+/+}* (SK3) and human undifferentiated SH-SY5Y (SK3), as well as targeting the SK4 channel in human MOG-G-UVW cells.

The work in this chapter targeted the expression of SK channel subtypes and their roles in human and mouse neuronal cell types in combatting oxidative stress. The hypothesis of this work was proposed in order to address previous studies interested in the underlying mechanisms of aging-related neuronal demise, namely Alzheimer's, Parkinson's, as well as Huntington's degenerative diseases (Fatokun *et al.* 2008). It has been proposed that the loss of normal oxidative stress modulation underlies neuropathology, and this proceeds to neuronal loss in the CNS (Lin and Beal 2006). It is not clear whether stress disturbance is a driver or is the consequence in the pathogenesis of neurodegenerative diseases (Andersen 2004). However, two detrimental factors, Ca^{2+} excess and oxidative stress, have been linked and suggested to cooperate in the neuronal dying processes. It is not known however how abnormal mitochondrial stress is initiated in neurodegeneration pathogenesis (Ermak and Davies 2002). Recent work showed that aberrant increased calcium entry into the cytosol of vagal neurons perturbed mitochondrial stress (Goldberg *et al.* 2012). In neuronal physiology, SK1-4 channels through control of firing rate operate as a fundamental determinant in this regard (Adelman *et al.* 2012; King *et al.* 2015) through Ca^{2+} regulation. Experiments here first used human neuroblastoma cells, the SH-SY5Y line, as a human cell model to attack this question. Three SK channel subtypes, which include SK1, SK3, and SK4, were found as resident channels in undifferentiated and differentiated cells. Retinoic acid (10 μM) for 7 days unveiled a neuronal marker, namely growth associated protein-43, and this was heavily expressed after 5 days exposure at the protein level. Recent work has revealed that this protein is required for the reshaping of morphology, and importantly to strengthen neuronal communication. In fact a lack of GAP-43 induces neuronal casualties through loss of information

exchange between synapses (Buizza *et al.* 2013). The *in vitro* investigation on neuronal cells presented here then established whether SK1-4 modulation, either activation or inhibition, does affect cell growth for the indicated time. In SH-SY5Y cell culture, neither SK1 nor SK3 channel activation by GW542573X (10-50 μM) and CyPPA (10-50 μM) respectively in both undifferentiated and differentiated cells (Figures 3.6-3.9, respectively), nor SK1 and SK3 channel inhibition by SK1-3 channel blockers (Figures 3.10-3.13, respectively), using UCL1684 (3-10 nM) and NS8593 (300 nM-1 μM), significantly modified cell viability in undifferentiated and differentiated cells. Estimating LD₅₀ for H₂O₂ on both undifferentiated and differentiated cells showed that the insult produced a similar cytotoxic effect on both cell types (Figures 3.14 and 3.15, respectively), where LD₅₀s were 450 μM . It has been accepted that H₂O₂ diffuses through membranes in bacteria and yeast (Bienert *et al.* 2006): in fact at a toxic concentration *in vitro* it increased Ca²⁺ entry into the primary neurons of mouse cerebral cortex after 1 hour (Hu *et al.* 1998), and exogenous H₂O₂, again at toxic concentrations, also exacerbated mitochondrial dysfunction, thereby enhancing cellular reactive oxygen species generation (Richter *et al.* 2015). In experiments with challenged resident SK channels in the presence of H₂O₂, it was not surprising that in MTS assays it was found that SK1 and SK3 channel opening reversed H₂O₂ action ($P < 0.0001$ versus insult), this resulting in SH-SY5Y cell protection (Figures 3.16, 18, 20 and 23, respectively). It has been previously reported that SK2 channel activation rescues hippocampal HT-22 cells from H₂O₂-induced oxidative stress through remodelling of mitochondrial function (Richter *et al.* 2015), using an SK2-3 channel activator, CyPPA (25 μM). Other work identified the SK1 channel subtype activator, GW542573X, which can actually activate SK1 channels with an EC₅₀ of 8.2 μM ,

being more potent at hSK1 over other channel subtypes, namely hSK2 and hSK3 (Hougaard et al. 2009). In this study, pharmacological tools for SK1-4 channel modulation were utilised, namely activators and blockers, and experiments attempted to confirm the channel target specificity by checking whether the relevant blocker can reverse the protective result of SK1 and SK3 channel activation. Here, an SK1-3 blocker, UCL1684 (3 nM), fully abolished the protection mediated by SK1 channel activation. However, UCL1684 (3 nM), did not affect the protection against H₂O₂ afforded by the SK3 channel activator CyPPA (Appendix 3, Figure 7.4). UCL1684 (10 nM) partially abrogated the protection established by the relevant activator in both undifferentiated and differentiated SH-SY5Y cells (Figures 3.21, and 24, respectively). This blocker is not thought to be as potent on the SK3 channel. In recombinant SK1-3 gene expression, pharmacological approaches with electrophysiology found that the SK1 and SK2 channels are more sensitive to UCL1684 than SK3 channels in HEK 293 cells (SK1 and SK2), and Jurkat cells (SK3). These studies obtained IC₅₀s of 0.76 nM (Strobaek *et al.* 2000), 0.36 nM (Strobaek et al. 2000), and 9.5 nM (Fanger et al. 2001), respectively. In this regard, another relevant SK1-3 blocker, NS8593, was screened against the SK3 channel. NS8593 (750 nM) entirely abolished the protective effect of CyPPA against H₂O₂ oxidative stress (Figures 3.22, and 25, respectively). This was the reason that in all subsequent sections pharmacological experiments used NS8593 when targeting the SK3 channel. In hippocampal CA1 neurons, electrical recording showed that the non-selective SK1-3 channel blocker (NS8593), decreases SK1-3 channel sensitivity to Ca²⁺ in this rank order of potency: 0.42, 0.60, and 0.73 µM (these representing *K_d* values respectively), but demonstrating no selectivity for the SK4 channel (Strobaek et al. 2006).

To understand whether SK channels are powerful targets for modulating oxidative stress, in CNS resident cells, this study tested the same hypothesis in mouse striatal cells. Curiously, the SK1-4 channel expression pattern was different between wild-type *STHdh⁺/Hdh⁺*, and mutant cells, namely heterozygous *STHdh^{Q111}/Hdh⁺* and homozygous *STHdh^{Q111}/Hdh^{Q111}*, and even between heterozygous and homozygous cells (Figures 3.26-3.28, respectively), a cell model of Huntington's disease (Trettel et al. 2000). *STHdh⁺/Hdh⁺* cells expressed SK1, SK3, and SK4 channel subtypes, whereas *STHdh^{Q111}/Hdh⁺* only expressed SK1 and SK2 channels, while *STHdh^{Q111}/Hdh^{Q111}* cells lacked SK2 and SK3 channels. Here, it is important to emphasise that SK1 channel cDNA does not provide a functional channel in the mouse and rat (Benton et al. 2003). This is a very attractive finding with *STHdh^{Q111}/Hdh^{Q111}* cells. Indeed, these striatal cells require SK channels for the medium AHP, and lacking this function influences neuronal excitability, and this proceeds to cell death. Intriguingly, it was found that huntingtin phenotype is more effective in homozygous than heterozygous dominant phenotype (Trettel et al. 2000). As in the case of SH-SY5Y cells, this work first assessed the effect of SK channel modulators alone on mouse striatal cell growth. In wild-type *STHdh⁺/Hdh⁺* cells, neither SK3 and SK4 channel activation, nor SK3 and SK4 inhibition, produced any significant effect on *STHdh⁺/Hdh⁺* cell growth (Figures 3.31, 32, 35, and 36 respectively). Similar results were found regarding the effect of the SK2-4 channel modulation on heterozygous, as well as homozygous cell growth. Here, the relevant SK channel modulators, both activators and blockers, did not produce any significant effect. Where the median toxic effect of the insult was estimated, dose-response curves showed that wild-type *STHdh⁺/Hdh⁺*, heterozygous *STHdh^{Q111}/Hdh⁺*, and homozygous *STHdh^{Q111}/Hdh^{Q111}* cells all invariably responded

to the H₂O₂, and the LD₅₀s were 1 mM (Figures 3.41-3.43, respectively). In the MTS viability assay, the impact of SK2-4 channels, in order, on oxidative stress was addressed. SK2 channel opening by an SK2-3 activator, CyPPA (20-40 μM), markedly increased cell numbers ($P < 0.0001$ versus insult) versus insult in heterozygous *STHdh^{Q111}/Hdh⁺* cells. Parallel blocking this channel by UCL1684, an SK1-3 channel inhibitor, abolished the protection against oxidative stress (Figures 3.44-3.45, respectively). Probing the next channel subtype, pharmacological experiments showed that SK3 channel activation through CyPPA (10-40 μM) also significantly ($P < 0.0001$ versus insult) rescued *STHdh⁺/Hdh⁺* cells (Figure 3.46). Again, the channel inhibition by NS8593 (750 nM), an SK1-3 channel blocker, blunted the protection against H₂O₂ afforded by the relevant activator (Figure 3.47). The reason that both wild-type and mutant cells were used in pharmacological experiments, was to test whether resident SK channels, in these mutant cells for Huntington's model, are still functional, and impact on oxidative stress. In this model, it has been found that mitochondria were extremely sensitive to changes in calcium entry and oxidative stress (Lim *et al.* 2008). In imaging living neurons in a mouse model of Alzheimer's disease, it was noticed that oxidative stress was generated in neurites near lesions, and it then gradually propagated into cell bodies, which caused caspase-dependent cell demise within 24h, while this was not observed in other neurons (Xie *et al.* 2013). Finally, SK4 activation by the SK4 channel activator, NS309 (20-40 nM), also afforded a significant protection ($P < 0.0001$ versus insult) against H₂O₂-induced oxidative stress in both cell types (Figures 3.48, and 51, respectively). Similarly, the SK4 channel blockers, TRAM-34 (100 nM) and NS618 (30 nM), effectively reversed SK4 activation and protection against H₂O₂ oxidative stress (Figures 3.49, 50, 52, and 53, respectively). An interesting study has shown

that NS309 acts more potently on the SK4 channels, this channel being four times more sensitive than other SK subtypes. Hence NS309 (≥ 30 nM) significantly induced in a dose-dependent manner an increase in hSK4 currents (Strobaek et al. 2004). It was also revealed that TRAM-34 distinguishes the SK4 channel from other SK channels (Wulff *et al.* 2007). In glioblastoma GL-15 cells, the SK4 protein is functionally expressed, and pharmacological screens showed that the IC₅₀ values of clotrimazole, TRAM-34, and charybdotoxin, were 257 nM, 55 nM, and 10.3 nM respectively (Fioretti et al. 2006). Further electrophysiological tests in CHO cells, have shown that the human SK4 channel can be fully inhibited by TRAM-34, with an IC₅₀ of 310 nM (John *et al.* 2007). In T-cells advances in channel pharmacology, include characterisation of a new SK4 blocker, NS6180, which is more potent at this channel than TRAM-34, with an IC₅₀ of 9 nM (Strobaek et al. 2013).

In addition to neurons, similar effects were found in human astrocytoma MOG-G-UVW cells, however, these cells are less sensitive to oxidative stress upmodulation (Wilson 1997). Their cell viability was reduced by ~50% using H₂O₂ (1 mM), which served as LD₅₀. Activation of the SK4 channel resident, the sole SK channel subtype (See next chapter), through NS309, also ($P < 0.0001$ versus insult) afforded significant protection against H₂O₂-induced oxidative stress. Here, the channel target blockade by the relevant SK4 blockers did completely abolish the rescuing effect of NS309 (Appendix 3, Figure 7.7 and 7.8). It has currently been accepted that Bcl-2 itself acts as leading protein among apoptotic regulators, triggering mitochondria, which eventually exceeds the apoptotic threshold, causing either cancer in case of scant upmodulation, or neurodegeneration when its downmodulated (Anilkumar and Prehn 2014; Czabotar et al. 2014). Importantly, Bcl-2 dysregulation in neuronal damage has been linked with oxidative stress

(Anilkumar and Prehn 2014). In this paradigm, *in vivo* work was shown that losing Bcl-2 in mice induced neuronal loss by 52% (Hochman *et al.* 1998). Moreover, simultaneous Bcl-2 expression in rat hippocampus in the presence of glutamate toxicity *in vivo* significantly diminished lesion size (Wong *et al.* 2005). Glutamate toxicity reduced SK2 channel expression in the cerebellum, and its activation with pharmacological experiments also markedly improved cell survival (Dolga *et al.* 2011). So, in the next step work here attempted to show whether SK channels “crosstalk” with Bcl-2 activity. Protein blotting discovered that H₂O₂ by itself produced pronounced reduction in Bcl-2 expression (Figure 3.54), and that SK3 or SK4 channel activation modestly (p -value<0.01) restored Bcl-2 at the protein level in a 24 hour challenge (Figure 3.54) in mouse wild-type striatal cells, and human neuroblastoma and astrocytoma cells. Moreover, CyPPA (20-40 μ M) activation of SK3 or SK2 channels also produced significant protection (P <0.0001 versus insult) against staurosporine-induced apoptosis that thought to work through Ca²⁺ entry through store-operated channels (Tojyo *et al.* 2013), at an LD₅₀ dose (30 nM) in *STHdh*^{+/+}/*Hdh*⁺ and *STHdh*^{Q111}/*Hdh*⁺ cells respectively (Appendix 3, Figures 7.9 and 7.10).

3.6 Conclusions

The results in this chapter revealed that SK channels can engage oxidative stress pathway in five CNS-related cell types. Most importantly, this work now may galvanise an examination of the mysterious mechanisms behind SK channel expression and a role in cells bearing neurodegenerative phenotypes, such as the Huntington's cell model. Of course healthy cells require SK1-4 channel activity to resist the cytotoxic stress of H₂O₂. Pertinently, this study delivers some mechanistic insight underling neurodegeneration. Homozygous *STHdh^{Q111}/Hdh^{Q111}* cells in fact lacked SK1-3 channel function, which explains why these cells cannot generate after hyperpolarisations, which is required for their physiology. Importantly, work here also observed that SK channel activity restores the abnormal apoptotic threshold through Bcl-2 regulation. These results could advance substantially an understanding of neurodegeneration pathogenesis, particularly the apoptotic role of SK channel.

3.7 Recommendations and future work

This study would urgently suggest mapping SK1-3 channel expression in all aging related CNS degenerative diseases, considering both *in vivo* and *in vitro* models. It would be fascinating if an SK1 channel role would also be determined in non-human species. Assessment of the effect of SK channel modulation on the other apoptotic pathways will also provide more clarification, particularly distinguishing between extrinsic and intrinsic modes. Also, it would be very interesting if future research explores whether plasma membrane and/or mitochondrial SK channels are responsible for such protection in these cells. Which SK channel subtype is expressed in the mitochondria of these cells also urgently needs to be addressed. Finally, there is a question about the efficiency or effectiveness of the antibody used here for SK4. Future consideration therefore might be given to producing a viable antibody for SK4.

4 Chapter Four: TRPM7 Ion Channel in Survival of Astrocytes and Neurons

4.1 Introduction

The TRPM7 ion channel occupies the seventh position of the melastatin subfamily (TRPM) in TRP channel classification (Wu *et al.* 2010). The TRPM7 ion channel, also termed the magnesium transporter (Zhang *et al.* 2011a), is composed of two domains, namely a channel and its kinase. Therefore, this bifunctional protein is an uncommon molecule amongst ion channels. The channel pore is permeant to various cations: Ca^{2+} ions, Mg^{2+} ions, and other metals (Monteilh-Zoller *et al.* 2003; Yamaguchi *et al.* 2001), which are touted as important ions in diseases, leading to perturbation in overall “cell fitness” such as cellular survival (Mattson 2007) and proliferation (Roderick and Cook 2008). Other trace metals such as Zn^{2+} also require the TRPM7 channel to cross the plasma membrane and thus be regulated (Yamaguchi *et al.* 2001). It has been shown that either intracellular Mg^{2+} or $\text{Mg}\cdot\text{ATP}$ finely regulates TRPM7 channel activity (Demeuse *et al.* 2006; Nadler *et al.* 2001). The TRPM7 channel subtype seems to be expressed in all cells (Runnels *et al.* 2001; Yee *et al.* 2014): indeed negative cell lines or types without this channel have not been reported so far, which is in fact very interesting, suggesting that this molecule is essential in all mammalian cell physiology (Yee *et al.* 2014). It is well established that for example Ca^{2+} and Mg^{2+} ions are implicated in the viability and growth avenues of different cell types (Chen *et al.* 2012; Jin *et al.* 2008; Mattson 2007). Such considerations of course predict that any dysregulation in either TRPM7 channel activity or its expression may produce ill effects through triggering disturbed Ca^{2+} and Mg^{2+} homeostasis in cells. Indeed, this member of TRPM channel

contributes to various physiological functions related to ionic homeostasis (Bae and Sun 2013). The TRPM7 channel seems a powerful prospective target in CNS injury. For instance, it was found that CA1 neurons possess the TRPM7 channel, and its role is critical in their survival. This study showed that lack of TRPM7 results in CA1 neurons, resistant to ischemic cell demise, compared to wild-type cells (Sun et al. 2009). It is still contentious that the TRPM7 kinase is a functional domain of the channel. By deletion of the TRPM7 channel in mice, interestingly early embryonic fatality was experienced in homozygous mice, while heterozygous generation produced only symptomatic illness (Ryazanova et al. 2010). This study reported that the kinase itself can actually regulate Mg^{2+} homeostasis at both cellular and organism levels. In contrast, recent research, again using mutant mice, indicated that kinase inactivation does not affect the overall channel function, and this protein acts as Mg^{2+} channel (Kaitsuka *et al.* 2014). Notably, however TRPM7 channel activity has been connected to cell survival, particularly in neurons. In this respect, an earlier study found that the TRPM7 channel in fact contributes to stroke pathogenesis through Ca^{2+} entry upregulation as well as by increasing reactive oxygen species in cortical neurons experiencing oxygen/glucose deprivation challenges (Aarts et al. 2003). This model indeed also produced mitochondrial dysfunction in neurons (Almeida *et al.* 2002), actually inducing apoptosis via caspase-3 awakening (Newcomb-Fernandez *et al.* 2001). The work in this chapter targeted this prospectively influential channel not only in neurons, but also in brain astrocytes. Importantly, the former cells were diseased neurons derived from homozygous Huntington's disease mice model. In the CNS, emerging research points to a vital role of astrocytes in CNS structure and function (Clarke and Barres 2013), $[Ca^{2+}]_i$ changes for example being shown in response to neurotransmitter

activity (Volterra *et al.* 2014). Intriguingly, this major CNS cell type is involved in synapse elimination through upmodulation of C1q component that serves as an initiator player in the complement pathway (Stevens *et al.* 2007), thereby inducing microglial phagocytosis (Clarke and Barres 2013). In this fine regulation, understanding such cross-talk between neurons, astrocytes, as well as microglial cells is extremely important, deciphering mechanisms in neurodegeneration processes. Thus, it is important that prospective studies should aim to examine the activities and roles of all CNS cell types in neurodegenerative diseases.

4.2 Hypothesis and aims

It is proposed here that inhibition of TRPM7 channel will have protective effects against H₂O₂-induced oxidative stress, CoCl₂-induced hypoxia, and staurosporine-induced apoptosis *in vitro*, since these mechanisms underlie degeneration processes in CNS.

The principal aims are:

1. To explore the expression of TRPM7 channel in mouse striatal homozygous mutant *STHdh^{Q111}/Hdh^{Q111}* cells.
2. To explore the expression of TRPM7 channel in human brain astrocytes, namely MOG-G-UVW cells.
3. To test the effect of TRPM7 channel blocking, if any, on the viability of these cells in pharmacological experiments.
4. To measure the LD₅₀ of these insults, which include H₂O₂, CoCl₂, and staurosporine on these cell types.
5. To show a protective role, if any, for the TRPM7 channel against the cytotoxic nature of these insults in both cell types.
6. To test whether channel target knock-out mimics pharmacological studies, using siRNA-mediated knockdown.

4.3 Materials and methods

4.3.1 Cell origins and features

The work in this chapter concentrated on CNS cell survival studies, using two CNS cell types, including mutant and wild-type cells. The former type was mouse striatal cells (*STHdh⁺/Hdh⁺*), which were mutated into the homozygous form of Huntington's cell model (*STHdh^{Q111}/Hdh^{Q111}*) that show a severe dominant phenotype (Trettel et al. 2000; Wheeler et al. 2000). The channel target (TRPM7) was also investigated in human brain astrocytoma MOG-G-UVW cells, which are derived from anaplastic astrocytoma (Frame et al. 1984). These cell types were described in chapter three (See section 3.3.1).

4.3.2 Polymerase chain reaction

The channel target transcripts, SK1-4 and TRPM7, were amplified in RT-PCR to test whether these targets are expressed at the mRNA level in these cells. First, extraction experiments isolated total RNA from the target cells after being lysed, and its concentration was then quantified in each sample. RNA purity and integrity in target samples were ensured. These samples were taken into the reverse transcription step, by generating their cDNA. In experiments that did not use the enzyme, reverse transcriptase, i.e. the negative control sample, this was labelled as No RT. The generated cDNA was then used in the PCR reaction. Specific primers for channel target genes, and β -actin, which serves as the reference, were used in these amplifications. Reaction conditions for various target genes indeed were validated, and in this respect, cycle number and temperature variations were considered. This found the following optimum profiles, for human primers: denaturation at 95°C for 5 minutes, followed by 30 cycles of incubation consisting

of 95°C for 30 seconds, 55°C for 30 seconds, followed by an extension step at 72°C for 1 minute, as well as 72°C for 5 minutes of final extension step. In the case of the mouse primers, experiments used the same PCR program, but these primers effectively annealed at 60°C instead of 55°C. In the final step, the amplicon sizes were UV visualised in electrophoresis experiments using 1% agarose gel.

Gene	Gene ID	Human primer sequences	Sizes (bp)
β-actin	NM_001101	F. 5'-CCCAGCCATGTACGTTGCTA-3'	126
		R. 5'-AGGGCATACCCCTCGTAGATG-3'	
KCNN1 (SK1)	NM_002248.4	F. 5'-TGGACACTCAGCTCACCAAG-3'	208
		R. 5'-TTAGCCTGGTCGTTTCAGCTT-3'	
KCNN2 (SK2)	AF397175.1	F. 5'-CAAGCAAACACTTTGGTGGA-3'	249
		R. 5'-CCGCTCAGCATTGTAAGTGA-3'	
KCNN3 (SK3)	NM_002249.5	F. 5'-AAGCGGAGAAGCACGTTTCATA-3'	180
		R. 5'-CTGGTGGATAGCTTGGAGGAA-3'	
KCNN4 (SK4)	AB128983.1	F. 5'-GAGAGGCAGGCTGTTATTGC-3'	215
		R. 5'-ACGTGCTTCTCTGCCTTGTT-3'	

Table 4.1 Primer sequences for human SK channel transcripts and positive control for the human cell type, and predicted identities. F. denotes forward primer and R. denotes reverse primer.

Gene	Gene ID	Mouse primer sequences	Sizes (bp)
β-actin	NM_007393.3	F. 5'-TGTTACCAACTGGGACGACA-3'	165
		R. 5'-GGGGTGTGGAAGGTCTCAA-3'	
KCNN1 (SK1)	NM_032397.2	F. 5'-GAAGCTTGGGTGAACTGAGC-3'	232
		R. 5'-CCATTAAGGAATCCCCAGGT-3'	
KCNN2 (SK2)	AY123778.1	F. 5'-TCTGATTGCCAGAGTCATGC-3'	250
		R. 5'-CCACATTGCTCCAAGGAAGT-3'	
KCNN3 (SK3)	AF357241.1	F. 5'-ACTTCAACACCCGATTCGTC-3'	191
		R. 5'-GGAAAGGAACGTGATGGAGA-3'	
KCNN4 (SK4)	BC010274.1	F. 5'-AAGCACACTCGAAGGAAGGA-3'	215
		R. 5'-CCGTCGATTCTCTTCTCCAG-3'	

Table 4.2 Primer sequences for mouse SK channel transcripts and positive control for the mouse cell type, and predicted identities. F. denotes forward primer and R. denotes reverse primer.

Gene	Gene ID	Primer sequences	Sizes (bp)
TRPM7 Human	NM_017672	F. 5'-TGCAGCAGAGCCCGATATTAT-3'	239
		R. 5'-CTCTATCCCATGCCAATGTAAGG-3'	
TRPM7 Mouse	NM_021450	F. 5'-GTCAGATTTGTCAGCAACTTGTC-3'	139
		R. 5'-GACCATTCTTCTATTGCCTGGTT-3'	

Table 4.3 Primer sequences for human and mouse TRPM7 channel transcript and positive control for the human and mouse cell types, and predicted identities. F. denotes forward primer and R. denotes reverse primer.

4.3.3 Small interference RNA

Knockdown protocol of the channel target, TRPM7, was consulted using the Eurofins Genomics database in order to obtain an effective target siRNA, the chosen candidate being top ranked with the highest percentile score, and like previous work this was used in knockdown experiments. Small interference RNA exploration used the following sequences:

Green fluorescent protein (GFP) siRNA which is non-targeting siRNA, served as non-specific control siRNA: 5'-GGCUACGUCCAGGAGCGCACC-3'. For targeting human TRPM7 channel gene in MOG-G-UVW cells, the siRNA sequence was 5'-UUAGGCAGUUCAUCUACUA-3' in exon 26. In the case of mouse TRPM7 gene the sequence was 5'-UUAGGCAGUUCACCUAAUA-3' also in exon 26. These are sense sequences through which complementary ends were determined, defining binding sites. Briefly, siRNA experiments were performed using TRPM7 siRNA oligonucleotide, this complexing with the transfection reagent, which was Oligofectamine™, in Opti-MEM® medium. Knockdown experiments first obtained the optimum concentrations of siRNAs within the 100 nM range on cell lines indicated, ensuring the effectiveness of the target siRNA.

To investigate whether siRNA-mediated downregulation of TRPM7 channel protein expression impacts on cell survival against cellular insults indicated, target cells were seeded in six-well plates at a density of 200×10^3 cells per well. Experiments first ensured the optimum cell density for these cell types in six-well plates for this protocol. After 24 hours, seeded plates were retrieved, and first observed under the microscope, to ensure the quality of the culture. Experiments used 100 nM and 80 nM to achieve successful delivery of the TRPM7 siRNAs in *STHdh^{Q111}/Hdh^{Q111}* and MOG-G-UVW cells respectively along with controls. After 72 hours, control and SK-

siRNA treated cells were harvested for MTS assays. These cells were counted and reseeded in the regular medium using 96-well plate format at the relevant densities, and then incubated for 24 hours recovery. The next day, control cells and treated cells were challenged with the cellular insults for 24 hours using the insult (serum-free) medium. This was followed by use of PMS-MTS mix (1:5) that in viable cells can be converted to formazan, thereby determining the relative cell viability.

4.3.4 Western blotting

In examining target protein, experiments first lifted control and treated cells in cold Dulbecco's phosphate buffered saline by aid of a cell scraper. Cell suspensions were then directly pipetted into fresh tubes in which pellets were formed after centrifugation. The supernatant was discarded, and cells in the full lysate were disintegrated in a mixture of Pierce lysis IP buffer and Halt™ protease inhibitor cocktail (100:1), which was then incubated on ice for 30 minutes. This was accomplished by partitioning of the suspended proteins in the supernatant, again after centrifugation. Extracted proteins were transferred into fresh tubes, and their concentrations were quantified in each sample via BCA assays.

Protein samples were then subjected to PAGE electrophoresis, thus separating protein molecules based on their sizes. Resultant gels were then used in Western blotting, commencing with the transferring step in which proteins were relocated on to blotting membranes, which were blocked in the blocking solution of 5% (w/v) dried skimmed milk and Tris buffered Saline with Tween®-20. These membranes were used in probing experiments to detect the target molecule, as well as loading control protein (See section 2.5.4). Anti-TRPM7 mouse monoclonal antibody (Abcam, ab85016) was applied in a dilution ratio (1:1000) in a blocking solution, this

normalising with a loading control, a mouse anti-GAPDH antibody (Sigma-Aldrich, G9295) in a ratio (1:50,000). The primary anti-TRPM7 antibody was incubated overnight for 16 hours, whereas the anti-GAPDH antibody was exposed for 45 minutes. Target signals were developed after the membrane was washed with Tris buffered Saline with Tween®-20, and expression was recorded at the following exposure times: 4 minutes and 30 seconds, respectively.

4.3.5 TRPM7 channel pharmacology

MTS cell viability assessments addressed in the *in vitro* cytotoxic effect, if any, of the insults and the TRPM7 channel modulator, as well as any combating action over 24 hours. The work here, unfortunately, did not confirm channel target specification through any pharmacological approach because selective TRPM7 channel modulators were not available, particularly any TRPM7 activator. Their role alone was first ensured in the cell viability test. Cellular insults at their LD₅₀s were also introduced in conjunction with TRPM7 channel blockade, MTS assays quantifying relative cell viability (See chapter two, section 2.7.2).

It is important to mention that the SK channel blockers used in the work here can block such channels at nanomolar concentrations, but can also block TRPM7 at micromolar ranges (Chubanov et al. 2012). Indeed, the SK1-3 channel blocker can fully block TRPM7 channel at 30 µM, for this reason pharmacological experiments bracketed this dose (30 µM).

4.4 Results

4.4.1 TRPM7 ion channel expression in mouse model of Huntington's homozygous *STHdh^{Q111}/Hdh^{Q111}* cells

4.4.1.1 TRPM7 channel mRNA and protein investigation in *STHdh^{Q111}/Hdh^{Q111}* cells

The work in this section used mouse striatal cells *STHdh^{Q111}/Hdh^{Q111}* cells for several reasons. For example, there was no previous study addressing TRPM7 channel expression in diseased cells such as a mouse striatal cell model of Huntington's disease. Also *STHdh^{Q111}/Hdh^{Q111}* cells do not generate SK2 and SK3 channels, and the SK1 channel subtype in mouse is not functional (Benton et al. 2003). This avoids pharmacological argument for using SK channel modulators in the context of TRPM7 channel blockade.

RT-PCR investigations found that *STHdh^{Q111}/Hdh^{Q111}* express the TRPM7 channel subtype of TRPM subfamily at the mRNA level, β -actin serving as the normalising control (Figure 4.1). This result was confirmed in Western blotting studies. This protein detection method used a specific antibody to recognise the channel target, and the expression was normalised by using GAPDH (Figure 4.2).

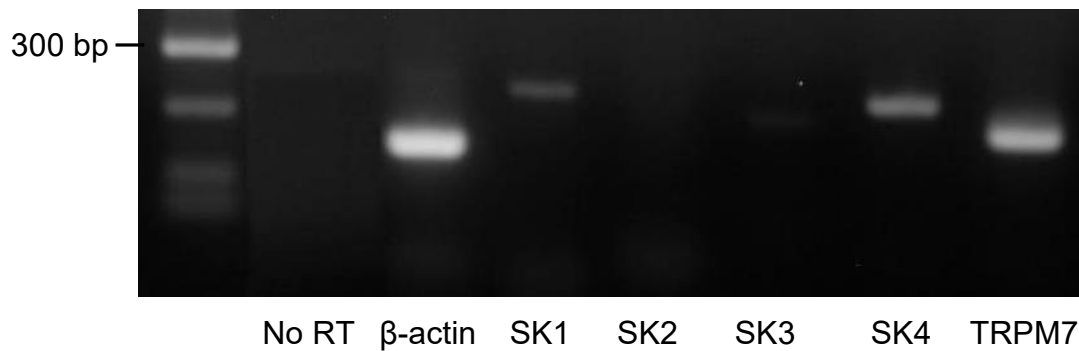


Figure 4.1 SK and TRPM7 channel mRNA in homozygous mutant *Hdh^{Q111}/Hdh^{Q111}* cells. Only the amplicons for SK1, SK4, and TRPM7 channels are present and the PCR products are of the predicted size. β -actin serves as the normalising control.

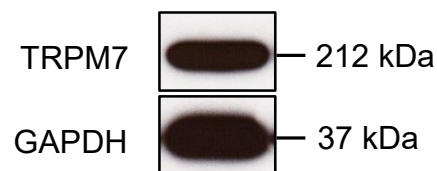


Figure 4.2 Representative immunoblot of TRPM7 channel subtype in homozygous mutant *Hdh^{Q111}/Hdh^{Q111}* cells. GAPDH serves as the normalising control.

4.4.1.2 The effect of pharmacological TRPM7 channel inhibition on

***STHdh^{Q111}/Hdh^{Q111}* cell viability**

The next question was: do these modulators alone affect *STHdh^{Q111}/Hdh^{Q111}* cell numbers in the viability assays. This determines whether constitutive TRPM7 channel activity modulates *STHdh^{Q111}/Hdh^{Q111}* cell proliferation. This question was addressed by the MTS assay using a 24 hour exposure. MTS cell viability quantification showed that neither NS8593 (20-40 μ M), nor UCL1684 (20-40 μ M), which are SK1-3 channel blockers, significantly modified *STHdh^{Q111}/Hdh^{Q111}* cell growth (Figures 4.3 and 4.4). Here, lower doses (5 and 10 μ M) for both SK1-3 blockers were also screened against *STHdh^{Q111}/Hdh^{Q111}* cell proliferation, but did not significantly change cell numbers compared to control (Appendix 3, Figures 7.11 and 7.12). These results enabled work to proceed to the next step where LD₅₀s of the insults were determined.

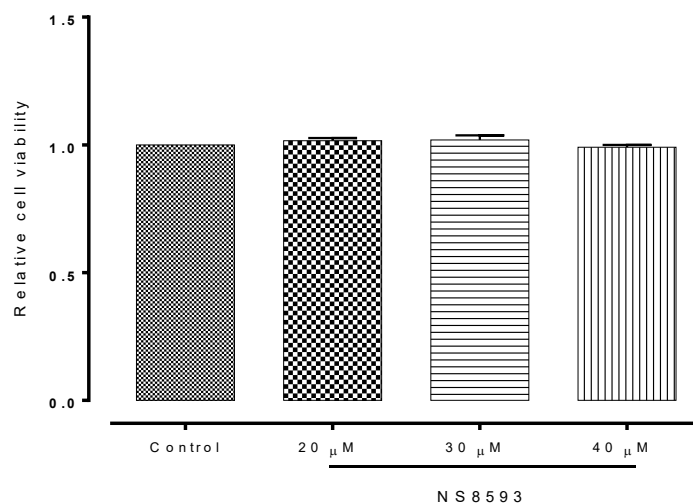


Figure 4.3 The effect of NS8593, TRPM7 channel inhibition, on homozygous mutant *Hdh^{Q111}/Hdh^{Q111}* cell viability. Data are shown as means \pm SEM. One-way ANOVA followed by Dunnett's post hoc test, n=6.

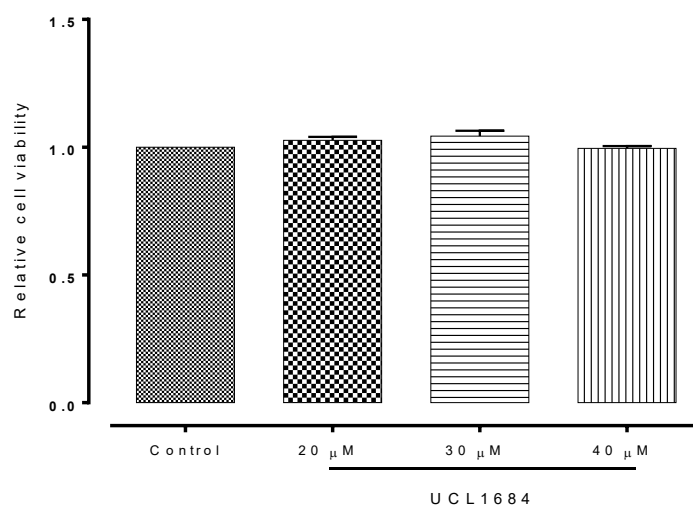


Figure 4.4 The effect of UCL1684, TRPM7 channel inhibition, on homozygous mutant *Hdh^{Q111}/Hdh^{Q111}* cell viability. Data are shown as means \pm SEM. One-way ANOVA followed by Dunnett's post hoc test, n=6.

4.4.1.3 The dose-response curve for cellular insults in *STHdh^{Q111}/Hdh^{Q111}* cells

Three different cellular insults were applied to induce cell injury in *STHdh^{Q111}/Hdh^{Q111}* cells, namely oxidative stress, hypoxia, and a pro-apoptotic challenge. Their cytotoxic action was estimated *in vitro* through MTS cell viability checks at 24 hours. The target cells were differentially sensitive to these insults with values from nanomolar up to millimolar ranges. H₂O₂ “killed” 50% of *STHdh^{Q111}/Hdh^{Q111}* cells with an approximate LD₅₀ of 1 mM (See chapter three, Figure 3.43). The next insult (CoCl₂) had an LD₅₀ of 60 μM on this cell type (Figure 4.5). These mutant cells were very sensitive to the apoptotic action of staurosporine, the MTS assay yielding 10 nM for this insult (Figure 4.6). All these LD₅₀s were determined from the dose-response data.

Following this step, work proceeded to the next stage, where TRPM7 channel inhibition-insult interactions were determined.

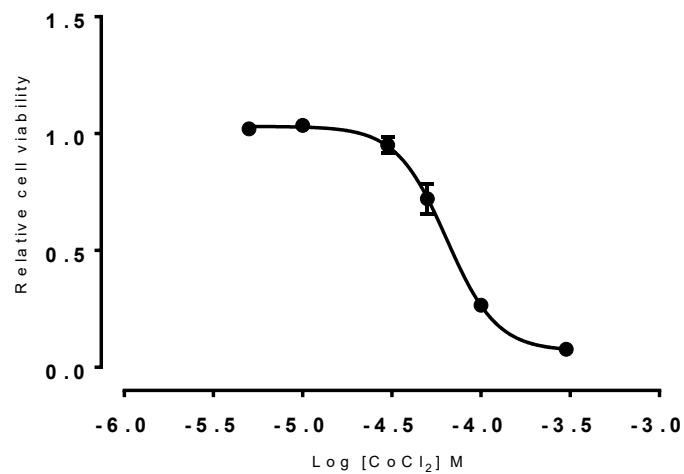


Figure 4.5 The effect of CoCl₂ on homozygous mutant *Hdh*^{Q111}/*Hdh*^{Q111} cell viability. From the line of best fit of the dose-response data, the LD₅₀ was 60 μM, n= 9.

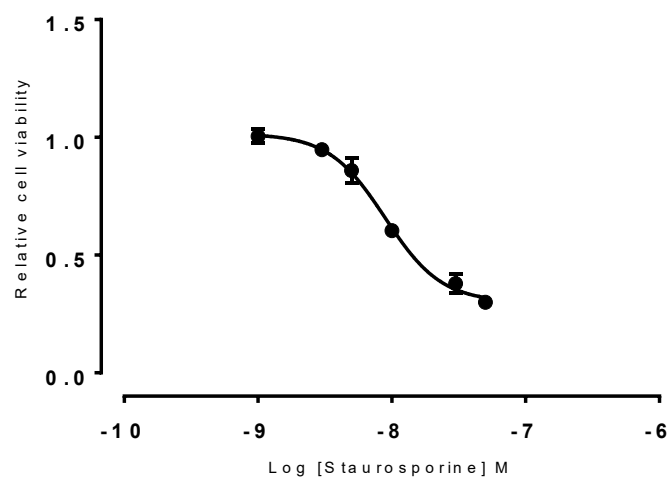


Figure 4.6 The effect of staurosporine on homozygous mutant *Hdh*^{Q111}/*Hdh*^{Q111} cell viability. From the line of best fit of the dose-response data, the LD₅₀ was 10 nM, n= 9.

4.4.1.4 Pharmacological inhibition of TRPM7 channel against striatal cell insults in *STHdh^{Q111}/Hdh^{Q111}* cells

The question posed here was whether TRPM7 ion channel blocking can rescue *STHdh^{Q111}/Hdh^{Q111}* cells from H₂O₂, CoCl₂, and staurosporine challenges. Again, pharmacological treatment to answer this question was for 24 hours. Interestingly, TRPM7 channel blocking by NS8593 and UCL1684 can remarkably ($P < 0.0001$ versus insult) reverse the decrease in *STHdh^{Q111}/Hdh^{Q111}* cell viability against the cytotoxic action of an LD₅₀ dose of H₂O₂ (Figures 4.7 and 4.8, respectively), CoCl₂ (Figures 4.9 and 4.10, respectively), and staurosporine (Figures 4.11 and 4.12, respectively), these insults mimicking oxidative stress, hypoxia, and apoptosis respectively. Both compounds, NS8593 (20-40 μ M) and UCL1684 (20-40 μ M), were protective in all cases, although these two compounds had no protective role at 10 μ M (N.B. not true for the H₂O₂-NS8593 interaction, Figure 4.7). This indicates that these modulators are potent at >10 μ M. This study did not pursue the channel specificity associated with the reversing the protection through TRPM7 channel opening because TRPM7 channel pharmacology is less advanced, and TRPM7 channel openers are not available.

These pharmacological results show that TRPM7 channel subtype has a crucial role in neuronal loss *in vitro* to oxidative stress, hypoxia, and apoptosis challenges, indicating that this channel is widely involved in cell survival mechanisms. This work was further progressed by TRPM7 gene silencing using the small interference RNA method.

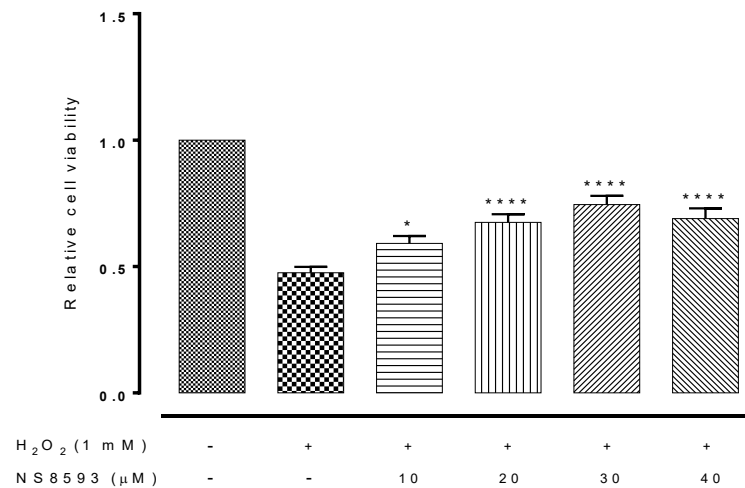


Figure 4.7 The effect of NS8593, TRPM7 channel inhibition, on the survival of homozygous mutant *Hdh*^{Q111}/*Hdh*^{Q111} cells exposed to H₂O₂-induced oxidative stress. Data are shown as means \pm SEM. *****p*-value < 0.0001 versus insult, one-way ANOVA followed by Dunnett's post hoc test, n= 9.

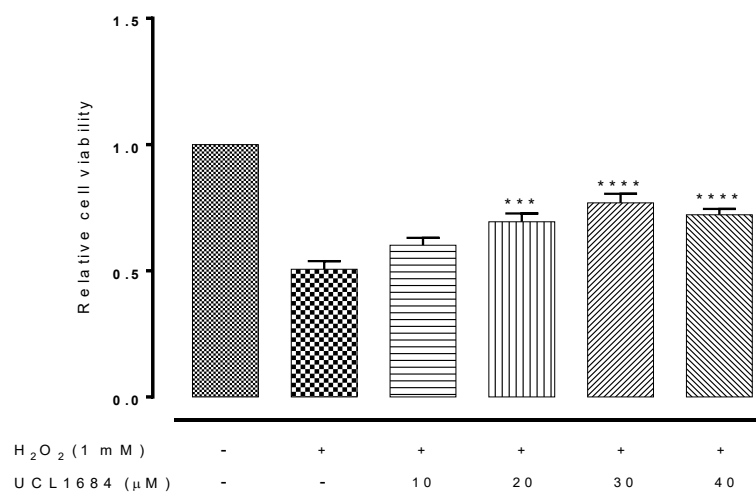


Figure 4.8 The effect of UCL1684, TRPM7 channel inhibition, on the survival of homozygous mutant *Hdh*^{Q111}/*Hdh*^{Q111} cells exposed to H₂O₂-induced oxidative stress. Data are shown as means \pm SEM. *****p*-value < 0.0001 versus insult, one-way ANOVA followed by Dunnett's post hoc test, n= 9.

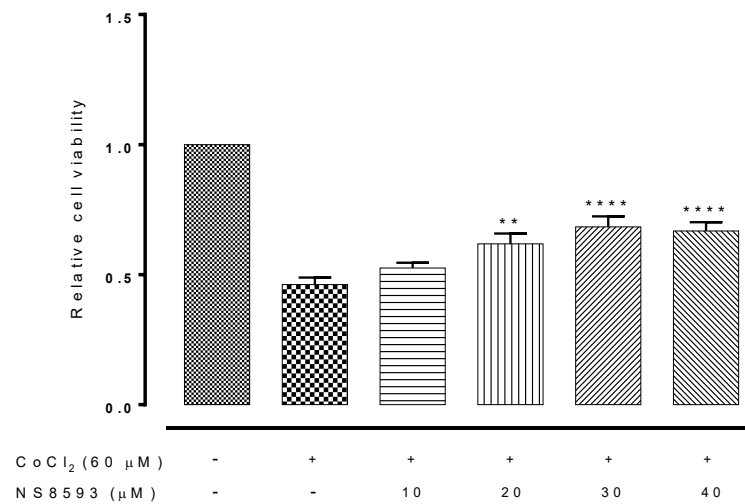


Figure 4.9 The effect of NS8593, TRPM7 channel inhibition, on the survival of homozygous mutant *Hdh^{Q111}/Hdh^{Q111}* cells exposed to CoCl₂-induced hypoxia. Data are shown as means ± SEM. *****p*-value < 0.0001 versus insult, one-way ANOVA followed by Dunnett's post hoc test, n= 9.

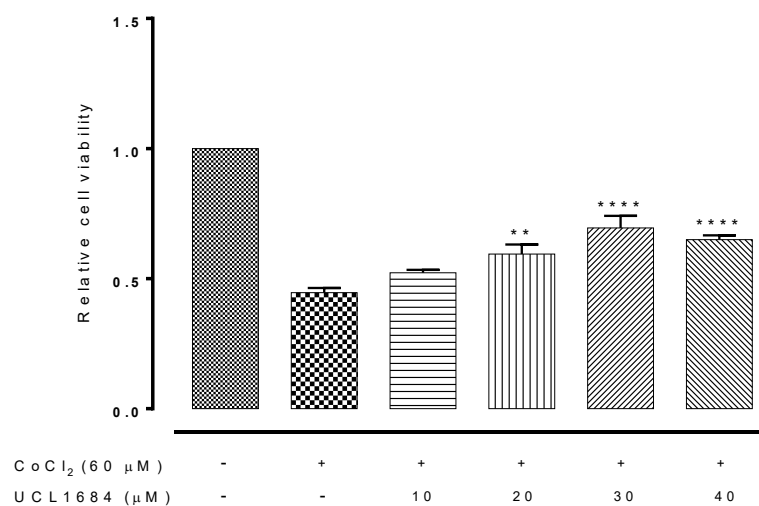


Figure 4.10 The effect of UCL1684, TRPM7 channel inhibition, on the survival of homozygous mutant *Hdh^{Q111}/Hdh^{Q111}* cells exposed to CoCl₂-induced hypoxia. Data are shown as means ± SEM. *****p*-value < 0.0001 versus insult, one-way ANOVA followed by Dunnett's post hoc test, n= 9.

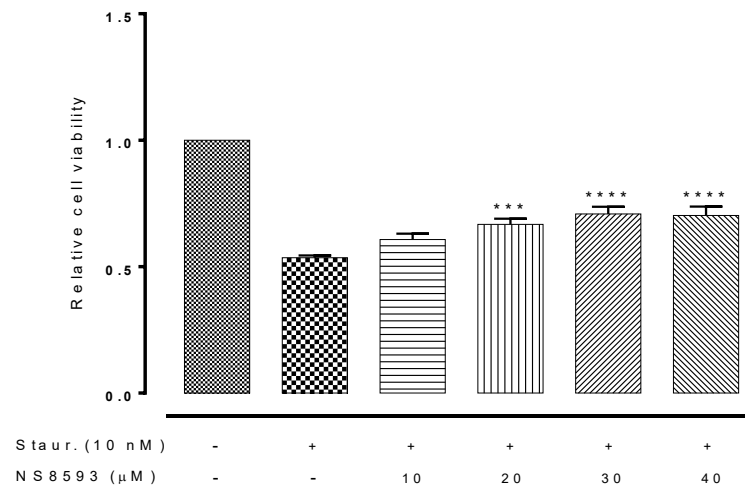


Figure 4.11 The effect of NS8593, TRPM7 channel inhibition, on the survival of homozygous mutant *Hdh^{Q111}/Hdh^{Q111}* cells exposed to staurosporine-induced apoptosis. Data are shown as means \pm SEM. *****p*-value < 0.0001 versus insult, one-way ANOVA followed by Dunnett's post hoc test, n= 9.

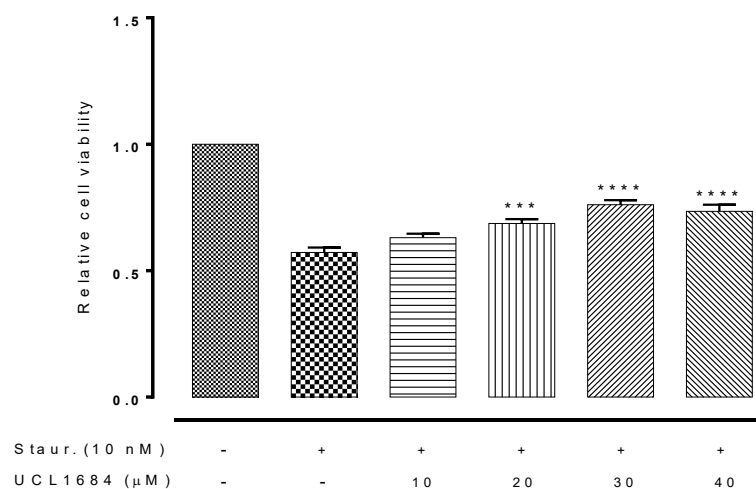


Figure 4.12 The effect of UCL1684, TRPM7 channel inhibition, on the survival of homozygous mutant *Hdh^{Q111}/Hdh^{Q111}* cells exposed to staurosporine-induced apoptosis. Data are shown as means \pm SEM. *****p*-value < 0.0001 versus insult, one-way ANOVA followed by Dunnett's post hoc test, n= 9.

4.4.1.5 Small interference RNA-mediated modulation of TRPM7 channel against cellular insults in *STHdh^{Q111}/Hdh^{Q111}* cells

To test whether lowering TRPM7 channel expression can mirror above pharmacological results, TRPM7 channel downregulation was performed via siRNA. This method used specific TRPM7-siRNA to knock-out this target in *STHdh^{Q111}/Hdh^{Q111}* cells after 72 hours. Its efficiency was first confirmed by Western blotting validation. This exploration used proteins from control cells i.e. non-treated cells, GFP-siRNA treated group, which expresses GFP-siRNA that serves as the normalising siRNA, as well as TRPM7-siRNA transfected cells, which express TRPM7-siRNA. Western blotting followed by densitometric analysis found that GFP-siRNA had no significant effect on TRPM7 channel expression level compared to control, in contrast TRPM7-siRNA produced an immense loss ($P < 0.0001$ versus control) in TRPM7 channel protein expression (Figures 4.13 and 4.14). After this determination, experiments further followed whether TRPM7 channel knockdown impacts on *STHdh^{Q111}/Hdh^{Q111}* cell viability in the presence of H₂O₂, CoCl₂, and staurosporine using the 24 hour exposure protocol. Intriguingly, the cell viability results revealed that this pre-treatment dramatically ($P < 0.0001$ versus insult) protected *STHdh^{Q111}/Hdh^{Q111}* cells from harm from H₂O₂, CoCl₂, and staurosporine. Cells lacking TRPM7 channels are more resistant to these toxic effects, namely oxidative stress, hypoxia, as well as apoptotic induction (Figures 4.15, 4.16 and 4.17), which by themselves caused a vast decrease in normal *STHdh^{Q111}/Hdh^{Q111}* cell numbers. Cells receiving GFP-siRNA were similarly sensitive as control cells (Figures 4.15, 4.16 and 4.17) to all insults.

These data clearly demonstrate that not only TRPM7 channel blockade, but also its downregulation is neuroprotective in these diseased cells.

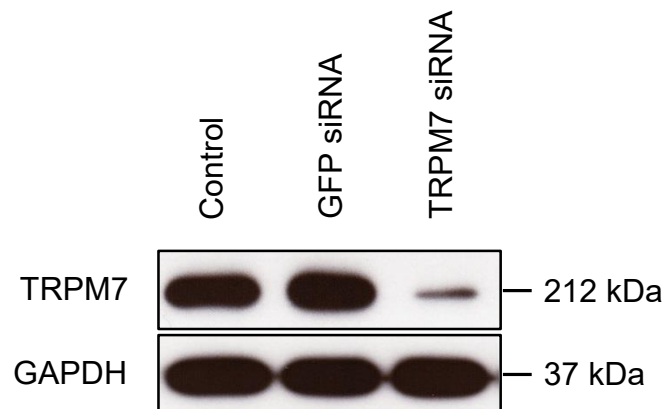


Figure 4.13 Representative immunoblot of TRPM7 channel in homozygous mutant *Hdh^{Q111/} Hdh^{Q111}* cells transfected with specific TRPM7-siRNA. TRPM7 channel protein expression is markedly downregulated compared to control. GAPDH serves as the normalising control.

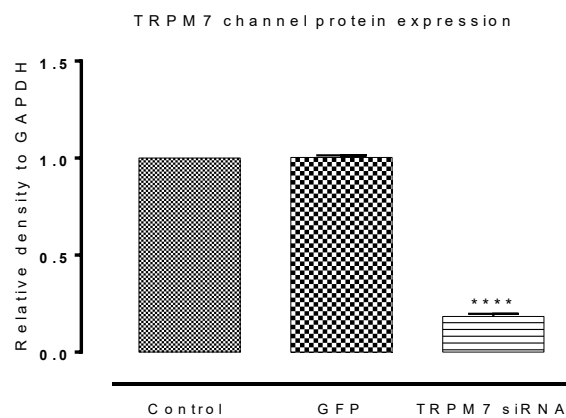


Figure 4.14 Densitometric measurement of TRPM7 channel in homozygous mutant *Hdh^{Q111/} Hdh^{Q111}* cells transfected with specific TRPM7-siRNA. Data are shown as means \pm SEM. *****p*-value < 0.0001 versus control, one-way ANOVA followed by Dunnett's post hoc test, *n* = 3.

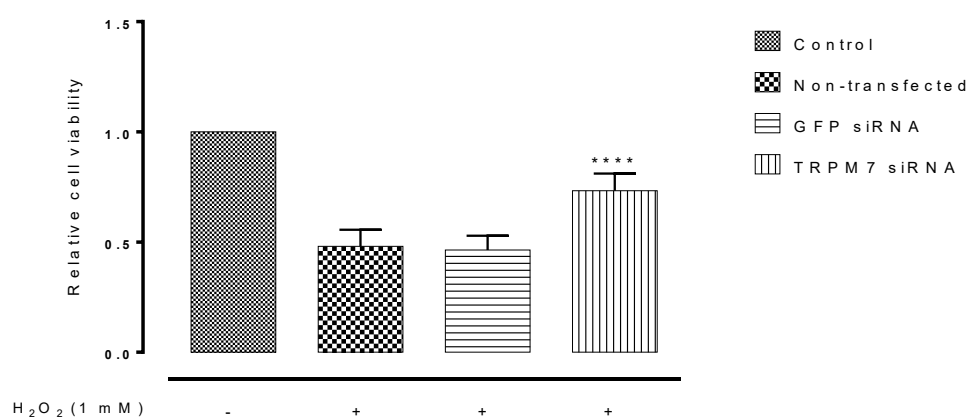


Figure 4.15 The effect of siRNA-mediated knockdown of TRPM7 channel on the survival of homozygous mutant *Hdh*^{Q111}/*Hdh*^{Q111} cells exposed to H₂O₂-induced oxidative stress. Data are shown as means ± SEM. *****p*-value < 0.0001 versus insult, one-way ANOVA followed by Dunnett's post hoc test, n= 9.

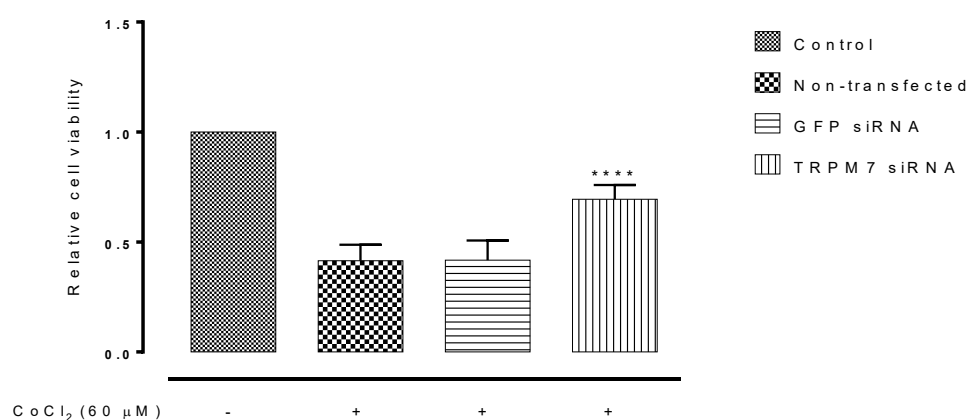


Figure 4.16 The effect of siRNA-mediated knockdown of TRPM7 channel on the survival of homozygous mutant *Hdh*^{Q111}/*Hdh*^{Q111} cells exposed to CoCl₂-induced hypoxia. Data are shown as means ± SEM. *****p*-value < 0.0001 versus insult, one-way ANOVA followed by Dunnett's post hoc test, n= 9.

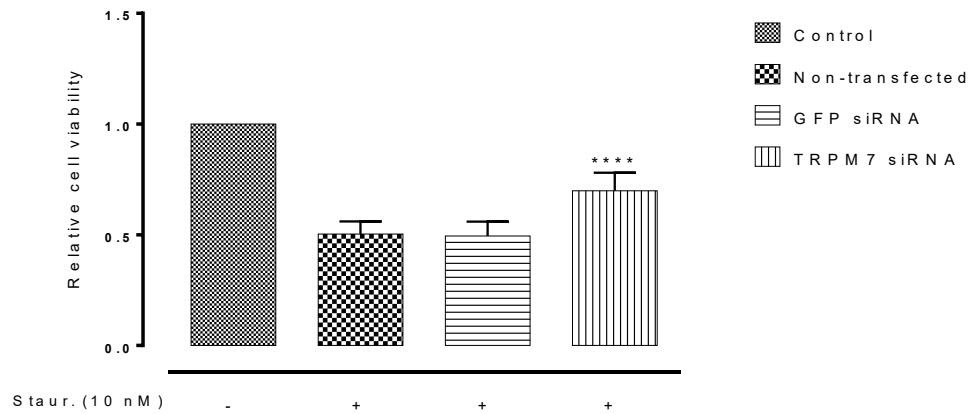


Figure 4.17 The effect of siRNA-mediated knockdown of TRPM7 channel on the survival of homozygous mutant *Hdh*^{Q111}/*Hdh*^{Q111} cells exposed to staurosporine-induced apoptosis. Data are shown as means \pm SEM. **** p -value $<$ 0.0001 versus insult, one-way ANOVA followed by Dunnett's post hoc test, $n = 9$.

4.4.2 TRPM7 ion channel expression in human astrocytoma MOG-G-UVW cells

4.4.2.1 TRPM7 channel mRNA and protein investigation in MOG-G-UVW cells

In the second part of this work, experiments tested the same hypothesis using another CNS derived cell type, a human brain astrocytoma. Similar questions and aims were addressed as shown in part one of this work. Wild-type MOG-G-UVW cells are less frequently used in research activities compare to other cell lines used in neuroscience to date. RT-PCR first investigated the TRPM7 channel message in MOG-G-UVW cells at the mRNA level (Figure 4.19). This was further examined by Western blotting to test whether the gene target also formed the channel protein. It was found that these channels are also expressed at the protein level (Figure 4.20). It is important to emphasise again that this cell line only has the SK4 subtype of SK channel (Figure 4.18), so helping to avert target confusion since this study used two SK1-3 channel blockers, in the micromolar range to produce TRPM7 channel blockade.

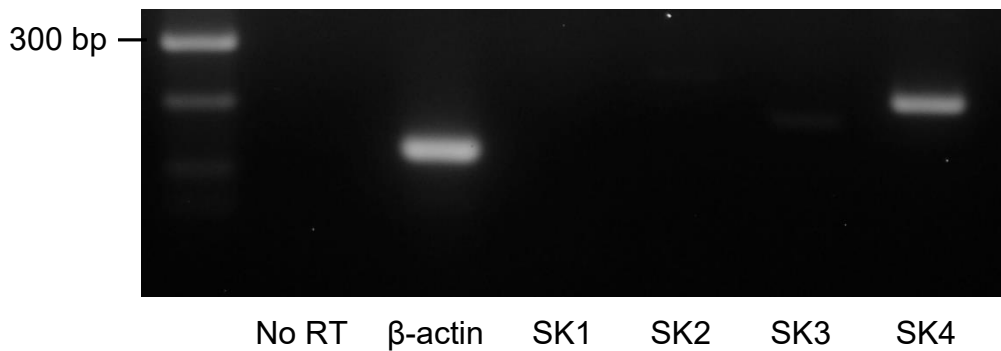


Figure 4.18 SK channel mRNA investigation in MOG-G-UVW cells. Only the amplicon for SK4 channel is present and the PCR products are of the predicted size. β -actin serves as the normalising control.

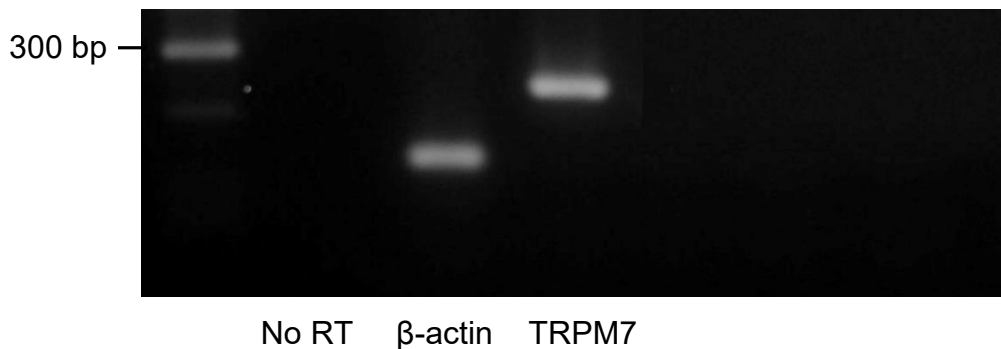


Figure 4.19 TRPM7 channel mRNA investigation in MOG-G-UVW cells. The amplicon for TRPM7 channel is present and the PCR products are of the predicted size. β -actin serves as the normalising control.

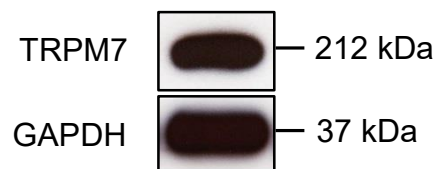


Figure 4.20 Representative immunoblot of TRPM7 channel subtype in MOG-G-UVW cells. GAPDH serves as the normalising control.

4.4.2.2 The effect of pharmacological TRPM7 channel inhibition on MOG-G-UVW cell viability

The pharmacological approach first assessed the effect TRPM7 channel blocking alone on MOG-G-UVW cell viability over 24 hours. In the MTS assay, SK1-3 channel blockers NS8593 (20-40 μM) and UCL1684 (20-40 μM) were tested on the proliferation of MOG-G-UVW cells (Figures 4.21 and 4.22, respectively). This screening did not significantly affect MOG-G-UVW cell numbers compared to control for the time indicated. This shows that these cells do not adopt constitutive TRPM7 channel activity for their proliferation. In this respect, experiments also considered the effect of lower doses of NS8593 (5 and 10 μM) and UCL1684 (5 and 10 μM): these concentrations were also inactive on MOG-G-UVW cell viability (Appendix 3, Figures 7.13 and 7.14).

These data encouraged this work to be progressed to the next stage, as these compounds did not modulate normal cell growth in MOG-G-UVW cells.

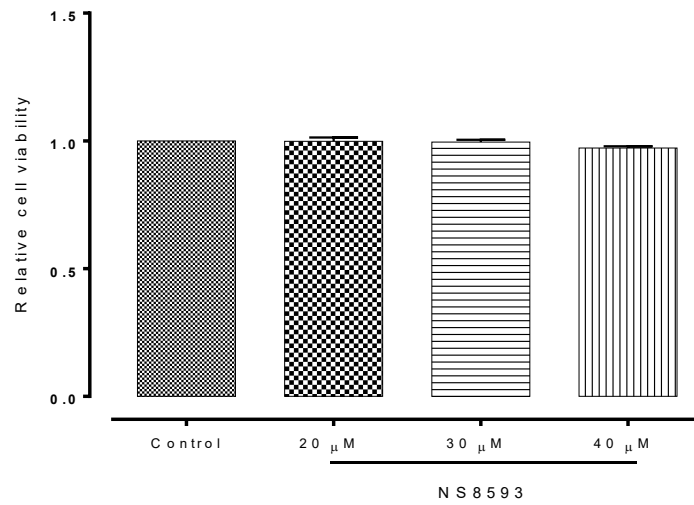


Figure 4.21 The effect of NS8593, TRPM7 channel inhibition, on MOG-G-UVW cell viability. Data are shown as means \pm SEM. One-way ANOVA followed by Dunnett's post hoc test, n=6.

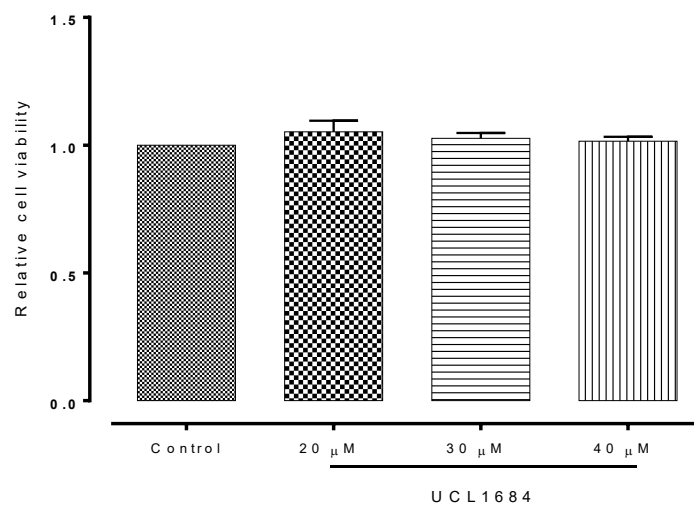


Figure 4.22 The effect of UCL1684, TRPM7 channel inhibition, on MOG-G-UVW cell viability. Data are shown as means \pm SEM. One-way ANOVA followed by Dunnett's post hoc test, n=6.

4.4.2.3 The dose-response curve for cellular insults in MOG-G-UVW cells

Again *in vitro* pharmacological experiments determined the LD₅₀s of cellular insults by the aid of dose-response measures, using H₂O₂, CoCl₂, and staurosporine to induce oxidative stress, hypoxia, and apoptosis respectively. These agents challenged cell viability and MTS assays estimated different LD₅₀s of the insults against MOG-G-UVW cell viability. MOG-G-UVW cells were less sensitive to H₂O₂ with an LD₅₀ 1 mM (Figure 4.23), while these cells showed a moderate sensitivity to CoCl₂ with an LD₅₀ 32 μM (Figure 4.24), and they were more sensitive to staurosporine toxic effect with an LD₅₀ of 50 nM (Figure 4.25).

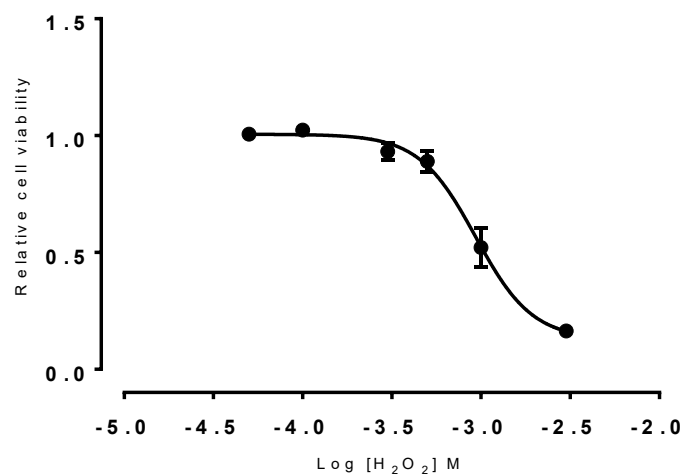


Figure 4.23 The effect of H₂O₂ on MOG-G-UVW cell viability. From the line of best fit of the dose-response data, the LD₅₀ was 1 mM, n= 9.

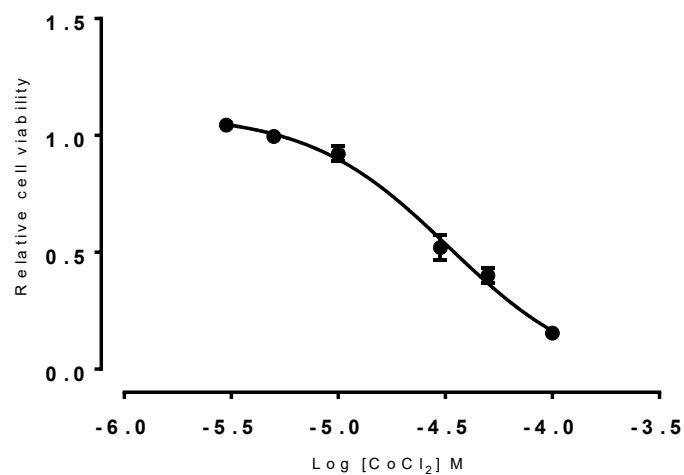


Figure 4.24 The effect of CoCl₂ on MOG-G-UVW cell viability. From the line of best fit of the dose-response data, the LD₅₀ was 32 μM, n= 9.

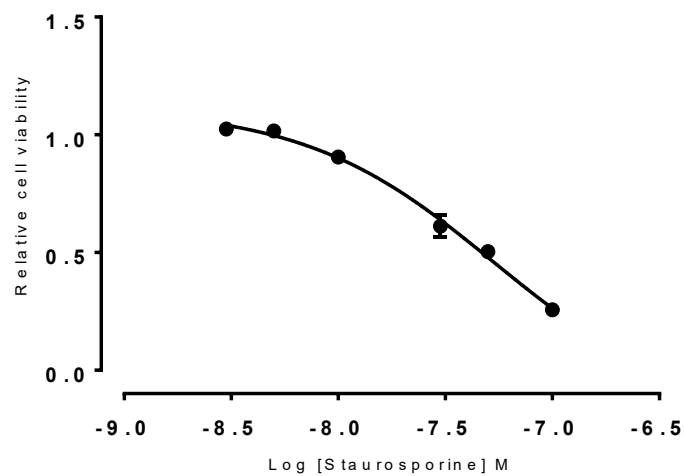


Figure 4.25 The effect of staurosporine on MOG-G-UWV cell viability. From the line of best fit of the dose-response data, the LD₅₀ was 50 nM, n= 9.

4.4.2.4 Pharmacological inhibition of TRPM7 channel against cellular insults in MOG-G-UVW cells

The next series of experiments checked whether TRPM7 channel inhibition promotes cell survival in the face of various cell death mechanisms, namely H₂O₂, CoCl₂, and staurosporine insults. This established that NS8593 (20-40 μM) and UCL1684 (20-40 μM), SK1-3 channel blockers, by blocking TRPM7 significantly protected ($P < 0.0001$ versus insult) cells against oxidative stress (Figures 4.26 and 4.27, respectively), hypoxia (Figures 4.28 and 4.29, respectively), and apoptosis (Figure 4.30 and 4.31, respectively). As expected, these modulators did not always have a protective role at 10 μM, where NS8593 did not oppose CoCl₂ and staurosporine induced effects (Figures 4.28 and 4.30, respectively). These data were encouraging, and the question was further pursued in siRNA experiments.

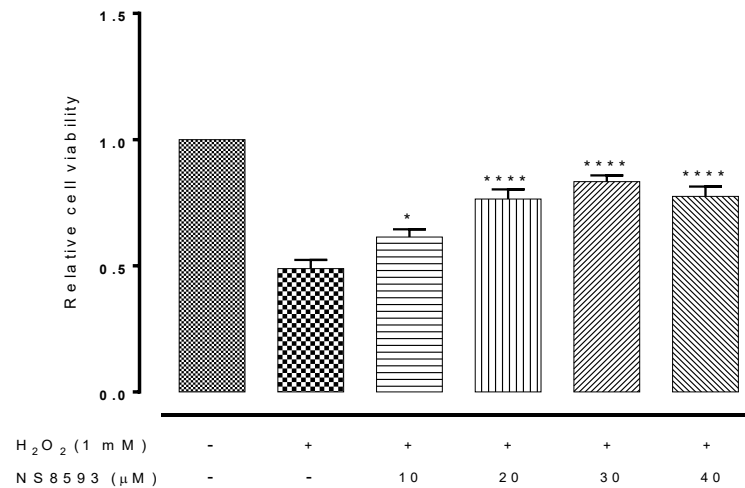


Figure 4.26 The effect of NS8593, TRPM7 channel inhibition, on the survival of MOG-G-UWV cells exposed to H₂O₂-induced oxidative stress. Data are shown as means \pm SEM. *****p*-value < 0.0001 versus insult, one-way ANOVA followed by Dunnett's post hoc test, *n* = 9.

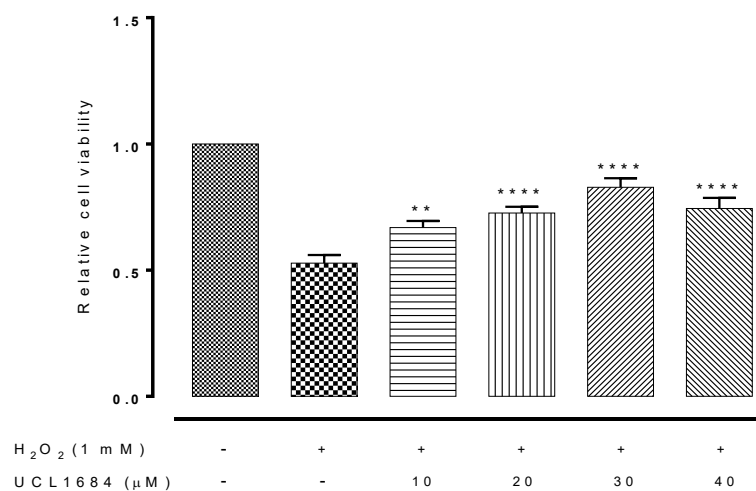


Figure 4.27 The effect of UCL1684, TRPM7 channel inhibition, on the survival of MOG-G-UWV cells exposed to H₂O₂-induced oxidative stress. Data are shown as means \pm SEM. *****p*-value < 0.0001 versus insult, one-way ANOVA followed by Dunnett's post hoc test, *n* = 9.

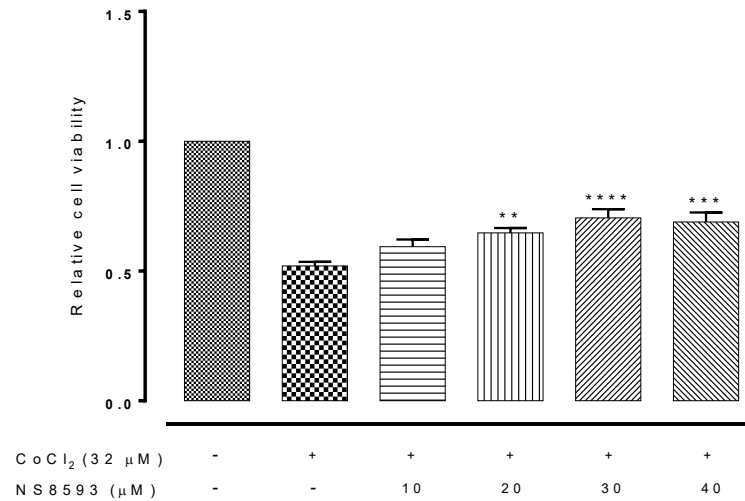


Figure 4.28 The effect of NS8593, TRPM7 channel inhibition, on the survival of MOG-G-UVW cells exposed to CoCl₂-induced hypoxia. Data are shown as means \pm SEM. **** p -value < 0.0001 versus insult, one-way ANOVA followed by Dunnett's post hoc test, $n = 9$.

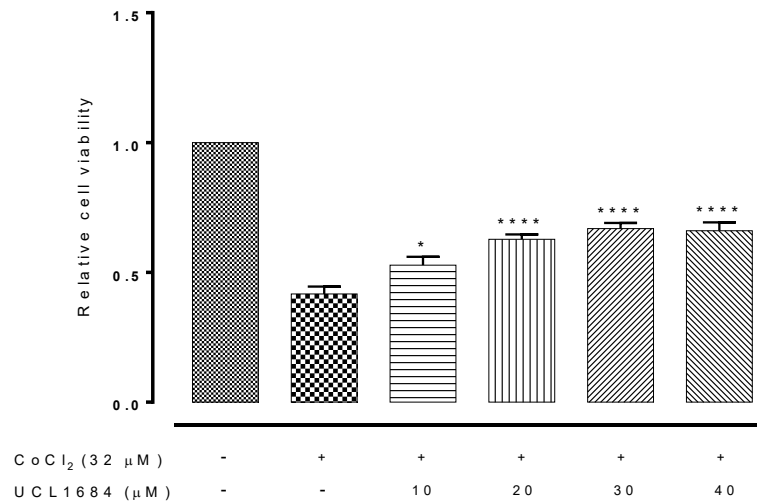


Figure 4.29 The effect of UCL1684, TRPM7 channel inhibition, on the survival of MOG-G-UVW cells exposed to CoCl₂-induced hypoxia. Data are shown as means \pm SEM. **** p -value < 0.0001 versus insult, one-way ANOVA followed by Dunnett's post hoc test, $n = 9$.

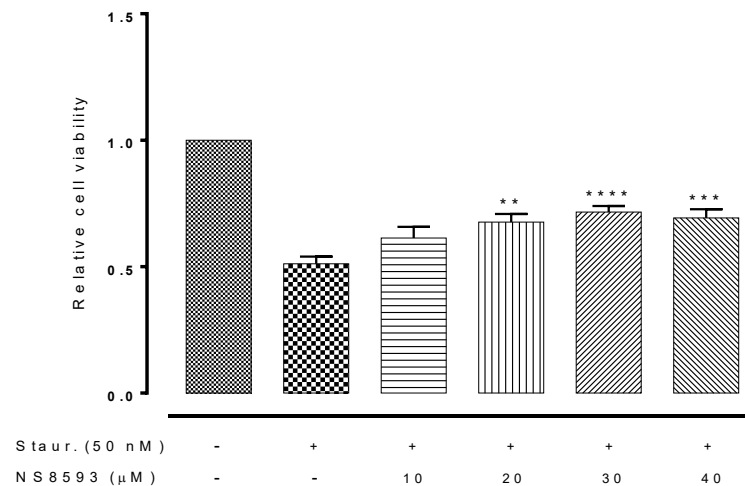


Figure 4.30 The effect of NS8593, TRPM7 channel inhibition, on the survival of MOG-G-UVW cells exposed to staurosporine-induced apoptosis. Data are shown as means \pm SEM. **** p -value $<$ 0.0001 versus insult, one-way ANOVA followed by Dunnett's post hoc test, $n = 9$.

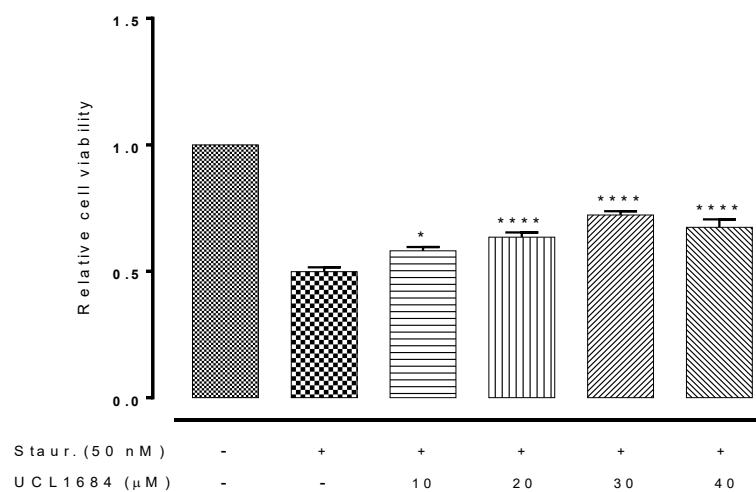


Figure 4.31 The effect of UCL1684, TRPM7 channel inhibition, on the survival of MOG-G-UVW cells exposed to staurosporine-induced apoptosis. Data are shown as means \pm SEM. **** p -value $<$ 0.0001 versus insult, one-way ANOVA followed by Dunnett's post hoc test, $n = 9$.

4.4.2.5 Small interference RNA-mediated modulation of TRPM7 channel against cellular insults in MOG-G-UVW cells

Small interference RNA experiments then tested whether TRPM7 channel knockdown can result in MOG-G-UVW cells resistant against death insults delivered through different mechanisms. These experiments used specific human TRPM7-siRNA to dampen TRPM7 channel expression in MOG-G-UVW cells. Western blotting results indicated that TRPM7 expression in GFP-treated cells was entirely normal (Figures 4.32 and 4.33). Importantly, densitometric analysis also showed that TRPM7-siRNA caused a marked reduction ($P < 0.0001$ versus control) in TRPM7 channel protein expression (Figures 4.32 and 4.33) 72 hours post-transfection. In the cell viability monitoring 24 hours after transfection, MTS results from knockdown of TRPM7 channels mirrored the pharmacological results. MOG-G-UVW deficient of TRPM7 channels were in fact significantly more viable ($P < 0.0001$ versus insult) in the face of H_2O_2 -induced oxidative stress (Figure 4.34), $CoCl_2$ -induced hypoxia (Figure 4.35), and staurosporine-induced apoptosis (Figure 4.36) than normal cells.

The data in this chapter are very compelling, TRPM7 channel inhibition in the face of three important models of cell death plays a central role in combating these three stressors, namely H_2O_2 -induced oxidative stress, $CoCl_2$ -induced hypoxia, and staurosporine-induced apoptosis. This indicates that this channel has a big role in survival of these CNS resident cells, i.e. both normal brain astrocytes, and the mouse cell model of Huntington's disease.

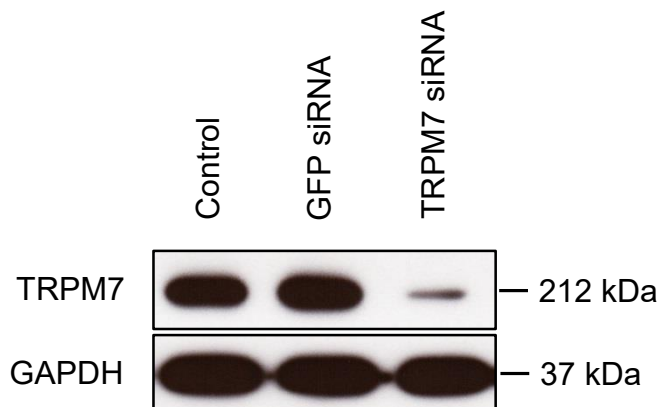


Figure 4.32 Representative immunoblot of TRPM7 channel in MOG-G-UVW cells transfected with specific TRPM7-siRNA. TRPM7 channel protein expression is considerably downregulated compared to control. GAPDH serves as the normalising control.

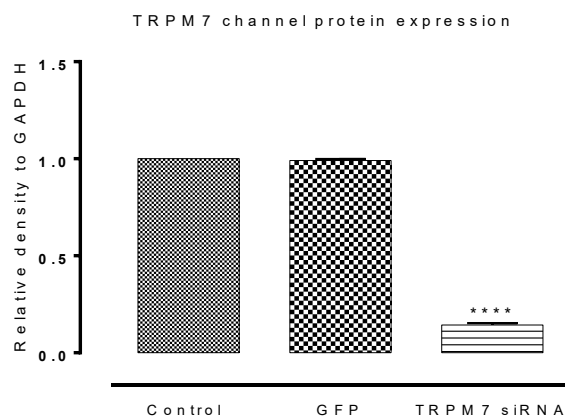


Figure 4.33 Densitometric measurement of TRPM7 channel in MOG-G-UVW cells transfected with specific TRPM7-siRNA. Data are shown as means \pm SEM. **** p -value < 0.0001 versus control, one-way ANOVA followed by Dunnett's post hoc test, $n = 3$.

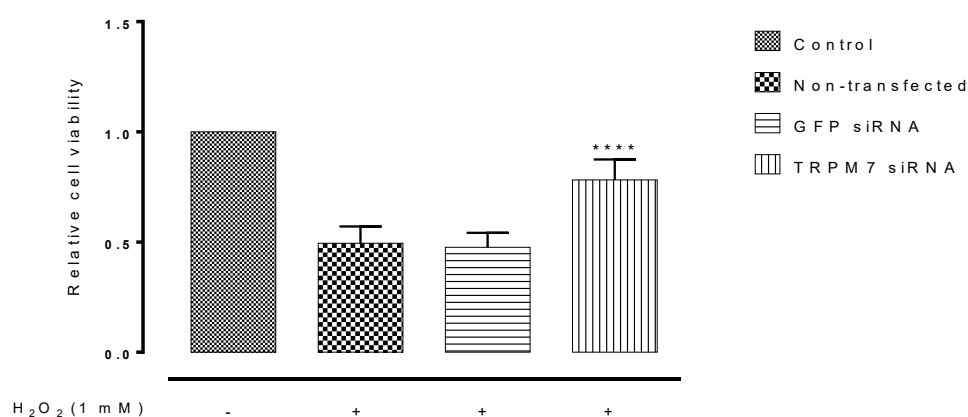


Figure 4.34 The effect of siRNA-mediated knockdown of TRPM7 channel on the survival of MOG-G-UVW cells exposed to H₂O₂-induced oxidative stress. Data are shown as means \pm SEM. **** p -value $<$ 0.0001 versus insult, one-way ANOVA followed by Dunnett's post hoc test, $n = 9$.

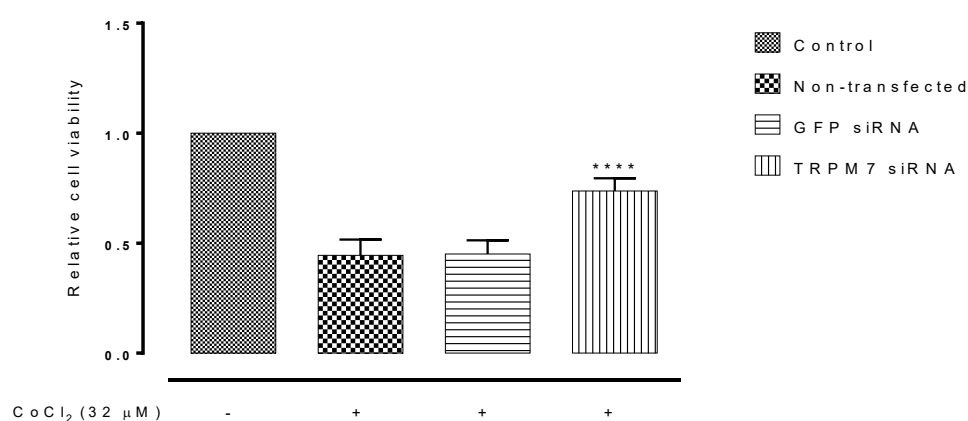


Figure 4.35 The effect of siRNA-mediated knockdown of TRPM7 channel on the survival of MOG-G-UVW cells exposed to CoCl₂-induced hypoxia. Data are shown as means \pm SEM. **** p -value $<$ 0.0001 versus insult, one-way ANOVA followed by Dunnett's post hoc test, $n = 9$.

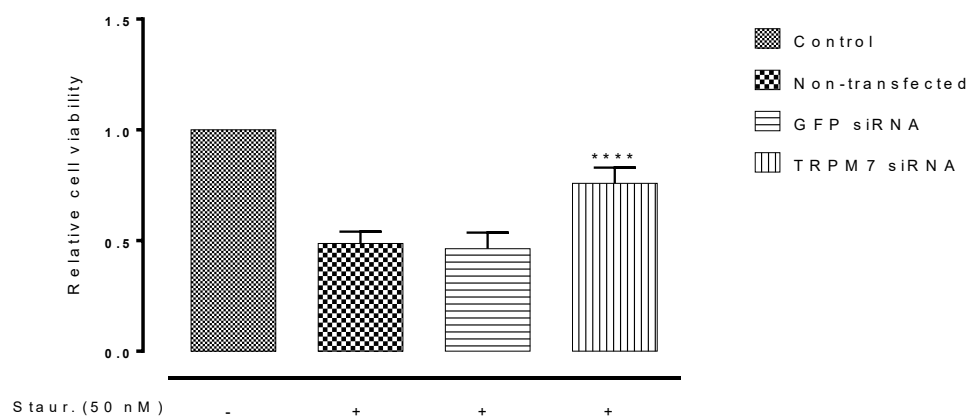


Figure 4.36 The effect of siRNA-mediated knockdown of TRPM7 channel on the survival of MOG-G-UVW cells exposed to staurosporine-induced apoptosis. Data are shown as means \pm SEM. **** p -value < 0.0001 versus insult, one-way ANOVA followed by Dunnett's post hoc test, $n = 9$.

4.5 Discussion

The principal findings of this work are:

1. In ***STHdh^{Q111}/Hdh^{Q111}*** cells, a mouse homozygous cell model of Huntington's disease, it was found that TRPM7 channels are expressed at both mRNA and protein levels in RT-PCR and Western blotting experiments.
2. Pharmacological screening indicated that TRPM7 channel blockade in *STHdh^{Q111}/Hdh^{Q111}* cells did not significantly modify the cell proliferation rate, indicating that this channel does not inhibit constitutive growth.
3. MTS cell viability assays also found that these cells were more sensitive to staurosporine-induced apoptosis than CoCl₂ and H₂O₂.
4. Pharmacological blocking of TRPM7 afforded significant protection against cell death mechanisms, namely staurosporine-induced apoptosis, CoCl₂-induced hypoxia, and H₂O₂-induced oxidative stress.
5. Intriguingly, pharmacological results were well supported by the channel target knockdown in siRNA experiments. This revealed that TRPM7 channel knock-out also significantly protected *STHdh^{Q111}/Hdh^{Q111}* against all insults indicated.
6. In **MOG-G-UVW** cells, a human brain astrocyte, RT-PCR and Western blotting investigations determined the presence of TRPM7 channels at both mRNA and protein levels respectively.
7. MTS assays showed that TRPM7 channel blocking had no effect on MOG-G-UVW proliferation, again indicating no impact of these channels on normal growth.
8. These cells were also more sensitive to staurosporine than other insults.

9. TRPM7 channel blockade in the presence of staurosporine-induced apoptosis, CoCl_2 -induced hypoxia, and H_2O_2 -induced oxidative stress, was also markedly protective, compared to the insult alone.
10. TRPM7 siRNA-mediated knock-out in MOG-G-UVW cells reflected the pharmacological TRPM7 channel results. Downregulation produced MOG-G-UVW cells more resistant against all the insults above.

The main focus of this work was to determine whether the TRPM7 channel promises to be a neuroprotectant molecule in human brain astrocytes and a mouse homozygous cell model of Huntington's disease against dysfunction mediated by staurosporine-induced apoptosis, CoCl_2 -induced hypoxia, and H_2O_2 -induced oxidative stress. There is a growing bank of knowledge that indicates that the TRPM7 channel is an impressive target in both neurodegeneration (Park et al. 2014) and the cancers (Deliot and Constantin 2015; Guilbert *et al.* 2009). Expression experiments of this present study first showed that the channel of interest is expressed in *STHdh^{Q111}/Hdh^{Q111}* and MOG-G-UVW cells (Figures 4.1-4.2 and 4.19-20, respectively) using RT-PCR and Western blotting methods. A later step checked whether the channel protein is functionally generated. This began with pharmacological probing in MTS cell viability assays. It is important to stress that the pharmacological approach used SK1-3 channel modulators for TRPM7 channel modulation, since it was recently shown that SK channel modulators can also block the TRPM7 ion channel at micromolar concentrations (see Figure 4.37), as in electrophysiological experiments NS8593 (30 μM) fully inhibited the TRPM7 channel current (Chubanov et al. 2012). SK1-3 blockers used in this work block the SK1-3 channels at nanomolar ranges, bypassing profile overlapping. Importantly, *STHdh^{Q111}/Hdh^{Q111}* cells expressed no SK2-3 channels (Figure 4.1), and the SK1 channel cDNA does not form a functional ion channel (Benton et al. 2003; D'Hoedt et al. 2004). In MOG-G-UVW cells, no SK1-3 channel transcripts were present at the mRNA level (Figure 4.18). Experiments screened the TRPM7 channel, bracketing the 30 μM dose as this concentration is more potent on channel activity (Chubanov et al. 2012). First, the effect of the modulators alone, namely NS8593

and UCL1684 was tested in the viability assays at 24 hours: here no significant effect on the cell numbers was found (Figures 4.3, 4.4 and 4.21, 4.22, respectively).

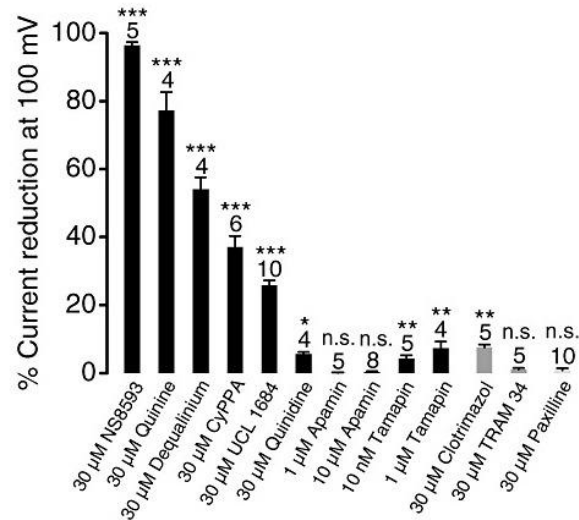


Figure 4.37 TRPM7 channel blocking by the SK channel modulators. NS8593 (30 μ M) can fully block TRPM7 channel current. Other SK channel modulators can also significantly block the channel target as indicated (Chubanov et al. 2012).

In the next phase, LD₅₀s of the insults were determined from the dose-response curves (Figures 3.43, 4.5, 4.6 and 4.23, 4.24, 4.25 respectively). In this regard, it has been documented that exogenous hydrogen peroxide (H₂O₂) can reach the cytosol by crossing the plasma membrane (Bienert et al. 2006; Fatokun et al. 2008). This stressor can react with active metals, particularly copper and iron, thus producing highly reactive cytotoxic radicals such as hydroxyl radicals (Bourassa and Miller 2012), which cause detrimental cell injury. Intriguingly, TRPM7 channel blocking ($P < 0.0001$ versus insult) reversed the cytotoxic effect of H₂O₂ in *STHdh^{Q111}/Hdh^{Q111}* and MOG-G-UVW cells. In this challenge and all subsequent challenges in this work the modulators, NS8593 and UCL1684, were protective at

(20-40 μM) in the presence of all insults indicated, but in some cases 10 μM of blockers did not significantly challenge the insults used (Figures 4.7-4.8 and 4.26-4.27, respectively). Nowadays, the involvement of TRPM7 channels in ischaemic conditions and cellular ROS regulation is accepted. Studies report that H_2O_2 caused TRPM7 activation and this elevated $[\text{Ca}^{2+}]_i$ (Coombes *et al.* 2011). In a detailed investigation of oxidative stress in Parkinson's disease (PD), interestingly, PD lesions, through α -Synuclein, exacerbated the physiological stress via mitochondria. This possible stress elevation is physiologically generated because it can be eliminated through inhibition of voltage dependent L-type calcium channels (Dryanovski *et al.* 2013). Silencing of TRPM7 channel gene in *STHdh^{Q111}/Hdh^{Q111}* and MOG-G-UVW cells mimicked the pharmacological picture (Figures 4.15 and 4.34, respectively), affording a profound increase ($P < 0.0001$ versus control) in cell viability. In aerobic organisms, oxygen (O_2) is required for normal tissue wellbeing, and hypoxia-inducible transcription factor 1 (HIF-1) plays a critical role that can be activated by CoCl_2 (Caltana *et al.* 2009). In Hep3B cells, real hypoxia mediates transcription in a mitochondrial-dependent manner, causing an increase in ROS, but CoCl_2 can induce transcription via ROS generation in a mitochondrial-independent pattern (Chandel *et al.* 1998). MTS viability assessments showed that TRPM7 channel blocking also significantly dampened ($P < 0.0001$ versus insult) the harmful delivery of CoCl_2 in *STHdh^{Q111}/Hdh^{Q111}* and MOG-G-UVW cells (Figures 4.9-4.10 and 4.28-4.29, respectively). Again, siRNA-mediated elimination of the TRPM7 channel made *STHdh^{Q111}/Hdh^{Q111}* and MOG-G-UVW cells less vulnerable ($P < 0.0001$ versus control) to the CoCl_2 hypoxia-mimetic effect (Figures 4.16 and 4.35, respectively). It has been revealed that knockdown of TRPM7 channels in hippocampal neurons, significantly attenuated an increase in intracellular $[\text{Mg}^{2+}]_i$

caused by anoxia (Zhang et al. 2011a). Moreover, TRPM7 dampening also improved ischaemia-induced long term potentiation and memory tasks (Sun et al. 2009). It is accepted that staurosporine creates apoptosis via PKC inhibition, but it is not selective. It may also inhibit other kinases such as tyrosine kinase (Ruegg and Burgess 1989), and more recently, staurosporine has been linked to store-operated Ca^{2+} entry (SOCE). Single cell imaging in staurosporine-induced cells shows that this entry remained activated after Ca^{2+} replenishment (Tojyo et al. 2013). Screening TRPM7 channel activity against staurosporine-induced apoptosis, showed that its inhibition markedly saved ($P < 0.0001$ versus insult) *STHdh^{Q111}/Hdh^{Q111}* and MOG-G-UVW cells from apoptosis (Figures 4.11-4.12 and 4.30-4.31, respectively). Invariably, TRPM7 abolishment through siRNA also showed an increase ($P < 0.0001$ versus control) in cell viability level (Figures 4.17 and 4.36, respectively). TRPM7 channel seems therefore a powerful target in neurodegeneration, being also linked to apoptosis, since it has been shown that TRPM7 knockdown increases fibroblast resistance to apoptotic stimuli through lowering ROS levels in a Mg^{2+} -dependent manner (Chen et al. 2012).

Excitatory neurotransmission has been recently linked to microglial activation, revealing that activated microglial cells release ATP, that can be amplified by astrocytes and binds to purinergic receptors (P2Y1R) on astrocytes, and ultimately this stimulation increases excitatory postsynaptic currents through a glutamate receptor-dependent pathway (Pascual *et al.* 2012). Interestingly, experiments here found that LPS-induced microglia caused remarkable upregulation of the TRPM7 channel expression in these cells (Appendix 3, Figure 7.15). MTS viability assays determined that this phenotype killed microglia in cultures, a fascinating result, requiring a detailed examination.

4.6 Conclusions

The data from this *in vitro* work showed that the TRPM7 channel is present in mouse homozygous mutant *STHdh^{Q111}/Hdh^{Q111}* and human brain wild-type MOG-G-UVW cells. This ion channel plays a big role in their survival in the face of various cell death mechanisms. It is fascinating that this channel rescues cells from oxidative stress, hypoxia, as well as apoptosis. Not only modulation of its activity, but also lowering of channel numbers improves cell viability in these abnormal conditions. This is the first study to question TRPM7 channel expression and any role in diseased mutant cells of this neurodegenerative model, namely *STHdh^{Q111}/Hdh^{Q111}*. These data illustrate that TRPM7 gene generates a functional channel in these cells, and this channel represents a robust target for neuroprotection.

4.7 Recommendations and future work

TRPM7 channel pharmacology is not well advanced. Thus, advances in this area to develop selective modulators will be very important. Mapping TRPM7 expression and its significance in other cells, particularly in cell models of neurodegenerative diseases would also provide further understanding in this field. Future investigations that can determine further knowledge about TRPM7 role *in vivo* will shed significant progress regarding this protein. Another task will be the elucidation of the channel regulatory mechanisms, including the importance of the channel kinase.

5 Chapter Five: SK Ion Channel in Death of Breast Cancer Cells

5.1 Introduction

SK potassium ion channels, namely small conductance (SK1-3) and a closely allied intermediate conductance (SK4) calcium-activated K^+ channel (Adelman et al. 2012; Kohler et al. 1996), significantly shape the symphony of Ca^{2+} signaling at both cellular (Xia et al. 1998) and molecular (Dolga et al. 2013) levels, thereby governing the myriad of cellular activities in the biology of excitable, and non-excitable cells. In such biology, SK ion channels possess a definite canonical role, which facilitates K^+ efflux and produces an hyperpolarisation (Alger and Nicoll 1980), thus reducing Ca^{2+} influx and potential Ca^{2+} overload. Activation alters firing patterns and memory, although the precise links between cellular events and higher order functions such as memory are not well defined. SK channels also regulate calcium flux in the later biology in the form of non-canonical roles (Pardo and Stuhmer 2014). This role offers compelling oncological relevance in the delineation of cancer hallmarks, judging from frequently highlighted outcomes of studies (Huang and Jan 2014) with the theme of Ca^{2+} levels in cancer featuring and supporting the notion that these SK molecules are notoriously implicated in the cancer phenotype. Indeed, this has increased the interest in cancer, as calcium affects physiological processes at different levels (Roderick and Cook 2008), driving cancer progression, migration, as well as mediating metastasis (Azimi *et al.* 2014). In this respect, it is not surprising that triple negative breast cancer cells, MDA-MB-435, require $K_{Ca2.3}$ (SK3) channels for cell migration by regulating calcium fluxes and membrane potential (Potier *et al.* 2006). *In vivo* profiling of the $K_{Ca3.1}$ (SK4) blocker, TRAM-34, on the infiltrative

behavior of glioblastoma multiforme, further improved the understanding of the SK channel role in this scenario, whereby blocking of the resident SK4 channels in malignant glioblastoma multiforme curbs diffusing of malignant cells, and in fact reduces the resultant astrocytosis (D'Alessandro *et al.* 2013). *In vitro* experiments also indicate that SK4 inhibition exclusively disrupts the crosstalk between tumours and neighboring resident cells, reactive astrocytes and microglia, in the brain. Recent work strengthens this notion, and points to astrocytes underlying life decisions of tumour cells, favouring their growth (Biasoli *et al.* 2014). In the gating of the SK class of K^+ ion channels, these proteins do not provide an inherent domain for Ca^{2+} binding, instead they use a modular protein, termed calmodulin (CaM), to chelate Ca^{2+} ions (Maylie *et al.* 2004). More recently it has been shown that CaM exists as an intrinsic partner in the SK channel complex (Adelman 2015). Moreover, the channel activity is tightly regulated by a bound casein kinase 2 (CK2) and protein phosphatase 2A (PP2A) (Allen *et al.* 2007), but their role on other cell functions, such as proliferation, remains to be addressed. Novel mechanisms, in the adult human, orchestrate highly programmed pathways through which approximately 60 billion cells (Diaz *et al.* 2005; Reed 2008), undergo daily cell division, thus keeping normal tissue homeostasis throughout. Disappointingly, in certain cancers cells escape from programmed cell death, destabilising physiological cell death, which is literally defection. The central question to be addressed is how cancer cells resist death choices? This facet of their physiology, considering a central for K^+ ion channels, is well reviewed by Huang and Jan (2014). This paper concludes there are four mechanisms. First, changes in cell membrane potential (V_m) throughout the cell cycle seems informative (Yang and Brackenbury 2013). For example, proliferating cancer and stem cells are more depolarized (-20 to -40 mV) than other

cells, namely neurons and cardiomyocytes, which hold their membrane potential at -60 to -80 mV. Moreover, cells throughout the cell cycle in fact have a depolarized V_m in the G2/M transition. K^+ ion channels have another traditional role, regulating cellular proliferation through cell volume control. It has been shown that during the cell cycle the EAG2 voltage-gated K^+ channels sit in different positions, moving from inside the cell to the plasma membrane where they serve as a checkpoint before mitotic entry at G2/M phase (Huang *et al.* 2012). An additional notion is that K^+ ion channel induced membrane hyperpolarisation facilitates Ca^{2+} entry through TRP ion channels (Wulff and Kohler 2013), thereby increasing $[Ca^{2+}]_i$, which positively triggers cell proliferation (Huang and Jan 2014). In addition to these canonical roles, it is worth highlighting their emerging roles as non-conducting channels. Indeed, it has been reported that when a nonconducting mutant, Kv1.3 channel, is expressed in HEK cells, and these cells do not lose growth capacities (Cidad *et al.* 2012).

In the light of this last idea, this study will address the non-canonical role of SK potassium ion channels in the context of breast cancer biology, particularly cell proliferation, as well as questioning a putative mechanism that links these ion channels to the signalling cascades. The International Agency for Research on Cancer currently reported that the global burden through this type of cancer in females reaches approximately 22.9% as an invasive cancer.

5.2 Hypothesis and aims

That SK ion channel activity promotes proliferation in breast cancer lines, and hence SK channel blockade may inhibit cancer cell growth.

The principal objectives are:

1. To determine the profile of expression of SK1-4 channels in five breast cancer cell lines.
2. To establish a role, if any, for SK channels using siRNA-mediated knockdown.
3. To probe any cytotoxic effects of SK channel blockade on breast cancer cell lines using selective small molecule blockers of SK channels.
4. To test whether changes in apoptotic mechanisms are involved in any of the effects observed.

5.3 Materials and methods

5.3.1 Cell origins and features

This *in vitro* study accessed a panel of widely studied breast cancer cell lines, which express various biological and pathological features, as well as endocrine responsiveness as summarised below:

Cell type	Type/Drug	Gene cluster	ER status	PR status	HER2 status	Source and Tumour type
MCF-7	Wild	Luminal	+	+	-	PE, IDC
TamR	Tamoxifen					
FasR	Fulvestrant					
BT-474	Wild	Luminal	+	+	+	P Br., IDC
MDA-MB-231	Wild	Basal B	-	-	-	PE, AC

Table 5.1 Biological features of breast cancer cell lines indicated (Knowlden *et al.* 2005; Knowlden *et al.* 2003; Neve *et al.* 2006). PE denotes pleural effusion, P. Br. denotes primary breast, IDC denotes invasive ductal carcinoma, and AC denotes adenocarcinoma.

The target cells were maintained in their culture using established growth medium and methodologies (See chapter two).

5.3.2 Polymerase chain reaction

The mRNA messages were investigated for all SK family members of K⁺ channels in the target cells. Total RNA was lysed and quantified, its purity and its integrity ensured. The cDNA samples were then synthesized using predesigned primer sequences for the transcripts of SK channel and β -actin which was the necessary reference (See table 5.2). For the negative control, the reaction excluded reverse transcriptase activity, which was referred to as No RT. The target DNA sequences were amplified, conditions being optimised for the PCR reactions of each pair of primers, by varying the temperatures. After the identification of the optimum

conditions for the cell lines, this profile was used in all reactions (PCR). First, denaturation at 95°C for 5 minutes, followed by 30 cycles of incubation consisting of 95°C for 30 seconds, 55°C for 30 seconds, followed by an extension step at 72°C for 1 minute, and final extension step (72°C for 5 minutes). RT-PCR products were stained and then visualised by UV light after being run on an 1% agarose gel electrophoresis.

Gene	Gene ID	Primer sequences	Sizes (bp)
β-actin	NM_001101	F. 5'-CCCAGCCATGTACGTTGCTA-3'	126
		R. 5'-AGGGCATAACCCCTCGTAGATG-3'	
KCNN1 (SK1)	NM_002248.4	F. 5'-TGGACACTCAGCTCACCAAG-3'	208
		R. 5'-TTAGCCTGGTCGTTTCAGCTT-3'	
KCNN2 (SK2)	AF397175.1	F. 5'-CAAGCAAACACTTTGGTGGGA-3'	249
		R. 5'-CCGCTCAGCATTGTAAGTGA-3'	
KCNN3 (SK3)	NM_002249.5	F. 5'-AAGCGGAGAAGCACGTTTCATA-3'	180
		R. 5'-CTGGTGGATAGCTTGGAGGAA-3'	
KCNN4 (SK4)	AB128983.1	F. 5'-GAGAGGCAGGCTGTTATTGC-3'	215
		R. 5'-ACGTGCTTCTCTGCCTTGTT-3'	

Table 5.2 Primer sequences for both human SK channel transcripts and the positive control for the human cell lines, and predicted identities. F. denotes forward primer and R. denotes reverse primer.

In the MCF-7 cell lineage, changes in gene quantity across cell types were analysed, samples from MCF-7 sensitive cells being compared with MCF-7 endocrine resistant cells, which include TamR and FasR cells, to identify whether SK channel transcripts were differentially regulated in endocrine resistant cells, by consulting the Affymetrix microarray database.

5.3.3 Small interference RNA

In order to render an effective knockdown of the channel of interest the Eurofins Genomics database was consulted, to choose the most effective candidate, i.e. one that gained the top rank and highest percentile score based on previous work. Experiments used the following sequences:

For non-targeting siRNA, namely green fluorescent protein (GFP), which serves as non-specific control siRNA: 5'-GGCUACGUCCAGGAGCGCACC-3'. For targeting siRNA, SK2 target sequence: 5'-GCAUUGGAGCACUAAUAA-3' in exon 1, and SK3 specific sequence: 5'-UUGUUGUUAUGGUGAUAGA-3' in exon 3. These were the sequences for the sense in which complementary ends were defined, thereby restricting the sites.

The specific SK siRNA oligonucleotides were complexed with Oligofectamine™ transfection reagent in Opti-MEM® medium. Experiments first monitored the effect of variable concentrations of siRNAs up to 100 nM on the cell lines, optimising the effectiveness of the siRNA transfection.

For studies of siRNA-mediated changes in cellular proliferation and apoptosis, the proliferating cells were seeded a density of 200×10^3 cells per well using six-well plates. After 24 hours, siRNA experiments were conducted using 50 nM and 75 nM to deliver the SK2 and SK3 siRNAs respectively along with controls. After 72 hours, MTS assays were carried out on both control and SK-siRNA treated cells, to test whether SK2-3 gene knockdown impacts on the growth of the cells at one time-point. Cells expressing SK-siRNA along with the controls, were counted, re-plated in 96-well plates and allowed to grow in the regular (siRNA-free) medium, and the medium refreshed every 24 hours. After this expansion, the assay was accomplished by applying the PMS-MTS mix (1:5), thus producing formazan by

functional cells. Cells, non-transfected cells (control), control siRNA (GFP), and SK-siRNA treated, were also examined to uncover the possible mechanisms, if any, which tip the balance between cell growth (Anti-apoptotic proteins) and cell death (Pro-apoptotic proteins), using western blotting. This step was performed 72 hours post-transfection.

5.3.4 Western blotting

Cells were lifted and harvested in cold Dulbecco's phosphate buffered saline by aid of the cell scraper. Next, the pellet was formed, cells (full lysate) were disintegrated in a mixture of Pierce lysis IP buffer and Halt™ protease inhibitor cocktail (100:1), and suspended proteins were left for 30 minutes. After centrifugation, the supernatants that carry proteins, were pipetted into fresh tubes. Protein concentrations were then measured in the BCA assays. PAGE electrophoresis and Immunoblotting used the standard procedure (See chapter two). Following the electrophoresis step, westerns (proteins) were blotted onto membranes, and incubated in a blocking solution, 5% (w/v) dried skimmed milk and Tris buffered Saline with Tween®-20, and were then probed with a variety of specific or loading control antibodies: the noted suppliers' dilution ratios are rabbit polyclonal anti-SK2 long and short isoforms (Abcam ab85401, 1:1000), rabbit polyclonal anti-SK3 (Abcam ab28631, 1:1000), rabbit monoclonal anti-Bcl-2 (Abcam ab32124, 1:1000), rabbit monoclonal anti-Caspase-7 full length and cleaved forms (Cell Signalling Technology #9492, 1:1000), rabbit polyclonal anti- cleaved caspase-9 (Cell Signalling Technology #Asp315, 1:1000), and mouse anti-GAPDH (Sigma-Aldrich G9295, 1:50,000). These were all diluted in the blocking solution. All antibodies, with the exception of anti-GAPDH mouse monoclonal antibody, were incubated

overnight for 16 hours. The following day, membranes were incubated with anti-GAPDH mouse monoclonal antibody after being washed with Tris buffered Saline with Tween®-20. Signals were developed and the exposure times were: 2 minutes, 3 minutes, 2 minutes, 2 minutes, 2 minutes and 30 seconds, for the detection, respectively. The resulting bands (signals) were analysed by densitometry.

5.3.5 SK channel pharmacology

Pharmacological probing of proliferating cells was also employed to examine any changes in the proliferative capacity of the cells in response to the challenge or stimulation with SK channel modulators, namely blockers and activators. After seventy two hours, the levels of cell viability were determined.

5.4 Results

5.4.1 SK channel expression and modulation in wild-type and endocrine resistant MCF-7 cells

5.4.1.1 SK channel mRNA investigation and analysis

In this section RT-PCR was used to investigate the presence of SK channel mRNA message in the MCF-7 (ER⁺, PR⁺, HER2⁻) adenocarcinoma cell line. This indicated that only K_{ca}2.2 (SK2) and K_{ca}3.1 (SK4) channel transcripts were present at the mRNA level (Figure 5.1). These cells can become less sensitive, thus eventually developing resistance to endocrine therapy, namely Tamoxifen and Fulvestrant. In order to test a putative mechanism of resistance, both Tamoxifen-resistant (TamR) and Fulvestrant-resistant (FasR) cell models, were also questioned as to the existence of the message for SK channel transcripts. Similar results were found regarding the presence of SK2 and SK4 channel mRNA in both TamR (Figure 5.2) and FasR (Figure 5.3) cells by RT-PCR. Such qualitative measures of SK channel transcripts (SK1-4) in these models compared to that of wild-type MCF-7 cells were further probed by consulting microarray. There was consistent expression of the SK subtypes in these cell lines, and only FasR cells express significantly increased SK4 channels (p -value < 0.01 versus control) compared to MCF-7 cells (Figure 5.4).

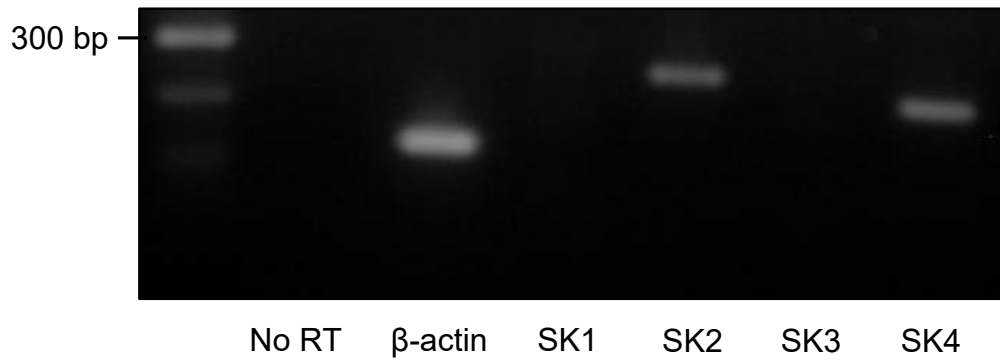


Figure 5.1 SK channel mRNA investigation in wild-type MCF-7 cells. Only the amplicons for SK2 and SK4 channels are present and the PCR products are of the predicted size. β -actin serves as the normalising control.

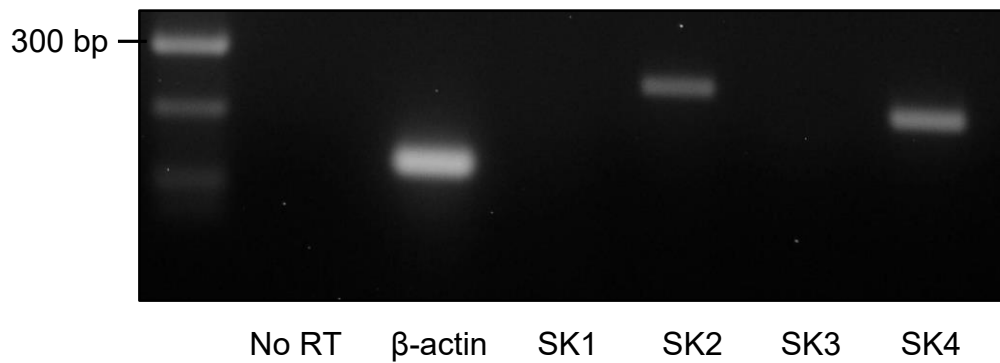


Figure 5.2 SK channel mRNA investigation in endocrine resistant TamR cells. Only the amplicons for SK2 and SK4 channels are present and the PCR products are of the predicted size. β -actin serves as the normalising control.

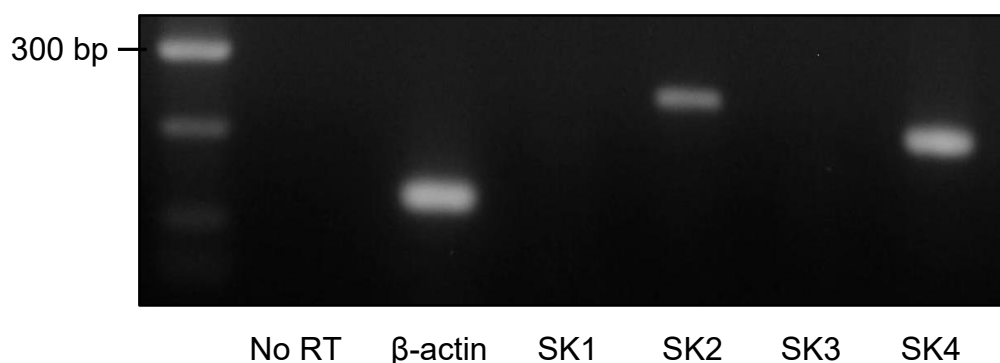


Figure 5.3 SK channel mRNA investigation in endocrine resistant FasR cells. Only the amplicons for SK2 and SK4 channels are present and the PCR products are of the predicted size. β -actin serves as the normalising control.

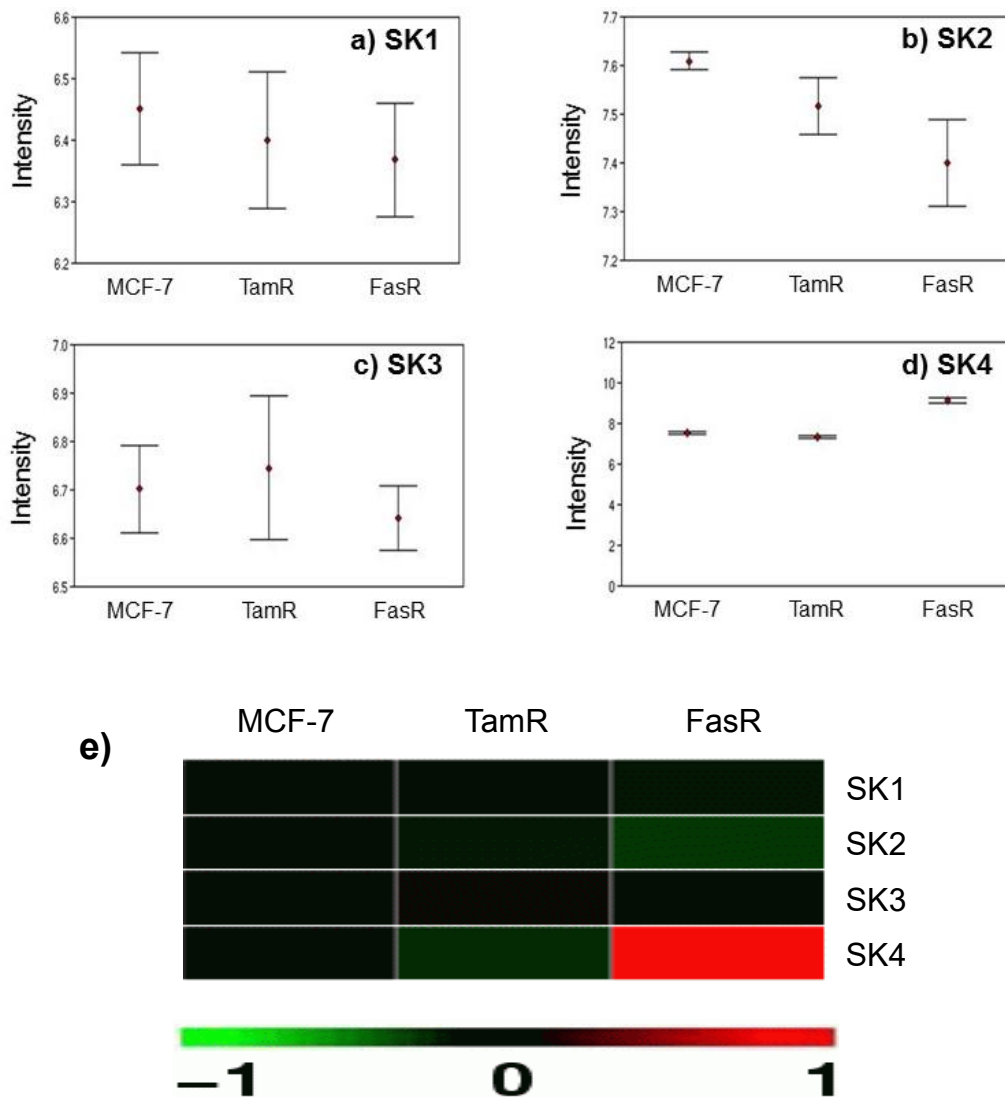


Figure 5.4 Microarray analysis of SK channel transcripts in the MCF-7 cell lineage. a) SK1 gene expression b) SK2 gene expression c) SK3 gene expression d) SK4 gene expression e) Heatmap of SK1-4 gene expression in the indicated cell types. Black boxes denote no change in gene expression. Green boxes denote downregulation. Red boxes denote upregulation. Gene expression intensities are presented in log₂ form. FasR cells express significantly higher SK4 channel expression upon fulvestrant treatment for 27 months, compared to MCF-7 cells, ** p -value < 0.01 versus control, one-way ANOVA followed by Tukey's post hoc test, $n = 3$.

5.4.1.2 SK2 channel protein expression in wild-type MCF-7 cells

The SK2 mRNA message was expressed across the MCF-7 cell lineage (See figures 5.1-5.4), thus cellular expression of SK2 channel was next assessed at the protein level by Western blotting. Because this channel has not been questioned and catalogued in cancer biology, this led to increased interest that it was a channel target. Here, however, it was shown pharmacologically that SK4 inhibition did not significantly (Figure 5.13) block cell growth. In these three cell lines, Western blots revealed two isoforms of the SK2 channel at the protein level (Figure 5.5), variant A that exhibits a long form of SK2, variant B containing a shorter N-terminal extension. Thus, they co-exist in the same tissue and are capable of generating a heteromultimeric channel, functioning in concert (Allen *et al.* 2011a). SK2 channel expression was noticeably higher in MCF-7 cells than resistant cell lines, TamR and FasR, which was consistent with the microarray analysis (see Figure 5.4).

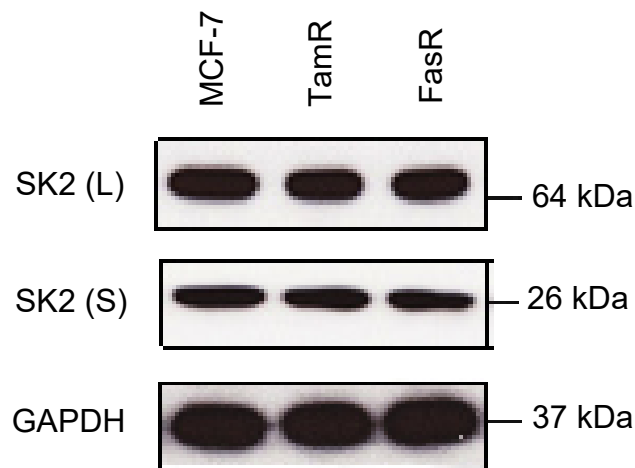


Figure 5.5 Immunoblot of SK2 channel subtype in the MCF-7 cell lineage. In TamR and FasR cells, SK2 channel protein expression is modestly downregulated. GAPDH serves as the normalising control.

5.4.1.3 siRNA-mediated modulation of SK2 channel in MCF-7 cells

Whether SK2 channel gene modulation impacts on MCF-7 cell viability was now tested. Following small interference RNA induction, Western blotting used samples from the following groups: control MCF-7 cells, which were only grown in normal medium, GFP-siRNA treated cells, which were transfected with GFP-siRNA that serves as the normalising siRNA, as well as SK2-siRNA treated cells, which were transfected with 50 nM of total siRNA. As the target gene express two isoforms, both proteins were detected in MCF-7 cells at the protein level (Figures 5.6) using a specific anti-SK2 antibody that itself detects both forms. Here, it is important to note that the siRNA can target both isoforms, having the same potential siRNA optimal binding site in a conserved region. Results showed that siRNA produced a near 45% ($P < 0.001$ versus control, densitometry relative to GAPDH expression) reduction in SK2-L proteins (Figures 5.6 and 5.7). It also achieved knockdown SK2-S channel proteins by a similar amount (Figure 5.6), despite no noticeable change in GFP-siRNA treated cells (Figure 5.6), compared to control.

To characterise the effect of SK2 channel knockdown on MCF-7 cell viability an MTS assay was used to determine relative viable cell numbers in the various groups after an additional 72 hours post-transfection in the normal culture condition. SK2 knockdown dramatically reduced ($P < 0.0001$ versus control) MCF-7 cell viability (Figure 5.8), repressing cell growth. Conversely, GFP-siRNA treated cell numbers were entirely normal, indicating that transfection *per se* did not induce obvious cytotoxic effects to the cells. Intriguingly, the results also indicate that removal of siRNA effect from the culture, did not allow recovery of the cell growth confirming that the effect is irreversible.

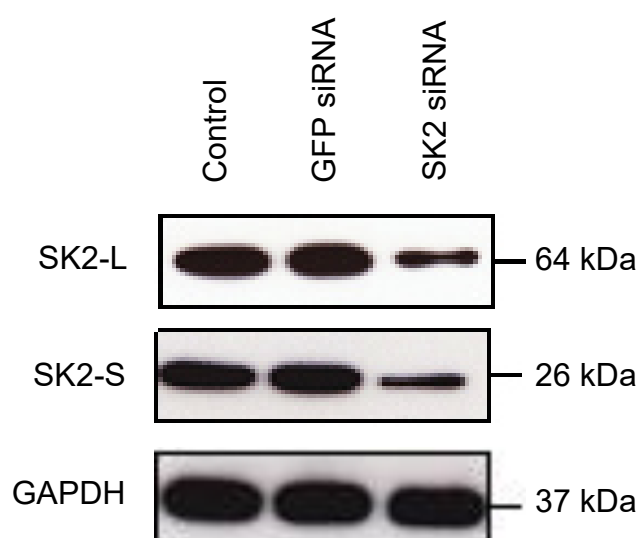


Figure 5.6 Representative immunoblot of SK2 channel in wild-type MCF-7 cells transfected with specific SK2-siRNA. SK2 channel protein expression is noticeably downregulated compared to control. GAPDH serves as the normalising control.

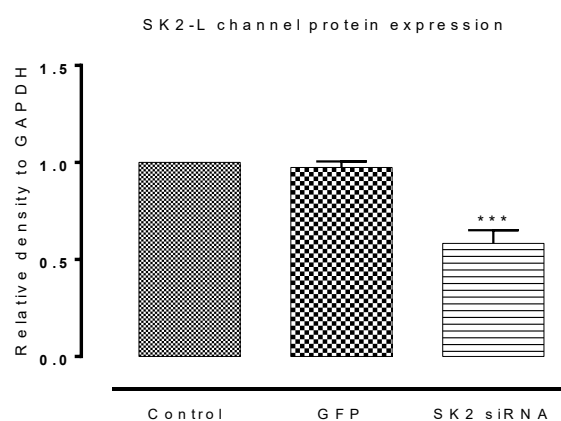


Figure 5.7 Densitometric measurement of SK2-long isoform (SK2-L) channel in wild-type MCF-7 cells transfected with specific SK2-siRNA. Data are shown as means \pm SEM. *** p -value $<$ 0.001 versus control, one-way ANOVA followed by Dunnett's post hoc test, $n = 3$.

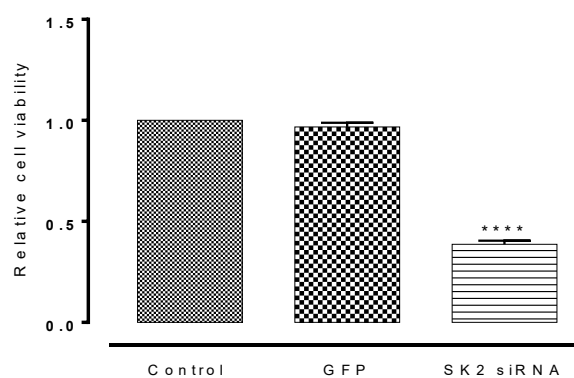


Figure 5.8 The effect of siRNA-mediated knockdown of the SK2 channel on MCF-7 cell viability. Data are shown as means \pm SEM. **** p -value $<$ 0.0001 versus control, one-way ANOVA followed by Dunnett's post hoc test, $n = 9$.

5.4.1.4 The effect of siRNA-mediated knockdown of SK2 channel on apoptosis in MCF-7 cells

Cells lacking SK2 channels have in fact low viability. A key question indeed is how then SK channel reduction contributes to cell loss? These channels have been implicated in apoptosis, which is arrested in cancer biology. This study addresses this question, thereby focusing on this pathway of cell death.

In Western blotting, direct targeting of SK2 channel by siRNA revealed that these channels were involved in regulating apoptosis. Knockdown of these proteins, not only caused a substantial loss ($P < 0.0001$ versus control) of Bcl-2 expression by 90% (Figures 5.9 and 5.10), but also coincided with a marked increase of ($P < 0.0001$ versus control) full length Caspase-7 by 370% (Figures 5.11 and 5.12), a member of the effector caspases. This antibody can detect both forms of the enzyme, and importantly Western blotting detected no cleaved (activated) form of caspase-7 (Figures 5.11) until SK2-siRNA treatment, and as expected there was no change in the controls. Conversely, control siRNA had no effect on Bcl-2 and caspase-7 activity. These results clearly show a negative correlation between SK2 channel and the apoptotic pathway through unbalancing, at least, these apoptotic markers, Bcl-2 and caspase-7. Indeed, SK2 channel inhibition by siRNA in these cells would augment apoptotic cell loss and thus hinder growth rate. This insightful crosstalk uncovers an event in the context of apoptosis biology, where Bcl-2 and caspase-7 are SK channel-dependent effectors, a result which is a first in this study. Therefore, SK2-dependent cell loss is associated with apoptosis or decreased cell viability.

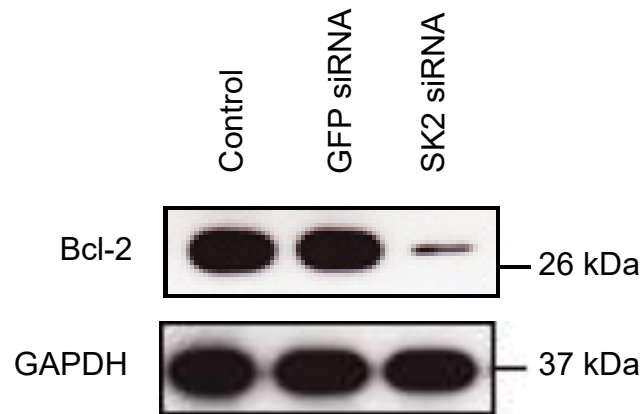


Figure 5.9 Representative immunoblot of anti-apoptotic Bcl-2 protein in wild-type MCF-7 cells transfected with specific SK2-siRNA. Bcl-2 expression is noticeably downregulated compared to control. GAPDH serves as the normalising control.

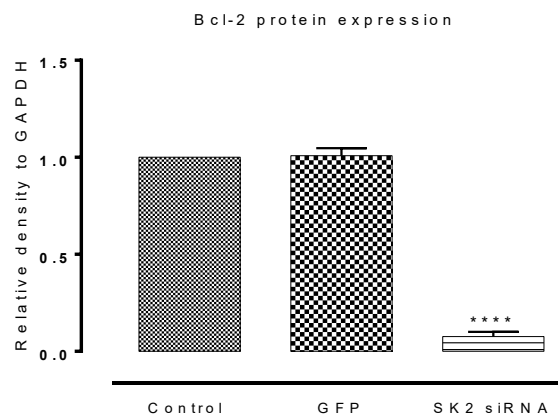


Figure 5.10 Densitometric measurement of anti-apoptotic Bcl-2 protein in wild-type MCF-7 cells transfected with specific SK2-siRNA. Data are shown as means \pm SEM. **** p -value < 0.0001 versus control, one-way ANOVA followed by Dunnett's post hoc test, $n = 3$.

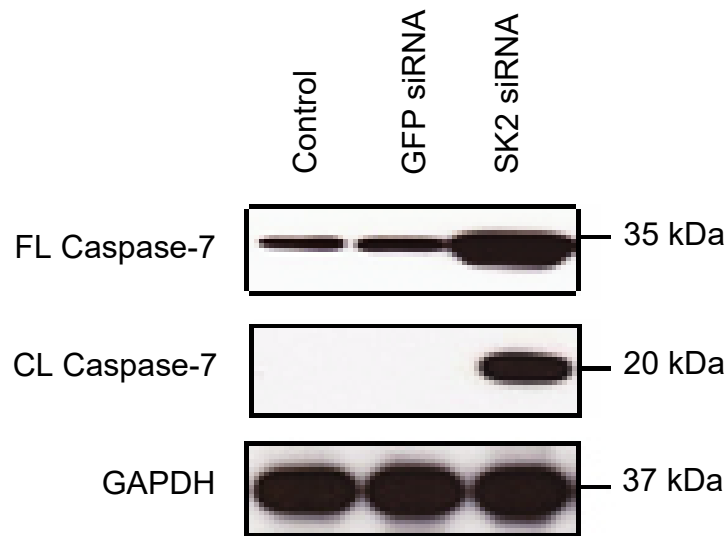


Figure 5.11 Representative immunoblot of pro-apoptotic caspase-7 protein in wild-type MCF-7 cells transfected with specific SK2-siRNA. Caspase-7 protein expression is noticeably upregulated compared to control. GAPDH serves as the normalising control.

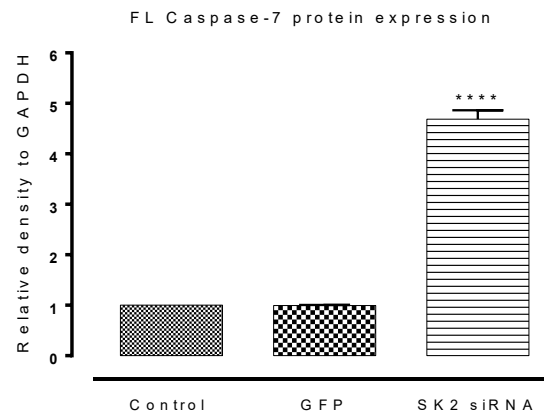


Figure 5.12 Densitometric measurement of full length (FL) pro-apoptotic caspase-7 protein in wild-type MCF-7 cells transfected with specific SK2-siRNA. Data are shown as means \pm SEM. **** p -value < 0.0001 versus control, one-way ANOVA followed by Dunnett's post hoc test, $n = 3$.

5.4.1.5 Pharmacological modulation of SK2 channel in the MCF-7 lineage

Given that these molecules are functionally expressed in MCF-7 and endocrine resistant cells, the next question was whether SK channel blockade drives cell loss or activation saves cells. SK channel modulators were dissolved in dimethyl sulfoxide following the supplier's instruction (See chapter two). There was no effect of working concentrations of the vehicle on relative cell numbers (Appendix 3, Figures 7.16, 7.17 and 7.18) over the period cell proliferation measured. In the SK channel blocking experiments, modulators were screened at multiple doses in increasing concentrations, considering the half maximal inhibitory concentrations (IC_{50} s), which were previously obtained, thereby generating dose-response curves. For SK activation experiments, three concentrations only were applied, and results are shown in the form of bar charts. SK channels modulators have currently been identified with known specificities. Pharmacological experiments were carried out in MCF-7 cells targeting both SK2 and SK4 channels. The SK1-3 blocker, UCL1684, caused a dose-dependent decrease ($IC_{50}= 6.2$ nM) in MCF-7 cell numbers after 72 hours (Figure 5.13).

With regard to specificity of the target and whether the opposite effect can be obtained, cells were also exposed to the SK2-3 channel activator, CyPPA (10-30 μ M), the latter appreciably enhancing cell growth ($P<0.0001$ versus control) by 160% (Figure 5.14). Over the same time course, inhibition of SK4 channels by NS6180, a new SK4 channel blocker, showed only a minor loss in MCF-7 cells (Figure 5.13). This was the reason this study did not attempt to examine this channel, SK4, in other cell types. Intriguingly, resistant TamR and FasR cells were also sensitive to the SK1-3 channel blocker, UCL1684, with IC_{50} values of 5.6 nM (Figure 5.15) and 3.5 nM (Figure 5.16), respectively.

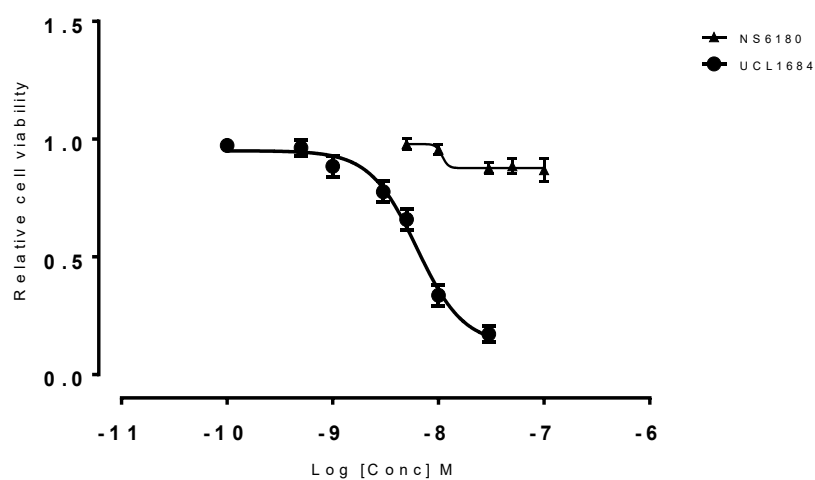


Figure 5.13 The effect of SK1-3 channel blocker, UCL1684, and SK4 channel blocker, NS6180, on MCF7 cell viability. From the line of best fit of the dose-response data, the IC_{50} was 6.2 nM, curve, $n = 9$.

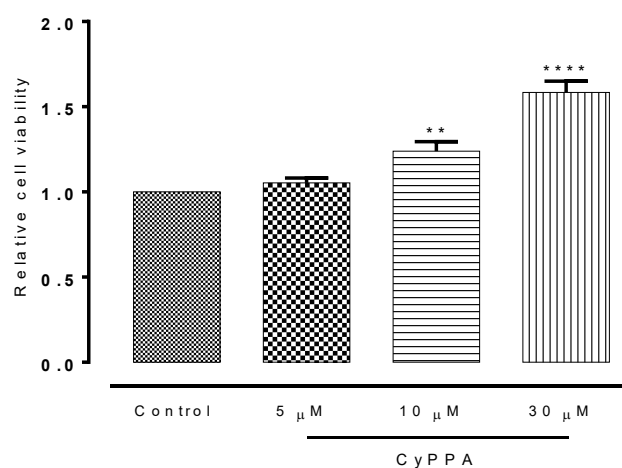


Figure 5.14 The effect of SK2-3 activator, CyPPA, on MCF-7 cell viability. Data are shown as means \pm SEM. **** p -value < 0.0001 versus control, one-way ANOVA followed by Dunnett's post hoc test, $n = 9$.

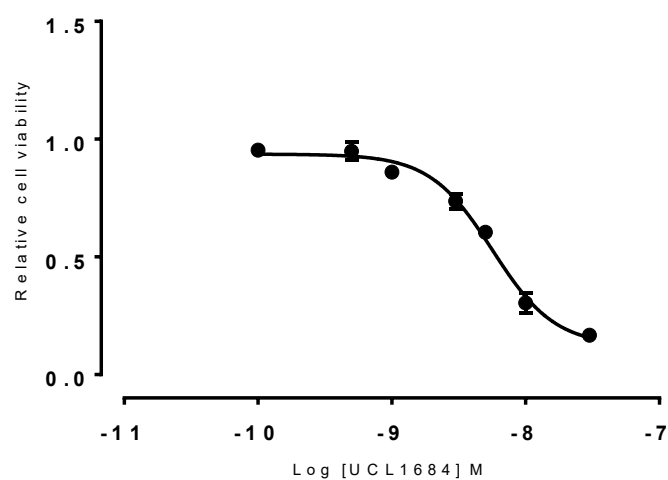


Figure 5.15 The effect of SK1-3 channel blocker, UCL1684, on TamR cell viability. From the line of best fit of the dose-response data, the IC_{50} was 5.6 nM, $n = 9$.

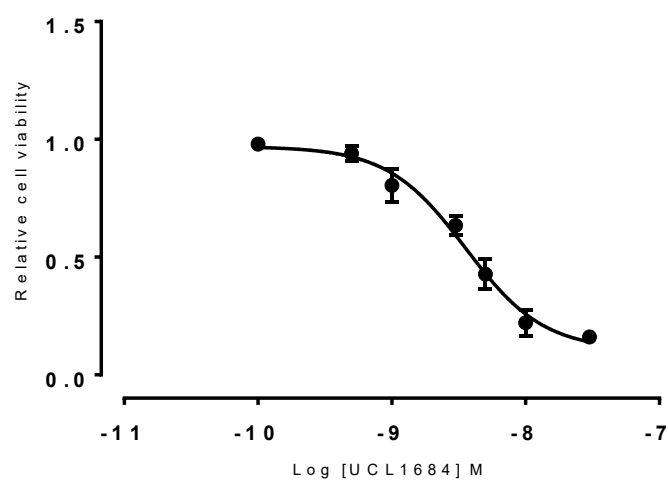


Figure 5.16 The effect of SK1-3 channel blocker, UCL1684, on FasR cell viability. From the line of best fit of the dose-response data, the IC_{50} was 3.5 nM, $n = 9$.

5.4.2 SK channel expression and modulation in BT-474 cells

5.4.2.1 SK channel mRNA investigation

To determine cell specificity the expression pattern of SK channels in other breast cancer cell lines was checked, and the question asked: are the subtypes of any SK channels still a target for blocking cell growth? To address this question, BT-474 cells (ER⁺, PR⁺, HER2⁺) were further examined. RT-PCR investigation for all transcripts, SK1-4, in BT-474 cells revealed only the presence of SK2 and SK4 channel messages (Figure 5.17) in a similar fashion to that of MCF-7 cells. No gene microarray data for the quantitative assessment of expressed channels was followed up.

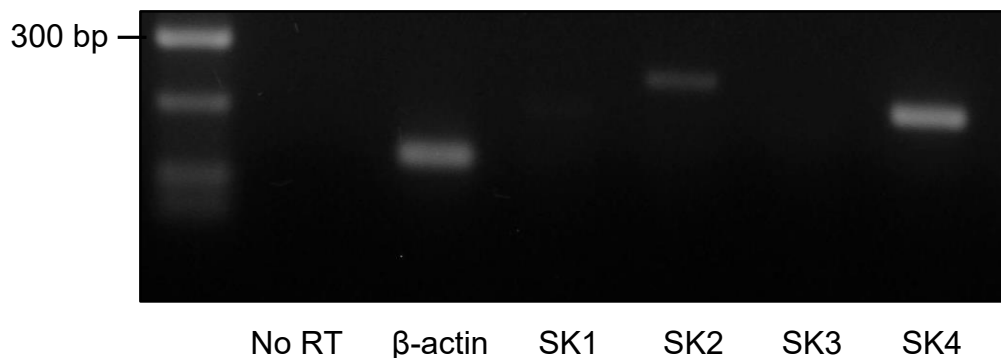


Figure 5.17 SK channel mRNA investigation in wild-type BT-474 cells. Only the amplicons for SK2 and SK4 channels are present and the PCR products are of the predicted size. β -actin serves as the normalising control.

5.4.2.2 SK2 channel protein expression and siRNA-mediated modulation of SK2 channel in BT-474 cells

As expected, immunoblots of control BT-474 cells found that SK2 channel was also expressed at the protein level (Figure 5.18), which was expressing both SK2-L and SK2-S isoforms, as shown using the specific anti-SK2 antibody.

In siRNA-mediated experiments, 50 nM of total siRNA was used. This produced a profound reduction of near 85% ($P < 0.0001$ versus control) in SK2-L channel proteins (Figures 5.18 and 5.19) after SK2 gene silencing for 72 hours. Coincidentally, the siRNA effectively reduced SK2-S channel expression (Figure 5.18) to a level in which proteins barely remained, indicating that BT-474 cells probably have lower normal expression of SK2 channels than MCF-7 cells. Immunoblots of the siRNA control cells, which were GFP-siRNA treated, showed no significant changes compared to control.

To assess viability of the cell lines after siRNA, MTS assay was employed and showed that BT-474 cells were strikingly sensitive ($P < 0.0001$ versus control) to the same concentration of SK2-siRNA, ~29% of cells remaining normal (Figure 5.20) compared with MCF-7 cells, where approximately 39% of cells were normal after siRNA. GFP-siRNA treated cells remained unaffected (Figure 5.20) compared to control. Again, these results show that this molecule, SK2, is a strong candidate for cell growth repressing another breast cancer BT-474 cell line.

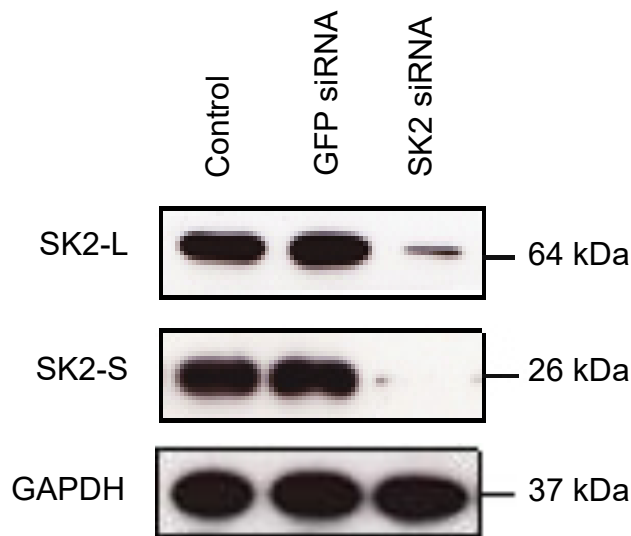


Figure 5.18 Representative immunoblot of SK2 channel in wild-type BT-474 cells transfected with specific SK2-siRNA. SK2 channel protein expression is noticeably downregulated compared to control. GAPDH serves as the normalising control.

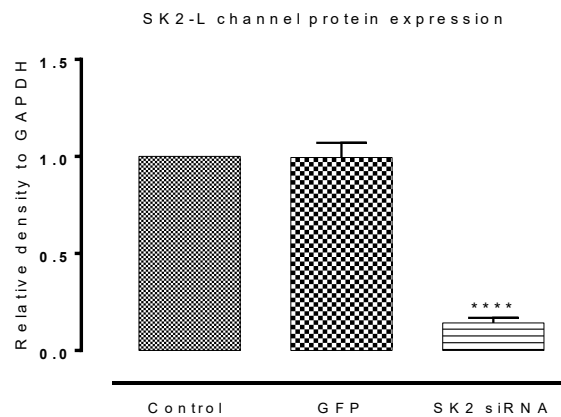


Figure 5.19 Densitometric measurement of SK2-long (SK2-L) isoform channel in wild-type BT-474 cells transfected with specific SK2-siRNA. Data are shown as means \pm SEM. **** p -value < 0.0001 versus control, one-way ANOVA followed by Dunnett's post hoc test, $n = 3$.

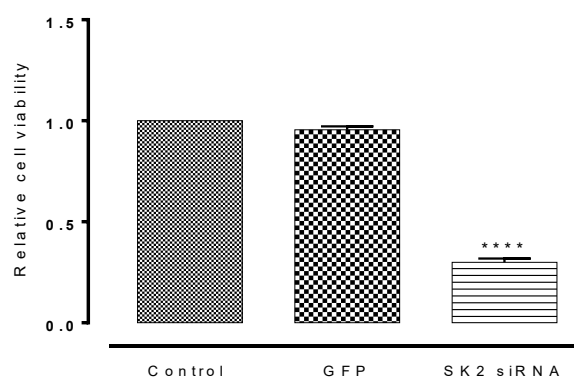


Figure 5.20 The effect of siRNA-mediated knockdown of SK2 channel on BT-474 cell viability. Data are shown as means \pm SEM. **** p -value $<$ 0.0001 versus control, one-way ANOVA followed by Dunnett's post hoc test, $n = 9$.

5.4.2.3 The effect of siRNA-mediated knockdown of SK2 channel on apoptosis in BT-474 cells

The molecular mechanism by which SK2 channels arrest cell growth activity is currently unknown. SK2 channel might regulate apoptosis in this cell line and to address this question, Western blotting was undertaken to monitor the activity of Bcl-2 and caspase-7 expression, as apoptotic markers after SK2 channel knockdown by siRNA for 72 hours. This treatment produced marked changes in apoptotic markers. Intriguingly, Bcl-2 expression was downregulated ($P < 0.0001$ versus control) by almost 90% (Figures 5.21 and 5.22), whereas a strong increase ($P < 0.0001$ versus control) in full length caspase-7 expression by near 470% (Figures 5.23 and 5.24), was revealed. Therefore, this result was consistent with detection of cleaved caspase-7 in SK2-siRNA treated cells (Figure 5.23). Control siRNA cells showed a slight decrease in protein expression, but Bcl-2 and caspase-7 activity was not significantly affected.

With regard to the effect of siRNA-mediated modulation on cell viability and apoptotic markers, results from MCF-7 and BT-474 cell lines were broadly consistent, so strengthening the main hypothesis. A minor exception was that BT-474 cells were more sensitive to the siRNA used than MCF-7 cells, as is explained in (5.4.2.2 section).

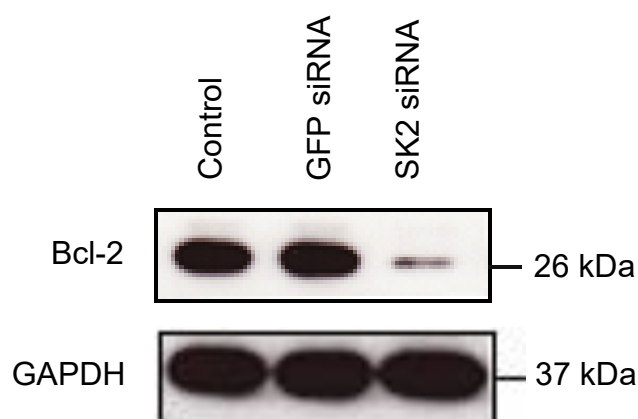


Figure 5.21 Representative immunoblot of anti-apoptotic Bcl-2 protein in wild-type BT-474 cells transfected with specific SK2-siRNA. Bcl-2 protein expression is noticeably downregulated compared to control. GAPDH serves as the normalising control.

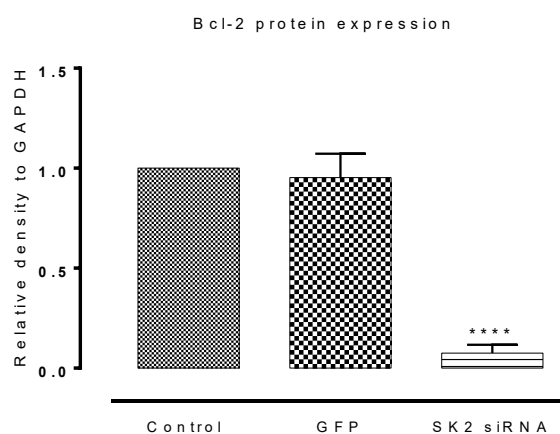


Figure 5.22 Densitometric measurement of anti-apoptotic Bcl-2 protein in wild-type BT-474 cells transfected with specific SK2-siRNA. Data are shown as means \pm SEM. **** p -value < 0.0001 versus control, one-way ANOVA followed by Dunnett's post hoc test, $n = 3$.

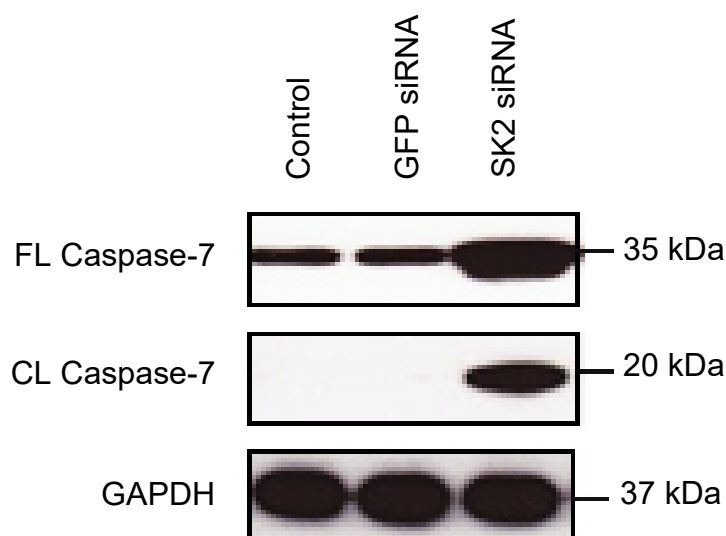


Figure 5.23 Representative immunoblot of pro-apoptotic caspase-7 protein in wild-type BT-474 cells transfected with specific SK2-siRNA. Caspase-7 protein expression is noticeably upregulated compared to control. GAPDH serves as the normalising control.

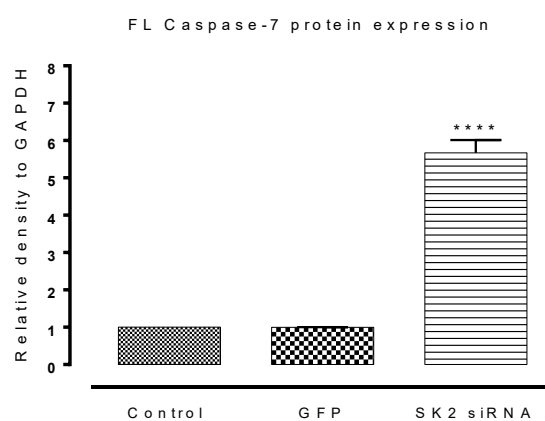


Figure 5.24 Densitometric measurement of full length (FL) pro-apoptotic caspase-7 protein in wild-type BT-474 cells transfected with specific SK2-siRNA. Data are shown as means \pm SEM. **** p -value < 0.0001 versus control, one-way ANOVA followed by Dunnett's post hoc test, $n = 3$.

5.4.2.4 Pharmacological modulation of SK2 channel in BT-474 cells

The BT-474 cell line was also questioned in respect of pharmacology, to determine whether pharmacological modulation of the subtype, SK2, of SK potassium ion channels can mirror siRNA results in terms of viability. The MTS assay showed that inhibition of SK2 channel in BT-474 cells caused vast cell loss with an IC_{50} = 3.7 nM over 72 hours (Figure 5.25). On the other hand, the SK2-3 activator, CyPPA (10-30 μ M), markedly ($P < 0.0001$ versus control) stimulated growth of BT-474 cells by near 160% (Figure 5.26), in a dose-dependent manner.

The viability tests revealed also no major differences in respect of SK2 channel pharmacology between MCF-7 and BT-474 cells, thus indicating that these cells were sensitive to SK2 channel modulation in a similar pattern.

The next question is:

Do breast cancer cells express only the subtype SK2 and SK4 of SK channels? To answer this question, this study was expanded, using another phenotype of breast cancer, MDA-MB-231, which is a triple negative (ER⁻, PR⁻, HER2⁻) cell line.

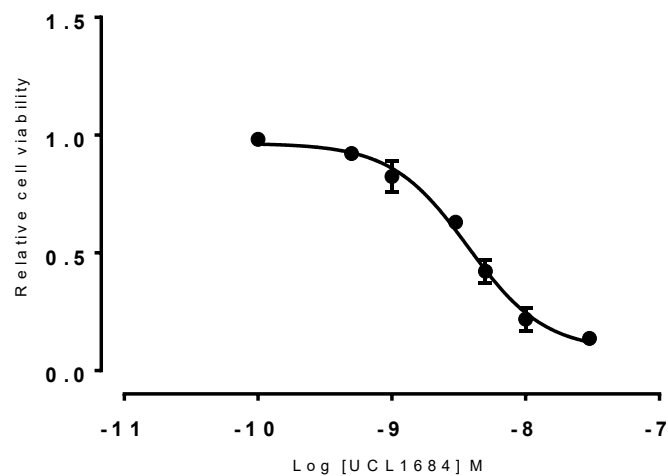


Figure 5.25 The effect of SK1-3 channel blocker, UCL1684, on BT-474 cell viability. From the line of best fit of the dose-response data, the IC_{50} was 3.7 nM, $n=9$.

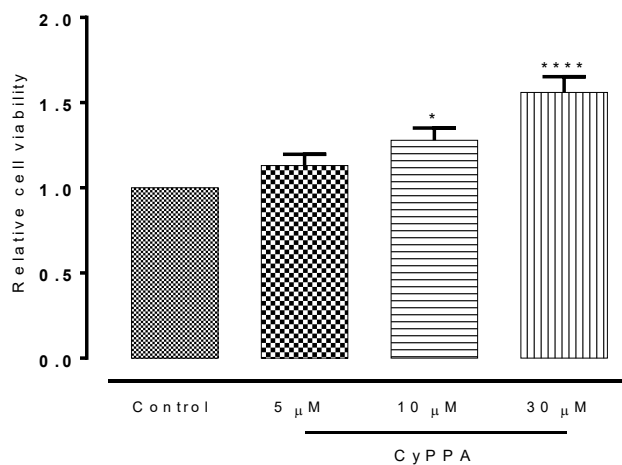


Figure 5.26 The effect of SK2-3 activator, CyPPA, on BT-474 cell viability. Data are shown as means \pm SEM. **** p -value < 0.0001 versus control, one-way ANOVA followed by Dunnett's post hoc test, $n=9$.

5.4.3 SK channel expression and modulation in MDA-MB-231 cells

5.4.3.1 SK channel mRNA investigation

To further test the hypothesis, the MDA-MB-231 cell line was also examined. These cells provided different and interesting insights regarding the expression pattern of the SK subtypes. RT-PCR determined that this cell line possesses $K_{Ca2.3}$ (SK3) channel rather than $K_{Ca2.2}$ (SK2) channel, as well as the SK4 subtype (Figure 5.27). Therefore, a new candidate, the SK3 channel, was examined in this cell line, using the same techniques.

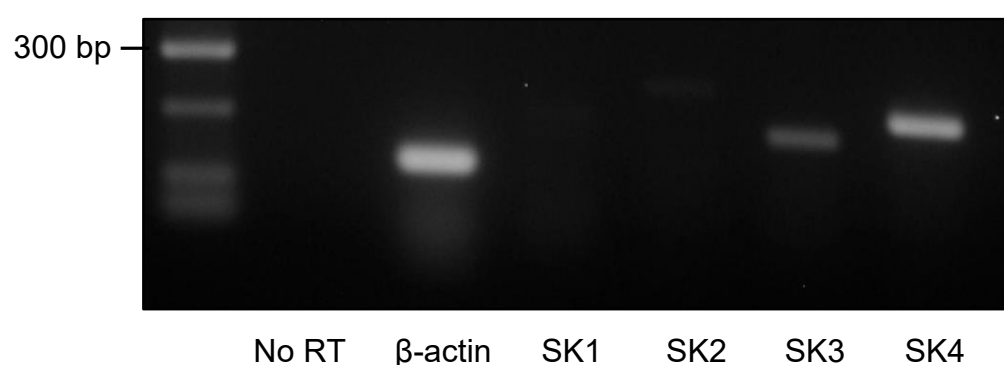


Figure 5.27 SK channel mRNA investigation in wild-type MDA-MB-231 cells. Only the amplicons for SK3 and SK4 channels are present and the PCR products are of the predicted size. β -actin serves as the normalising control.

5.4.3.2 SK3 channel protein expression and siRNA-mediated modulation of SK3 channel in MDA-MB-231 cells

Following a systematic study, Western blotting of lysates from control MDA-MB-231 cells showed that SK3 proteins were also expressed at the protein level (Figure 5.28) using a specific anti-SK3 antibody, this being consistent with the RT-PCR result. Silencing of the SK3 gene with specific-SK3 siRNA (75 nM) resulted in a significant ($P < 0.0001$ versus control) reduction of the SK3 channel protein expression by 50% in siRNA (Figure 5.28 and 5.29). Conversely, GFP-siRNA had no significant effect on the expression level of the SK3 channel proteins compared to control (Figure 5.28 and 5.29). MDA-MB-231 cell viability changes were monitored by MTS assay, over 72 hours. Cells lacking SK3 channels showed a significant ($P < 0.0001$ versus control) loss of MDA-MB-231 cells by near 60% (Figure 5.30), whereas cells in the GFP-siRNA treated group remained viable (Figure 5.30). In summary, siRNA results show that for the cell lines used namely MCF-7 (ER⁺, PR⁺, HER2⁻), BT-474 (ER⁺, PR⁺, HER2⁺), as well as MDA-MB-231 (ER⁻, PR⁻, HER2⁻) cells these possess SK channel-dependent cell growth, irrespective of the subtype through either SK2 or SK3 channel targeting.

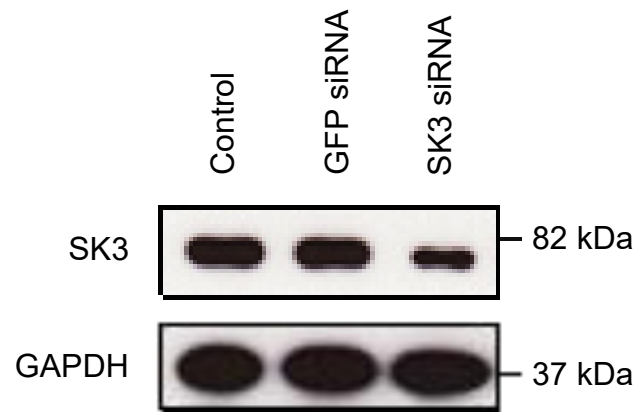


Figure 5.28 Representative immunoblot of SK3 channel in wild-type MDA-MB-231 cells transfected with specific SK3-siRNA. SK3 channel protein expression is noticeably downregulated compared to control. GAPDH serves as the normalising control.

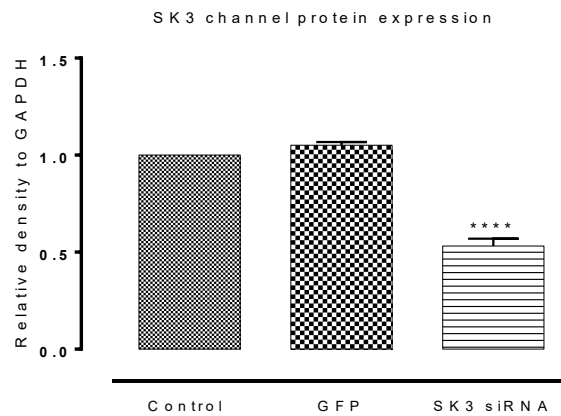


Figure 5.29 Densitometric measurement of SK3 channel in wild-type MDA-MB-231 cells transfected with specific SK3-siRNA. Data are shown as means \pm SEM. **** p -value < 0.0001 versus control, one-way ANOVA followed by Dunnett's post hoc test, $n = 3$.

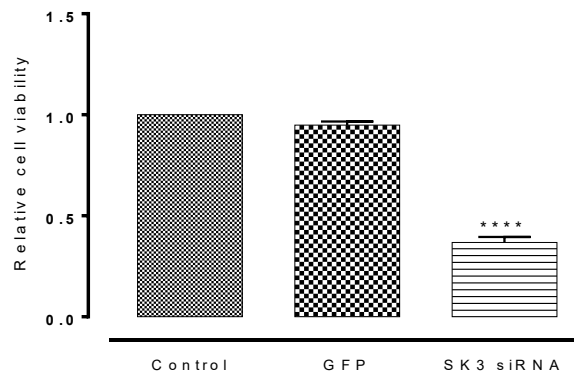


Figure 5.30 The effect of siRNA-mediated knockdown of SK3 channel on MDA-MB-231 cell viability. Data are shown as means \pm SEM. **** p -value $<$ 0.0001 versus control, one-way ANOVA followed by Dunnett's post hoc test, $n = 9$.

5.4.3.3 The effect of siRNA-mediated knockdown of SK3 channel on apoptosis in MDA-MB-231 cells

Since, SK2 channels use Bcl-2 and caspase-7 to regulate cell growth in the cell lines tested so far, the link of the SK3 channel to apoptosis was tested using the same apoptotic markers, namely Bcl-2 and caspase-7. In Western blotting experiments, application of SK3-siRNA for 72 hours produced a vast ($P < 0.0001$ versus control) decrease in Bcl-2 protein expression by up to 90% (Figures 5.31 and 5.32), but no significant difference between control and GFP-siRNA groups was observed (Figures 5.31 and 5.32). The siRNA results show that full length caspase-7 increases by 370% ($P < 0.0001$ versus control) following SK3 channel inhibition. Western blotting showed no cleaved caspase-7 expression until SK3-siRNA treatment (Figures 5.33 and 5.34). Moreover, controls demonstrate a minor, but not significant, difference in full length caspase-7 expression (Figures 5.33 and 5.34). These data are internally consistent amongst MCF-7 (ER⁺, PR⁺, HER2⁻), BT-474 (ER⁺, PR⁺, HER2⁺), as well as MDA-MB-231 (ER⁻, PR⁻, HER2⁻) cell lines in respect of apoptotic induction by SK2 and SK3 subtypes.

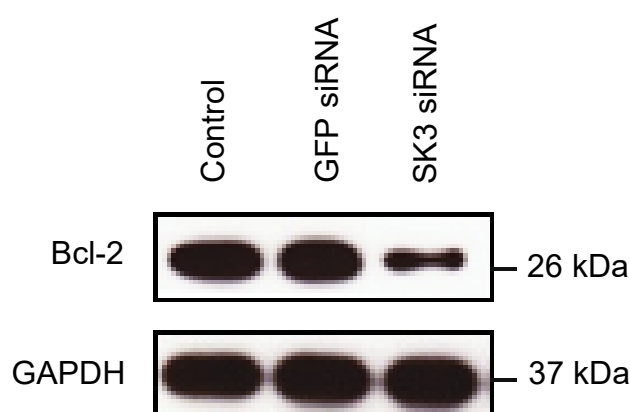


Figure 5.31 Representative immunoblot of anti-apoptotic Bcl-2 protein in wild-type MDA-MB-231 cells transfected with specific SK3-siRNA. Bcl-2 protein expression is noticeably downregulated compared to control. GAPDH serves as the normalising control.



Figure 5.32 Densitometric measurement of anti-apoptotic Bcl-2 protein in wild-type MDA-MB-231 cells transfected with specific SK3-siRNA. Data are shown as means \pm SEM. **** p -value < 0.0001 versus control, one-way ANOVA followed by Dunnett's post hoc test, $n = 3$.

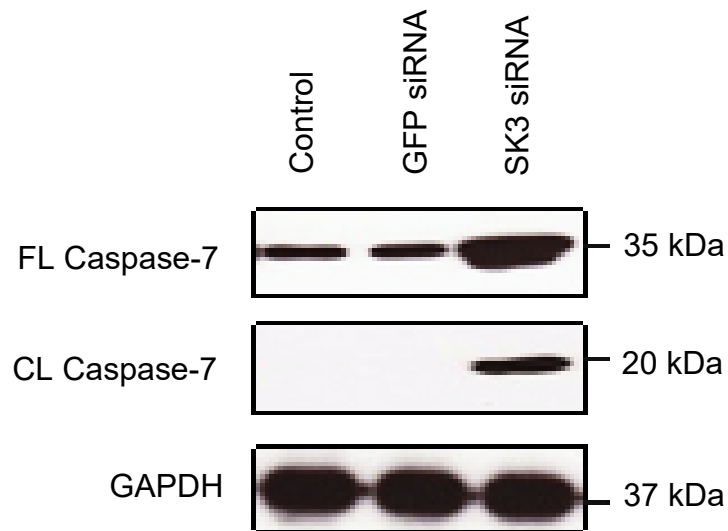


Figure 5.33 Representative immunoblot of pro-apoptotic caspase-7 protein in wild-type MDA-MB-231 cells transfected with specific SK3-siRNA. Caspase-7 protein expression is noticeably upregulated compared to control. GAPDH serves as the normalising control.

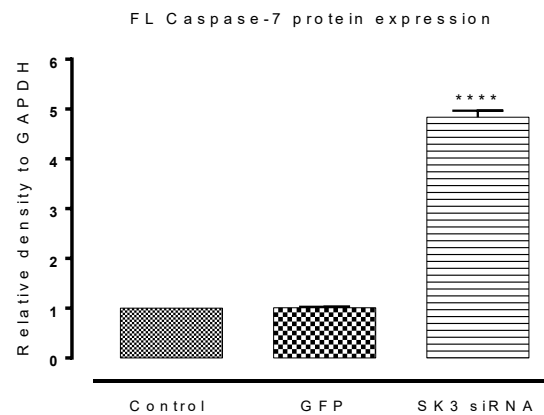


Figure 5.34 Densitometric measurement of full length (FL) pro-apoptotic caspase-7 protein in wild-type MDA-MB-231 cells transfected with specific SK3-siRNA. Data are shown as means \pm SEM. **** p -value $<$ 0.0001 versus control, one-way ANOVA followed by Dunnett's post hoc test, $n = 3$.

5.4.3.4 Pharmacological modulation of SK3 channel in MDA-MB-231 cells

As seen above in MCF-7 (ER⁺, PR⁺, HER2⁻) and BT-474 (ER⁺, PR⁺, HER2⁺) cells SK2 channel inhibition by the SK1-3 blocker, UCL1684, led to cell growth suppression. The anti-proliferative effects of two SK small molecule inhibitors, which include UCL1684 and NS8593, were tested in the viability MTS assays using MDA-MB-231 cells and the same time course. Screening of UCL1684 against MDA-MB-231 cells, negatively affected cell growth (IC₅₀= 5.9 nM) over 72 hours (Figure 5.35), mimicking the siRNA result. To check for SK3 channel specificity, another generic SK1-3 blocker, NS8593, was tested. This different blocker produced the same result on cell viability with an IC₅₀ of 814 nM in MDA-MB-231 cells (Figure 5.36). Opening of SK3 channels by CyPPA (10-30 μM) caused an increase ($P < 0.0001$ versus control) in cell numbers to 160% (Figure 5.37), further demonstration that the anti-proliferative effect is indeed specific to the SK3 channel.

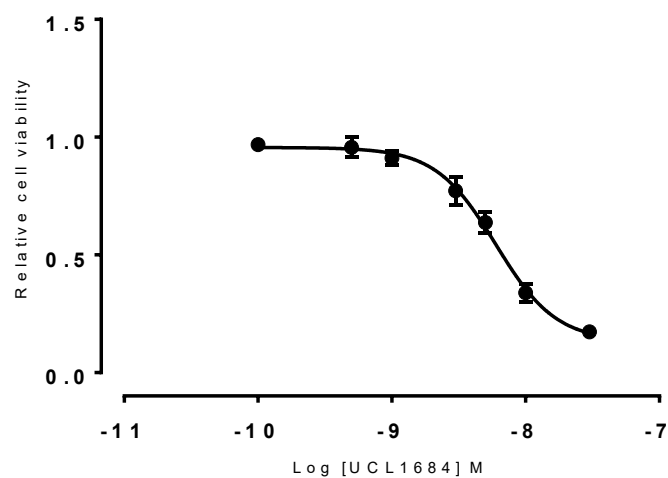


Figure 5.35 The effect of SK1-3 channel blocker, UCL1684, on MDA-MB-231 cell viability. From the line of best fit of the dose-response data, the IC_{50} was 5.9 nM, $n=9$.

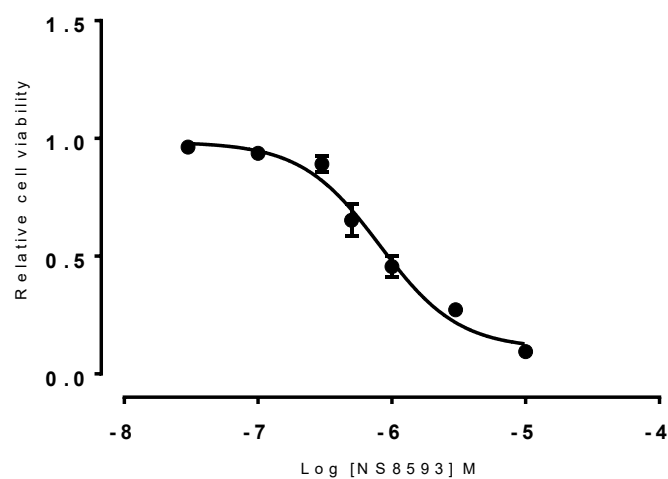


Figure 5.36 The effect of SK1-3 channel blocker, NS8593, on MDA-MB-231 cell viability. From the line of best fit of the dose-response data, the IC_{50} was 8.1 nM, $n=9$.

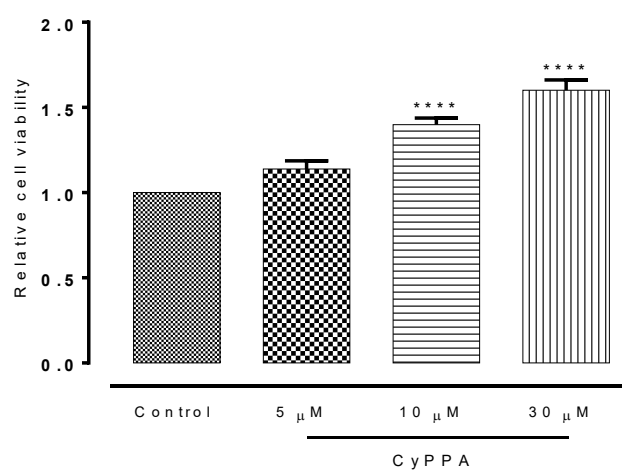


Figure 5.37 The effect of the SK2-3 activator, CyPPA, on MDA-MB-231 cell viability. Data are shown as means \pm SEM. **** p -value $<$ 0.0001 versus control, one-way ANOVA followed by Dunnett's post hoc test, $n = 9$.

5.5 Discussion

The main findings of this study are:

1. $K_{Ca2.2}$ (SK2) and $K_{Ca3.1}$ (SK4) channels are expressed in four widely used breast cancer cell lines, which include wild-type, MCF-7 and BT-474, and endocrine resistant, TamR and FasR, cell types.
2. $K_{Ca2.3}$ (SK3) and $K_{Ca3.1}$ (SK4) channels are expressed in another commonly used, triple negative cell line, namely MDA-MB-231 cells.
3. Pharmacological inhibition of SK2 ion channels in MCF-7, BT-474, as well as endocrine resistant cells, TamR and FasR, significantly blocked cell growth with drugs in the low nanomolar range.
4. Pharmacological inhibition of SK3 ion channels in MDA-MB-231 cells also significantly blocked cell growth.
5. In contrast, activation of SK2 and SK3 channels in all wild-type lines used, staves off cell loss and markedly enhanced cell growth.
6. Small interference RNA-mediated knockdown of SK2 ion channels in MCF-7 and BT-474 cells significantly arrested cell growth.
7. Small interference RNA-mediated knockdown of SK3 ion channels in MDA-MB-231 cells also significantly arrested cell growth.
8. Intriguingly, siRNA-mediated knockdown of SK2 and SK3 channels in the cell lines indicated produced a considerable downregulation of the anti-apoptotic protein Bcl-2, and a corresponding upregulation of the activated form of caspase-7 of effector caspases.
9. In addition, siRNA-mediated knockdown of SK2 and SK3 channels also markedly increased caspase-9 protein expression, but not caspase-8,

indicating that these SK channels cross-talk with an intrinsic pathway of apoptosis.

To begin this discussion and to give some SK channel background, this potassium channel was first found in red blood cells, as well as excitable cells such as neurons, where they are involved laterally in hyperpolarisation (Alger and Nicoll 1980; Gardos 1958). Since this work, similar studies raised the possibility that these molecules are also involved in other cellular functions where they regulate ion flux, K^+ and Ca^{2+} (indirectly), at cellular levels, which can trigger intracellular signaling (Kaczmarek 2006). Thus it was extremely hard to limit their role to “one way pathway”. Returning to the CNS system, SK1-4 channels are differentially distributed in the brain, SK1-3 subtypes being principally and largely expressed in central neurons (Sailer et al. 2004), but not the SK4 subtype (Adelman et al. 2012). In brain tissue, the SK2-long isoform controls the excitatory postsynaptic potential, which is, of course, an important component in synaptic signaling, plasticity, as well as learning (Allen et al. 2011a).

Intriguingly, in this study it was found that some neurons not only express SK1-3 channel subtypes, but also the SK4 subtype at the mRNA level, for instance in the case of wild-type mouse striatal *STHdh⁺/Hdh⁺* cells (See chapter three). This investigation also showed that other CNS resident cells, namely astrocytic and microglial cells, express in fact only SK4 channel (See chapters three and four).

Work in chapter three showed that SK1-4 channel subtype activation in cells of CNS origin cells, namely neurons and astrocytes, had no effect on cell viability after 24 hours, but importantly reversed any reduction in the viability caused by neuronal insults. Use of the relevant channel inhibitor abolished the protection afforded by SK channel activation. Here, it is important to highlight that in contrast to cancer cells, the relevant SK blockers and activators used had no effect on the “normal” viability of the CNS cells (See chapter three).

The cancer work here was carried out in four breast cancer cell lines, which include wild-type, MCF-7 and BT-474, and endocrine resistant, namely TamR and FasR cells, and it was found that these cells have a consistent SK subtype expression pattern, expressing SK2 and SK4 channel subtypes, while another widely used cell line, MDA-MB-231, lacks SK2 channel subtype cell but also expresses the SK3 subtype alongside SK4. This cell line is triple negative (ER⁻, PR⁻, HER2⁻), while the MCF-7 line has (ER⁺, PR⁺, HER2⁻) status, and BT-474 cell has triple positive status (Neve et al. 2006). It is really intriguing that in non-tumorigenic cells, MCF 10A cells, results here have found that these do not express SK1, SK2, and SK3 channels (Appendix 3, Figures 7.19 and 7.20).

The hypothesis in the cancer work in this study was proposed to link the previous findings mentioned above. In this regard it is interesting to note that SK2 channel subtype activation significantly reduces neuronal cell death caused by ischemia, by lowering Ca²⁺ entry in mouse hippocampal CA1 pyramidal neurons (Allen *et al.* 2011b). It is clear that this element, in numerous pathological conditions, behaves as “criminal ion” when fluctuations are deregulated, thus triggering numerous cellular processes. Significantly, it is well documented that Ca²⁺ drives cancerous processes, especially proliferation, apoptosis, as well as cell cycle progression (Farfariello et al. 2015; Prevarskaya *et al.* 2010).

The work presented here was limited to small (SK1-3) and intermediate (SK4) conductance calcium activated K⁺ channels. There were several reasons for eliminating the big (BK) conductance calcium activated K⁺ channels. First, these channels are less sensitive to Ca²⁺ than SK channels (Latorre and Brauchi 2006). In this respect, it is accepted that SK1-4 channel subtypes are comparably sensitive to Ca²⁺ fluctuations (Latorre and Brauchi 2006), this being the sole activator (Xia et

al. 1998). Importantly, it is curious that only few published works have questioned the role of SK1-3 channels in breast cancer (Potier et al. 2006), rather than SK4 and BK channels (Girault *et al.* 2012).

SK channel pharmacology to date is well advanced (Wulff and Kohler 2013). Here, experiments examined the cytotoxic effect, if any, of SK1-4 channel modulation on the cell lines indicated. Pharmacological experiments first approached the question of the SK4 channel subtype in MCF-7 cells, using the up to date SK4 blocker, NS6180 (5-100 nM), which seems more potent (IC_{50} = 9 nM) on the SK4 channel (Strobaek et al. 2013). The MTS viability assay showed that the SK4 blocker did not significantly block MCF-7 cell growth (Figure 5.13). TRAM-34 a former SK4 channel blocker at low micromolar concentrations actually enhances cell growth capacity in MCF-7 cells, by stimulating estrogen receptors, not through SK4 channel blockade (Roy *et al.* 2010). Both TRAM-34 and NS6180, at concentrations more than 1 μ M, in fact cause off-target confusion, for example NS6180 blocks other ion channels such as $K_v1.3$ (Strobaek et al. 2013).

The next candidate, the resident SK2 channel was then challenged. Knock down experiments, using siRNA in MCF-7 and BT-474 cells showed that SK2 channel loss produced a marked reduction in the viability of the indicated cells (Figures 5.8, and 5.20), respectively. Similar outcomes were obtained in MDA-MB-231 cells, once again reducing SK3 channels curtailed cell growth (Figure 5.30), despite only a partial but significant lack of these channels at the protein level after siRNA treatment (Figure 5.28).

This work here now attempted to bring to light the underlying mechanism by which SK2-3 channels discourage cell growth. It should be noted that SK channels are critically expressed at a mitochondrial level (Dolga et al. 2014), and are implicated

as oncological targets (Leanza *et al.* 2014). Intriguingly, the protein analysis conducted here showed that knockdown of SK2 and SK3 channel subtypes resulted in a reduction of the anti-apoptotic Bcl-2 protein, and in contrast amplification of the activated caspase-7 form. This is an exciting breakthrough for cancer biology underlying that SK channels-related cell death can be achieved through apoptosis, and as a corollary reduced apoptosis is important in the initiation of cancer, see for example (Llambi and Green 2011). Bcl-2 regulates the mitochondrial outer membrane permeability, which controls the liberation and localisation of pro-apoptotic factors in the cytoplasm, thus committing cells to a death decision (Bender and Martinou 2013): hence it plays a pivotal role in creating either death or life decisions. Accordingly, results presented here clearly signify that SK2-3 channel blockade is offering a pro-apoptotic signal in these breast cancer cells.

To recapitulate the siRNA-mediated effect using pharmacology, the relevant SK2 and SK3 channel modulators were screened against the viability of cell lines, including resistant cells. Invariably, SK2 and SK3 channel inhibition markedly abated cell growth, mimicking the siRNA results. Against the MCF-7 lineage, namely MCF-7, TamR and FasR cells, the SK1-3 blocker, UCL1684, reduced cell number in a dose-dependent manner with an IC_{50} 6.2, 5.6 and 3.5 nM respectively (Figures 5.13, 5.15, and 5.16). In this respect, it was found that UCL1684 blocks SK1-3 channels in the low nanomolar range (IC_{50} 3-6 nM): for example in rat chromaffin cells (Campos Rosa *et al.* 2000; Dunn 1999). Similarly, the blocker was active against both BT-474 (Figure 5.25), and MDA-MB-231 (Figure 5.35) cell growth. In the case of the latter cell line, experiments also used another generic SK1-3 blocker, NS8593, which produced a similar response (Figure 5.36). The IC_{50} in MDA-MB-231

cells was 814 nM compared with the K_d of 0.73 μ M for the channel modulator in hippocampal CA1 neurons (Strobaek et al. 2006).

Previous work has reported that the growth of MCF-7 cells is not responsive to apamin, which is also a SK1-3 channel blocker. In this study apamin (100 nM) does not modulate the viability of MDA-MB-435 cells after 24 hours (Potier et al. 2006). This raises a question: why the sensitivity to small molecule inhibitors, namely UCL1684 and NS8593, but not apamin? This can perhaps be explained by the following: firstly, this study challenged cells over 72 hours, and this protocol is currently accepted generally in cancer work. Secondly, apamin is a peptide with no capacity to cross the cell membrane (Douda *et al.* 2015), so losing the prospect of targeting subcellular SK channels in the mitochondrial membrane. Thirdly, melanoma cells express higher level of SK2 channels under hypoxic than normoxic conditions, and they only respond to apamin in the former condition. Thus, levels of expression of SK2 channels dictates their response to pharmacological stimuli (Tajima *et al.* 2006). The results described in this chapter provide a rationale for effects observed. The conclusion is that cancer cells are 'high-jacking' SK2-3 channels to drive life decisions by resisting apoptosis, at least, through Bcl-2 regulation. This is further clarified by the finding that the relevant channel activator, CyPPA, which modulates SK2-3 by increasing the responsiveness of these channels to Ca^{2+} increments, increased cell growth in wild-type cell lines used in this cancer work after 72 hours. SK2 and SK3 channels respond to the modulator, CyPPA, with an EC_{50} 14 μ M and 5.6 μ M respectively in HEK293 cells (Hougaard et al. 2007). The concentrations used here bracketed these values. The findings of this work perfectly fit our hypothesis that these SK proteins are responsible for cellular life and death decisions.

5.6 Conclusions

The central big question in tumorigenesis is: Can we discover the biological processes and targets that deregulate cell growth and encourage tumorigenesis?

The work presented in this chapter identified two SK potassium channels that can effectively modulate cell growth through apoptosis. Knockdown of these targets was potently cytotoxic, and was relevant to cell lines used, their being little difference in responsiveness. These results were confirmed in pharmacological experiments employing MTS cell viability, where it was shown that small molecule inhibitors of SK2 and SK3 channels can mirror siRNA results. The experiments here generated (IC₅₀)s identical to published values for these SK blockers on their channel targets. Consolidating the pharmacological approach, activation of SK2 and SK3 channels, in contrast, further increased cell numbers. Results also showed that reductions of SK2 and SK3 channels in these breast cancer cell lines trigger apoptotic signals, through “off switch” of Bcl-2 and “on switch” of caspase-7 and caspase-9, including the activated form of the caspase. This study updates therefore the catalogue of oncological targets, to include the SK potassium channel family. These results provides healthy and robust evidence that these channels represent an attractive target controlling cell growth through a specific mechanism, thereby deregulating the balance in apoptosis. Thus, this study clearly highlights an SK role as players in the concept of tumorigenesis and in the hallmarks of cancer.

5.7 Recommendations and future work

This work used primary and resistant breast cancer cells in an *in vitro* study, although, it would be interesting to screen for an SK2-3 role against cell growth in *in vivo*. The argument can be strengthened if SK channel contributions are interrogated by the aid of clinicians. Further, it would be advantageous if an SK role can be pathologically mapped during the stages of cell cycle and tumour progression, not only in breast cancer but also in other cancer types. If researchers would examine an SK channel contribution in cancer stem cells, this may also help. But for these developments, tools, such as immunohistochemical tests, for examining SK channel expression in normal and cancer tissues need to be improved.

In this study several questions remained to be addressed. For example, examining Bcl-2 and caspase-7 expression after pharmacological treatment of these cells. This outcome needs to be measured using others techniques such as a Tunnel assay. It would be interesting if both proliferation and the journey through the cell cycle could also be investigated with an SK channel role in mind.

6 Chapter Six General Discussion

6.1 The major findings of this study:

- ✚ In normal and diseased CNS cell types (Chapter three), SK class of K⁺ channels are broadly present.
- ✚ In Huntington's affected neurons, SK1-4 channels are differentially expressed among dominant phenotypes and wild-type cells.
- ✚ It is alluring that severely affected neurons, *STHdh^{Q111}/Hdh^{Q111}* cells, lacked SK1-3 channel activities.
- ✚ SK channel activation improves CNS cell survival experiencing oxidative stress induced cell injury.
- ✚ Such channel activation also restores Bcl-2 proteins which were downregulated throughout oxidative stress.

- ✚ In breast cancer cells (Chapter five), SK channels are also variably present in cells with various phenotypes.
- ✚ SK1-3 channels are in fact absent in breast non-tumorigenic MCF 10A cells.
- ✚ SK2-3 channel blocking or downregulation is potently cytotoxic against breast cancer "constitutive" cell growth.
- ✚ Inhibition of these channels strongly reduces survival through Bcl-2, caspase-7, and caspase-9 factors.

- ✚ In brain astrocytes and Huntington's affected neurons (Chapter four), the TRPM7 channel member of TRP channels is present.

- ✚ TRPM7 channel blocking or downregulation improved cell survival against oxidative stress, hypoxia, as well as apoptosis in these cells.

6.2 SK channel role in cell survival

Membrane molecules which facilitate ion translocation, particularly ion channels that when opened, drive the membrane potential of the cell, result in the respective equilibrium potential of the permeant ion being achieved, which is crucial for normal cell wellbeing. It is previously accepted that these proteins are implicated in various diseases, controlling key ionic movements (Dolga and Culmsee 2012; Huber 2013). Indeed, such ion channels are implicated in abnormal cell growth and degeneration, which are mechanisms inducing cancers and neurodegenerative illness. Amongst ion channels, K^+ channels comprise nearly 50% (Wulff *et al.* 2009): ion channels in the human genome comprise $\sim 1.5\%$ (Huang and Jan 2014). In cellular physiology, though K^+ channel opening, cell membranes hyperpolarise, and gating Na^+ or Ca^{2+} channels shifts the membrane potential, in a depolarising direction. In excitable cells, it is well-known that their role (e.g. in nerve or muscle cells) is to modulate the excitable state, namely action potential firing patterns (Yuan and Chen 2006). In non-excitable cells, there are burgeoning data to support the view that, K^+ ion channels have emerging non-conducting roles, i.e. modifying other cellular features, relating to cancer progression, such as proliferation (Pardo and Stuhmer 2014). Because of the role that the Ca^{2+} activated K^+ channel family of K^+ channels has in regulating cytosolic Ca^{2+} , it is to be expected that these molecules are necessary in taking cell death or life decisions. This thesis concentrated on SK channel characterisation in normal CNS cells, also diseased CNS and breast cells since their role there was not previously well-studied. Therefore, the central question here was: Are the subtypes of the SK class of K^+ ion channels likely to be impressive targets for blocking neurodegeneration and cancer cell growth? Such an important question was addressed using thirteen diverse cell types.

This study used *in vitro* systems, cells being grown in optimum conditions. RT-PCR and Western blotting tools were deployed for examining the channel targets, assessing their mRNA and protein expression. This was followed by further asking whether these proteins are functionally occurring, this question being addressed with the aid of pharmacological and small interference RNA experiments, in concert with survival experiments in MTS assays. Experiments also used Western blotting checks to decipher underlying mechanisms in crosstalk with these ion channels. In certain cases, microarray Affymetrix analysed the quantitative expression of target genes.

This study first identified that SK1-4 channels are ubiquitous in several CNS resident cells, and excitingly, are differentially expressed between Huntington's mutant cells and wild-type cells. These channels have been shown to generate afterhyperpolarisations (Sah and Faber 2002) with medium duration, and are very responsive to cytosolic Ca^{2+} alterations (Park 1994). In this context it is not surprising that Ca^{2+} dysregulation is really a major player in Alzheimer's pathogenesis (LaFerla 2002). Pharmacological screening has shown that these channels contribute in oxidative stress, where SK channel activation rescued brain astrocytes and neurones from oxidative stress induced through toxic doses of H_2O_2 . However, mouse homozygous mutant *STHdh^{Q111}/Hdh^{Q111}* cells lacked functional SK1-3 channels, but expressed SK2 channels in heterozygous *STHdh^{Q111}/Hdh⁺* which are functional, and activation markedly challenged oxidative stress. SK molecules are resident channels in different zones of the brain: for example SK1 and SK2 channels are densely present in hippocampus and neocortex (Sailer *et al.* 2002). Broadly speaking, it is accepted that these channels are implicated in neuronal physiology regulating various functions, but in a feedback mode shaping

neuronal activity, including synaptic transmission (Fiorillo and Williams 1998) and dendritic integration (Sailer et al. 2002). Intriguingly, recent studies have discovered K^+ channels at a subcellular level (Trimmer 2015): for example human dopaminergic neurons possess mitochondrial SK2 channels, and this channel showed a neuroprotective outcome, its activation restoring mitochondrial wellbeing (Dolga et al. 2014).

The study presented here showed H_2O_2 -induced oxidative stress crosstalk with Bcl-2, which has a fundamental role in the intrinsic route of apoptosis, indeed the H_2O_2 stressor caused a vast reduction in Bcl-2 protein expression in both neurons and astrocytes (See chapter three). This effect was reversed by SK channel opening in pharmacological experiments in these cells. Previous work was shown that Bcl-2 expression has a negative impact on the reactive oxygen species balance in cells, this treatment rescuing GT1-7 neurons from ROS injury effect (Kane *et al.* 1993). Of course, apoptosis thinking is also of big interest in the cancer field, since cancer progression through lack of apoptosis is a leading factor in oncogenesis (Llambi and Green 2011). Nowadays, researchers have also highlighted an emerging target “mitochondrial ion channels” for cancer cure (Leanza et al. 2014). In this thesis, RT-PCR and Western blotting showed that SK1-4 channels are not only expressed in CNS cells, but also that breast cancer cells favoured these molecules. SK2 and SK3 channel subtypes being found at both the mRNA and protein levels, although unfortunately Western blotting did not show SK4 protein expression. Thus, the work here focused on SK2 and SK3 channel subtypes and whether they are functional proteins. It is additionally interesting that the work here discovered that in non-tumorigenic breast cells, MCF 10A, there are no SK1, SK2, and SK3 channel types. As highlighted above, these ion channels contribute in Ca^{2+} -related features of

“pathophysiology”, numerous studies showing that tumours in fact require more Ca^{2+} ions for their progress (Panner *et al.* 2005). This was the reason that SK channels were targeted in pharmacological and gene modulation experiments. In all the cell types used, SK2 or SK3 channel blocking significantly reduced breast cancer cell numbers. In contrast, opening of these channels markedly increased cell numbers in MTS viability assays. Not only SK2-3 channel activity dampening, but also SK2 or SK3 channel downregulation similarly produced a notable decrease in the cell viability. Linking this effect to life/death gates, experiments found that SK2 or SK3 channel inhibition in fact profoundly dampened Bcl-2 expression, whereas greatly upregulated caspase-7 and caspase-9 protein expression (See chapter five). This is a non-canonical role for these channels. A corollary of this is that the target domains which trigger intracellular machinery (e.g. Bcl-2) need not reside in the transmembrane region, but may form part of intracellular domains. This is compelling finding and is the first study to show that SK2 and SK3 channels control this avenue in cell viability, thereby potently triggering cancer cell growth. More recently, it has been highlighted that the Bcl-2 protein is really an emerging target in both neurodegeneration and cancer pathogenesis (Czabotar *et al.* 2014). In this sense, SK channels act as a promising target in both fields, and this study confirmed this window of opportunity.

6.3 TRPM7 channel role in CNS cell survival

In chapter four, the second channel candidate considered was TRPM7 of the TRPM channel family. Challenges for current neurodegeneration treatment are that other channelopathies (rather than SK dysfunction) such as TRPM7 deregulation occur. Therefore, the proposed study also aimed at identifying a TRPM family member, namely TRPM7, a potentially new target which may sidestep such a problem. The proposal is that modulation of one type of membrane protein, the so called TRPM7 channel is a potential strategy in developing a new generation of anti-degenerative effects against oxidative stress, hypoxia, as well as apoptosis. The work addressed therefore the key question “Is this particular channel a good target for blocking neuronal death?”

In physiology, TRPM7 has expanding cellular functions, from embryonic development to cell proliferation, and this extends to cell survival aspects (Yee et al. 2014), these roles being observed in different cell types, both excitable and non-excitable versions. It is clear that this channel allows various ions to cross the membrane, for instance Ca^{2+} and Mg^{2+} (Schmitz *et al.* 2003). Presumably, this channel is involved in pathologies where these ions play a decisive role in underlying mechanisms causing neuronal loss. The work here used mouse homozygous mutant *STHdh^{Q111}/Hdh^{Q111}* and MOG-G-UVW cells to test whether targeting this channel can improve cell survival against oxidative stress, hypoxia and apoptosis. TRPM7 presence was first determined through RT-PCR and Western blotting methods. These tools indicated that the TRPM7 channel is expressed at both the mRNA and protein levels. It was hypothesised here that either TRPM7 blocking or TRPM7 channel expression reduction through siRNA would rescue these cells from the toxic action of these insults above. MTS viability experiments showed that

indeed TRPM7 channel blocking significantly saved these cells from oxidative stress, hypoxia and apoptosis. Similar results were achieved via siRNA-mediated experiments. The channel knock-out afforded significant protection then against mechanisms which of course activate cell death. It is very interesting that one molecule challenges three different cell demise mechanisms, namely oxidative stress, hypoxia and apoptosis, and the underlying mechanism(s) behind this powerful role of TRPM7 needs to be elucidated. It has been reported that the TRPM7 channel can improve neuronal cell survival not only against oxidative stress, but also by eliminating excitotoxicity (Aarts and Tymianski 2005).

Ion channels such as the SK or TRP family are differentially expressed in tissues and even within tissues (Pardo and Stuhmer 2014). For example, in the cancer work presented here some cell lines expressed SK2 and SK4 (MCF-7) and others SK3 and SK4 (MDA-MB-231) channels, and “normal” non-tumorigenic breast epithelial cells did not express SK1, SK2 and SK3 channels. Perhaps the differences in SK channel expression are in part responsible for the different growth rates i.e. cancerous versus non-tumorigenic cells. This could be investigated systematically in future work. The work with neuronal cells showed similarly that differences exist. Hence human SH-SY5Y cells express SK1 and SK3 channels and mouse Huntington’s cells, which express mutant Huntington protein (Trettel et al. 2000), express either SK1, SK3, SK4 (Wild-type, *Hdh⁺/Hdh⁺*), SK1 and SK2 (Heterozygous, *STHdh^{Q111}/Hdh⁺*) or SK1 and SK4 (Homozygous, *STHdh^{Q111}/Hdh^{Q111}*). Further, SK1 channels are not functional in the mouse (Benton et al. 2003), but are in the human (Shah and Haylett 2000). In this regard future work could use a human Huntington’s model in order that such differences do not impact on interpretations. In astrocytes (MOG-G-UVW) and microglia (BV-2) only SK4 channels are expressed at an RNA level, although whether the SK4 channel is expressed at the protein level or not remains to be established. To begin to answer this question the antibody used here needs to be checked against a positive SK4 control to determine the effectiveness, or otherwise. Also single channel electrophysiology, along with pharmacology, could be deployed to determine the existence of SK4 channel. In addition, SK channels are also expressed in non-excitabile cells, such as T-lymphocytes (Strobaek et al. 2013). This presents both opportunities and challenges for therapeutic strategies. Since most SK channel modulators were not water soluble penetration into the brain

across the blood-brain barrier, i.e. delivery to a CNS target, should in principle be less of a problem. Based on tissue expression described here the preferred targets in cancer cells would be SK2, SK4 (MCF-7) and SK3, SK4 (MDA-MB-231), in human neurons SK1, SK3 (SH-SY5Y), and in mouse neurons SK2 (*STHdh^{Q111}/Hdh⁺*) and SK4 (*STHdh^{Q111}/Hdh^{Q111}*). Consistent with this is that CyPPA (25 μ M), an SK2-3 activator, markedly improved *in vitro* rat hippocampal cell viability against glutamate-induced mitochondrial dysfunction (Dolga et al. 2013) through SK2 channel modulation (See also *in vivo* work below). Three other important points are worth making. Firstly, the cancer work shows that knocking out one of the SK targets, and only one, is adequate to blunt growth indicating that in this case at least “compensation” by the remaining SK channel (SK4) is not suffice. Secondly, SK channel activation in CNS cell lines does not impact on constitutive growth, whereas that is not the case in cancer cells. This offers the prospect of selective targeting of activity against cancer cells when CNS cells are not “stressed” and also poses a question. What renders the SK channel susceptible to modulation only in the face of a stress such as hypoxia etc? How does that insult bring about that change? Thirdly, attention needs to be paid to concentrations since in all instances the effects of the modulators were biphasic, protecting at low, and affording less protection at a higher concentration (See e.g. Fig 3.18).

All of the work presented here was carried out on *in vitro* cell systems and it remains to be seen how any of the effects reported here translate to the *in vivo* situation. There are precedents for this proposed strategy however in other clinical settings. An *in vivo* rat study showed that CyPPA (5 mg/kg) prevents psychiatric symptoms occurring through amygdala hyperactivity (Atchley et al. 2012). In addition, the SK4 channel opener, NS309, seems to modulate hippocampal pyramidal firing

properties, which are related to neuronal hyperexcitability (Pedarzani *et al.* 2005), for example ataxia. In inflammatory bowel disease, *in vivo* rat studies showed that the IK (SK4) blocker, NS6180 (10 mg/kg), significantly improved inflammatory bowel disease outcome. Furthermore, SK channels are also implicated in heart disorders, and it has been reported that *in vivo* SK2 channel subtype inhibition by NS8593 (5 mg/kg) in the horse demonstrated a clear antiarrhythmic property (Haugaard *et al.* 2015). In the context of cancer work, future experiments should examine the prospective activity of the SK modulators we have tested against tumours in one of the many transgenic or knockout mouse models of breast cancer available, taking the argument one step closer to a drug design strategy.

In the case of the TRP channel work described in chapter four, TRPM7 was expressed in both cell lines (*STHdh^{Q111}/Hdh^{Q111}* and MOG-G-UVW) tested. For the pharmacology, selective modulators were unfortunately not available, hence the reason that this study used SK channel modulators to probe TRPM7 channel (Chubanov *et al.* 2012). TRPM7 ion channel modulators have been previously tested in different disease models of cancer and neurodegeneration. For example, in the brain, *In vivo* studies with mice showed that carvacrol (10 mg/kg) markedly reversed neuronal injury and behavioural abnormalities in a neonatal hypoxia-ischemia model (Chen *et al.* 2015a). Also it has been found that TRPM7 channel inhibition *in vitro* by carvacrol (500 μ M) actually dampened human glioblastoma cell properties, namely proliferation, migration and invasion (Chen *et al.* 2015b). Here we described that TRPM7 channel blocking (Over a narrow concentration range) also produced cells more resistant to cellular stressors, namely neuronal insults, making it an attractive target to focus on therapeutically. Perhaps future work should confirm that these blockers showed better protection against oxidative stress c.f.

hypoxia and apoptosis. Once again more importantly, and intriguingly, the blockers did not affect the constitutive growth of the cells tested, raising the same question about how the insult or the consequences of it modulate TRPM7 properties.

A final consideration for future work is what is happening to intracellular Ca^{2+} in response to SK channel or TRPM7 blockade or SK channel activation? Any changes which must surely be important for cell growth or survival could be measured using cell imaging with either fluorescent (e.g. FURA-2) or bioluminescent indicators.

In conclusion, these molecules regulate ionic homeostasis, and when dysregulated alter life and death decisions that cells make. It is worth espousing that SK and TRPM7 channels act as channels of life or death. The wider implications are that the results here add weight to an emerging view that these channels have fundamental unsuspected non-canonical roles in the cancers, roles which are also highly relevant to degenerative diseases in the brain.

7 Appendix

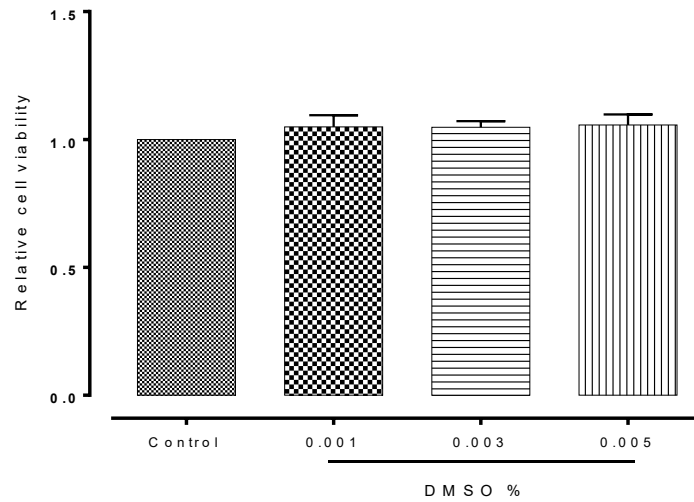
1. Charcoal stripped foetal bovine serum protocol

This serum was used in endocrine resistant cell cultures. To treat 100 ml of foetal bovine serum the following protocol was used. First, the pH in normal foetal bovine serum was adjusted to 4.2 using HCl (5 M), and then allowed to equilibrate at 4 °C. A solution of: 18 ml distilled water, 2 gram activated charcoal, and 0.01 gram dextran T70 was mixed, this being stirred for one hour. From this solution, 5 ml was added into each 100 ml of foetal bovine serum (pH= 4.2), and gently agitated overnight at 4 °C in the dark, using a stirrer for at least 16 hours. The following day, the charcoal was removed after centrifugation at 12,000 g for 40 minutes, and the supernatant filtered in Whatman filter paper, at least 4 times. Finally, the resultant pH was readjusted to 7.2 using NaOH (5 M) before being filtered through a syringe filter (0.2 µm).

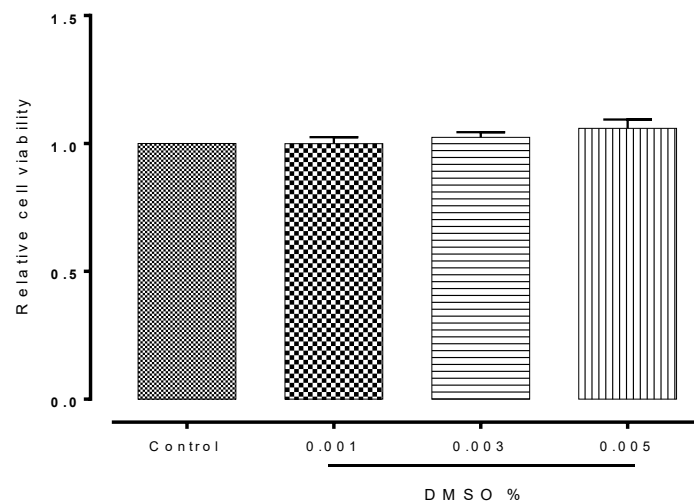
2. Protocols for running and stacking gels in Western blotting

Ingredients	Running gel	Stacking gel
Double distilled water	10.4 ml	6.4 ml
ProtoGel (30%)	6 ml	1.7 ml
Trisaminomethane (1.5 M)	5.7 ml	-
Trisaminomethane (1 M)	-	1.25 ml
Sodium dodecyl sulphate (10%)	0.23 ml	0.1 ml
Ammonium persulfate (10%)	0.23 ml	0.1 ml
Tetramethylethylenediamine	0.014 ml	0.01 ml

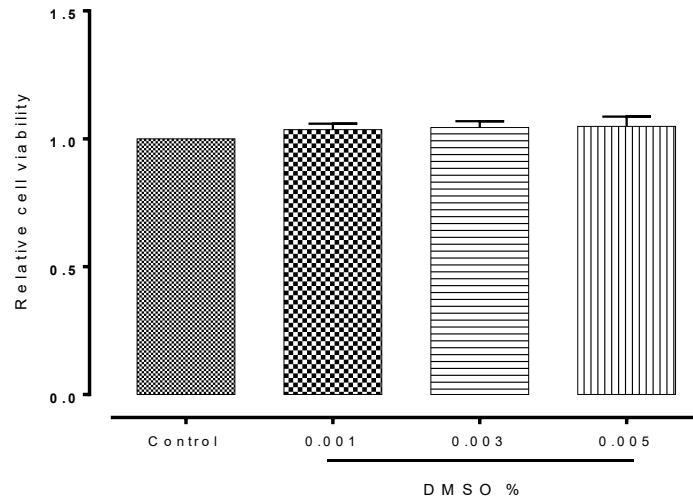
3. Results



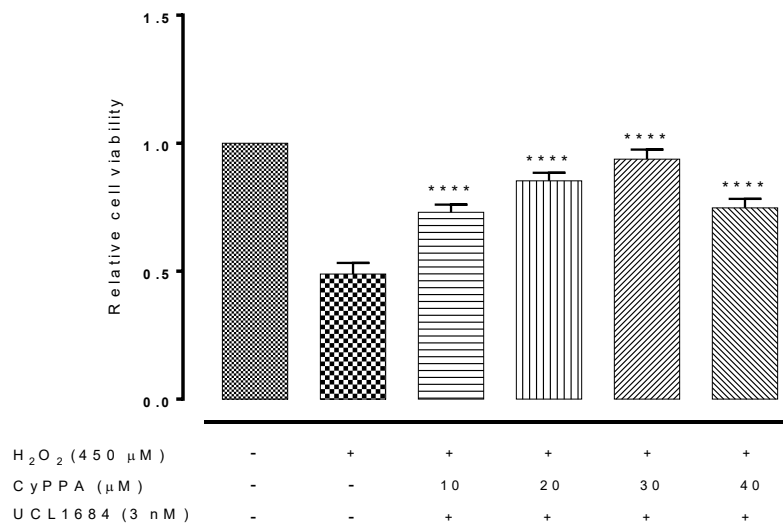
7.1 The effect of the drug vehicle, DMSO, on undifferentiated SH-SY5Y cell viability. Data are shown as means \pm SEM. One-way ANOVA followed by Dunnett's post hoc test, n=6.



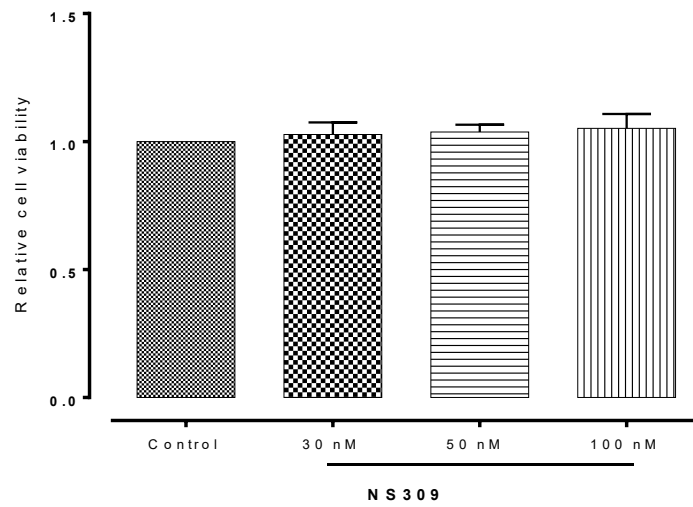
7.2 The effect of the drug vehicle, DMSO, on wild-type *Hdh*^{+/+} cell viability. Data are shown as means \pm SEM. One-way ANOVA followed by Dunnett's post hoc test, n=6.



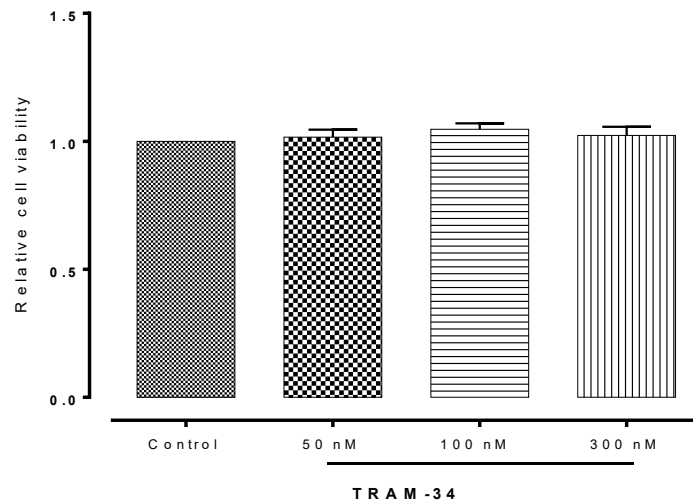
7.3 The effect of the drug vehicle, DMSO, on MOG-G-UVW cell viability. Data are shown as means \pm SEM. One-way ANOVA followed by Dunnett's post hoc test, n=6.



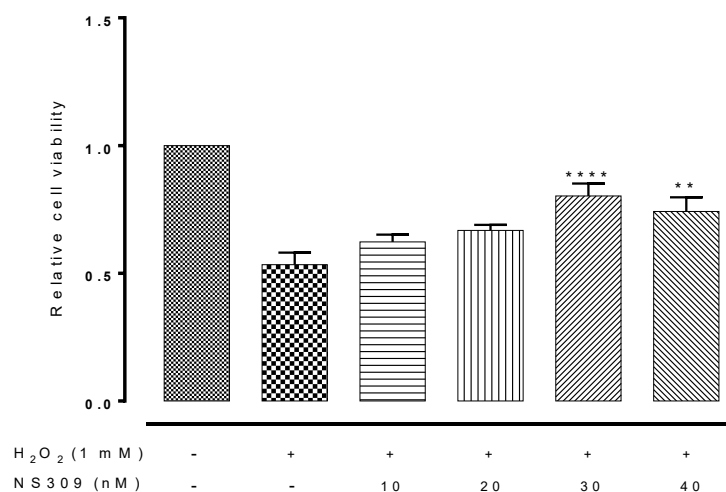
7.4 The effect of CyPPA, an SK2-3 channel activator, in the presence of the SK1-3 channel blocker, UCL1684, on the survival of undifferentiated SH-SY5Y cells exposed to H₂O₂-induced oxidative stress. Data are shown as means \pm SEM. ****p-value < 0.0001 versus insult, one-way ANOVA followed by Dunnett's post hoc test, n =9.



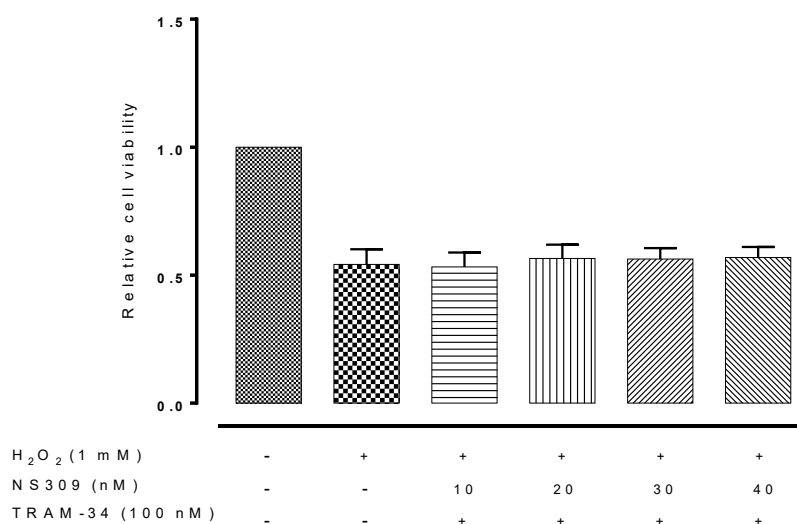
7.5 The effect of the SK4 channel activator, NS309, on MOG-G-UVW cell viability. Data are shown as means \pm SEM. One-way ANOVA followed by Dunnett's post hoc test, n=6.



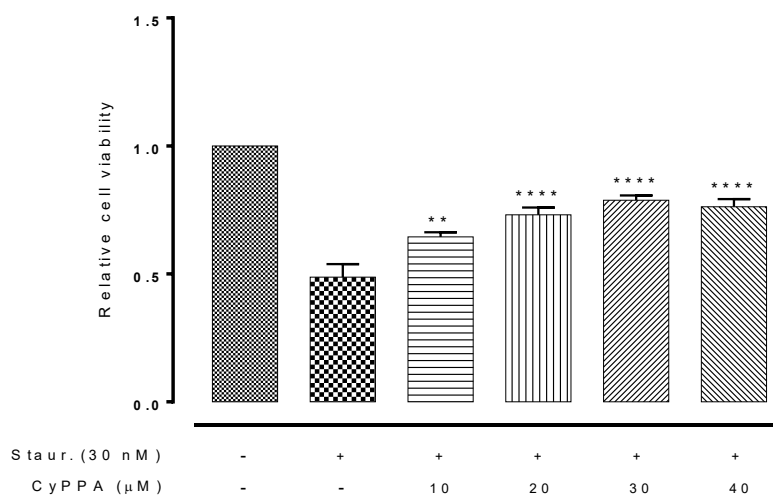
7.6 The effect of the SK4 channel blocker, TRAM-34, on MOG-G-UVW cell viability. Data are shown as means \pm SEM. One-way ANOVA followed by Dunnett's post hoc test, n=6.



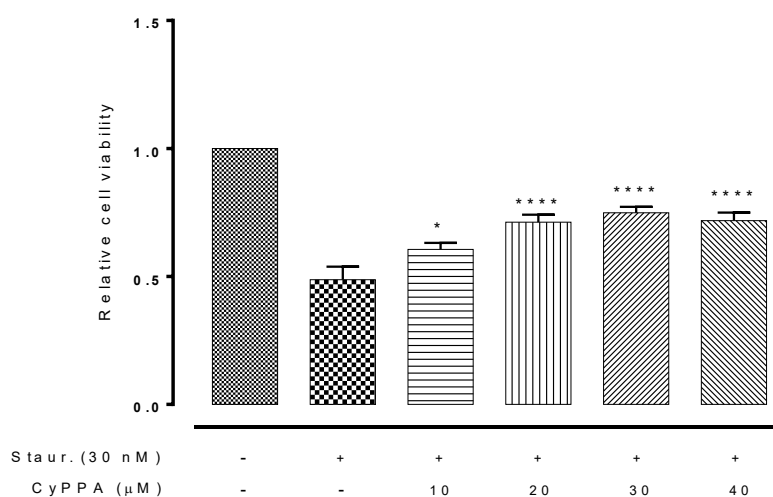
7.7 The effect of NS309, SK4 channel activation, on the survival of MOG-G-UVW cells exposed to H₂O₂-induced oxidative stress. Data are shown as means ± SEM. *****p*-value < 0.0001 versus insult, one-way ANOVA followed by Dunnett's post hoc test, n =9.



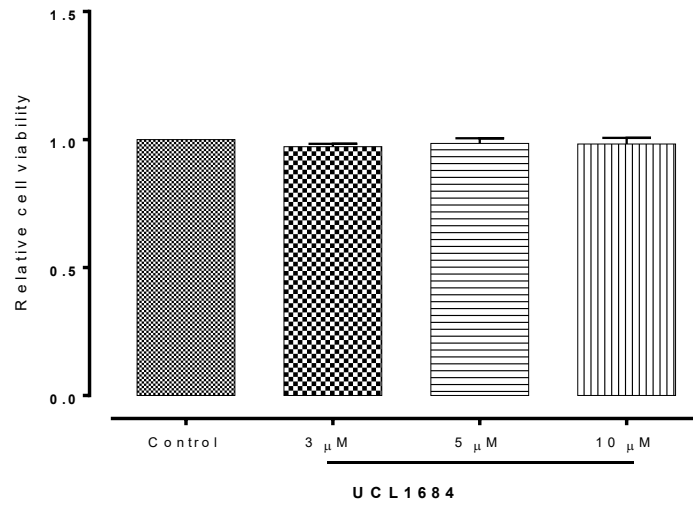
7.8 The effect of NS309, an SK4 channel activator, in the presence of the SK4 channel blocker, TRAM-34, on the survival of MOG-G-UVW cells exposed to H₂O₂-induced oxidative stress. Data are shown as means ± SEM. One-way ANOVA followed by Dunnett's post hoc test, n =9.



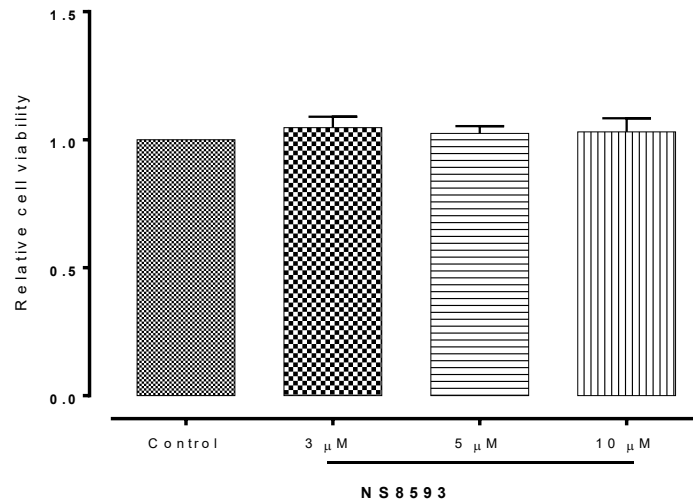
7.9 The effect of CyPPA, SK3 channel activation, on the survival of wild-type *Hdh⁺/Hdh⁺* cells exposed to staurosporine-induced apoptosis. Data are shown as means \pm SEM. *****p*-value < 0.0001 versus insult, one-way ANOVA followed by Dunnett's post hoc test, n = 9.



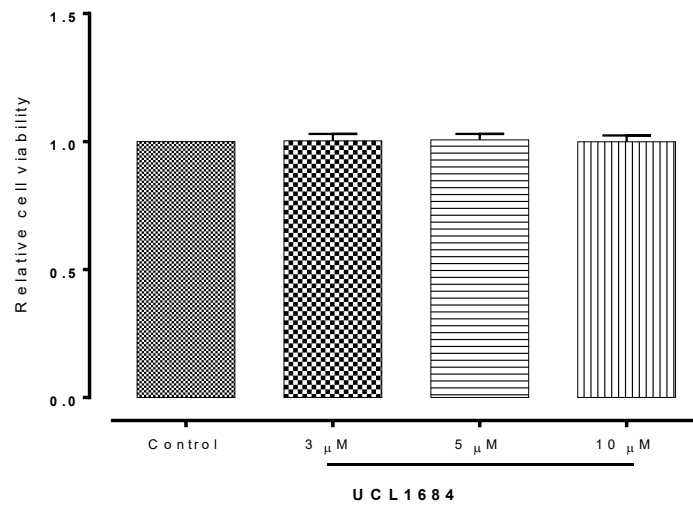
7.10 The effect of CyPPA, SK2 channel activation, on the survival of heterozygous *Hdh^{Q111}/Hdh⁺* cells exposed to staurosporine-induced apoptosis. Data are shown as means \pm SEM. *****p*-value < 0.0001 versus insult, one-way ANOVA followed by Dunnett's post hoc test, n = 9.



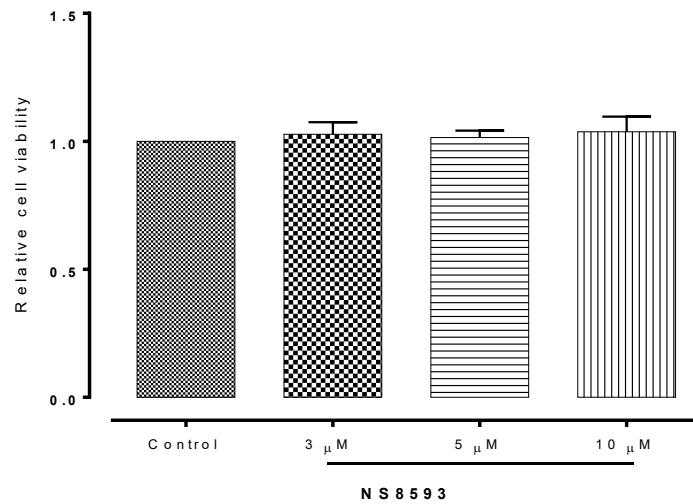
7.11 The effect of SK1-3 ion channel blocker, UCL1684, on homozygous mutant *Hdh^{Q111}/Hdh^{Q111}* cell viability. Data are shown as means ± SEM. One-way ANOVA followed by Dunnett's post hoc test, n=6.



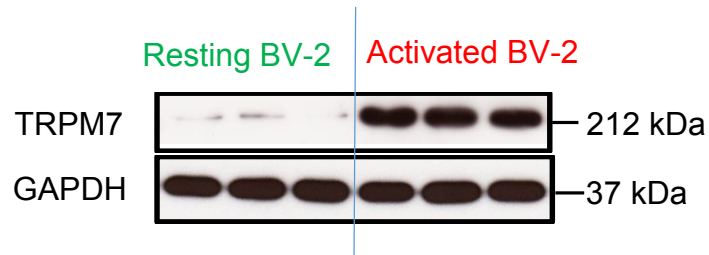
7.12 The effect of SK1-3 ion channel blocker, NS8593, on homozygous mutant *Hdh^{Q111}/Hdh^{Q111}* cell viability. Data are shown as means ± SEM. One-way ANOVA followed by Dunnett's post hoc test, n=6.



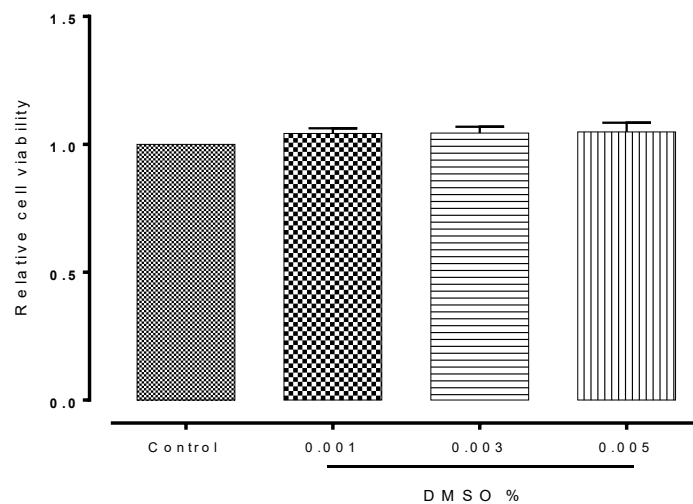
7.13 The effect of SK1-3 ion channel blocker, UCL1684, on MOG-G-UVW cell viability. Data are shown as means \pm SEM. One-way ANOVA followed by Dunnett's post hoc test, n=6.



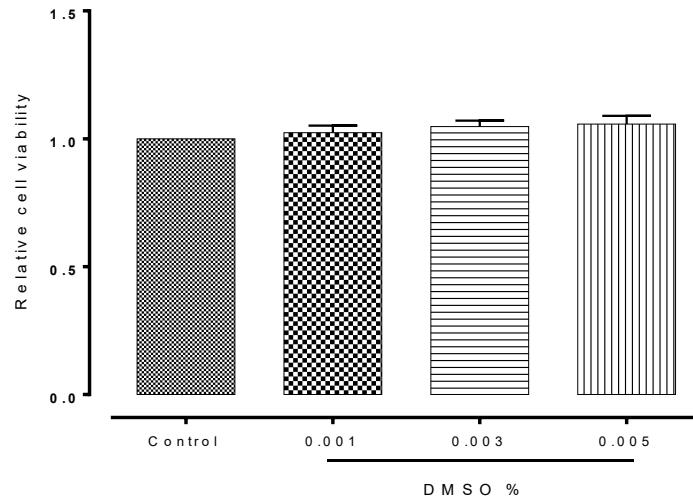
7.14 The effect of SK1-3 ion channel blocker, NS8593, on MOG-G-UVW cell viability. Data are shown as means \pm SEM. One-way ANOVA followed by Dunnett's post hoc test, n=6.



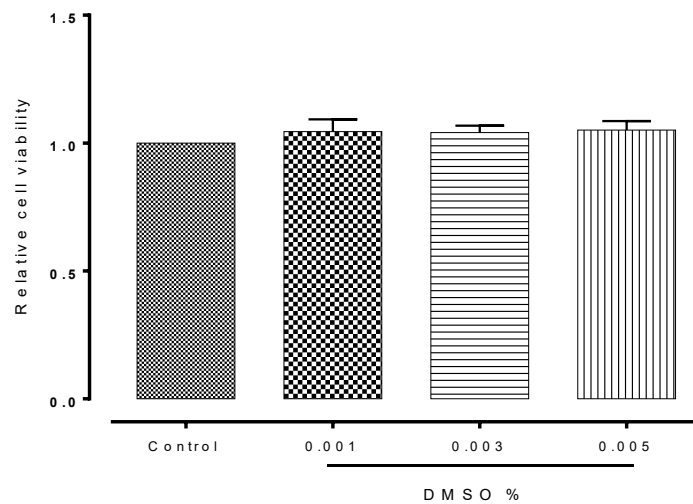
7.15 Representative immunoblot of TRPM7 channel in BV-2 cells. TRPM7 protein expression is distinctly upregulated after treatment with lipopolysaccharides (20 ng/ml) after 24 hours. GAPDH serves as the normalising control.



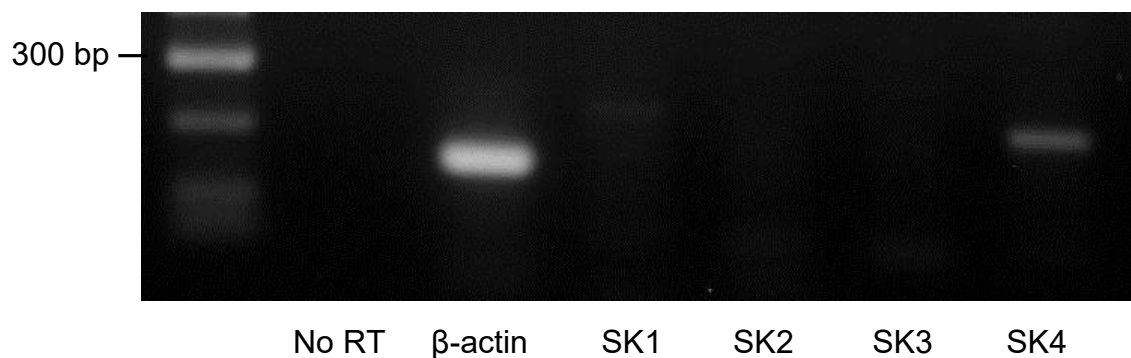
7.16 The effect of the drug vehicle, DMSO, on MCF-7 cell viability. Data are shown as means \pm SEM. One-way ANOVA followed by Dunnett's post hoc test, n=6.



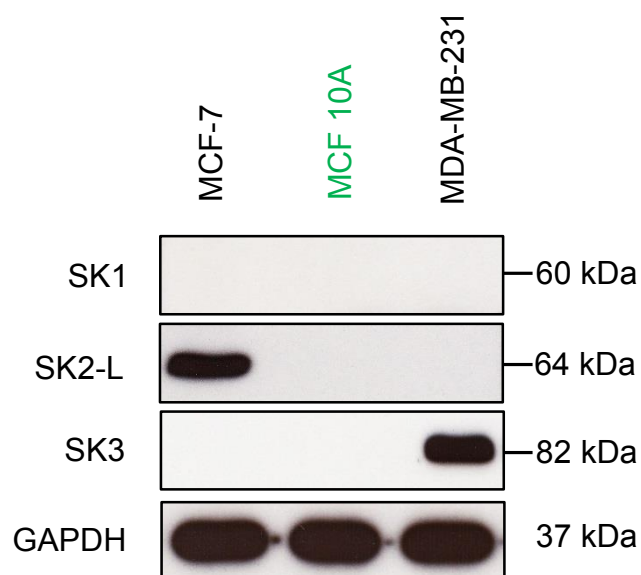
7.17 The effect of the drug vehicle, DMSO, on BT-474 cell viability. Data are shown as means \pm SEM. One-way ANOVA followed by Dunnett's post hoc test, n=6.



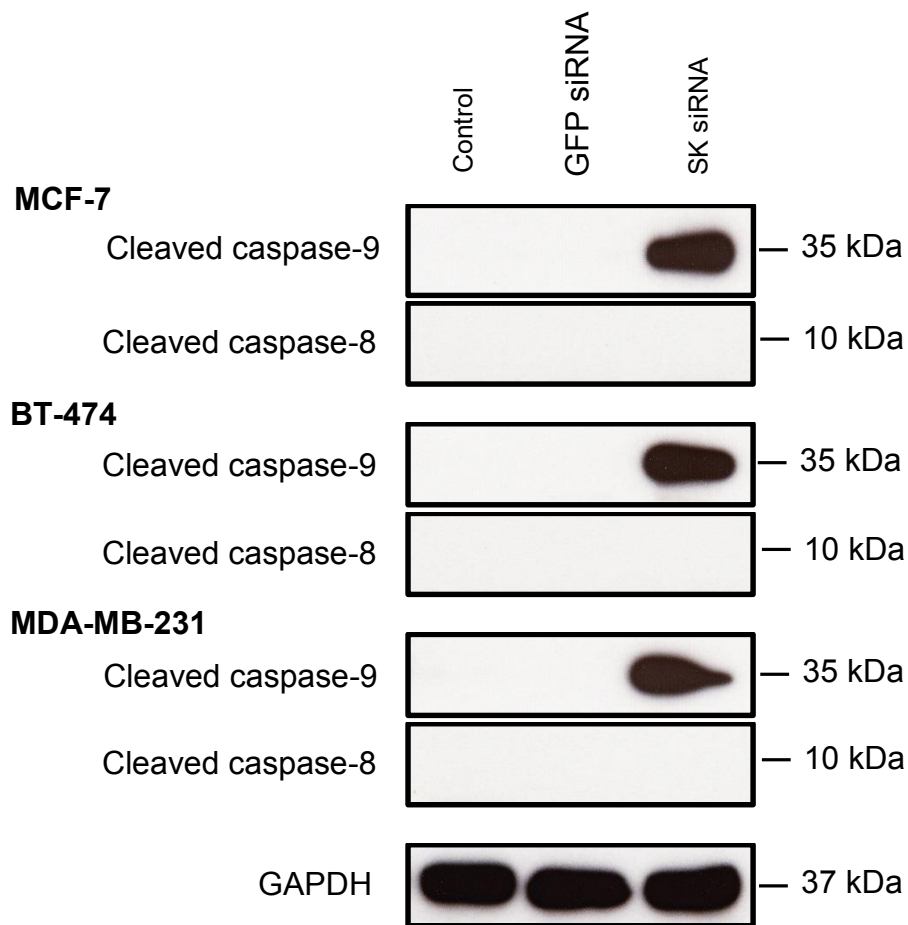
7.18 The effect of the drug vehicle, DMSO, on MDA-MB-231 cell viability. Data are shown as means \pm SEM. One-way ANOVA followed by Dunnett's post hoc test, n=6.



7.19 SK ion channel mRNA investigation in MCF 10A cells. Only the amplicons for SK4 channel is present and the PCR products are of the predicted size. β -actin serves as the normalising control.



7.20 Representative immunoblot of SK1-3 ion channel expression. SK1, SK2-L and SK3 ion channels are not expressed at the protein level in MCF 10A cells. GAPDH serves as the normalising control.



7.21 Representative immunoblot of cleaved caspase-8 and -9 protein in wild-type breast cancer cells transfected with specific SK2 (MCF-7 and BT-474) or SK3 (MDA-MB-231) siRNA. GAPDH serves as the normalising control.

8 References

(1993). A novel gene containing a trinucleotide repeat that is expanded and unstable on Huntington's disease chromosomes. The Huntington's Disease Collaborative Research Group. *Cell* **72**:971-983.

Aarts, M., Iihara, K., Wei, W. L., Xiong, Z. G., Arundine, M., Cerwinski, W., MacDonald, J. F. *et al.* (2003). A key role for TRPM7 channels in anoxic neuronal death. *Cell* **115**:863-877.

Aarts, M. M. and Tymianski, M. (2005). TRPMs and neuronal cell death. *Pflugers Arch* **451**:243-249.

Acehan, D., Jiang, X., Morgan, D. G., Heuser, J. E., Wang, X. and Akey, C. W. (2002). Three-dimensional structure of the apoptosome: implications for assembly, procaspase-9 binding, and activation. *Mol Cell* **9**:423-432.

Adelman, J. P. (2015). SK Channels and Calmodulin. *Channels (Austin)* **0**.

Adelman, J. P., Maylie, J. and Sah, P. (2012). Small-conductance Ca²⁺-activated K⁺ channels: form and function. *Annu Rev Physiol* **74**:245-269.

Al Soraj, M., He, L., Peynshaert, K., Cousaert, J., Vercauteren, D., Braeckmans, K., De Smedt, S. C. *et al.* (2012). siRNA and pharmacological inhibition of endocytic pathways to characterize the differential role of macropinocytosis and the actin cytoskeleton on cellular uptake of dextran and cationic cell penetrating peptides octaarginine (R8) and HIV-Tat. *J Control Release* **161**:132-141.

Alba, E., Albanell, J., de la Haba, J., Barnadas, A., Calvo, L., Sanchez-Rovira, P., Ramos, M. *et al.* (2014). Trastuzumab or lapatinib with standard chemotherapy for HER2-positive breast cancer: results from the GEICAM/2006-14 trial. *Br J Cancer* **110**:1139-1147.

Alger, B. E. and Nicoll, R. A. (1980). Epileptiform burst afterhyperpolarization: calcium-dependent potassium potential in hippocampal CA1 pyramidal cells. *Science* **210**:1122-1124.

Allen, D., Bond, C. T., Lujan, R., Ballesteros-Merino, C., Lin, M. T., Wang, K., Klett, N. *et al.* (2011a). The SK2-long isoform directs synaptic localization and function of SK2-containing channels. *Nat Neurosci* **14**:744-749.

Allen, D., Fakler, B., Maylie, J. and Adelman, J. P. (2007). Organization and regulation of small conductance Ca²⁺-activated K⁺ channel multiprotein complexes. *J Neurosci* **27**:2369-2376.

Allen, D., Nakayama, S., Kuroiwa, M., Nakano, T., Palmateer, J., Kosaka, Y., Ballesteros, C. *et al.* (2011b). SK2 channels are neuroprotective for ischemia-induced neuronal cell death. *J Cereb Blood Flow Metab* **31**:2302-2312.

Almeida, A., Almeida, J., Bolanos, J. P. and Moncada, S. (2001). Different responses of astrocytes and neurons to nitric oxide: the role of glycolytically generated ATP in astrocyte protection. *Proc Natl Acad Sci U S A* **98**:15294-15299.

Almeida, A., Delgado-Esteban, M., Bolanos, J. P. and Medina, J. M. (2002). Oxygen and glucose deprivation induces mitochondrial dysfunction and oxidative stress in neurones but not in astrocytes in primary culture. *J Neurochem* **81**:207-217.

Ames, J. B., Tanaka, T., Stryer, L. and Ikura, M. (1996). Portrait of a myristoyl switch protein. *Curr Opin Struct Biol* **6**:432-438.

Andersen, J. K. (2004). Oxidative stress in neurodegeneration: cause or consequence? *Nat Med* **10 Suppl**:S18-25.

Anilkumar, U. and Prehn, J. H. (2014). Anti-apoptotic BCL-2 family proteins in acute neural injury. *Front Cell Neurosci* **8**:281.

Atchley, D., Hankosky, E. R., Gasparotto, K. and Rosenkranz, J. A. (2012). Pharmacological enhancement of calcium-activated potassium channel function reduces the effects of repeated stress on fear memory. *Behav Brain Res* **232**:37-43.

Augustine, G. J., Santamaria, F. and Tanaka, K. (2003). Local calcium signaling in neurons. *Neuron* **40**:331-346.

- Avanzini, G., de Curtis, M., Panzica, F. and Spreafico, R. (1989). Intrinsic properties of nucleus reticularis thalami neurones of the rat studied in vitro. *J Physiol* **416**:111-122.
- Azimi, I., Roberts-Thomson, S. J. and Monteith, G. R. (2014). Calcium influx pathways in breast cancer: opportunities for pharmacological intervention. *Br J Pharmacol* **171**:945-960.
- Bae, C. Y. and Sun, H. S. (2011). TRPM7 in cerebral ischemia and potential target for drug development in stroke. *Acta Pharmacol Sin* **32**:725-733.
- Bae, C. Y. and Sun, H. S. (2013). Current understanding of TRPM7 pharmacology and drug development for stroke. *Acta Pharmacol Sin* **34**:10-16.
- Barrett, E. F. and Barret, J. N. (1976). Separation of two voltage-sensitive potassium currents, and demonstration of a tetrodotoxin-resistant calcium current in frog motoneurones. *J Physiol* **255**:737-774.
- Bender, T. and Martinou, J. C. (2013). Where killers meet--permeabilization of the outer mitochondrial membrane during apoptosis. *Cold Spring Harb Perspect Biol* **5**:a011106.
- Benton, D. C., Monaghan, A. S., Hosseini, R., Bahia, P. K., Haylett, D. G. and Moss, G. W. (2003). Small conductance Ca²⁺-activated K⁺ channels formed by the expression of rat SK1 and SK2 genes in HEK 293 cells. *J Physiol* **553**:13-19.
- Berridge, M. J. (1998). Neuronal calcium signaling. *Neuron* **21**:13-26.
- Berridge, M. J. (2012). Calcium signalling remodelling and disease. *Biochem Soc Trans* **40**:297-309.
- Bezánilla, F. (2000). The voltage sensor in voltage-dependent ion channels. *Physiol Rev* **80**:555-592.
- Biasoli, D., Sobrinho, M. F., da Fonseca, A. C., de Matos, D. G., Romão, L., de Moraes Maciel, R., Rehen, S. K. *et al.* (2014). Glioblastoma cells inhibit astrocytic p53-expression favoring cancer malignancy. *Oncogenesis* **3**:e123.

- Biedler, J. L., Roffler-Tarlov, S., Schachner, M. and Freedman, L. S. (1978). Multiple neurotransmitter synthesis by human neuroblastoma cell lines and clones. *Cancer Res* **38**:3751-3757.
- Bienert, G. P., Schjoerring, J. K. and Jahn, T. P. (2006). Membrane transport of hydrogen peroxide. *Biochim Biophys Acta* **1758**:994-1003.
- Blasi, E., Barluzzi, R., Bocchini, V., Mazzolla, R. and Bistoni, F. (1990). Immortalization of murine microglial cells by a v-raf/v-myc carrying retrovirus. *J Neuroimmunol* **27**:229-237.
- Blatz, A. L. and Magleby, K. L. (1986). Single apamin-blocked Ca-activated K⁺ channels of small conductance in cultured rat skeletal muscle. *Nature* **323**:718-720.
- Bocchini, V., Mazzolla, R., Barluzzi, R., Blasi, E., Sick, P. and Kettenmann, H. (1992). An immortalized cell line expresses properties of activated microglial cells. *J Neurosci Res* **31**:616-621.
- Bond, C. T., Herson, P. S., Strassmaier, T., Hammond, R., Stackman, R., Maylie, J. and Adelman, J. P. (2004). Small conductance Ca²⁺-activated K⁺ channel knock-out mice reveal the identity of calcium-dependent afterhyperpolarization currents. *J Neurosci* **24**:5301-5306.
- Bootman, M. D. (2012). Calcium signaling. *Cold Spring Harb Perspect Biol* **4**:a011171.
- Bortner, C. D. and Cidlowski, J. A. (2014). Ion channels and apoptosis in cancer. *Philos Trans R Soc Lond B Biol Sci* **369**:20130104.
- Bourassa, M. W. and Miller, L. M. (2012). Metal imaging in neurodegenerative diseases. *Metallomics* **4**:721-738.
- Bourque, C. W. and Brown, D. A. (1987). Apamin and d-tubocurarine block the afterhyperpolarization of rat supraoptic neurosecretory neurons. *Neurosci Lett* **82**:185-190.
- Bredesen, D. E., Rao, R. V. and Mehlen, P. (2006). Cell death in the nervous system. *Nature* **443**:796-802.
- Brown, J. M. and Attardi, L. D. (2005). The role of apoptosis in cancer development and treatment response. *Nat Rev Cancer* **5**:231-237.

Bruening-Wright, A., Schumacher, M. A., Adelman, J. P. and Maylie, J. (2002). Localization of the activation gate for small conductance Ca²⁺-activated K⁺ channels. *J Neurosci* **22**:6499-6506.

Buizza, L., Prandelli, C., Bonini, S. A., Delbarba, A., Cenini, G., Lanni, C., Buoso, E. *et al.* (2013). Conformational altered p53 affects neuronal function: relevance for the response to toxic insult and growth-associated protein 43 expression. *Cell Death Dis* **4**:e484.

Burg, E. D., Remillard, C. V. and Yuan, J. X. (2006). K⁺ channels in apoptosis. *J Membr Biol* **209**:3-20.

Cailleau, R., Young, R., Olive, M. and Reeves, W. J., Jr. (1974). Breast tumor cell lines from pleural effusions. *J Natl Cancer Inst* **53**:661-674.

Cain, K., Bratton, S. B. and Cohen, G. M. (2002). The Apaf-1 apoptosome: a large caspase-activating complex. *Biochimie* **84**:203-214.

Caltana, L., Merelli, A., Lazarowski, A. and Brusco, A. (2009). Neuronal and glial alterations due to focal cortical hypoxia induced by direct cobalt chloride (CoCl₂) brain injection. *Neurotox Res* **15**:348-358.

Campbell, A. K. (2014). Intracellular Calcium. Wiley.

Campos Rosa, J., Galanakis, D., Piergentili, A., Bhandari, K., Ganellin, C. R., Dunn, P. M. and Jenkinson, D. H. (2000). Synthesis, molecular modeling, and pharmacological testing of bis-quinolinium cyclophanes: potent, non-peptidic blockers of the apamin-sensitive Ca(2+)-activated K(+) channel. *J Med Chem* **43**:420-431.

Casteels, R. and Droogmans, G. (1981). Exchange characteristics of the noradrenaline-sensitive calcium store in vascular smooth muscle cells or rabbit ear artery. *J Physiol* **317**:263-279.

Castle, N. A., London, D. O., Creech, C., Fajloun, Z., Stocker, J. W. and Sabatier, J. M. (2003). Maurotoxin: a potent inhibitor of intermediate conductance Ca²⁺-activated potassium channels. *Mol Pharmacol* **63**:409-418.

Catacuzzeno, L., Fioretti, B. and Franciolini, F. (2012). Expression and Role of the Intermediate-Conductance Calcium-Activated Potassium Channel KCa3.1 in Glioblastoma. *J Signal Transduct* **2012**:421564.

Catterall, W. A. (2010). Ion channel voltage sensors: structure, function, and pathophysiology. *Neuron* **67**:915-928.

Chandel, N. S., Maltepe, E., Goldwasser, E., Mathieu, C. E., Simon, M. C. and Schumacker, P. T. (1998). Mitochondrial reactive oxygen species trigger hypoxia-induced transcription. *Proc Natl Acad Sci U S A* **95**:11715-11720.

Chen, H. C., Su, L. T., Gonzalez-Pagan, O., Overton, J. D. and Runnels, L. W. (2012). A key role for Mg(2+) in TRPM7's control of ROS levels during cell stress. *Biochem J* **445**:441-448.

Chen, Q. H. and Toney, G. M. (2009). Excitability of paraventricular nucleus neurones that project to the rostral ventrolateral medulla is regulated by small-conductance Ca²⁺-activated K⁺ channels. *J Physiol* **587**:4235-4247.

Chen, W., Xu, B., Xiao, A., Liu, L., Fang, X., Liu, R., Turlova, E. *et al.* (2015a). TRPM7 inhibitor carvacrol protects brain from neonatal hypoxic-ischemic injury. *Mol Brain* **8**:11.

Chen, W. L., Barszczyk, A., Turlova, E., Deurloo, M., Liu, B., Yang, B. B., Rutka, J. T. *et al.* (2015b). Inhibition of TRPM7 by carvacrol suppresses glioblastoma cell proliferation, migration and invasion. *Oncotarget* **6**:16321-16340.

Choi, K., Kim, J., Kim, G. W. and Choi, C. (2009). Oxidative stress-induced necrotic cell death via mitochondria-dependent burst of reactive oxygen species. *Curr Neurovasc Res* **6**:213-222.

Chokshi, R., Fruasaha, P. and Kozak, J. A. (2012a). 2-aminoethyl diphenyl borinate (2-APB) inhibits TRPM7 channels through an intracellular acidification mechanism. *Channels (Austin)* **6**:362-369.

Chokshi, R., Matsushita, M. and Kozak, J. A. (2012b). Detailed examination of Mg²⁺ and pH sensitivity of human TRPM7 channels. *Am J Physiol Cell Physiol* **302**:C1004-1011.

Christofferson, D. E. and Yuan, J. (2010). Necroptosis as an alternative form of programmed cell death. *Curr Opin Cell Biol* **22**:263-268.

Chubanov, V., Mederos y Schnitzler, M., Meissner, M., Schafer, S., Abstiens, K., Hofmann, T. and Gudermann, T. (2012). Natural and synthetic modulators of SK (K(ca)²) potassium channels inhibit magnesium-dependent activity of the kinase-coupled cation channel TRPM7. *Br J Pharmacol* **166**:1357-1376.

Chubanov, V., Waldegger, S., Mederos y Schnitzler, M., Vitzthum, H., Sassen, M. C., Seyberth, H. W., Konrad, M. *et al.* (2004). Disruption of TRPM6/TRPM7 complex formation by a mutation in the TRPM6 gene causes hypomagnesemia with secondary hypocalcemia. *Proc Natl Acad Sci U S A* **101**:2894-2899.

Cidad, P., Jimenez-Perez, L., Garcia-Arribas, D., Miguel-Velado, E., Tajada, S., Ruiz-McDavitt, C., Lopez-Lopez, J. R. *et al.* (2012). Kv1.3 channels can modulate cell proliferation during phenotypic switch by an ion-flux independent mechanism. *Arterioscler Thromb Vasc Biol* **32**:1299-1307.

Clapham, D. E. (2003). TRP channels as cellular sensors. *Nature* **426**:517-524.

Clapham, D. E., Julius, D., Montell, C. and Schultz, G. (2005). International Union of Pharmacology. XLIX. Nomenclature and structure-function relationships of transient receptor potential channels. *Pharmacol Rev* **57**:427-450.

Clarke, L. E. and Barres, B. A. (2013). Emerging roles of astrocytes in neural circuit development. *Nat Rev Neurosci* **14**:311-321.

Coombes, E., Jiang, J., Chu, X. P., Inoue, K., Seeds, J., Branigan, D., Simon, R. P. *et al.* (2011). Pathophysiologically relevant levels of hydrogen peroxide induce glutamate-independent neurodegeneration that involves activation of transient receptor potential melastatin 7 channels. *Antioxid Redox Signal* **14**:1815-1827.

Correia, C., Lee, S. H., Meng, X. W., Vincelette, N. D., Knorr, K. L., Ding, H., Nowakowski, G. S. *et al.* (2015). Emerging understanding of Bcl-2 biology: Implications for neoplastic progression and treatment. *Biochim Biophys Acta* **1853**:1658-1671.

Cosens, D. J. and Manning, A. (1969). Abnormal electroretinogram from a *Drosophila* mutant. *Nature* **224**:285-287.

Crawley, S. W. and Cote, G. P. (2009). Identification of dimer interactions required for the catalytic activity of the TRPM7 alpha-kinase domain. *Biochem J* **420**:115-122.

Czabotar, P. E., Lessene, G., Strasser, A. and Adams, J. M. (2014). Control of apoptosis by the BCL-2 protein family: implications for physiology and therapy. *Nat Rev Mol Cell Biol* **15**:49-63.

D'Alessandro, G., Catalano, M., Sciaccaluga, M., Chece, G., Cipriani, R., Rosito, M., Grimaldi, A. *et al.* (2013). KCa3.1 channels are involved in the infiltrative behavior of glioblastoma in vivo. *Cell Death Dis* **4**:e773.

D'Hoedt, D., Hirzel, K., Pedarzani, P. and Stocker, M. (2004). Domain analysis of the calcium-activated potassium channel SK1 from rat brain. Functional expression and toxin sensitivity. *J Biol Chem* **279**:12088-12092.

Decuypere, J. P., Monaco, G., Missiaen, L., De Smedt, H., Parys, J. B. and Bultynck, G. (2011). IP(3) Receptors, Mitochondria, and Ca Signaling: Implications for Aging. *J Aging Res* **2011**:920178.

Deignan, J., Lujan, R., Bond, C., Riegel, A., Watanabe, M., Williams, J. T., Maylie, J. *et al.* (2012). SK2 and SK3 expression differentially affect firing frequency and precision in dopamine neurons. *Neuroscience* **217**:67-76.

Deliot, N. and Constantin, B. (2015). Plasma membrane calcium channels in cancer: Alterations and consequences for cell proliferation and migration. *Biochim Biophys Acta*.

Demeuse, P., Penner, R. and Fleig, A. (2006). TRPM7 channel is regulated by magnesium nucleotides via its kinase domain. *J Gen Physiol* **127**:421-434.

Diaz, L. F., Chiong, M., Quest, A. F., Lavandero, S. and Stutzin, A. (2005). Mechanisms of cell death: molecular insights and therapeutic perspectives. *Cell Death Differ* **12**:1449-1456.

Dolga, A. M. and Culmsee, C. (2012). Protective Roles for Potassium SK/K(Ca)² Channels in Microglia and Neurons. *Front Pharmacol* **3**:196.

Dolga, A. M., de Andrade, A., Meissner, L., Knaus, H. G., Hollerhage, M., Christophersen, P., Zischka, H. *et al.* (2014). Subcellular expression and neuroprotective effects of SK channels in human dopaminergic neurons. *Cell Death Dis* **5**:e999.

Dolga, A. M., Netter, M. F., Perocchi, F., Doti, N., Meissner, L., Tobaben, S., Grohm, J. *et al.* (2013). Mitochondrial small conductance SK2 channels prevent glutamate-induced oxytosis and mitochondrial dysfunction. *J Biol Chem* **288**:10792-10804.

Dolga, A. M., Terpolilli, N., Kepura, F., Nijholt, I. M., Knaus, H. G., D'Orsi, B., Prehn, J. H. *et al.* (2011). KCa₂ channels activation prevents [Ca²⁺]_i deregulation and reduces neuronal death following glutamate toxicity and cerebral ischemia. *Cell Death Dis* **2**:e147.

Douda, D. N., Khan, M. A., Grasemann, H. and Palaniyar, N. (2015). SK3 channel and mitochondrial ROS mediate NADPH oxidase-independent NETosis induced by calcium influx. *Proc Natl Acad Sci U S A* **112**:2817-2822.

Dringen, R. (2000). Metabolism and functions of glutathione in brain. *Prog Neurobiol* **62**:649-671.

Dryanovski, D. I., Guzman, J. N., Xie, Z., Galteri, D. J., Volpicelli-Daley, L. A., Lee, V. M., Miller, R. J. *et al.* (2013). Calcium entry and alpha-synuclein inclusions elevate dendritic mitochondrial oxidant stress in dopaminergic neurons. *J Neurosci* **33**:10154-10164.

Du, J., Xie, J., Zhang, Z., Tsujikawa, H., Fusco, D., Silverman, D., Liang, B. *et al.* (2010). TRPM7-mediated Ca²⁺ signals confer fibrogenesis in human atrial fibrillation. *Circ Res* **106**:992-1003.

Duncan, L. M., Deeds, J., Hunter, J., Shao, J., Holmgren, L. M., Woolf, E. A., Tepper, R. I. *et al.* (1998). Down-regulation of the novel gene melastatin correlates with potential for melanoma metastasis. *Cancer Res* **58**:1515-1520.

Dunn, P. M. (1999). UCL 1684: a potent blocker of Ca²⁺-activated K⁺ channels in rat adrenal chromaffin cells in culture. *Eur J Pharmacol* **368**:119-123.

Dutta, A. K., Khimji, A. K., Sathe, M., Kresge, C., Parameswara, V., Esser, V., Rockey, D. C. *et al.* (2009). Identification and functional characterization of the intermediate-conductance Ca(2+)-activated K(+) channel (IK-1) in biliary epithelium. *Am J Physiol Gastrointest Liver Physiol* **297**:G1009-1018.

Edgerton, J. R. and Reinhart, P. H. (2003). Distinct contributions of small and large conductance Ca²⁺-activated K⁺ channels to rat Purkinje neuron function. *J Physiol* **548**:53-69.

Eijkelkamp, N., Quick, K. and Wood, J. N. (2013). Transient receptor potential channels and mechanosensation. *Annu Rev Neurosci* **36**:519-546.

Ermak, G. and Davies, K. J. (2002). Calcium and oxidative stress: from cell signaling to cell death. *Mol Immunol* **38**:713-721.

Fanger, C. M., Rauer, H., Neben, A. L., Miller, M. J., Rauer, H., Wulff, H., Rosa, J. C. *et al.* (2001). Calcium-activated potassium channels sustain calcium signaling in T lymphocytes. Selective blockers and manipulated channel expression levels. *J Biol Chem* **276**:12249-12256.

Farfariello, V., Iamshanova, O., Germain, E., Fliniaux, I. and Prevarskaya, N. (2015). Calcium homeostasis in cancer: A focus on senescence. *Biochim Biophys Acta*.

Fatokun, A. A., Stone, T. W. and Smith, R. A. (2008). Oxidative stress in neurodegeneration and available means of protection. *Front Biosci* **13**:3288-3311.

Federico, A., Cardaioli, E., Da Pozzo, P., Formichi, P., Gallus, G. N. and Radi, E. (2012). Mitochondria, oxidative stress and neurodegeneration. *J Neurol Sci* **322**:254-262.

Fiers, W., Beyaert, R., Declercq, W. and Vandenabeele, P. (1999). More than one way to die: apoptosis, necrosis and reactive oxygen damage. *Oncogene* **18**:7719-7730.

Fioretti, B., Castigli, E., Micheli, M. R., Bova, R., Sciacaluga, M., Harper, A., Franciolini, F. *et al.* (2006). Expression and modulation of the intermediate-conductance Ca^{2+} -activated K^{+} channel in glioblastoma GL-15 cells. *Cell Physiol Biochem* **18**:47-56.

Fiorillo, C. D. and Williams, J. T. (1998). Glutamate mediates an inhibitory postsynaptic potential in dopamine neurons. *Nature* **394**:78-82.

Fleig, A. and Penner, R. (2004). The TRPM ion channel subfamily: molecular, biophysical and functional features. *Trends Pharmacol Sci* **25**:633-639.

Foskett, J. K., White, C., Cheung, K. H. and Mak, D. O. (2007). Inositol trisphosphate receptor Ca^{2+} release channels. *Physiol Rev* **87**:593-658.

Frame, M. C., Freshney, R. I., Vaughan, P. F., Graham, D. I. and Shaw, R. (1984). Interrelationship between differentiation and malignancy-associated properties in glioma. *Br J Cancer* **49**:269-280.

Franchi, L., Munoz-Planillo, R. and Nunez, G. (2012). Sensing and reacting to microbes through the inflammasomes. *Nat Immunol* **13**:325-332.

Friedlander, R. M. (2003). Apoptosis and caspases in neurodegenerative diseases. *N Engl J Med* **348**:1365-1375.

Gardos, G. (1958). The function of calcium in the potassium permeability of human erythrocytes. *Biochim Biophys Acta* **30**:653-654.

Gassmann, M., Grenacher, B., Rohde, B. and Vogel, J. (2009). Quantifying Western blots: pitfalls of densitometry. *Electrophoresis* **30**:1845-1855.

Gees, M., Colsoul, B. and Nilius, B. (2010). The role of transient receptor potential cation channels in Ca^{2+} signaling. *Cold Spring Harb Perspect Biol* **2**:a003962.

Ghavami, S., Shojaei, S., Yeganeh, B., Ande, S. R., Jangamreddy, J. R., Mehrpour, M., Christoffersson, J. *et al.* (2014). Autophagy and

apoptosis dysfunction in neurodegenerative disorders. *Prog Neurobiol* **112**:24-49.

Ghosh, A. and Greenberg, M. E. (1995). Calcium signaling in neurons: molecular mechanisms and cellular consequences. *Science* **268**:239-247.

Gilany, K., Van Elzen, R., Mous, K., Coen, E., Van Dongen, W., Vandamme, S., Gevaert, K. *et al.* (2008). The proteome of the human neuroblastoma cell line SH-SY5Y: an enlarged proteome. *Biochim Biophys Acta* **1784**:983-985.

Girault, A., Haelters, J. P., Potier-Cartereau, M., Chantome, A., Jaffres, P. A., Bougnoux, P., Joulin, V. *et al.* (2012). Targeting SKCa channels in cancer: potential new therapeutic approaches. *Curr Med Chem* **19**:697-713.

Glenner, G. G. and Wong, C. W. (1984). Alzheimer's disease: initial report of the purification and characterization of a novel cerebrovascular amyloid protein. *Biochem Biophys Res Commun* **120**:885-890.

Goldberg, J. A., Guzman, J. N., Estep, C. M., Ilijic, E., Kondapalli, J., Sanchez-Padilla, J. and Surmeier, D. J. (2012). Calcium entry induces mitochondrial oxidant stress in vagal neurons at risk in Parkinson's disease. *Nat Neurosci* **15**:1414-1421.

Goldberg, J. A. and Wilson, C. J. (2005). Control of spontaneous firing patterns by the selective coupling of calcium currents to calcium-activated potassium currents in striatal cholinergic interneurons. *J Neurosci* **25**:10230-10238.

Grunnet, M., Jensen, B. S., Olesen, S. P. and Klaerke, D. A. (2001). Apamin interacts with all subtypes of cloned small-conductance Ca²⁺-activated K⁺ channels. *Pflugers Arch* **441**:544-550.

Guilbert, A., Gautier, M., Dhennin-Duthille, I., Haren, N., Sevestre, H. and Ouadid-Ahidouch, H. (2009). Evidence that TRPM7 is required for breast cancer cell proliferation. *Am J Physiol Cell Physiol* **297**:C493-502.

Guo, J. L., Covell, D. J., Daniels, J. P., Iba, M., Stieber, A., Zhang, B., Riddle, D. M. *et al.* (2013). Distinct alpha-synuclein strains differentially promote tau inclusions in neurons. *Cell* **154**:103-117.

Habermann, E. (1984). Apamin. *Pharmacol Ther* **25**:255-270.

Hallworth, N. E., Wilson, C. J. and Bevan, M. D. (2003). Apamin-sensitive small conductance calcium-activated potassium channels, through their selective coupling to voltage-gated calcium channels, are critical determinants of the precision, pace, and pattern of action potential generation in rat subthalamic nucleus neurons in vitro. *J Neurosci* **23**:7525-7542.

Hardie, R. C. (2011). A brief history of trp: commentary and personal perspective. *Pflugers Arch* **461**:493-498.

Hardie, R. C. and Franze, K. (2012). Photomechanical responses in *Drosophila* photoreceptors. *Science* **338**:260-263.

Haugaard, M. M., Hesselkilde, E. Z., Pehrson, S., Carstensen, H., Flethoj, M., Praestegaard, K. F., Sorensen, U. S. *et al.* (2015). Pharmacologic inhibition of small-conductance calcium-activated potassium (SK) channels by NS8593 reveals atrial antiarrhythmic potential in horses. *Heart Rhythm* **12**:825-835.

Henn, A., Lund, S., Hedtjarn, M., Schrattenholz, A., Porzgen, P. and Leist, M. (2009). The suitability of BV2 cells as alternative model system for primary microglia cultures or for animal experiments examining brain inflammation. *Altex* **26**:83-94.

Higley, M. J. and Sabatini, B. L. (2012). Calcium signaling in dendritic spines. *Cold Spring Harb Perspect Biol* **4**:a005686.

Hirschberg, B., Maylie, J., Adelman, J. P. and Marrion, N. V. (1998). Gating of recombinant small-conductance Ca-activated K⁺ channels by calcium. *J Gen Physiol* **111**:565-581.

Hochman, A., Sternin, H., Gorodin, S., Korsmeyer, S., Ziv, I., Melamed, E. and Offen, D. (1998). Enhanced oxidative stress and altered antioxidants in brains of Bcl-2-deficient mice. *J Neurochem* **71**:741-748.

Hodgkin, A. L. and Huxley, A. F. (1952). A quantitative description of membrane current and its application to conduction and excitation in nerve. *J Physiol* **117**:500-544.

Hofer, A., Kovacs, G., Zappatini, A., Leuenberger, M., Hediger, M. A. and Lochner, M. (2013). Design, synthesis and pharmacological characterization of analogs of 2-aminoethyl diphenylborinate (2-APB), a known store-operated calcium channel blocker, for inhibition of TRPV6-mediated calcium transport. *Bioorg Med Chem* **21**:3202-3213.

Hosseini, R., Benton, D. C., Dunn, P. M., Jenkinson, D. H. and Moss, G. W. (2001). SK3 is an important component of K(+) channels mediating the afterhyperpolarization in cultured rat SCG neurones. *J Physiol* **535**:323-334.

Hougaard, C., Eriksen, B. L., Jorgensen, S., Johansen, T. H., Dyhring, T., Madsen, L. S., Strobaek, D. *et al.* (2007). Selective positive modulation of the SK3 and SK2 subtypes of small conductance Ca²⁺-activated K⁺ channels. *Br J Pharmacol* **151**:655-665.

Hougaard, C., Jensen, M. L., Dale, T. J., Miller, D. D., Davies, D. J., Eriksen, B. L., Strobaek, D. *et al.* (2009). Selective activation of the SK1 subtype of human small-conductance Ca²⁺-activated K⁺ channels by 4-(2-methoxyphenylcarbamoyloxymethyl)-piperidine-1-carboxylic acid tert-butyl ester (GW542573X) is dependent on serine 293 in the S5 segment. *Mol Pharmacol* **76**:569-578.

Hu, Q., Corda, S., Zweier, J. L., Capogrossi, M. C. and Ziegelstein, R. C. (1998). Hydrogen peroxide induces intracellular calcium oscillations in human aortic endothelial cells. *Circulation* **97**:268-275.

Huang, X., Dubuc, A. M., Hashizume, R., Berg, J., He, Y., Wang, J., Chiang, C. *et al.* (2012). Voltage-gated potassium channel EAG2 controls mitotic entry and tumor growth in medulloblastoma via regulating cell volume dynamics. *Genes Dev* **26**:1780-1796.

Huang, X. and Jan, L. Y. (2014). Targeting potassium channels in cancer. *J Cell Biol* **206**:151-162.

Huber, S. M. (2013). Oncochannels. *Cell Calcium* **53**:241-255.

Ishii, T. M., Maylie, J. and Adelman, J. P. (1997). Determinants of apamin and d-tubocurarine block in SK potassium channels. *J Biol Chem* **272**:23195-23200.

Jafaar, Z. M., Litchfield, L. M., Ivanova, M. M., Radde, B. N., Al-Rayyan, N. and Klinge, C. M. (2014). beta-D-glucan inhibits endocrine-resistant breast cancer cell proliferation and alters gene expression. *Int J Oncol* **44**:1365-1375.

Jiang, J., Li, M. and Yue, L. (2005). Potentiation of TRPM7 inward currents by protons. *J Gen Physiol* **126**:137-150.

Jin, J., Desai, B. N., Navarro, B., Donovan, A., Andrews, N. C. and Clapham, D. E. (2008). Deletion of *Trpm7* disrupts embryonic development and thymopoiesis without altering Mg²⁺ homeostasis. *Science* **322**:756-760.

Jin, J., Wu, L. J., Jun, J., Cheng, X., Xu, H., Andrews, N. C. and Clapham, D. E. (2012). The channel kinase, TRPM7, is required for early embryonic development. *Proc Natl Acad Sci U S A* **109**:E225-233.

John, V. H., Dale, T. J., Hollands, E. C., Chen, M. X., Partington, L., Downie, D. L., Meadows, H. J. *et al.* (2007). Novel 384-well population patch clamp electrophysiology assays for Ca²⁺-activated K⁺ channels. *J Biomol Screen* **12**:50-60.

Joiner, W. J., Wang, L. Y., Tang, M. D. and Kaczmarek, L. K. (1997). hSK4, a member of a novel subfamily of calcium-activated potassium channels. *Proc Natl Acad Sci U S A* **94**:11013-11018.

Ju, T. C., Chen, H. M., Lin, J. T., Chang, C. P., Chang, W. C., Kang, J. J., Sun, C. P. *et al.* (2011). Nuclear translocation of AMPK-alpha1 potentiates striatal neurodegeneration in Huntington's disease. *J Cell Biol* **194**:209-227.

Kaczmarek, L. K. (2006). Non-conducting functions of voltage-gated ion channels. *Nat Rev Neurosci* **7**:761-771.

Kaitsuka, T., Katagiri, C., Beesetty, P., Nakamura, K., Hourani, S., Tomizawa, K., Kozak, J. A. *et al.* (2014). Inactivation of TRPM7 kinase activity does not impair its channel function in mice. *Sci Rep* **4**:5718.

Kane, D. J., Sarafian, T. A., Anton, R., Hahn, H., Gralla, E. B., Valentine, J. S., Ord, T. *et al.* (1993). Bcl-2 inhibition of neural death: decreased generation of reactive oxygen species. *Science* **262**:1274-1277.

Kang, R., Zeh, H. J., Lotze, M. T. and Tang, D. (2011). The Beclin 1 network regulates autophagy and apoptosis. *Cell Death Differ* **18**:571-580.

Kawamoto, E. M., Vivar, C. and Camandola, S. (2012). Physiology and pathology of calcium signaling in the brain. *Front Pharmacol* **3**:61.

Keen, J. E., Khawaled, R., Farrens, D. L., Neelands, T., Rivard, A., Bond, C. T., Janowsky, A. *et al.* (1999). Domains responsible for constitutive and Ca(2+)-dependent interactions between calmodulin and small conductance Ca(2+)-activated potassium channels. *J Neurosci* **19**:8830-8838.

Kerr, J. F., Wyllie, A. H. and Currie, A. R. (1972). Apoptosis: a basic biological phenomenon with wide-ranging implications in tissue kinetics. *Br J Cancer* **26**:239-257.

King, B., Rizwan, A. P., Asmara, H., Heath, N. C., Engbers, J. D., Dykstra, S., Bartoletti, T. M. *et al.* (2015). IKCa Channels Are a Critical Determinant of the Slow AHP in CA1 Pyramidal Neurons. *Cell Rep*.

Knowlden, J. M., Hutcheson, I. R., Barrow, D., Gee, J. M. and Nicholson, R. I. (2005). Insulin-like growth factor-I receptor signaling in tamoxifen-resistant breast cancer: a supporting role to the epidermal growth factor receptor. *Endocrinology* **146**:4609-4618.

Knowlden, J. M., Hutcheson, I. R., Jones, H. E., Madden, T., Gee, J. M., Harper, M. E., Barrow, D. *et al.* (2003). Elevated levels of epidermal growth factor receptor/c-erbB2 heterodimers mediate an autocrine growth regulatory pathway in tamoxifen-resistant MCF-7 cells. *Endocrinology* **144**:1032-1044.

Kohler, M., Hirschberg, B., Bond, C. T., Kinzie, J. M., Marrion, N. V., Maylie, J. and Adelman, J. P. (1996). Small-conductance, calcium-activated potassium channels from mammalian brain. *Science* **273**:1709-1714.

- Kozak, J. A., Matsushita, M., Nairn, A. C. and Cahalan, M. D. (2005). Charge screening by internal pH and polyvalent cations as a mechanism for activation, inhibition, and rundown of TRPM7/MIC channels. *J Gen Physiol* **126**:499-514.
- Krishna, A., Biryukov, M., Trefois, C., Antony, P. M., Hussong, R., Lin, J., Heinaniemi, M. *et al.* (2014). Systems genomics evaluation of the SH-SY5Y neuroblastoma cell line as a model for Parkinson's disease. *BMC Genomics* **15**:1154.
- Krnjevic, K. and Lisiewicz, A. (1972). Injections of calcium ions into spinal motoneurons. *J Physiol* **225**:363-390.
- Kunzelmann, K. (2005). Ion channels and cancer. *J Membr Biol* **205**:159-173.
- LaFerla, F. M. (2002). Calcium dyshomeostasis and intracellular signalling in Alzheimer's disease. *Nat Rev Neurosci* **3**:862-872.
- Lamy, C., Goodchild, S. J., Weatherall, K. L., Jane, D. E., Liegeois, J. F., Seutin, V. and Marrion, N. V. (2010). Allosteric block of KCa₂ channels by apamin. *J Biol Chem* **285**:27067-27077.
- Lang, F., Foller, M., Lang, K. S., Lang, P. A., Ritter, M., Gulbins, E., Vereninov, A. *et al.* (2005). Ion channels in cell proliferation and apoptotic cell death. *J Membr Biol* **205**:147-157.
- Langeslag, M., Clark, K., Moolenaar, W. H., van Leeuwen, F. N. and Jalink, K. (2007). Activation of TRPM7 channels by phospholipase C-coupled receptor agonists. *J Biol Chem* **282**:232-239.
- Lasfargues, E. Y., Coutinho, W. G. and Redfield, E. S. (1978). Isolation of two human tumor epithelial cell lines from solid breast carcinomas. *J Natl Cancer Inst* **61**:967-978.
- Latorre, R. and Brauchi, S. (2006). Large conductance Ca²⁺-activated K⁺ (BK) channel: activation by Ca²⁺ and voltage. *Biol Res* **39**:385-401.
- Leanza, L., Zoratti, M., Gulbins, E. and Szabo, I. (2014). Mitochondrial ion channels as oncological targets. *Oncogene* **33**:5569-5581.

- Lehen'kyi, V., Shapovalov, G., Skryma, R. and Prevarskaya, N. (2011). Ion channels and transporters in cancer. 5. Ion channels in control of cancer and cell apoptosis. *Am J Physiol Cell Physiol* **301**:C1281-1289.
- Li, M. and Xiong, Z. G. (2011). Ion channels as targets for cancer therapy. *Int J Physiol Pathophysiol Pharmacol* **3**:156-166.
- Li, W. and Aldrich, R. W. (2011). Electrostatic influences of charged inner pore residues on the conductance and gating of small conductance Ca²⁺ activated K⁺ channels. *Proc Natl Acad Sci U S A* **108**:5946-5953.
- Li, W., Halling, D. B., Hall, A. W. and Aldrich, R. W. (2009). EF hands at the N-lobe of calmodulin are required for both SK channel gating and stable SK-calmodulin interaction. *J Gen Physiol* **134**:281-293.
- Lim, D., Fedrizzi, L., Tartari, M., Zuccato, C., Cattaneo, E., Brini, M. and Carafoli, E. (2008). Calcium homeostasis and mitochondrial dysfunction in striatal neurons of Huntington disease. *J Biol Chem* **283**:5780-5789.
- Lin, M. T. and Beal, M. F. (2006). Mitochondrial dysfunction and oxidative stress in neurodegenerative diseases. *Nature* **443**:787-795.
- Litan, A. and Langhans, S. A. (2015). Cancer as a channelopathy: ion channels and pumps in tumor development and progression. *Front Cell Neurosci* **9**:86.
- Llambi, F. and Green, D. R. (2011). Apoptosis and oncogenesis: give and take in the BCL-2 family. *Curr Opin Genet Dev* **21**:12-20.
- Lujan, R. (2010). Organisation of potassium channels on the neuronal surface. *J Chem Neuroanat* **40**:1-20.
- Lumachi, F., Brunello, A., Maruzzo, M., Basso, U. and Basso, S. M. (2013). Treatment of estrogen receptor-positive breast cancer. *Curr Med Chem* **20**:596-604.
- MacKinnon, R. (2004). Potassium channels and the atomic basis of selective ion conduction (Nobel Lecture). *Angew Chem Int Ed Engl* **43**:4265-4277.

Madison, D. V. and Nicoll, R. A. (1982). Noradrenaline blocks accommodation of pyramidal cell discharge in the hippocampus. *Nature* **299**:636-638.

Maher, B. J. and Westbrook, G. L. (2005). SK channel regulation of dendritic excitability and dendrodendritic inhibition in the olfactory bulb. *J Neurophysiol* **94**:3743-3750.

Majno, G. and Joris, I. (1995). Apoptosis, oncosis, and necrosis. An overview of cell death. *Am J Pathol* **146**:3-15.

Mangiarini, L., Sathasivam, K., Seller, M., Cozens, B., Harper, A., Hetherington, C., Lawton, M. *et al.* (1996). Exon 1 of the HD gene with an expanded CAG repeat is sufficient to cause a progressive neurological phenotype in transgenic mice. *Cell* **87**:493-506.

Marambaud, P., Dreses-Werringloer, U. and Vingtdeux, V. (2009). Calcium signaling in neurodegeneration. *Mol Neurodegener* **4**:20.

Martin, L. J. (2010). Mitochondrial and Cell Death Mechanisms in Neurodegenerative Diseases. *Pharmaceuticals (Basel)* **3**:839-915.

Marty, A. (1989). The physiological role of calcium-dependent channels. *Trends Neurosci* **12**:420-424.

Mattson, M. P. (2007). Calcium and neurodegeneration. *Aging Cell* **6**:337-350.

Maylie, J., Bond, C. T., Herson, P. S., Lee, W. S. and Adelman, J. P. (2004). Small conductance Ca²⁺-activated K⁺ channels and calmodulin. *J Physiol* **554**:255-261.

McIlwain, D. R., Berger, T. and Mak, T. W. (2013). Caspase functions in cell death and disease. *Cold Spring Harb Perspect Biol* **5**:a008656.

Mederos y Schnitzler, M., Waring, J., Gudermann, T. and Chubanov, V. (2008). Evolutionary determinants of divergent calcium selectivity of TRPM channels. *FASEB J* **22**:1540-1551.

Meech, R. W. (1972). Intracellular calcium injection causes increased potassium conductance in *Aplysia* nerve cells. *Comp Biochem Physiol A Comp Physiol* **42**:493-499.

Mikoshiba, K. (2007). IP3 receptor/Ca²⁺ channel: from discovery to new signaling concepts. *J Neurochem* **102**:1426-1446.

Miller, D. J. (2004). Sydney Ringer; physiological saline, calcium and the contraction of the heart. *J Physiol* **555**:585-587.

Monaghan, A. S., Benton, D. C., Bahia, P. K., Hosseini, R., Shah, Y. A., Haylett, D. G. and Moss, G. W. (2004). The SK3 subunit of small conductance Ca²⁺-activated K⁺ channels interacts with both SK1 and SK2 subunits in a heterologous expression system. *J Biol Chem* **279**:1003-1009.

Monteilh-Zoller, M. K., Hermosura, M. C., Nadler, M. J., Scharenberg, A. M., Penner, R. and Fleig, A. (2003). TRPM7 provides an ion channel mechanism for cellular entry of trace metal ions. *J Gen Physiol* **121**:49-60.

Montell, C. (2005). The TRP superfamily of cation channels. *Sci STKE* **2005**:re3.

Montell, C. and Rubin, G. M. (1989). Molecular characterization of the *Drosophila* trp locus: a putative integral membrane protein required for phototransduction. *Neuron* **2**:1313-1323.

Muraki, K., Iwata, Y., Katanosaka, Y., Ito, T., Ohya, S., Shigekawa, M. and Imaizumi, Y. (2003). TRPV2 is a component of osmotically sensitive cation channels in murine aortic myocytes. *Circ Res* **93**:829-838.

Nadler, M. J., Hermosura, M. C., Inabe, K., Perraud, A. L., Zhu, Q., Stokes, A. J., Kurosaki, T. *et al.* (2001). LTRPC7 is a Mg.ATP-regulated divalent cation channel required for cell viability. *Nature* **411**:590-595.

Nahorski, S. R. (1988). Inositol polyphosphates and neuronal calcium homeostasis. *Trends Neurosci* **11**:444-448.

Neve, R. M., Chin, K., Fridlyand, J., Yeh, J., Baehner, F. L., Fevr, T., Clark, L. *et al.* (2006). A collection of breast cancer cell lines for the study of functionally distinct cancer subtypes. *Cancer Cell* **10**:515-527.

Newcomb-Fernandez, J. K., Zhao, X., Pike, B. R., Wang, K. K., Kampfl, A., Beer, R., DeFord, S. M. *et al.* (2001). Concurrent assessment of

calpain and caspase-3 activation after oxygen-glucose deprivation in primary septo-hippocampal cultures. *J Cereb Blood Flow Metab* **21**:1281-1294.

Nicholson, R. I., Hutcheson, I. R., Hiscox, S. E., Knowlden, J. M., Giles, M., Barrow, D. and Gee, J. M. (2005). Growth factor signalling and resistance to selective oestrogen receptor modulators and pure anti-oestrogens: the use of anti-growth factor therapies to treat or delay endocrine resistance in breast cancer. *Endocr Relat Cancer* **12 Suppl 1**:S29-36.

Nishihara, E., Hiyama, T. Y. and Noda, M. (2011). Osmosensitivity of transient receptor potential vanilloid 1 is synergistically enhanced by distinct activating stimuli such as temperature and protons. *PLoS One* **6**:e22246.

Nolting, A., Ferraro, T., D'Hoedt, D. and Stocker, M. (2007). An amino acid outside the pore region influences apamin sensitivity in small conductance Ca²⁺-activated K⁺ channels. *J Biol Chem* **282**:3478-3486.

Numata, T., Shimizu, T. and Okada, Y. (2007). Direct mechano-stress sensitivity of TRPM7 channel. *Cell Physiol Biochem* **19**:1-8.

Oliver, D., Klocker, N., Schuck, J., Baukowitz, T., Ruppertsberg, J. P. and Fakler, B. (2000). Gating of Ca²⁺-activated K⁺ channels controls fast inhibitory synaptic transmission at auditory outer hair cells. *Neuron* **26**:595-601.

Ouadid-Ahidouch, H. and Ahidouch, A. (2013). K(+) channels and cell cycle progression in tumor cells. *Front Physiol* **4**:220.

Panner, A., Cribbs, L. L., Zainelli, G. M., Origitano, T. C., Singh, S. and Wurster, R. D. (2005). Variation of T-type calcium channel protein expression affects cell division of cultured tumor cells. *Cell Calcium* **37**:105-119.

Pardo, L. A. and Stuhmer, W. (2014). The roles of K(+) channels in cancer. *Nat Rev Cancer* **14**:39-48.

Park, H. S., Hong, C., Kim, B. J. and So, I. (2014). The Pathophysiologic Roles of TRPM7 Channel. *Korean J Physiol Pharmacol* **18**:15-23.

- Park, Y. B. (1994). Ion selectivity and gating of small conductance Ca(2+)-activated K⁺ channels in cultured rat adrenal chromaffin cells. *J Physiol* **481** (Pt 3):555-570.
- Pascual, O., Ben Achour, S., Rostaing, P., Triller, A. and Bessis, A. (2012). Microglia activation triggers astrocyte-mediated modulation of excitatory neurotransmission. *Proc Natl Acad Sci U S A* **109**:E197-205.
- Pedarzani, P., McCutcheon, J. E., Rogge, G., Jensen, B. S., Christophersen, P., Hougaard, C., Strobaek, D. *et al.* (2005). Specific enhancement of SK channel activity selectively potentiates the afterhyperpolarizing current I(AHP) and modulates the firing properties of hippocampal pyramidal neurons. *J Biol Chem* **280**:41404-41411.
- Pedarzani, P. and Stocker, M. (2008). Molecular and cellular basis of small--and intermediate-conductance, calcium-activated potassium channel function in the brain. *Cell Mol Life Sci* **65**:3196-3217.
- Perou, C. M., Jeffrey, S. S., van de Rijn, M., Rees, C. A., Eisen, M. B., Ross, D. T., Pergamenschikov, A. *et al.* (1999). Distinctive gene expression patterns in human mammary epithelial cells and breast cancers. *Proc Natl Acad Sci U S A* **96**:9212-9217.
- Perou, C. M., Sorlie, T., Eisen, M. B., van de Rijn, M., Jeffrey, S. S., Rees, C. A., Pollack, J. R. *et al.* (2000). Molecular portraits of human breast tumours. *Nature* **406**:747-752.
- Perraud, A. L., Knowles, H. M. and Schmitz, C. (2004). Novel aspects of signaling and ion-homeostasis regulation in immunocytes. The TRPM ion channels and their potential role in modulating the immune response. *Mol Immunol* **41**:657-673.
- Perraud, A. L., Schmitz, C. and Scharenberg, A. M. (2003). TRPM2 Ca²⁺ permeable cation channels: from gene to biological function. *Cell Calcium* **33**:519-531.
- Polymeropoulos, M. H., Lavedan, C., Leroy, E., Ide, S. E., Dehejia, A., Dutra, A., Pike, B. *et al.* (1997). Mutation in the alpha-synuclein gene identified in families with Parkinson's disease. *Science* **276**:2045-2047.

- Potier, M., Joulin, V., Roger, S., Besson, P., Jourdan, M. L., Leguennec, J. Y., Bougnoux, P. *et al.* (2006). Identification of SK3 channel as a new mediator of breast cancer cell migration. *Mol Cancer Ther* **5**:2946-2953.
- Pouladi, M. A., Morton, A. J. and Hayden, M. R. (2013). Choosing an animal model for the study of Huntington's disease. *Nat Rev Neurosci* **14**:708-721.
- Power, J. M. and Sah, P. (2008). Competition between calcium-activated K⁺ channels determines cholinergic action on firing properties of basolateral amygdala projection neurons. *J Neurosci* **28**:3209-3220.
- Prevarskaya, N., Skryma, R. and Shuba, Y. (2010). Ion channels and the hallmarks of cancer. *Trends Mol Med* **16**:107-121.
- Pugazhenthii, S., Wang, M., Pham, S., Sze, C. I. and Eckman, C. B. (2011). Downregulation of CREB expression in Alzheimer's brain and in Aβ-treated rat hippocampal neurons. *Mol Neurodegener* **6**:60.
- Putney, J. W. (2011). The physiological function of store-operated calcium entry. *Neurochem Res* **36**:1157-1165.
- Razik, M. A. and Cidlowski, J. A. (2002). Molecular interplay between ion channels and the regulation of apoptosis. *Biol Res* **35**:203-207.
- Reed, J. C. (2008). Bcl-2-family proteins and hematologic malignancies: history and future prospects. *Blood* **111**:3322-3330.
- Richter, M., Nickel, C., Apel, L., Kaas, A., Dodel, R., Culmsee, C. and Dolga, A. M. (2015). SK channel activation modulates mitochondrial respiration and attenuates neuronal HT-22 cell damage induced by H₂O₂. *Neurochem Int* **81**:63-75.
- Roderick, H. L. and Cook, S. J. (2008). Ca²⁺ signalling checkpoints in cancer: remodelling Ca²⁺ for cancer cell proliferation and survival. *Nat Rev Cancer* **8**:361-375.
- Roy, J. W., Cowley, E. A., Blay, J. and Linsdell, P. (2010). The intermediate conductance Ca²⁺-activated K⁺ channel inhibitor TRAM-34 stimulates proliferation of breast cancer cells via activation of oestrogen receptors. *Br J Pharmacol* **159**:650-658.

Ruegg, U. T. and Burgess, G. M. (1989). Staurosporine, K-252 and UCN-01: potent but nonspecific inhibitors of protein kinases. *Trends Pharmacol Sci* **10**:218-220.

Runnels, L. W., Yue, L. and Clapham, D. E. (2001). TRP-PLIK, a bifunctional protein with kinase and ion channel activities. *Science* **291**:1043-1047.

Ryazanova, L. V., Rondon, L. J., Zierler, S., Hu, Z., Galli, J., Yamaguchi, T. P., Mazur, A. *et al.* (2010). TRPM7 is essential for Mg(2+) homeostasis in mammals. *Nat Commun* **1**:109.

Sah, P. and Clements, J. D. (1999). Photolytic manipulation of [Ca²⁺]_i reveals slow kinetics of potassium channels underlying the afterhyperpolarization in hippocampal pyramidal neurons. *J Neurosci* **19**:3657-3664.

Sah, P. and Faber, E. S. (2002). Channels underlying neuronal calcium-activated potassium currents. *Prog Neurobiol* **66**:345-353.

Sah, P. and McLachlan, E. M. (1992). Potassium currents contributing to action potential repolarization and the afterhyperpolarization in rat vagal motoneurons. *J Neurophysiol* **68**:1834-1841.

Sailer, C. A., Hu, H., Kaufmann, W. A., Trieb, M., Schwarzer, C., Storm, J. F. and Knaus, H. G. (2002). Regional differences in distribution and functional expression of small-conductance Ca²⁺-activated K⁺ channels in rat brain. *J Neurosci* **22**:9698-9707.

Sailer, C. A., Kaufmann, W. A., Marksteiner, J. and Knaus, H. G. (2004). Comparative immunohistochemical distribution of three small-conductance Ca²⁺-activated potassium channel subunits, SK1, SK2, and SK3 in mouse brain. *Mol Cell Neurosci* **26**:458-469.

Sassone, J., Maraschi, A., Sassone, F., Silani, V. and Ciammola, A. (2013). Defining the role of the Bcl-2 family proteins in Huntington's disease. *Cell Death Dis* **4**:e772.

Savic, N., Pedarzani, P. and Sciancalepore, M. (2001). Medium afterhyperpolarization and firing pattern modulation in interneurons of stratum radiatum in the CA3 hippocampal region. *J Neurophysiol* **85**:1986-1997.

Scherzinger, E., Lurz, R., Turmaine, M., Mangiarini, L., Hollenbach, B., Hasenbank, R., Bates, G. P. *et al.* (1997). Huntingtin-encoded polyglutamine expansions form amyloid-like protein aggregates in vitro and in vivo. *Cell* **90**:549-558.

Scherzinger, E., Sittler, A., Schweiger, K., Heiser, V., Lurz, R., Hasenbank, R., Bates, G. P. *et al.* (1999). Self-assembly of polyglutamine-containing huntingtin fragments into amyloid-like fibrils: implications for Huntington's disease pathology. *Proc Natl Acad Sci U S A* **96**:4604-4609.

Schmitz, C., Perraud, A. L., Johnson, C. O., Inabe, K., Smith, M. K., Penner, R., Kurosaki, T. *et al.* (2003). Regulation of vertebrate cellular Mg²⁺ homeostasis by TRPM7. *Cell* **114**:191-200.

Schonherr, R. (2005). Clinical relevance of ion channels for diagnosis and therapy of cancer. *J Membr Biol* **205**:175-184.

Schug, Z. T., Gonzalez, F., Houtkooper, R. H., Vaz, F. M. and Gottlieb, E. (2011). BID is cleaved by caspase-8 within a native complex on the mitochondrial membrane. *Cell Death Differ* **18**:538-548.

Schwindt, P. C., Spain, W. J., Foehring, R. C., Chubb, M. C. and Crill, W. E. (1988). Slow conductances in neurons from cat sensorimotor cortex in vitro and their role in slow excitability changes. *J Neurophysiol* **59**:450-467.

Shah, M. and Haylett, D. G. (2000). The pharmacology of hSK1 Ca²⁺-activated K⁺ channels expressed in mammalian cell lines. *Br J Pharmacol* **129**:627-630.

Shepard, P. D. and Stump, D. (1999). Nifedipine blocks apamin-induced bursting activity in nigral dopamine-containing neurons. *Brain Res* **817**:104-109.

Shiozaki, E. N., Chai, J. and Shi, Y. (2002). Oligomerization and activation of caspase-9, induced by Apaf-1 CARD. *Proc Natl Acad Sci U S A* **99**:4197-4202.

Simon, F., Varela, D. and Cabello-Verrugio, C. (2013). Oxidative stress-modulated TRPM ion channels in cell dysfunction and pathological conditions in humans. *Cell Signal* **25**:1614-1624.

Singh, S., Syme, C. A., Singh, A. K., Devor, D. C. and Bridges, R. J. (2001). Benzimidazolone activators of chloride secretion: potential therapeutics for cystic fibrosis and chronic obstructive pulmonary disease. *J Pharmacol Exp Ther* **296**:600-611.

Soule, H. D., Maloney, T. M., Wolman, S. R., Peterson, W. D., Jr., Brenz, R., McGrath, C. M., Russo, J. *et al.* (1990). Isolation and characterization of a spontaneously immortalized human breast epithelial cell line, MCF-10. *Cancer Res* **50**:6075-6086.

Soule, H. D., Vazquez, J., Long, A., Albert, S. and Brennan, M. (1973). A human cell line from a pleural effusion derived from a breast carcinoma. *J Natl Cancer Inst* **51**:1409-1416.

Stevens, B., Allen, N. J., Vazquez, L. E., Howell, G. R., Christopherson, K. S., Nouri, N., Micheva, K. D. *et al.* (2007). The classical complement cascade mediates CNS synapse elimination. *Cell* **131**:1164-1178.

Stocker, M. (2004). Ca(2+)-activated K⁺ channels: molecular determinants and function of the SK family. *Nat Rev Neurosci* **5**:758-770.

Stocker, M., Hirzel, K., D'Hoedt, D. and Pedarzani, P. (2004). Matching molecules to function: neuronal Ca²⁺-activated K⁺ channels and afterhyperpolarizations. *Toxicon* **43**:933-949.

Stocker, M. and Pedarzani, P. (2000). Differential distribution of three Ca(2+)-activated K(+) channel subunits, SK1, SK2, and SK3, in the adult rat central nervous system. *Mol Cell Neurosci* **15**:476-493.

Storm, J. F. (1987). Action potential repolarization and a fast after-hyperpolarization in rat hippocampal pyramidal cells. *J Physiol* **385**:733-759.

Strobaek, D., Brown, D. T., Jenkins, D. P., Chen, Y. J., Coleman, N., Ando, Y., Chiu, P. *et al.* (2013). NS6180, a new K(Ca) 3.1 channel inhibitor prevents T-cell activation and inflammation in a rat model of inflammatory bowel disease. *Br J Pharmacol* **168**:432-444.

Strobaek, D., Hougaard, C., Johansen, T. H., Sorensen, U. S., Nielsen, E. O., Nielsen, K. S., Taylor, R. D. *et al.* (2006). Inhibitory gating modulation of small conductance Ca²⁺-activated K⁺ channels by the synthetic compound (R)-N-(benzimidazol-2-yl)-1,2,3,4-tetrahydro-1-naphthylamine (NS8593) reduces afterhyperpolarizing current in hippocampal CA1 neurons. *Mol Pharmacol* **70**:1771-1782.

Strobaek, D., Jorgensen, T. D., Christophersen, P., Ahring, P. K. and Olesen, S. P. (2000). Pharmacological characterization of small-conductance Ca(2+)-activated K(+) channels stably expressed in HEK 293 cells. *Br J Pharmacol* **129**:991-999.

Strobaek, D., Teuber, L., Jorgensen, T. D., Ahring, P. K., Kjaer, K., Hansen, R. S., Olesen, S. P. *et al.* (2004). Activation of human IK and SK Ca²⁺ -activated K⁺ channels by NS309 (6,7-dichloro-1H-indole-2,3-dione 3-oxime). *Biochim Biophys Acta* **1665**:1-5.

Stutzmann, G. E. and Mattson, M. P. (2011). Endoplasmic reticulum Ca(2+) handling in excitable cells in health and disease. *Pharmacol Rev* **63**:700-727.

Suh, S. W., Shin, B. S., Ma, H., Van Hoecke, M., Brennan, A. M., Yenari, M. A. and Swanson, R. A. (2008). Glucose and NADPH oxidase drive neuronal superoxide formation in stroke. *Ann Neurol* **64**:654-663.

Sun, H. S., Jackson, M. F., Martin, L. J., Jansen, K., Teves, L., Cui, H., Kiyonaka, S. *et al.* (2009). Suppression of hippocampal TRPM7 protein prevents delayed neuronal death in brain ischemia. *Nat Neurosci* **12**:1300-1307.

Sutko, J. L. and Airey, J. A. (1996). Ryanodine receptor Ca²⁺ release channels: does diversity in form equal diversity in function? *Physiol Rev* **76**:1027-1071.

Syme, C. A., Gerlach, A. C., Singh, A. K. and Devor, D. C. (2000). Pharmacological activation of cloned intermediate- and small-conductance Ca(2+)-activated K(+) channels. *Am J Physiol Cell Physiol* **278**:C570-581.

Szatkowski, M., Barbour, B. and Attwell, D. (1990). Non-vesicular release of glutamate from glial cells by reversed electrogenic glutamate uptake. *Nature* **348**:443-446.

Tajima, N., Schonherr, K., Niedling, S., Kaatz, M., Kanno, H., Schonherr, R. and Heinemann, S. H. (2006). Ca²⁺-activated K⁺ channels in human melanoma cells are up-regulated by hypoxia involving hypoxia-inducible factor-1 α and the von Hippel-Lindau protein. *J Physiol* **571**:349-359.

Takahashi, N., Kozai, D. and Mori, Y. (2012). TRP channels: sensors and transducers of gasotransmitter signals. *Front Physiol* **3**:324.

Teshima, K., Kim, S. H. and Allen, C. N. (2003). Characterization of an apamin-sensitive potassium current in suprachiasmatic nucleus neurons. *Neuroscience* **120**:65-73.

Togashi, K., Inada, H. and Tominaga, M. (2008). Inhibition of the transient receptor potential cation channel TRPM2 by 2-aminoethoxydiphenyl borate (2-APB). *Br J Pharmacol* **153**:1324-1330.

Tojyo, Y., Morita, T., Nezu, A. and Tanimura, A. (2013). Staurosporine maintains the activation of store-operated Ca(2)(+) entry even after the refilling of Ca(2)(+) stores. *Cell Calcium* **53**:349-356.

Tong, H., Steinert, J. R., Robinson, S. W., Chernova, T., Read, D. J., Oliver, D. L. and Forsythe, I. D. (2010). Regulation of Kv channel expression and neuronal excitability in rat medial nucleus of the trapezoid body maintained in organotypic culture. *J Physiol* **588**:1451-1468.

Trettel, F., Rigamonti, D., Hilditch-Maguire, P., Wheeler, V. C., Sharp, A. H., Persichetti, F., Cattaneo, E. *et al.* (2000). Dominant phenotypes produced by the HD mutation in STHdh(Q111) striatal cells. *Hum Mol Genet* **9**:2799-2809.

Trimmer, J. S. (2015). Subcellular localization of K⁺ channels in mammalian brain neurons: remarkable precision in the midst of extraordinary complexity. *Neuron* **85**:238-256.

Tsokas, P., Ma, T., Iyengar, R., Landau, E. M. and Blitzer, R. D. (2007). Mitogen-activated protein kinase upregulates the dendritic translation

machinery in long-term potentiation by controlling the mammalian target of rapamycin pathway. *J Neurosci* **27**:5885-5894.

Ullrich, N. D., Voets, T., Prenen, J., Vennekens, R., Talavera, K., Droogmans, G. and Nilius, B. (2005). Comparison of functional properties of the Ca²⁺-activated cation channels TRPM4 and TRPM5 from mice. *Cell Calcium* **37**:267-278.

Varfolomeev, E. E., Schuchmann, M., Luria, V., Chiannikulchai, N., Beckmann, J. S., Mett, I. L., Rebrikov, D. *et al.* (1998). Targeted disruption of the mouse Caspase 8 gene ablates cell death induction by the TNF receptors, Fas/Apo1, and DR3 and is lethal prenatally. *Immunity* **9**:267-276.

Vargas, M. R. and Johnson, J. A. (2009). The Nrf2-ARE cytoprotective pathway in astrocytes. *Expert Rev Mol Med* **11**:e17.

Venkatachalam, K. and Montell, C. (2007). TRP channels. *Annu Rev Biochem* **76**:387-417.

Visan, V., Fajloun, Z., Sabatier, J. M. and Grissmer, S. (2004). Mapping of maurotoxin binding sites on hKv1.2, hKv1.3, and hKCa1 channels. *Mol Pharmacol* **66**:1103-1112.

Volterra, A., Liaudet, N. and Savtchouk, I. (2014). Astrocyte Ca²⁺(+) signalling: an unexpected complexity. *Nat Rev Neurosci* **15**:327-335.

Weerasinghe, P. and Buja, L. M. (2012). Oncosis: an important non-apoptotic mode of cell death. *Exp Mol Pathol* **93**:302-308.

Wei, A. D., Gutman, G. A., Aldrich, R., Chandy, K. G., Grissmer, S. and Wulff, H. (2005). International Union of Pharmacology. LII. Nomenclature and molecular relationships of calcium-activated potassium channels. *Pharmacol Rev* **57**:463-472.

Wes, P. D., Chevesich, J., Jeromin, A., Rosenberg, C., Stetten, G. and Montell, C. (1995). TRPC1, a human homolog of a *Drosophila* store-operated channel. *Proc Natl Acad Sci U S A* **92**:9652-9656.

Wheeler, V. C., White, J. K., Gutekunst, C. A., Vrbanac, V., Weaver, M., Li, X. J., Li, S. H. *et al.* (2000). Long glutamine tracts cause nuclear localization of a novel form of huntingtin in medium spiny striatal

neurons in HdhQ92 and HdhQ111 knock-in mice. *Hum Mol Genet* **9**:503-513.

Williams, S., Serafin, M., Muhlethaler, M. and Bernheim, L. (1997). Distinct contributions of high- and low-voltage-activated calcium currents to afterhyperpolarizations in cholinergic nucleus basalis neurons of the guinea pig. *J Neurosci* **17**:7307-7315.

Wilson, J. X. (1997). Antioxidant defense of the brain: a role for astrocytes. *Can J Physiol Pharmacol* **75**:1149-1163.

Wong, F., Schaefer, E. L., Roop, B. C., LaMendola, J. N., Johnson-Seaton, D. and Shao, D. (1989). Proper function of the *Drosophila* trp gene product during pupal development is important for normal visual transduction in the adult. *Neuron* **3**:81-94.

Wong, L. F., Ralph, G. S., Walmsley, L. E., Bienemann, A. S., Parham, S., Kingsman, S. M., Uney, J. B. *et al.* (2005). Lentiviral-mediated delivery of Bcl-2 or GDNF protects against excitotoxicity in the rat hippocampus. *Mol Ther* **11**:89-95.

Wu, L. J., Sweet, T. B. and Clapham, D. E. (2010). International Union of Basic and Clinical Pharmacology. LXXVI. Current progress in the mammalian TRP ion channel family. *Pharmacol Rev* **62**:381-404.

Wulff, H., Castle, N. A. and Pardo, L. A. (2009). Voltage-gated potassium channels as therapeutic targets. *Nat Rev Drug Discov* **8**:982-1001.

Wulff, H., Gutman, G. A., Cahalan, M. D. and Chandy, K. G. (2001). Delineation of the clotrimazole/TRAM-34 binding site on the intermediate conductance calcium-activated potassium channel, IKCa1. *J Biol Chem* **276**:32040-32045.

Wulff, H. and Kohler, R. (2013). Endothelial small-conductance and intermediate-conductance KCa channels: an update on their pharmacology and usefulness as cardiovascular targets. *J Cardiovasc Pharmacol* **61**:102-112.

Wulff, H., Kolski-Andreaco, A., Sankaranarayanan, A., Sabatier, J. M. and Shakkottai, V. (2007). Modulators of small- and intermediate-

conductance calcium-activated potassium channels and their therapeutic indications. *Curr Med Chem* **14**:1437-1457.

Xia, X. M., Fakler, B., Rivard, A., Wayman, G., Johnson-Pais, T., Keen, J. E., Ishii, T. *et al.* (1998). Mechanism of calcium gating in small-conductance calcium-activated potassium channels. *Nature* **395**:503-507.

Xie, H., Hou, S., Jiang, J., Sekutowicz, M., Kelly, J. and Bacskai, B. J. (2013). Rapid cell death is preceded by amyloid plaque-mediated oxidative stress. *Proc Natl Acad Sci U S A* **110**:7904-7909.

Xie, H. R., Hu, L. S. and Li, G. Y. (2010). SH-SY5Y human neuroblastoma cell line: in vitro cell model of dopaminergic neurons in Parkinson's disease. *Chin Med J (Engl)* **123**:1086-1092.

Xu, S. Z., Zeng, F., Boulay, G., Grimm, C., Harteneck, C. and Beech, D. J. (2005). Block of TRPC5 channels by 2-aminoethoxydiphenyl borate: a differential, extracellular and voltage-dependent effect. *Br J Pharmacol* **145**:405-414.

Yamaguchi, H., Matsushita, M., Nairn, A. C. and Kuriyan, J. (2001). Crystal structure of the atypical protein kinase domain of a TRP channel with phosphotransferase activity. *Mol Cell* **7**:1047-1057.

Yang, J., Liu, X., Bhalla, K., Kim, C. N., Ibrado, A. M., Cai, J., Peng, T. I. *et al.* (1997). Prevention of apoptosis by Bcl-2: release of cytochrome c from mitochondria blocked. *Science* **275**:1129-1132.

Yang, M. and Brackenbury, W. J. (2013). Membrane potential and cancer progression. *Front Physiol* **4**:185.

Yee, N. S., Kazi, A. A. and Yee, R. K. (2014). Cellular and Developmental Biology of TRPM7 Channel-Kinase: Implicated Roles in Cancer. *Cells* **3**:751-777.

Yeh, W. C., de la Pompa, J. L., McCurrach, M. E., Shu, H. B., Elia, A. J., Shahinian, A., Ng, M. *et al.* (1998). FADD: essential for embryo development and signaling from some, but not all, inducers of apoptosis. *Science* **279**:1954-1958.

Yuan, L. L. and Chen, X. (2006). Diversity of potassium channels in neuronal dendrites. *Prog Neurobiol* **78**:374-389.

Zhang, J., Zhao, F., Zhao, Y., Wang, J., Pei, L., Sun, N. and Shi, J. (2011a). Hypoxia induces an increase in intracellular magnesium via transient receptor potential melastatin 7 (TRPM7) channels in rat hippocampal neurons in vitro. *J Biol Chem* **286**:20194-20207.

Zhang, L. and Krnjevic, K. (1987). Apamin depresses selectively the after-hyperpolarization of cat spinal motoneurons. *Neurosci Lett* **74**:58-62.

Zhang, L. and McBain, C. J. (1995). Potassium conductances underlying repolarization and after-hyperpolarization in rat CA1 hippocampal interneurons. *J Physiol* **488** (Pt 3):661-672.

Zhang, M., Abrams, C., Wang, L., Gizzi, A., He, L., Lin, R., Chen, Y. *et al.* (2012). Structural basis for calmodulin as a dynamic calcium sensor. *Structure* **20**:911-923.

Zhang, S., Fritz, N., Ibarra, C. and Uhlen, P. (2011b). Inositol 1,4,5-trisphosphate receptor subtype-specific regulation of calcium oscillations. *Neurochem Res* **36**:1175-1185.

Zorov, D. B., Isaev, N. K., Plotnikov, E. Y., Zorova, L. D., Stelmashook, E. V., Vasileva, A. K., Arkhangelskaya, A. A. *et al.* (2007). The mitochondrion as janus bifrons. *Biochemistry (Mosc)* **72**:1115-1126.